SHEAR RESISTANCE AT NORMAL AND HIGH TEMPERATURES OF REINFORCED CONCRETE MEMBERS WITH LINKS AND CENTRAL BARS

By

Satish Balkrishna Desai

A thesis submitted in fulfilment of
the requirement for the award of
the Degree of Doctor of Philosophy
in Civil Engineering

Structures Research Centre
Department of Civil Engineering
City University, London EC1V 0HB

September, 1995

TABLE OF CONTENTS

LIST OF TABLES

LIST OF FIGURES

Sketches

LIST OF PHOTOGRAPHS

ACKNOWLEDGEMENTS

The writer carried out the work described in this thesis working on the projects funded jointly by the Department of Environment (DOE) and the British Cement Association (BCA). The writer is grateful to the DOE and the BCA for allowing him to present this work and the BCA research staff for their advice and help in planning the experimental work.

The writer would like to thank his supervisor Professor K S Virdi for his help and advice. The writer would also thank Professor A W Beeby of the University of Leeds and Professor P Regan of the University of Westminster for some thought-provoking discussions on this subject.

The staff of the Pavus Institute Laboratory (Veseli, near Prague) and the structural engineering laboratories at the BCA, Imperial College, the City University and the University of Dundee have helped with the experimental work described in this thesis and the writer acknowledges their enthusiastic assistance with gratitude.

DECLARATION

I grant powers of discretion to the University Librarian to allow this thesis to be copied in whole or in part without further reference to me. This permission covers only single copies made for study purposes, subject to normal conditions of acknowledgement.

ABSTRACT

This report, in its earlier part, reviews some important aspects of research and development in the design of reinforced concrete members against shear. This review includes a study of the background of design method for shear resistance given in the British Standard code of practice and a comparison of this method with the methods recommended by the Eurocode and the American code of practice for concrete structures. Based on this study, the contributions to shear resistance of a member afforded by concrete, the tension steel and the links are identified. The influence of these constituents on the modes of transfer of shear has been investigated, in order to examine the method for estimating the overall shear resistance of the member. A test programme is reported, concerning horizontal steel at the centre of the cross-section as an alternative form of shear reinforcement. Tests on some fifty beam specimens were carried out, allowing for variation in the main parameters; for example, the span of beams, the strength of concrete and the amount of tension steel. Also, some beams did not have any shear reinforcement and some were provided with central bars, some with links and some with the combination of central bar and links. A design method has been derived on the basis of these tests, for estimating the contribution of central steel to the shear resistance of beams. This method has been verified with the help of measurement of stresses in the web steel, using strain gauges fixed on the reinforcement of two of the test beams. A similar design method is proposed for using central steel to enhance the punching shear resistance of slabs, based on the results of tests on fifteen slab specimens, allowing for variations in thickness of slabs, the strength of concrete and the amount of central steel. The design methods for beams and slabs have been examined with the help of a finite element computer program capable of using the non-linear properties of structural materials. Finally, the normal temperature design rules for beams have been modified and a method is proposed for design of beams exposed to high temperatures. This method has been verified on the basis of fire exposure tests on ten beam specimens provided with differing amount and type of web steel and with gauges for measurement of temperatures inside the beams.

LIST OF NOTATIONS

b	width of the cross-section of a beam	(mm)
d	effective depth of the cross-section (measured from the extreme compression fibre to the centroid of the tension reinforcement)	(mm)
f_{cu}	Characteristic cube strength of concrete	(N/mm^2)
f_{ck}	Characteristic cylinder strength of concrete	"
f_{yv}	yield stress for steel reinforcement	"
ϱ	$100A_{st}/bd$, where A_{st} is the amount of tension steel	
A_{sw}	area of cross-section of links	(mm^2)
A_b	area of cross-section of central horizontal bar	"
s	spacing of links along the length of the member	(mm)
s_b	spacing of bars in central mesh in slabs	"
ϱ_b	$100A_b/bd$, for beams and $100A_b/bs_b$ for slabs	
V_D	design shear resistance of a section	(kN)
V_C	contribution of concrete to V_D	"
V_L	contribution of links to V_D	"
V_B	contribution of central bar to V_D	"
a_1	shear span	
a	shear span ratio (a_1/d)	
t	fire exposure time	(minutes)
T	temperature developed (° C) at x mm from the face of the member exposed to fire, corresponding to the fire exposure time "t"	
	b_T, d_T the effective dimensions of the cross-section corresponding to the fire exposure time "t", assuming that the concrete reaching a temperature in excess of 750° C is structurally ineffective.	
f_{cT}	Revised f_{cu} corresponding to the time "t"	(N/mm^2)
f_{yT}	Revised f_{yv} " "	
E_T	Revised E_{st} " "	
	(The suffix "T" is used generally to show the revised dimensions, material strengths and the load carrying capacity of a member after a fire exposure time "t")	

CHAPTER 1
INTRODUCTION

1.1 Development of technology and design methods

The history of concrete[1] has records of its progress from about 5600 BC onwards. The oldest concrete so far discovered was used in floors of dwellings on the banks of the river Danube in central Europe. The technology and construction methods have evolved over the centuries and there are some important landmarks in this development; for example, the use of reinforcement in the first century in Rome and, in the United Kingdom, the invention of Portland Cement in 1824 and the construction of a reinforced concrete bridge in Suffolk in 1870. During the twentieth century, the concrete technology has made a rapid progress, leading to improvements in the strength and performance of concrete.

The progress in concrete technology has promoted research, theoretical as well as experimental, for developing methods for design of reinforced concrete structures. The design methods are aimed at securing the safety of buildings with due regard to the economy of construction, maintaining a balance between the influence of the past experience and the findings of research. The stages of development of the design methods range from permissible stress design up to the limit state design of modern times.

1.2 Role of research in development of design methods

The main reasons for developing design methods by the application of research are found in the basic expectations from engineering. Firstly, an engineer has to have a quantified objective in the form of a specified performance of a building; for example, the load carrying capacity and the serviceability of the structural frame. This makes it essential to have a plan for achieving this objective, in advance of starting the construction. Secondly, such a plan has to be perceptible to his peers and, in more modern times, it has to be documented in a verifiable manner.

The development of design methods is expected to account for the effect of changes in construction practices. For example, some detailing practices have become virtually obsolete for reasons of economy, such as beams with haunches at the supports and bent-up bars as shear reinforcement. Also, the design of structural elements may have to account for steel and concrete with higher strength and performance which may differ from the time when the design rules were formulated. It is necessary, therefore, to examine the design rules from time to time and to revise them with the assistance of research.

The dimensions of structural elements, particularly the flat slabs, are expected to meet the requirements of making the optimum use of space and the economy of construction. Also, the potential of precast concrete elements as transportable products requires the use of slimmer and lighter elements, with adequate load carrying capacity under normal and fire exposure conditions. The dimensions of structural members are often governed by the requirements of provision against shear; for example, thin slabs. The design against shear, therefore, may require special attention for members with dimensions less than those considered as the minimum acceptable according to the earlier practice. Also, the placing of concrete in members with reduced widths requires careful detailing to avoid any congestion of reinforcement at the supports. This could be assisted by consideration of an alternative form of web reinforcement.

Shear failure is brittle and it could occur suddenly, without any perceptible warning. It is essential, therefore, that a safe design provision is made to avoid such a failure. Additionally, as the nature of shear failure is complex, the solution may not meet the precise requirements of a particular interpretation of the problem. The main objective of research should be, therefore, to develop a safe design method for estimating the shear resistance, allowing an extra reserve for an assessed lack of exactness of the model and the complexity of mechanisms such as shear failure. Such a solution should envelop the critical interpretations of the problem, assuming only the justifiable assessment of resistance afforded by the design provision.

1.3 The present position

The design of reinforced concrete members is required to address a number of issues such as; the limited understanding of the mechanical properties of concrete, its non-homogeneous internal structure and the difference in its tensile strength and its compressive strength. These issues have had a greater influence on design rules for shear compared with those for flexure. Analytical methods for flexural design have been developed satisfactorily, while a large proportion of research on shear design has opted for development of empirical methods for predicting shear resistance capacity of beams, based on loads causing failure of test specimens.

With the progress of computer technology, computer programs can be used to evaluate the effects of axial force, bending moment, shear and torsion on members of a structural frame using rules derived from the principles of mathematics, physics and mechanics. It is possible to solve complex frames, three-dimensional as well as plane, for any conceivable combination of loads.

In principle, these analyses are based on compatibility of slopes, deflections and rotations at the joints of structural frames. The modern analyses are able to include the formation of plastic hinges, to match the concepts of limit state philosophy. However, the evaluation of load carrying capacity of the members of the frame is based on the behaviour of members in flexure and the corresponding limit state characteristics of the constituent material of the members.

There are computer programs which can account for the properties of "cracked" sections and which are based on the compatibility of deformation of components of frames. These analyses also concern flexural capacity and not the shear strength of the components of frames. Such computer programs are able to account for a design condition with high temperatures or the effects of a rise in temperature during a certain period of time, in accordance with a time-temperature relationship. This is based on the evaluation of temperature contours in the cross-sections of members of frame and the corresponding change in the strength of concrete or steel. These calculations concern the effect of high temperature on

only the flexural capacities of the members of the frame and they do not account for shear.

1.4 Scope of the project

1.4.1 General plan

It is proposed to develop a method for shear design which could be suitable for use in design of reinforced concrete members subjected to normal as well as fire exposure conditions. The design rules will be based on an examination of the roles of various components; concrete, tension steel and web reinforcement. These rules will generally accord with the principles supporting the design methods given in the current codes of practice, the British Standards and Eurocodes.

For fire exposure conditions, the codes of practice include prescriptive rules which are based on a limited test data. These rules give minimum sizes of members and cover to the reinforcement, appropriate to achieve the required fire resistance rating. However, the rules are not related to the effect of fire exposure on shear resistance of members and the strength of the constituent materials at normal temperatures.

The shear resistance of a reinforced concrete member is expected to decrease as a result of reduction in the strength of its component materials (concrete and steel) under fire exposure conditions. Also, in the case of a member with tension face exposed to fire, the loss of stiffness of the tension steel could result in a reduced resistance to widening of cracks. It is important, therefore, to understand the roles of components of a member in providing the shear resistance at normal temperatures. With this understanding, the reduction in strength of these components can be duly accounted for in the estimate of shear resistance of the member under fire exposure conditions.

It is intended to develop design rules for estimating the safe shear-carrying capacity of a beam exposed to fire for a certain period of time. These rules could be used for estimating the shear resistance and, also, the flexural capacity of a

beam. These rules require a method for estimating the temperatures inside the beam. The rise in temperature in a concrete section, as a response to the external high temperatures, depends on a large number of factors. These factors include the moisture content in the concrete and the chemical composition of the aggregate and cement. Also, the development of temperature in a beam depends on the heating conditions and the heat transfer characteristics of the environment. However, these factors cannot be conveniently evaluated for the purposes of developing a general design rule. It is decided, therefore, to use data based on tests for deriving rules for estimating the temperatures inside a beam exposed to fire for a certain period of time.

It is also intended to look beyond the present practice of providing shear reinforcement in the form of links only. An alternative form of web reinforcement is considered in the form of central bars. A central bar, protected from fire and bonded with the surrounding concrete, could provide a strong core resisting the progress of a shear crack into the compression zone. The central bars could also afford some ductility and reduce the undesirable brittleness of shear failure.

Links are considered unsuitable as shear reinforcement for slabs less than 200 mm deep for anchorage reasons. Such slabs could be reinforced against punching shear using small diameter central bars, which will have dependable bond and anchorage. Although links are commonly used as web reinforcement in beams, central bars could offset some proportion of the links. This combination could ease the congestion of links and improve the detailing of reinforcement.

1.4.2 Outline of the contents of the project

Previous research, which is relevant to the development of shear design under normal temperature conditions, is reviewed in Chapter 2. (The review of previous research, applicable to the design of reinforced concrete beams under fire exposure conditions, is given in Chapter 5.) Two broad categories of research have been examined in Chapter 2; the shear-compression theory and the truss analogy. Chapter 2 also gives a comparison of the methods of shear design recommended in various codes of practice.

Rules for shear design under normal temperature conditions are proposed in Chapter 3. These rules are in harmony with the principles supporting the rules given in the current codes of practice. The rules are based on an examination and understanding of contributions of the constituents of the section; concrete, the tension steel and the web steel. It is proposed that the web steel should be treated as reinforcement for enhancing the shear resistance of a concrete member and not as an independent component of any analogous truss.

Chapter 3 also includes the derivation of design rules for enhancement to the shear resistance afforded by the horizontal steel as web reinforcement. These rules are compatible with the method selected for assessing the other contributions to the shear resistance. The rules are based on a test programme for beams and flat slabs carried out during the past four years.

A non-linear finite element computer program is used for examination of the design rules as shown in Chapter 4.

Chapter 5 gives a brief review of previous research and a report on tests on beams exposed to fire. The test results are compared with the estimates of shear resistance given by the proposed design method. The design method is also shown to be applicable for estimating flexural capacity of beams at elevated temperatures, using test results from previous research. A LOTUS Spreadsheet computer program is used to demonstrate the potential use of the method. A similar method could be developed for assessment of the punching shear capacity of flat slabs under fire exposure conditions. However, tests for validation of such a rule could not be accommodated in this project.

Chapter 6 gives an overall summary and the conclusions. Also, some important topics for research have been identified in Chapter 6, which could not be accommodated in this project.

CHAPTER 2

REVIEW OF PREVIOUS RESEARCH ON REINFORCED CONCRETE DESIGN AT NORMAL TEMPERATURES

2.1 Introduction

During the past hundred years, the methods of design of reinforced concrete structures have been reviewed and improved through research, using analytical as well as experimental techniques. A significant proportion of research on shear design, however, has opted for development of empirical rules for estimating the shear resistance. These rules are supported by a large number of tests on beams and slabs, using a number of parameters. However, these empirical rules could not be verified satisfactorily, using a theoretical approach.

Figure 2.1 shows two load cases, the first being that of a load directly over the support resulting mainly in direct compression. In the second case, the load is at mid-span and the resulting flexure in the mid-span region is resisted by a couple, provided by tension in the bottom steel and compressive stresses in the top half of the beam giving smooth trajectories of stresses. The beam could fail if the magnitude of the load exceeds a certain critical limit and resulting failure mechanism in these two cases has been sufficiently investigated. But, in contrast, the stresses at a location in the vicinity of the support could reach a disturbed state when a critical load is applied in the span of a beam with certain depth and at a certain critical distance from the support. Here, the stress distribution is different compared with the flexural stress distribution. The mode of failure in this region is generally known as the diagonal shear failure and it has not been analytically explained to any degree of satisfaction, despite several decades of study.

It is generally agreed that, when a certain load is applied, a beam will fail in shear only if the shear cracks form. The reactive mechanism within the structure of a beam, which resists the applied shear, has been viewed differently by different researchers. The two main categories are commonly known as the truss analogy and the shear-compression theory.

2.2 The initial concepts of design against shear

2.2.1 Mörsch truss analogy

Mörsch truss analogy was introduced in about 1903[2] and it was aimed at estimating the shear resistance of a concrete section. If the applied shear exceeded the shear resistance of concrete, the early classical Mörsch truss analogy method required provision of shear reinforcement in the form of links for the entire applied shear.

Mörsch assumed an elastic behaviour of concrete in compression and no tensile stresses in the concrete between the neutral axis and the tension steel. As shown in figure 2.2, a triangular shape of flexural compressive stress block was assumed and the shear stress variation was parabolic above the neutral axis (d_n). Below the neutral axis, there was no variation in the flexural stresses and, therefore, the shear stress was constant. With these assumptions, it seemed that a large part of the shear was carried by the cracked portion of the beam below the neutral axis. The limiting shear stress was expressed as a fraction of its compressive strength.

If the applied shear exceeded the shear resistance capacity of concrete, the beam was treated as a cracked beam, acting like a truss with the compression block and the tension steel as the two chords. The diagonal compression struts, inclined at 45°, were provided by concrete strips in between the cracks and the vertical links provided the tension members. (Figure 2.3). The entire applied shear was carried by the tension in the links subjected to a permissible tensile stress, a fraction of the yield stress of steel.

2.2.2 Developments following the Mörsch truss analogy

Mörsch[3] commented in 1922 that it was not possible to carry out a mathematical evaluation of the slope of shear cracks, which determined the inclination of concrete struts. He accepted the value of 45° for this slope and arrived at the usual calculation for links, 45° being an assumption as unfavourable

as possible for all practical purposes.

It was recognised in 1907 by Talbot[4] that the shear strength depended on a the strength of concrete, the tension reinforcement and the length of beam. He concluded that the stirrups did not actually develop stresses as high as predicted by the 45° truss analogy. He deduced, therefore, that part of the shear force must be carried by concrete. Similar observations were made by Richard[5] in 1927.

Following the initial development of truss analogy, the research reported in the following sections comes under two broad categories; the shear-compression theory and the modified truss analogy.

2.3 Combined consideration of shear and bending

2.3.1 Tooth model

This model was developed by Kani[6, 7] during the 1960's. Kani's concept was based on the idealisation of the flexural shear failure mechanism as the breaking off of a concrete tooth between two flexural cracks. Kani looked upon a concrete beam with cracks as being comparable to a comb, the "teeth" being the segments of concrete between the cracks and the spine being the uncracked compression zone.

The tension steel was at the lower edge of a tooth. The tooth was subjected to bending due to the action of a load at this level, produced by the difference in tensile steel force between the two faces of the tooth and the bond between tension steel and the concrete. The tensile steel force varied linearly from zero at the support to the maximum where the bending moment applied to the beam was the greatest, generally at the point of application of the load (Figure 2.4). Failure of the beam was caused by the flexural failure of teeth and a long beam would fail immediately if the teeth broke. A short beam, however, would carry on supporting the load by acting as a tied arch with the tension steel providing the tie.

Kani produced two relations which showed that the shear strength

interacted with "shear span", as shown by the tests. (Figure 2.5) The line showing capacity of teeth assumes linear variation of the applied "bond force load". The line representing the arch action strength was derived from a geometrical consideration that the beam strength was a function of the compression block at the load point. The depth of the compression block was taken as "y_o" initially from consideration of flexure. As shown in figure 2.6 and in figure 3.1 of Chapter 3, the compressive trajectories lie within a certain zone converging at a point "O". As the beam cracks along the directions of these trajectories, concrete strips form and lose their support. They virtually "peel" away from the load outwards until a strip finds an unyielding support. Thus, the depth of compressive zone reduces from y_o to y. The ratio of arch strength to the beam flexural strength was y/y_o , which, in its turn, was a function of the shear span ratio. Kani used this approach to obtain the ratio of the ultimate bending resistance (M_u) and the theoretical flexural capacity (M_{fl}).(Figure 2.6)

Kani ignored the presence of shear forces on the concrete teeth. For particular dimensions of tooth taken from tests, he plotted the curves shown in figure 2.5, analyzing the tooth-section at the top of only the vertical faces of the crack (Figure 2.7). He assumed that this tooth-section was critical for considering the failure of a tooth since the cracks extended and became inclined only when the arch action started. Additionally, Kani did not consider the effects of dowel action and aggregate interlock across the crack. (These modes of shear transfer will be discussed in section 2.5.)

Fenwick[8] did research on beams without web reinforcement and generally agreed with Kani's approach. He, however, considered the full "cantilever" length of the teeth and estimated the aggregate interlock and dowel force contribution. He considered that the "bond force moment" was resisted by a combination of the couples provided by the reactive forces developed in concrete. The contribution of the reactions (V_{1A} and V_{1B}) at the head of the tooth was 20%. The contributions of the reactions provided by the dowel action (V_{2A} and V_{2B}) and aggregate interlock (V_{3A} and V_{3B}) were 20% and 60% respectively. (Figure 2.8)

Remarkably, researchers who have worked on the effects of aggregate

interlock and dowel action have found that Kani's graphs, based on theoretical results which exclude these aspects (Figure 2.5), nevertheless correspond closely with the graphs in figure 2.9 summarising the test results.

This is a case of two mutually compensating factors in Kani's analysis; omission of the transfer of shear through aggregate interlock and the dowel action, balanced by a less onerous consideration of vertical face of the "tooth". However, Kani's analysis illustrates the importance of the basic concept of associating shear failure with the reduction in the depth of compression block. Kani's analysis also shows that it is possible to arrive at a design rule for estimating the shear resistance without quantifying the effects of the individual shear transfer mechanisms.

2.3.2 Shear-compression theory

This approach has been described in the report published in 1969 by the Institution of Structural Engineers[9]. Generally, this approach concerns the condition of a beam after a shear crack has formed and a further increase in the applied load has caused dowel failure of the tension steel. At this stage, the beam is looked upon as a tied arch and the external load is assumed to be supported by an inclined compression force in the compression block above the tip of the shear crack. (Figure 2.10) The horizontal component of this force "C" is balanced by the tension in the steel. The "dowel action" of the tension steel is ignored and the tension steel is assumed to be anchored sufficiently to support the tie action.

The beam is able to carry the applied load if there are adequate reactive forces to sustain the ultimate bending moment "m_s", taken about the point of intersection of the applied load and the axis of the tension steel. (Figure 2.10) The basic simplified equation is given as follows:

$$m_s = Q_{ult}(ad)$$

$$= C \times (1 - 0.375n_1)d + A_{sw} f_{yv} c^2/2s$$

where

Q_{ult} = ultimate applied shear force

C	=	$0.67f_{ck}$ x $(n_1)bd$ ($0.67f_{ck}$ is the average longitudinal compressive stress in compression zone at failure[9])
n_1d	=	depth of compression block above the tip of a shear crack
a	=	M/Qd, shear span ratio ("ad" is the ratio of the bending moment (M) to the shear force (Q). For a point load, it is the distance between the point of application of the load and the support.)
c	=	horizontal projection of the crack-length

The theoretical evaluation of n_1 required calculation of the neutral axis depth before the onset of action of shear and an evaluation of crack length, for a certain shear span ratio and an amount of tension steel. The IStructE report[9, p 74] commented that the use of shear span ratio in the calculation of n_1 would present problems related to the effects of continuity of a beam over supports. For calculating the shear span ratio for a continuous beam or for a beam with rigid connection with a column, it would be necessary to assume a distribution of moments using elastic analysis. However, this distribution would be unlikely to correspond to the actual distribution of moments at failure. Hence, the value of (M/Qd) used in the calculation of n_1 would be incorrect and this could undermine the basis of design.

Although this theory did not lead directly to any practical design method, it established some basic principles; for example, association of shear failure with the reduction in the depth of compression block to a fraction of its value before the onset of shear, influence of tension reinforcement on the shear-carrying capacity of a member, etc. These topics will be discussed in details in Chapter 3.

2.3.3 Semi-empirical solutions influenced by shear-compression theory

Placas and Regan[10] discussed two primary modes of shear failure:

i) Compression failure in the concrete caused by an excessive bending moment (m_s, defined in the previous paragraph) and a critical reduction in the depth of compression block and

ii) "shearing" involving mainly vertical displacements, when the applied shear

exceeds the sum of the contribution to shear resistance of the compression block concrete, aggregate interlock and the force in the shear reinforcement crossing the crack.

(The authors believed that the dowel action of the tension steel could be neglected when considering the shear resistance of beams provided with links. Such interaction of links and tension steel and the modes of shear transfer will be discussed in paragraph 2.5.)

The authors gave the following semi-empirical rule for shear cracking resistance (V_{cr}, in psi units) for beams without web reinforcement:

$$V_{cr} = 8(f_{ck}\rho)^{1/3} bd \leq 12(f_{ck})^{1/3} bd \quad \ldots \quad 2.3.1$$

Placas and Regan proposed that both the aggregate interlock and the dowel forces could be accounted for in an equation containing strength of concrete and the percentage of tension reinforcement ϱ, with an empirically adjusted constant.

In equation 2.3.1 the constant "8" was evaluated on the basis of tests. With this value, it was considered that the aggregate interlock and the dowel action effects could be accounted for, without any need for an explicit and separate quantification of these mechanisms.

Additionally, the links would have influence on aggregate interlock and, even more substantially, on the dowel action. This should make an explicit evaluation of aggregate interlock and dowel action very complex, as structural beams would invariably have links. The same is true for slabs, as the transverse reinforcement provides an influence on the dowel action, comparable to that of links in case of beams.

Zsutty[11] proposed the following empirical rule for shear cracking resistance (V_{cr}, in psi units) for beams without web reinforcement:

$$V_{cr} = 60\left(\frac{f_{ck}\rho}{100\,a}\right)^{1/3} bd \quad \ldots \quad 2.3.2$$

Zsutty's rule agrees with equation 2.3.1 when the value of shear-span ratio

"a" is 4.22 and, for a value of "a" of 2.5, it gives an estimate of V_{cr} 20% higher than that given by equation 2.3.1. In other words, Regan's equation 2.3.1 does not include the shear-span ratio but, in comparison with equation 2.3.2, it affords 20% extra reserve for the critical case of shear-span ratio of 2.5. Equation 2.3.1 resembles the rule for design concrete shear stress given in the current British Standard, which also excludes the shear-span ratio. This rule will be examined in paragraph 2.7.

2.4 Modified truss analogies

2.4.1 Stuttgart tests

A detailed test programme was carried out during the period 1961-63 at the University of Stuttgart. The report and results of this programme were published in seven parts by Leonhardt and Walther[12]. Leonhardt has reported on some selected topics of this programme, suggesting a method for reducing shear reinforcement[13], and recorded the following important conclusions:

i) The most unfavourable shear condition is given by one or two concentrated loads per span with a moment/shear ratio between 2.4 and 3.5. All other load patterns can be considerably more favourable.

ii) The tensile stresses in links are less than those calculated according to the Mörsch truss analogy. (f_v as shown in figure 2.11)

Leonhardt described the requirement of web reinforcement according to the traditional 45° truss as "full shear coverage". Figure 2.12 shows a diagrammatical plot of the stress f_{v1} in links observed in the tests, as a function of load (P) plotted on the X-axis. The graph also shows f_v , the stress in links given by the Mörsch truss analogy, which is calculated as follows:

$$f_v = v/r$$

where

$v = V/(b'jd)$

V = the total applied shear force

b' = width of the beam

jd = lever arm of the section

r = A_{sw} /b's

The line representing f_{v1} runs almost parallel to that representing f_v or "the full shear coverage", giving an offset on the X-axis. Leonhardt proposed that the X-axis offset is defined as "P_{crack}" or V_1 under which a shear crack reaches the link. V_1 represents the portion of total shear (V) carried by the compression members of the truss and it is represented by a stress "v_1" (V_1/b'jd) which is related linearly to the compressive strength f_{ck} (cylinder strength). Leonhardt deduced the following rule and proposed the following empirical values for v_1.

$f_{v1} = (v - v_1)/r$

$v_1 = (1/16)\ f_{ck}$ [for single-span beams]

$v_1 = (1/22)\ f_{ck}$ [for continuous beams]

Leonhardt has suggested that the shear reinforcement can be reduced subject to the following main conditions:

i) closely spaced links in preference to bent-up bars; the spacing should decrease with increasing values of shear stress from 1/2 to 1/6 of the overall depth.

ii) curtailment and proper anchorage of the tension steel to account for the increase in the tie force corresponding to the component of increased strut force.

Leonhardt's improved truss model is reflected in the rules given in the CEB code**[31]** and more recently, the "variable strut inclination method" given in Eurocode EC2**[30]** which will be discussed later in this chapter.

2.4.2 Moosecker's model

Further improvement in truss model is seen in the statically indeterminate truss shown in figure 2.13, as proposed by Moosecker**[14]**. He used an iterative

process, considering the bending stiffness of the compression chord. The depth of the compression chord was also determined using an iterative process, starting with the depth corresponding to flexure and then reducing it if the tensile stress at the top of the crack exceeded the tensile strength of concrete. Moosecker carried out a statistical analysis of 145 tests, to confirm the validity of this model.

2.4.3 Compression field theory

(Truss analogy with compatibility conditions for strains)

Collins' compression field theory[15] considers equilibrium of average stresses and a compatibility of average strains in the diagonal compression struts and the transverse and longitudinal steel members. The theory, in its simplified form , assumes that the longitudinal steel is placed symmetrically, the web steel is vertical and the effect of bending moment can be ignored.

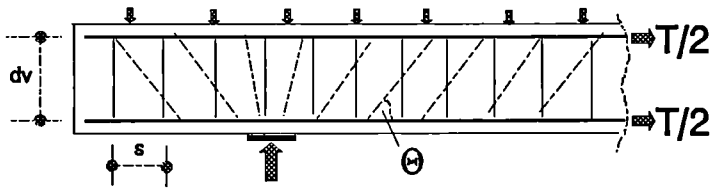

Sketch 2.4 : Compression field theory model of beam

The shear force (V) is resisted by the vertical component of the diagonal compression in the field or a series of struts inclined at an angle θ with the horizontal, formed in the concrete web of the beam. With b_v as the effective web width and d_v as the effective shear depth, the diagonal compressive stress (f_d) is given by:

$$f_d = \frac{V}{b_v\, d_v \sin\theta \cos\theta}$$

The horizontal component of the compression in struts is balanced by the tension in transverse steel, to satisfy the condition of equilibrium of longitudinal

forces at "Zero moment" section.

$$T = \frac{V}{\tan\theta}$$

The equilibrium of transverse forces is provided by tension in the links with tensile stress f_v and area A_{sw}.

$$\frac{A_{sw} f_v d_v}{s} = V \tan\theta$$

The angle θ is given by the following compatibility relationship between strains; ϵ_l (longitudinal tensile strain), ϵ_t (transverse tensile strain) and ϵ_d (diagonal compressive strain).

$$\tan^2\theta = \frac{\epsilon_l + \epsilon_d}{\epsilon_t + \epsilon_d}$$

The compressive stress f_d in concrete is limited to a maximum of f_{du}. Since the corresponding strains are average strains in a cracked section, this limit could not be the same as the cylinder strength (f_{ck}) and Collins proposed the following rule:

$$f_{du} = \frac{5.5 f_{ck}}{4 + \frac{\gamma_m}{\epsilon_d}}$$

$\gamma_m = (2\epsilon_d + \epsilon_l + \epsilon_t)$
(ϵ_d at failure is taken as 0.002)

With the knowledge of stress-strain relationship, failure criteria of materials and on the basis of equilibrium and compatibility conditions, the behaviour of a beam can be studied from an initial stage to its failure. The angle θ is determined by trial and error until the equilibrium and compatibility conditions are satisfied for an initially assumed value of shear stress and working out the corresponding stresses and strains. Finally, shear failure will occur when the diagonal compressive stress f_d reaches the maximum permissible value of f_{du} .

2.4.4 Modified Compression Field Theory

The compression field theory assumed that, after cracking, the concrete cannot resist any tensile stresses. This limitation was removed and the theory was modified and improved by Vecchio and Collins[16] in the following aspects:

i) consideration of the presence of tensile stresses between cracks;
ii) treatment of the principal compressive stress as a function of compressive strain and the corresponding tensile strain.
iii) assumption that the concrete and the steel are perfectly bonded together at the boundaries of the elements (i.e., no overall slip) and the strain in concrete is equal to that in the steel;
iv) assumption that the principal strain axis is coincidental with the principal stress axis;
v) evaluation of the relationship of both tensile and compressive stresses with the corresponding strains; and
vi) inclination of the compressive fields as a function of the longitudinal, diagonal and transverse strains in the concrete.

2.4.5 A brief summary of the Unified Theory Models[17]

A simultaneous consideration of axial forces, bending, shear and torsion could be vital for designing the walls and shells of structures, such as those of submerged containers, offshore platforms and nuclear container vessels. A combined application of these actions on a two-dimensional element produces an important state of stress known as the membrane stress. Hsu[17] has described this two-dimensional element as the membrane element, which forms the basic building block of a large variety of structures made of walls and shells. Using the information given by Hsu, a rational analysis and design of such structures could be carried out to meet the fundamental compliance criteria: stress equilibrium, strain compatibility and the constitutive laws of mechanics of materials (steel and concrete). Hsu has described the application of various unified theory models to the design of reinforced concrete members. Some of these models are generally similar to those which have been dealt with earlier in paragraphs 2.4.3 and 2.4.4. A summary of two other models is given in paragraphs 2.4.5.1 and 2.4.5.2.

2.4.5.1 Strut-and-tie model

This model could be particularly useful for designing knee-joints of a portal frame, corbels, openings in beams, articulated or halved joints, etc. In these regions, there is a static or geometric discontinuity and the stresses and strains are too disturbed and too irregular to be treated mathematically. These regions are known as D regions, to draw attention to the disturbed state of stresses and strains and discontinuous nature of the region. In such cases, application of the compatibility conditions is not feasible. In the design of members in such local or D regions, the stresses are usually determined by only the equilibrium conditions and the strain conditions are ignored.

The strut-and-tie model is based on arranging struts and ties within the member (Figure 2.14) in such a way that the internal forces are in equilibrium with the boundary forces. This technique is very well illustrated by Schlaich et al[18] who give many examples of the application of this model. For structural design of special importance, use of this model for local regions could be supplemented by complex Finite Element Methods, to achieve compatibility conditions as well as equilibrium conditions.

This model is suitable for estimating shear resistance as well as flexural resistance as shown in figure 2.14. The model combines the contribution of diagonal concrete struts as well as the vertical tension in links for resistance to shear. The inclination of concrete compression struts is α, the same as the angle assumed to be made by the inclined cracks with respect to the longitudinal axis of the beam. If d_v is the lever arm of the truss, each cell of the truss will have a horizontal dimension of $d_v \cot\alpha$, except for the end cell, which will have half this dimension.

For the design of compression struts and checking the acceptability of its dimensions, uniaxial concrete strength could be used as the criterion, with due regard to the stress conditions and steel anchorage requirement at the nodes where the struts and ties intersect. Although there are general recommendations for the selection and the proportioning of the struts and ties, there are no definite

objective criteria for this task. Also, forces in every strut and tie must be calculated and proportioned for each load combination and a different set of internal forces and member sizes may be necessary for each of them. This model, therefore, is difficult to use in the actual design of main regions.

This model has been refined with considerable research, resulting in an improved understanding of shear flow, the behaviour of the nodes and sizing the dimensions of the struts and ties.

2.4.5.2 Softened Truss Model

As opposed to the prediction of a linear behaviour of membrane element corresponding to Hooke's law for concrete and steel, this model employs the actual stress-strain relationship for the materials. For concrete, the stress-strain curve has two characteristics: first, it is non-linear and second, as a result of cracking, the compression in concrete is "softened", apparently due to the diagonal shear cracking of concrete caused by the tensile stresses.

This model uses the softened biaxial constitutive law of concrete. Figure 2.15 shows the shape of compressive stress-strain curve for concrete. According to Hsu, the softening effect of concrete is represented by a "softening coefficient", which must be a function of the most important measure of the severity of cracking, considered to be the tensile strain in concrete in the direction normal to the diagonal compression. To a lesser extent, this softening coefficient is also a function of the diagonal compressive strain in the concrete.

This model can predict shear and torsional strengths, as well as the corresponding load-deformation behaviour of a structure throughout its post-cracking loading history. Hsu has proposed a number of simplifications to the theoretical use of the models, subject to certain limitations. However, he has recommended that these simplifications should be used only by designers who know the subject, in order to avoid unsafe solutions through incorrect applications.

2.4.6 Conclusions based on the review of truss analogies

The early truss analogy has been known to give grossly conservative design requirements. Leonhardt showed that it was an oversimplification and he proposed an improved truss model leading to a reduction in shear reinforcement. This model, however, does not account for the modes of shear transfer, which were identified in section 2.3, and roles of constituents of a member (concrete, tension steel and the web steel) in contributing to these transfers of shear, as described in the next section.

The scope for the application of the modified compression field theory to practical design is limited to the regions of a member where stress trajectories are parallel and the shear distribution is uniform. The Canadian Code (1984)**[19]** has used it with substantial approximations. The angle of inclination of the compression field is prescribed to be constant for the span of the beam. Also, the longitudinal and transverse strains are prescribed to be 0.002. For the reasons explained in paragraph 2.4.5.1, the D-region design is excluded and a strut-and-tie method is recommended for such regions.

The strut-and-tie method has its limitations as it complies only with equilibrium condition and, where necessary, supplementary calculations are needed for considerations of the compatibility conditions. It is recommended that an understanding of the stress flows, the bond between the steel and concrete and the steel anchorage requirements in a local region may help to improve serviceability and to prevent undesirable and premature failures. A good design for a local region, therefore, depends largely on the skills and experience of the engineer, since the application of the strut-and-tie model by itself does not cover these points.

It is concluded that these and the other models proposed by Hsu could serve specific design requirements when used with care. However, they could not lead to a design method for general use or for arriving at a solution for the shear resistance of concrete suitable for common structural design.

2.5 The modes of shear transfer

2.5.1 Introduction

In section 2.3, a reference was made to the shear transfer modes for a beam without web reinforcement. These modes are illustrated diagrammatically in figure 2.16; V_{cb} , V_d and V_a being the contributions of the compression block concrete, the dowel action of tension steel and the aggregate interlock respectively. The following paragraphs give a brief summary of research on estimating their relative magnitudes.

The aggregate interlock is the resistance to slippage, attributed to friction along the crack. This friction is generated after the crack is initiated by an applied shear exceeding the shear cracking load. The contribution of this mode of transfer of shear depends on the compressive strength of concrete and the size of the aggregates which are looked upon as rigid spheres distributed and embedded to various depths within the cement matrix[20]. The shear force is resisted by a combination of crushing and sliding of the rigid spheres into and over the softer cement matrix. This mode of shear transfer is believed to interact and develop along with the dowel action of tension steel up to certain stage.

The contribution of dowel action to the shear resistance of a beam is mobilised when the shear crack crosses the tension steel. As the shear force increases, the diagonal crack opens up. This action of the increasing shear force produces tensile stresses in concrete surrounding the tension steel and an increase in the dowel force. This combination produces splitting cracks in concrete along the line of the tension steel and a reduction in the bond between concrete and the steel. This triggers redistribution of stresses as the stiffness of the dowel bar and the surrounding concrete is rapidly lost. This loss of dowel stiffness reduces the resistance afforded by the dowel to the rotation of beam segments on either side of the crack. The dowel splitting is accelerated as the initial crack opens up with further increase in shear, leading to the final failure.

2.5.2 Taylor's research on the modes of shear transfer

2.5.2.1 Compression zone[21]

Taylor initially sought to evaluate the shear carried by the compression zone concrete and reported tests on rectangular beams 203 x 406 mm deep with 1.03% tension steel. Beams 7, 8 and 9 had shear spans of 860 mm, 1170 mm and 1470 mm or shear span ratios of 2.32, 3.16 and 3.99 respectively. An additional beam 10 was the same as beam 9, but with 150 mm deep vertical cracks at 150 mm centres, as shown in figure 2.17. The cracks were formed using 0.5 mm thick aluminium alloy crack-formers.

The beams had strain measurement gauges at locations as shown in figure 2.17. The measured strains were multiplied by the Elastic Modulus of concrete, $4.5\sqrt{U_w} \times 10^3$, for obtaining the direct stress distribution. U_w was the 150 mm cube strength of the concrete at the time of the corresponding test.

A computer program was used for calculating the shear stresses at each gauge location and an initial input was the slope of the longitudinal stress-moment curve, obtained from the longitudinal strain measurements. The shear stress (τ_{xy}) was taken to be a function of the longitudinal stress (σ_x) in the compression block (with linear variation of stress), using the following standard relationship.

$$(\tau_{xy})_y = \int_0^y \frac{\partial (\sigma_x)_y}{\partial x} \, dy$$

The applied shear (V) was assumed to be carried by a combination of the compression zone shear (V_{cb}) and V_2 , the sum of aggregate interlock and dowel action combined together ($V_a + V_d$). This established the equilibrium of vertical forces. Taylor used the principles of shear-compression theory for establishing the equilibrium of moments. The externally applied moment, M, ($M = Vad_t$) was counteracted by the couple provided by the internal reactions, about the point of intersection of the horizontal centre line of tension steel with the vertical line of application of the load. (Figure 2.18)

$$M = C\left(d_1 - \frac{d_n}{3}\right) + V_2 s \quad \ldots \quad 2.5.1$$

where

C = compression zone force

V_2 = $V_a + V_d$

d_1 = effective depth

d_n = depth of compression zone evaluated by computer program at each load stage

Initially, the line of action of V_2 was taken as shown in figure 2.18. The integral of the computed shear stress at each gauge location gave the shear force (V_{cb}) carried by the compression zone. The computer calculation of the shear stress, which led to the evaluation of V_{cb}, was developed with the use of equation 2.5.1 and it needed an estimate of a value for V_2 , so that the resulting V_{cb} was equal to (V - V_2). For this purpose, V_2 was initially provided as 0.2V and increased progressively in steps of 0.1V, until the computer programme evaluated V_{cb} close to (V - V_2), within 0.01V. The line of action of V_2, assumed initially as shown in figure 2.18, was modified to take account of the expected value of V_2, simultaneously satisfying the compatibility between the applied bending moment and the resisting moment and the equilibrium of vertical forces.

Taylor had also taken measurements of vertical and horizontal displacements at the cracks (ΔV and ΔH respectively) using rosettes, for the purposes of aggregate interlock study as described in paragraph 2.5.2.2 below. These rosettes were put on the beam as soon as the first sign of a flexural crack was observed, at a horizontal distance δH and at a vertical distance δV from the tip of the crack. (Figure 2.19) This was successful in case of beams where the selected crack extended as expected. In other cases, alternative cracks developed and the selected crack did not extend.

Taylor made an important observation that the compression block depth reduced with the increasing influence of shear, which will be discussed in chapter 3. This depth, or the neutral axis depth at a section, was taken as a function of the

moment and the distance of the section from the end of the beam. At the point of application of load, the initial neutral axis depths under the action of 20-25% of the failure load were 195 mm for beams 7, 8 and 9 and 135 mm for beam 10.

The final depths of compression block (d_n) were nearly 50% of their initial values. Table 2.5.1 shows V_{cb} related to V, the applied shear, for all the beams. For beam 8, d_n (112 mm*) is related to an applied shear of 75.5 kN and not 106.8 kN which is the shear at failure. This was due to some problem with the recording using a logger and measurement during the last stages of application of load. For beams 7, 9 and 10, table 2.5.1 shows d_n related to V, the shear at failure.

The test on beam 10 with pre-formed cracks was carried out mainly for comparison purposes. The total shear carried by this beam was quoted by Taylor as 75% of the corresponding beam 9 without the cracks. Taylor attributed this reduction to the non-availability of aggregate interlock over 45% of the crack depth in case of beam 10. However, beam 10 had a lower cube strength, 49.5 N/mm^2 compared with 60 N/mm^2 for beam 9. For comparison between the failure loads for beams 10 and 9, account should have been taken of their concrete strengths. The failure load for beam 9, 89 kN, should have been converted into an equivalent failure load, by using the ratio of cube-root of the concrete strength of beam 10 to that of beam 9. (BS8110 rule, section 2.7) The true comparison, therefore, is that the failure load for beam 10 was 71 kN, 85% of the equivalent failure load 83.5 kN $[89x(49.5/60)^{0.33}]$ for beam 9 and not 75% as Taylor has suggested.

Table 2.5.1: Depth of Compression Block (d_n) and its contribution to the Shear Resistance

Beam no	f_{cu} N/mm^2	V kN	d_n mm	V_{cb} kN	% V_{cb}
7	57.5	75.6	102	29.8	39 %
8	57.5	106.8	112*	24.4	23 %
9	60.0	89.0	107	34.2	38 %
10	49.5	71.0	69	25.3	37 %

(* This reading corresponds to V = 75.5 kN, and not 106.8 kN.)

2.5.2.2 Aggregate interlock[22]

Taylor carried out two types of tests. The first type concerned tests on interlock independent of a beam environment. The second type concerned tests for confirming the presence of such interlock forces in a beam, with sufficient instrumentation to enable assessment of the forces.

For the first type, Taylor used a "block-test" rig (Figure 2.20) for displacement-controlled tests. This rig was used to measure displacements normal to the induced crack and shear displacements across the induced crack, ΔN and ΔS respectively. The effect of the following variables was studied in a total of 35 tests:

i) $\Delta N/\Delta S$: displacement ratio
ii) concrete strength
iii) aggregate size
iv) aggregate type (eg, gravel and limestone)

The shear stress (f_S) and the normal stress(f_N) produced by aggregate interlock were derived from the strain measurements. f_{Su} and f_{Nu} were the ultimate values of these stresses.

For the second type of testing, beam specimens 150 x 300 mm deep without web reinforcement and with preformed cracks and notches were used as shown in figure 2.21. The notches in these specimens in compression and tension zones were meant to eliminate any shear transfer other than the aggregate interlock. However, certain trials were needed for developing a method to form an induced crack. In the end, results of two of the six beam tests were considered as reliable and satisfactory for comparison with the block tests. (Figure 2.23) Taylor used the results from the block tests for actually evaluating the aggregate interlock contribution.

The relationship between displacements and stresses derived from the block tests was used for calculating the aggregate interlock contribution for beams 7, 8,

9 and 10. The rosette measurements of vertical and horizontal displacements at the cracks (ΔV and ΔH respectively) were used for calculating the equivalent interlock stresses.

2.5.2.3 Dowel action

Taylor carried out tests on scale models to estimate the effect of dowel action mode of shear transfer[23]. Figure 2.22 shows the test arrangement used by Taylor. The specimens were 87 mm deep and the width varied between 450 and 800 mm, but most of the beams were 625 mm wide.

The central part of the specimen was a separate precast element, with a preformed crack separating it from the rest of the beam. A gradually increasing downward force was applied to the precast element, until a splitting crack developed. The force causing the splitting crack and the model displacements were used in relation with the data corresponding to a study of tests on prototype beams, to derive a relative magnitude of dowel action contribution.

It can be argued, however, that the measured quantitative load deformation response of a part-precast composite beam may not represent the complex state of stresses in a beam constructed with in-situ concrete, in the region influenced by dowel splitting. The downward force on the central rigid precast section would induce vertical movement at the steel level. This could not be compared with the deformation corresponding to a rotation about the apex of an inclined shear crack, as described in paragraph 2.5.3 below.

2.5.2.4 Observations on Taylor's work

i) Influence of type of aggregate and the strength of concrete

Block test results showed that the specimens with gravel aggregate performed better than those with limestone and lightweight aggregate. (Figure 2.23). Taylor considered the strength of aggregate and matrix within the concrete as an influential parameter. Although the highest stresses in concrete systems are

in the matrix, the stress concentration caused by the aggregate could make the aggregate-matrix bond critical. Breakdown of this bond may be the cause of shear failure in members made with normal strength concrete.

In fact, this demonstrates the similarity between the action of the aggregate interlock mechanism in inclined cracks and the action of aggregate interlock resisting compressive stresses in a concrete cube. Morrell and Chia[24] have explained that, when a concrete cube specimen is subjected to external loading, the local shear stresses develop in the interfaces between aggregate and the cement paste, causing initial cracks or pre-cracks. The local shear stresses occur as a result of the difference in elastic properties of the two materials and the pre-cracks first appear when the shear stresses exceed the weakest bond strength. This exposes the coarse aggregate and a mechanical interlock occurs, which enables concrete specimens to sustain load after initial pre-cracking.

It can be concluded, therefore, that the parameter "aggregate-matrix bond" governing the cube strength of normal grade concrete (f_{cu}) also controls the aggregate interlock strength (f_{Su}). Also, figure 2.23 shows that the values of f_{Su} increase with increasing f_{cu} , confirming the dependence of aggregate interlock on the strength of concrete.

ii) Relative magnitude of the shear forces in a beam carried by compression zone concrete, aggregate interlock and dowel action

It is apparently impracticable to do a precise evaluation of these individual contributions. The researchers have been able to propose only the relative upper limits or a range of proportions of shear resistance attributable to aggregate interlock and dowel action. In this context, Taylor's estimates for the range of values are examined for some of their details. (Table 2.5.2)

a) Taylor observed that the aggregate interlock mechanism appeared to carry approximately half the applied shear[22]. For beam 7 with shear-span ratio of 2.32, the compression zone contribution (V_{cb}) was nearly 40% of the applied shear (V). This was the case for beams 9 and 10 as well, where the

shear-span ratio was 3.99. For beam 8 with an intermediate shear-span ratio of 3.16, however, the percentage of V_{cb} was 23%. The reduction in V_{cb} could be due to the discontinuity in the recorded strain plot and due to a sudden increase in strain which was noted at an intermediate load stage by Taylor.

b) The individual estimates of the three contributions did not add up to the applied shear level near failure, especially for beam 8 as shown below. Taylor observed that the rosettes could be applied only after the appearance of visual cracks, for measurement of displacement at cracks. The contributions of aggregate interlock (V_a) and dowel action (V_d) derived from these measurements, therefore, could not account for the part which could have been mobilised due to the earlier cracking which was undetectable. Taylor claimed that this may have resulted in an underestimate of the combination ($V_a + V_d$). However, the difference between the applied shear and $\Sigma(V_{cb} + V_a + V_d)$ is more significant for beam 8. This could be attributed to the underestimate of V_{cb} , as discussed in the previous paragraph. V_{cb} and $\Sigma(V_{cb} + V_a + V_d)$ for beam 8 are shown as (**) in table 2.5.2. The details given in table 2.5.2 are extracted from Taylor's graphs[22].

Table 2.5.2: ($V_{cb} + V_a + V_d$) expressed as a percentage of the applied shear for beams 7, 8, 9 & 10

Beam no	V_{cb}	V_a	V_d	$\Sigma (V_{cb} + V_a + V_d)$
7	39%	40%	14%	93%
8	23%**	36%	13%	72%(**)
9	38%	36%	16%	90%
10	37%	31%	20%	88%

Taylor gave an apportionment for V_{cb} , V_a and V_d , the three components of shear resistance of a beam without any web reinforcement, which is unduly influenced by his low estimate of V_{cb} for beam 8. It is submitted that the apportionment should be revised as shown in brackets.

		Taylor's conclusions %	Proposed revision %
Compression zone concrete	:	20 - 40	(40)
Aggregate interlock	:	33 - 50	(60)
Dowel action	:	15 - 25	

2.5.3 Dowel Action research by Chana

Chana[25] has done rigorous work to study the role and importance of dowel action. Using a high-speed tape recorder, he observed that the dowel cracking took place just before the beam failed and he considered it a trigger for shear failure of beams without web reinforcement. He carried out tests to show that links are effective in controlling dowel splitting, not only across the crack but also for some distance away.

Chana observed that the movement of cracked portion of the beam was purely rotational about the apex of the critical crack. This is not in accord with the vertical movement induced at the steel level in Taylor's dowel action model specimens described in paragraph 2.5.2.3. Chana noted that the maximum width of an inclined crack at peak load was 0.25 mm at the base of the crack. An average width of dowel crack, based on readings of dowel gauges placed in some specimens, was 0.08 mm. (Figure 2.24)

2.5.4 Contribution of aggregate interlock and dowel action for beams with links

R N Swamy and A D Andriopoulos[26] reported tests on 87 beam specimens, 75 x 115 mm deep, with and without shear reinforcement. The specimens were provided with gauges to measure strains in tension steel, links and compression block concrete. Longitudinal concrete strains were also measured at various depths along one or two adjacent sections near the head of the diagonal crack. These longitudinal strains were used for assessing the shear carried by the compression block concrete (V_{cb}). The shear carried by links (V_L) was obtained

directly from the strain measurements. The applied shear was (V_u). The sum of the contributions of dowel action (V_d) and aggregate interlock (V_a) was derived as follows:

$$(V_d + V_a) = V_u - (V_{cb} + V_L)$$

The tests demonstrated the influence of various factors on the combination of ($V_d + V_a$) represented by a ratio r_{da} [$r_{da} = (V_d + V_a)/V_u$]. The variations in specimen-types were as follows:

i) concrete strength : 24 to 69 N/mm^2

ii) amount of tension steel : 2% to 4%

iii) shear-span ratio, a : 2 to 6

iv) rf_{yv}, a ratio representing the amount of web reinforcement ($r = A_{sw}/bs$; s = spacing of links) : 0.4 to 8.25

The general conclusions drawn by the authors are briefly given below:

i) The ratio r_{da} decreases linearly with the shear span ratio, a. The rate of decrease is higher for beams with links than beams without links. For example, for the range of "2 < a < 5", r_{da} drops from 0.85 to 0.5 for beams without links. The same reduction for beams with links is from 0.7 to 0.18, for rf_{yv} of 0.3 N/mm^2.

ii) The ratio r_{da} is maximum when there are no links. r_{da} reduces with the increasing amount of links and it reaches a level of about "0.2" when flexural failure occurs with higher amounts of links. This is attributed to transfer of shear from aggregate interlock to the shear carried by links.

iii) For low amounts of links ($rf_{yv} < 0.6$), the ratio r_{da} is higher for specimens with 2% of tension steel than those with 4% of tension steel. For larger amounts of links, the ratio r_{da} is higher for specimens with 4% of tension steel than those with 2% of tension steel, with other parameters (shear span

ratio, concrete strength etc.) remaining the same. This explains the interdependence of V_d and V_a. For higher rf_{yv}, the links take over the aggregate interlock effect. The combination, therefore, is dictated by the amount of tension steel which governs the dowel action component.

2.5.6 Conclusions from the review given in section 2.5

It is not practicable to quantify the separate contribution of aggregate interlock to the shear resistance of a member. Calculation of crack-width and the control of inclined crack widths are not suitable for generalisation and developing practical guidance and design rules. Also, isolated evaluation of this mechanism could become obscured by its interaction with shear reinforcement and dowel action of longitudinal steel.

The dowel action contribution is estimated to be of the order of 15% for beams without links. This contribution is largely dependent on the elastic modulus of steel and the amount of tension steel. These factors also govern the capacity of the concrete section to resist the widening of cracks. However, provision of links could have significant effect on the estimate of dowel action contribution. Chana[25] has demonstrated that the links have an important role in controlling the dowel-action cracking, in addition to their own contribution to the shear resistance. Most structural beams would normally have links to provide this beneficial effect of controlling cracking. Slabs have transverse steel with a similar beneficial effect. It is not practicable, however, to isolate and quantify this beneficial effect.

The major factors governing the contributions of these two modes of shear transfer are the strength of concrete and the tension steel. If a rule for the design shear stress includes these factors, the benefit afforded by these mechanisms can be accounted for by adjusting a constant multiplier in the rule. This will be discussed in chapter 3.

The beneficial effect of aggregate interlock increases with the increase in size of aggregate. The effect of the size of aggregate on aggregate interlock and, hence, on the shear resistance of a member is represented by a multiplier,

commonly known as the "depth factor" which also includes other effects which will be discussed in the section 2.7. If the size of aggregate is the same, the aggregate interlock will have a greater benefit for shallower sections compared with the benefit for deeper sections. The size of coarse aggregate (say 20 mm) is normally the same for different strengths of concrete, used in beams with different depths. An allowance is, therefore, made to the shear strength based purely on the compressive strength of concrete and without any regard to the size of aggregate.

2.6 Background of the current codes of practice

In 1962, a detailed report was published in the American Concrete Institute (ACI) Proceedings[27], which addressed the question of reinforced concrete shear resistance. The ACI Committee, who prepared the report, claimed that some 2500 specimens were tested and over 450 papers were published on this subject in different parts of the world, during the period between 1899 and 1960. The report concluded, however, that:

> "The problems of shear and diagonal tension have not been fundamentally and conclusively solved."

The Committee strongly recommended further research work, not only to explore other areas of the problem, but also to establish a basically rational theory for effects of shear and diagonal tension on the behaviour of reinforced concrete members.

In the United Kingdom, the Institution of Structural Engineers formed a "Shear Study Group"[9] in 1965, under the chairmanship of Professor A L L Baker, with the following terms of reference:

i) To consider the available information on shear in concrete in various scientific papers and foreign codes.

ii) To decide what further tests are required.

iii) To put forward suggestions for a research programme which will eventually enable a relationship to be established between design formulae and the various modes of failure that can occur.

The Group published a report in January 1969 and concluded that it was necessary to review the method for design against shear based on the traditional Mörsch truss analogy. This method was used in CP114, the code of practice which was in use at that time. The Group commented on this method as follows:

i) It was an over-simplification as it was based on the inclination of compression struts and the shear cracks at 45^0;
ii) It gave a poor relationship with test results and it was often grossly conservative;
iii) It ignored the contribution of compression block concrete; and
iv) It predicted the cause of failure to be yielding of links.

The Study Group Report made some recommendations which had a considerable influence on the shear design method in the British Standard CP110[28], which emerged in 1972. This code introduced fundamental changes to the earlier design practice, mainly due to the adoption of Limit State Philosophy. These changes also included a new set of rules for shear resistance, allowing addition of the contribution of concrete to that of links, even when the applied shear exceeded the resistance of concrete on its own.

CP110 was superseded in 1985 by BS8110[29] which has retained the CP110 method in principle. This is also similar in certain aspects to the "Standard Method" in the current draft of Eurocode EC2[30], which itself has been influenced by the CEB code MC78[31]. (This CEB code was revised to MC90[32].) These methods are examined in the following section.

The changes brought about by the introduction of CP110 were not appreciated by some engineers at that time. This was similar to the reactions on the American Concrete Institute Code[33]. In 1984, MacGregor[34] called the shear provision rules in the ACI Code of Practice as "semi-empirical mumbo-jumbo".

In spite of such disparaging general opinions, the problem of shear resistance of reinforced concrete has continued to interest many talented

researchers. On the positive side, it has to be said that "mumbo-jumbo" or otherwise, the design rules in most codes of practice have been supported by a large test database. Within the limitations on their use, they appear to have been satisfactory in meeting the overall objective of avoiding the sudden, brittle and undesirable shear failures.

2.7 General comparison between BS8110, EC2 and ACI codes

2.7.1 Introduction

The design methods in the British Standard BS8110, Eurocode EC2 and the ACI code generally require separate consideration of resistance against bending moment and shear. For estimating the shear resistance of a reinforced concrete member, the BS8110, ACI code and the "standard method" in Eurocode EC2 employ an "addition principle". This principle allows an addition of the contribution of concrete (V_C) and the contribution of links (V_L), to cater for applied shears in excess of V_C.

The evaluation of contribution of the links (V_L) is similar in BS8110 and the "standard method" given in Eurocode EC2. EC2, however, has an alternative method called the "variable strut inclination method" which does not allow any additional contribution of concrete to the shear resistance. This method is based on the assumption of a truss with the compression zone concrete and the tension steel as the parallel chords to resist the bending moment. The shear force in a panel is resisted by the vertical component of web reinforcement as a tension member and a concrete strut as a compression member. For the purposes of this project, only the standard method given in EC2 is used for comparison with BS8110 and the ACI code.

2.7.2 Depth factor

The depth factor is meant to account for the "size effect". It is an empirical multiplier to the nominal shear stress based on the width and depth of the cross-section. Many researchers including Chana[35] and Bazant and Sun[36] have

shown that the shallower beams fail at higher nominal shear stress. The simplest explanation is the enhanced benefit of aggregate interlock afforded to shallower beams, which was noted in section 2.5. There are also two other explanations, concerning beams without web reinforcement.

First, the rate of change of stress across the cross-section or the strain gradient is higher in shallower beams[37]. This causes an enhanced confinement of compression zone concrete resulting in an increase in the tensile strength of concrete in the neutral axis region. The cracking is delayed, therefore, and, hence, an increase in the nominal shear carrying capacity for shallower beams.

Second explanation concerns the fracture energy[36]. In homogeneous but brittle materials, a fracture could occur almost at a point. In contrast, concrete members suffer fracture over a relatively large fracture process zone and the progressive microcracking causes deterioration of the tensile strength. In larger concrete members, the release of strain energy into the cracking zone is greater compared to smaller members and, hence, the nominal shear strength is smaller.

In beams with web reinforcement, it would seem that the size effect caused by confinement resulting from high strain gradients in shallower beams should be mitigated when links are provided. However, Bazant and Sun[36] have demonstrated that the size effect does apply to beams with links, although on a reduced scale.

2.7.3 General rules for the design concrete stress (v_c)

The BS8110 notations are used for terms which have similar meaning in the other codes (v_c , etc), for the sake of a convenient comparison.

a) BS8110

$$v_c = \frac{0.27}{\gamma_m} (\rho f_{cu})^{1/3} \left(\frac{400}{d}\right)^{1/4} \quad N/mm^2 \quad (a \geq 2) \quad \ldots \quad 2.7.1$$

[If "a" is less than 2, v_c is obtained by multiplying the value of v_c given by

equation 2.7.1, by a factor of (2/a).]

$$\rho = 100\frac{A_{st}}{bd} \qquad \leq 3.0$$

f_{cu} $\leq$ 40 N/mm^2

400/d $\geq$ 1.0 (depth factor)

γ_m = 1.25 (partial safety factor for shear strength without shear reinforcement, which differs from γ_m of 1.5 for concrete in flexure or axial load)

BS8110 does not allow the applied shear stress, v, to exceed $0.8(f_{cu})^{0.5}$ or 5 N/mm^2, whichever is the lesser. Beyond this limit, the shear carrying capacity of the member cannot be enhanced with provision of shear reinforcement. This is to ensure a safe limit on the compressive stresses in the web concrete.

b) Eurocode EC2

The EC2 presentation is not the same as that of BS8110. The following equations are adopted from the actual text of EC2, modified for the ease of comparison with BS8110. EC2 requires a designer to compare the applied shear force (V) with the following values of shear resistance.

i) If the applied shear force exceeds V_c (V_{Rd1}, according to EC2 notation), links have to be provided.

$$V_C = \frac{0.0525 f_{ck}^{\frac{2}{3}}}{\gamma_c} \frac{K(1.2 + 0.4\rho)bd}{1000} \quad kN \quad (a \geq 2.5) \quad .. \; 2.7.2$$

[If "a" is less than 2.5, V_c is obtained by multiplying the value of V_c given by equation 2.7.2, by a factor of (2.5/a).]

γ_c = partial factor for concrete = 1.5

f_{ck} $\leq$ 50 N/mm^2 (characteristic cylinder strength of concrete = o.8f_{cu} approximately)

$\rho \leq 2.0$

K = $[(1600 - d)/1000] \geq 1.0$

(K is the depth factor. The value of K is limited to 1.00 only, if more than 50% of the tension reinforcement is curtailed.)

ii) Maximum design shear force, V_{Rd2} , which should not be exceeded irrespective of any provision of shear reinforcement. (This rule corresponds to the BS8110 rule which is meant to ensure a safe limit on the compressive stresses in the web concrete.)

$$V_{Rd2} = 0.5 \frac{f_{ck}}{\gamma_c} (\nu) \frac{0.9bd\ (1 + \cot\alpha)}{1000} \quad kN \quad \ldots \quad 2.7.3$$

$$\nu = (0.7 - \frac{f_{ck}}{200}) \quad \geq 0.5$$

α = angle of inclination of the shear reinforcement with the longitudinal axis (90° for vertical links)

c) ACI Code of practice

ACI code rule includes the terms V_u (the ultimate applied shear) and M_u (the ultimate bending moment). Also, this rule depends on a parameter l_n/d, where l_n is the span of the beam. The formula is written in a form similar to the above formulae, including the strength reduction factor ϕ. (ϕ = 0.85)

$$v_c = 0.134 \sqrt{f_{ck}} + 0.147\rho \frac{V_u\ d}{M_u} \qquad (\frac{l_n}{d} \geq 5.0) \ldots \quad 2.7.4$$

If l_n/d is less than 5, v_c is obtained by multiplying the value of v_c given by equation 2.7.4 by a factor $(3.5 - 2.5M_u/V_ud)$. This enhancement in v_c is limited by limiting the range of values of the factor, so that $1 < (3.5 - 2.5M_u/V_ud) < 2.5$.

2.7.4 Influence of various parameters on v_c

i) The percentage of tension steel

Table 2.7.1 gives a comparison based on the tests carried out by Kim and Park[38] using a range of values of A_{st}. The test specimens included in table 2.7.1 have the following general characteristics:

f_{ck} = 53.7 N/mm2 ($0.8f_{cu}$); a = 3.0 (shear-span ratio); and

v_f = [(failure load)/bd] N/mm^2.

Table 2.7.1 : Effect of percentage of steel on the design shear stress

b x d	$\%A_{st}$	v_f	BS8110 v_c	EC2 v_{Rd1}	ACI v_c
170 x 272	1.09	1.26 1.22	0.99	1.08	1.05
170 x 270	1.87	1.54 1.56	1.19	1.29	1.09
170 x 267	3.35	1.72 1.73	1.40	1.33	1.16
170 x 255	4.68	2.07 2.20	1.42	1.34	1.22
170 x 142	1.87	1.70 1.63	1.40	1.41	1.09
300 x 550	1.87	1.37 1.30	1.08	1.02	1.09
300 x 915	1.87	0.99 1.21	1.08	0.97	1.09

v_f is calculated for both tests on one specimen type. The values of v_c (N/mm^2) are design values inclusive of the appropriate partial factors. In this way, it is possible to account for the large difference in partial factors for strength of materials in the codes; for example, 1.25 in BS8110, 1.5 in EC2 and 1.18 in the ACI code. (inverse of the strength reduction factor, ϕ = 0.85.) The calculations

for v_c also ignore the various limitations on concrete strength. This is necessary for providing a general and equitable comparative study, since it is not intended to carry out an absolute validation of the rules given in the codes of practice.

For the normal levels of tension reinforcement, between 1% to 2%, the rules in all codes seem to give estimates of v_c which accord with the test data.

ii) The strength of concrete

All the three codes include an exponential function of the strength of concrete in the rule giving v_c. In table 2.7.1, the values of v_c are calculated with actual concrete strength, well in excess of the BS8110 limit of f_{cu} (40/N/mm^2). The test results show that these values of v_c are satisfactory.

Clarke[39] tested 12 beams with concrete cube strengths between 83 and 93 N/mm^2, shear span ratio of 3 and tension steel of 1.8 % and 2.6 %. He concluded that the BS8110 rule for v_c could allow for f_{cu} in excess of 40 N/mm^2. The writer believes that this BS8110 limit should be increased to 60 N/mm^2 (to correspond to the EC2 limit of $f_{ck} \leq 50$ N/mm^2) and the maximum applied shear stress "v" should be given as "$v \leq 0.8 f_{cu}^{0.5}$ or 6.2 N/mm^2 , whichever is the lesser".

iii) The shear-span ratio

Table 2.7.2 includes some values from tests on 200 x 300 mm beams which will be reported in chapter 3. It is noted that the estimates given by the BS8110 rule for v_c seem to come closer to the ACI rule predictions for shear-span ratios of 2.6 onwards. This shows that the BS8110 rule covers the critical zone with the shear span ratio of about 2.5, although this ratio is not a part of the formula.

Table 2.7.2: Effect of shear-span ratio on the design shear stress

b x d (% A_{st})	a	v_f	BS8110 v_c	EC2 v_{Rd1}	ACI v_c
170 x 270 (1.87) (f_{ck} = 53.7)	1.50	4.63 4.69	1.59	2.15	2.35
200 x 265 (1.78) (f_{cu} = 27.0)	2.60	1.09 1.13	0.87	0.69	0.73
200 x 265 (1.78) (f_{cu} = 43.0)	4.00	1.31 1.41	1.02	0.94	0.86
170 x 270 (1.87) (f_{ck} = 53.7)	4.50	1.45 1.39	1.19	1.29	1.06
170 x 270 (1.87) (f_{ck} = 53.7)	6.00	1.29 1.33	**	flexural failure	**

2.8 The review of research and the objectives of the project

The review of research in this chapter has revealed a wide range of indicators of shear failures, following Kani's "tooth model" and including the work by Regan, Taylor and others as described above. Some of the important points are as follows:

i) A concentrated load acting at a distance from the support corresponding to a shear span ratio in the region of 2.5, produces the most critical loading condition for shear failure of a beam.

ii) At the stage of reaching the shear failure, the depth of compression block is reduced to about 50% of its value before the onset of shear.

iii) The shear resistance of a member attributable to the concrete section is derived from the modes of shear transfer in the following proportions:

concrete in the compression zone: 40%

aggregate interlock and dowel action: 60%

iv) The constituents of a member (concrete, the tension steel and the web reinforcement) influence the individual modes of shear transfer and the overall shear resistance of the member, but the roles of these constituents are interrelated.

v) The total shear resistance of a member is provided by the sum of the contributions of concrete section and the web reinforcement.

Most of the points listed above have been noted by Regan[40] in his review presented in the "Structural engineer" of October 1993. This paper is considered to be a landmark in the assessment of research work on shear done during the past hundred years and the remarkable work done during the past 30 or 40 years. Regan has pointed out the importance of research on shear resistance under fire exposure conditions, which is an important part of this project and the subject of Chapter 5 of this report.

The study of research on the secondary mechanisms, aggregate interlock and the dowel action, has showed that there is no need for any quantitative evaluation of their contributions. The influence of each constituent of the member on these shear failure mechanisms may change with the change in the provision of web reinforcement and the tension steel, but these changes could be mutually compensating.

Bobrowski[41] has proposed the following plan, with regard to a rational evaluation of the ultimate shear resistance of a reinforced concrete member:

i) Drop the nominal "ultimate" shear stress concept and investigate alternative indicators of shear failure; and

ii) Try an empirical solution based on a sufficient number of parameters and, therefore, a large number of tests.

Bobrowski has commented that the ultimate capacity of a reinforced concrete beam should take account of the proportion of shear and bending moment. However, the comparative study of the rules in the codes of practice has demonstrated that a general rule excluding the parameter "shear-span ratio", for example the BS8110 rule, can provide safe results within its limitations.

The writer agrees with the concept of finding an empirical solution and rules based on a large number of tests, provided that the rules can be checked out using a rigorous analysis. These rules may appear to follow the nominal "ultimate" shear stress concept but they should be broadly derived from the considerations of the critical shear-span ratio, reduction in the depth of compression block due to the action of shear and the roles of constituents of the section. In chapter 3, rules are proposed and examined on this basis.

As discussed in section 2.7, the empirical rules follow an "addition principle". This principle allows an addition of the contribution of concrete and the contribution of the web steel for obtaining the design shear resistance. The truss models, which were reviewed in section 2.4, do not allow such addition of contributions to the shear resistance provided by concrete and the web steel. As described by Hsu **[17]**, these models are incapable of predicting the contribution of concrete because they are based on the assumption that the direction of cracks coincides with the direction of principal stresses and strains in concrete after cracking.

Hsu has observed from test results that the shear strength of membrane elements is made up of two terms, one attributable to steel and the other attributable to concrete, V_c. He has remarked that the existence of the term V_c is apparently caused by the fact that the actual direction of cracks is different from the assumed direction of post-cracking principal stresses and strains. A theoretical approach to account for this actual direction of cracks would require incorporation of the constitutive law relating shear stress to the shear strain in the direction of the cracks. This approach would also require very complex equilibrium and compatibility equations. Hsu has conceded that efficient algorithms to solve the

complex equations are needed before the "contribution of concrete" can be derived mathematically.

Although the design rules proposed in Chapter 3 follow the "addition principle" and they are mainly based on tests, it is decided to provide a cross-check using a non-linear finite element program. In chapter 4, the estimates of shear resistance given by the design rules will be compared with those given by the computer program, to examine the common trends between the two methods.

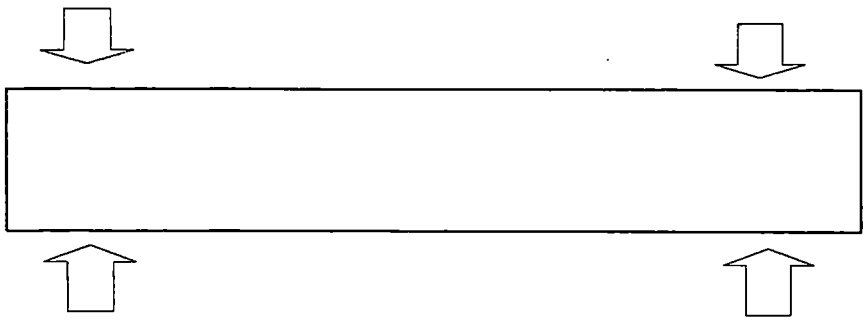

LOADS OVER SUPPORTS

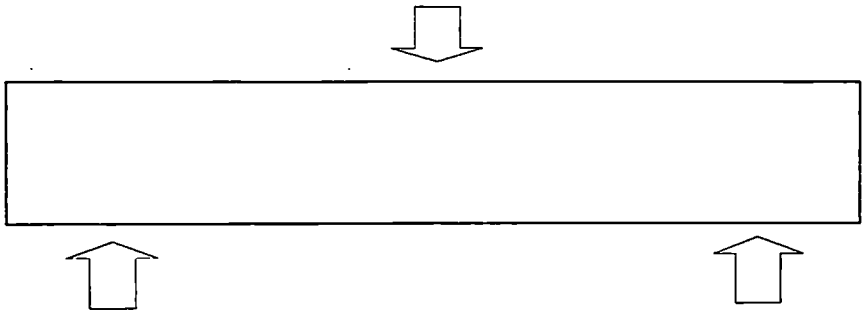

LOAD AT MID-SPAN

SIMPLE LOAD CONDITIONS FOR A BEAM

FIGURE 2.1

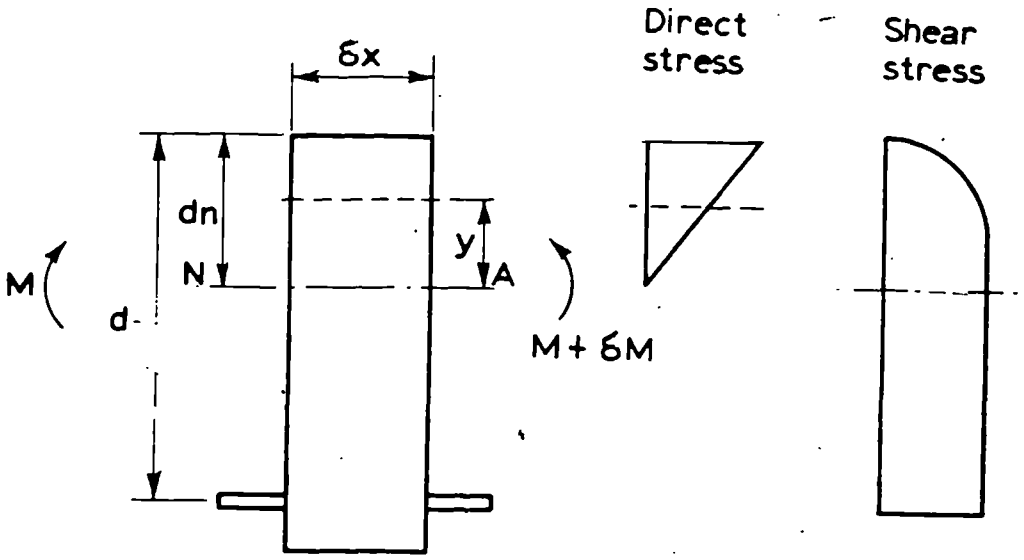

Shear stress distribution in a beam

FIGURE 2.2

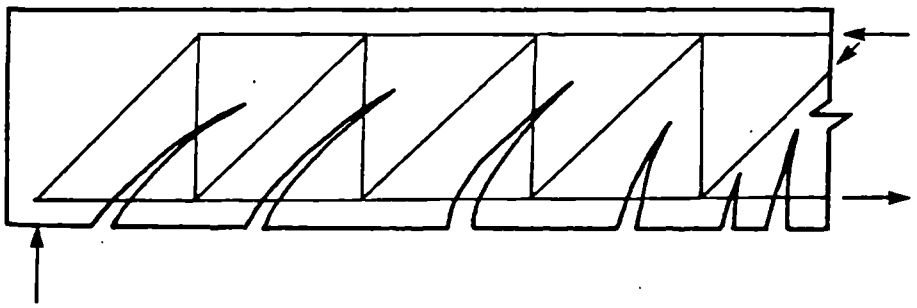

CLASSICAL TRUSS ANALOGY (MÖRSCH)

FIGURE 2.3

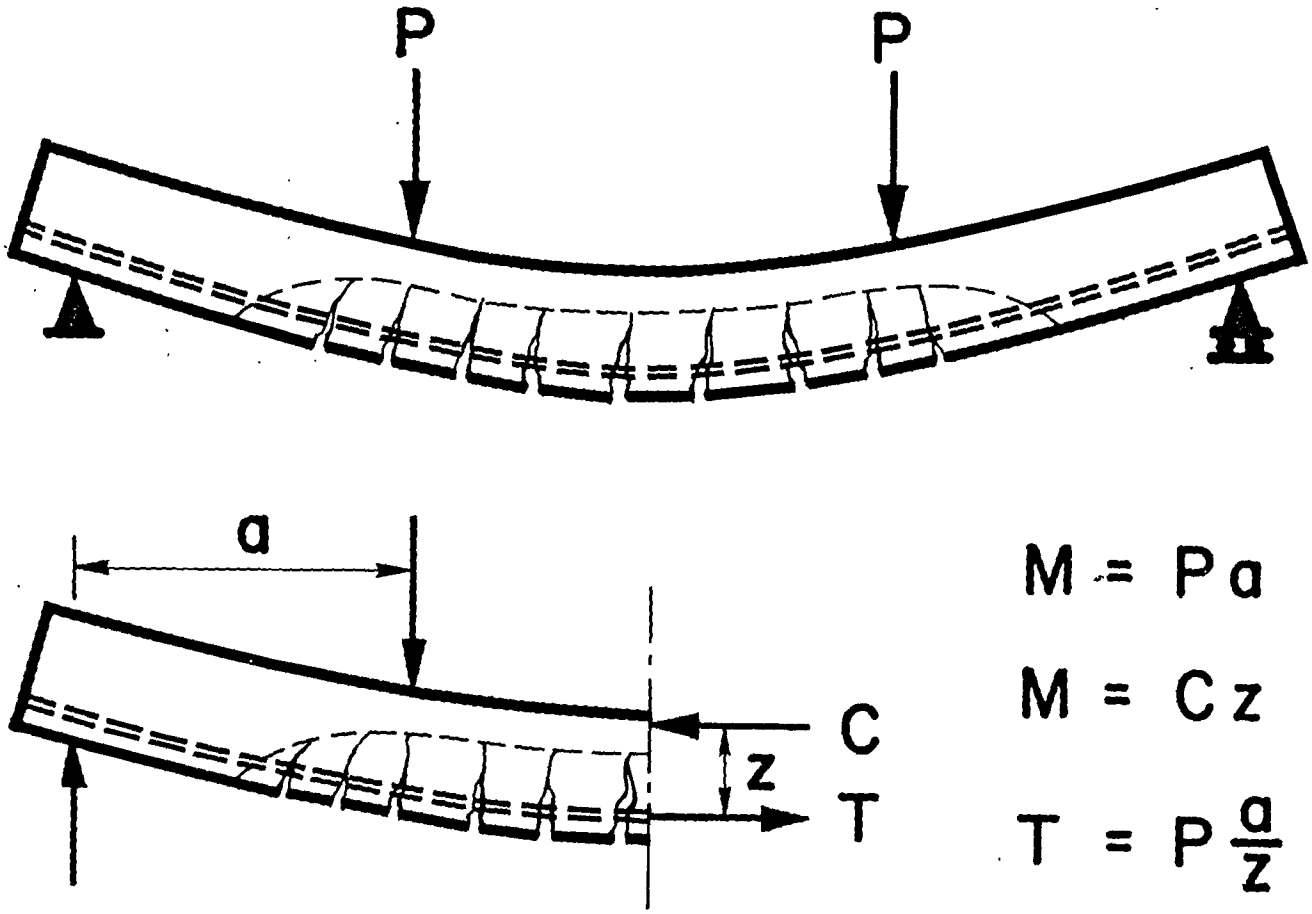

KANI'S CONCRETE TOOTH MODEL FIGURE 2.4

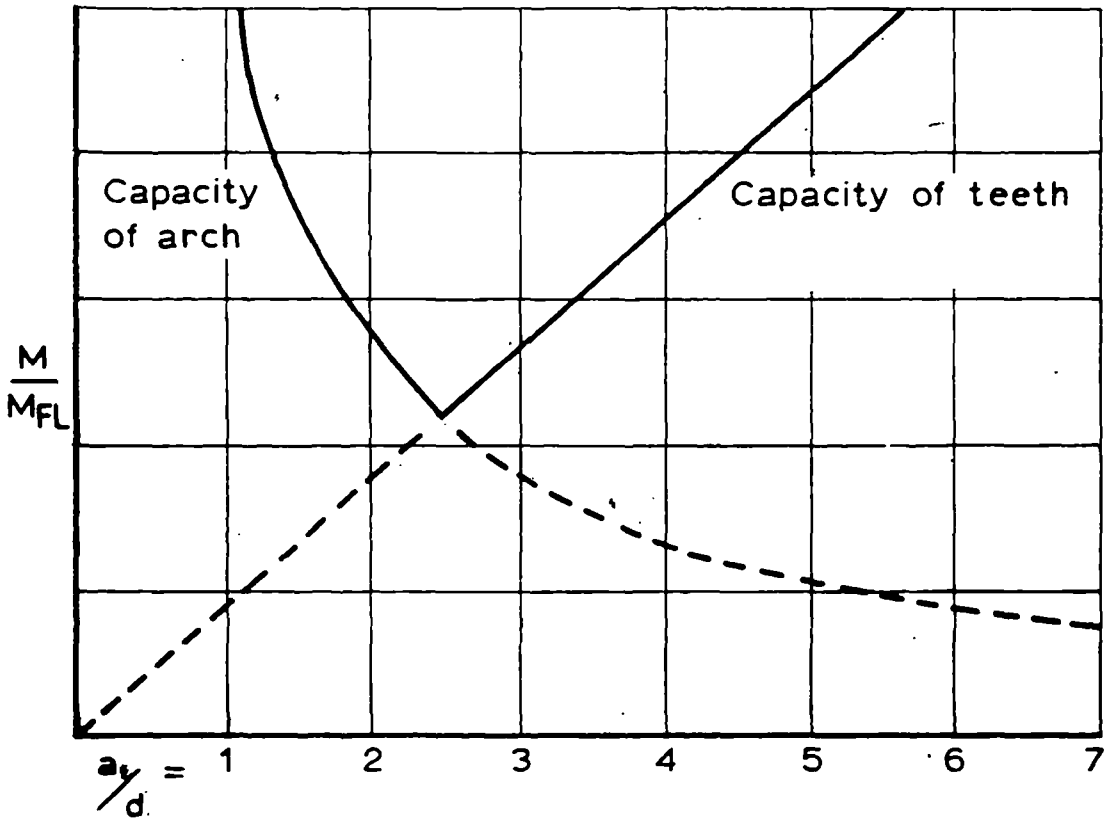

COMPARISON BETWEEN CAPACITY OF ARCH
AND
FLEXURAL CAPACITY OF TEETH

FIGURE 2.5

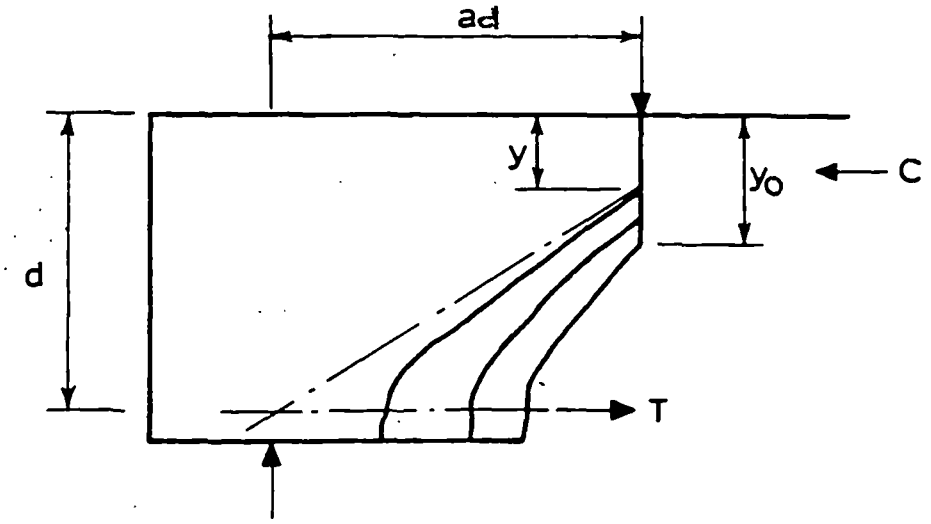

KANI'S ARCH MODEL

FIGURE 2.6

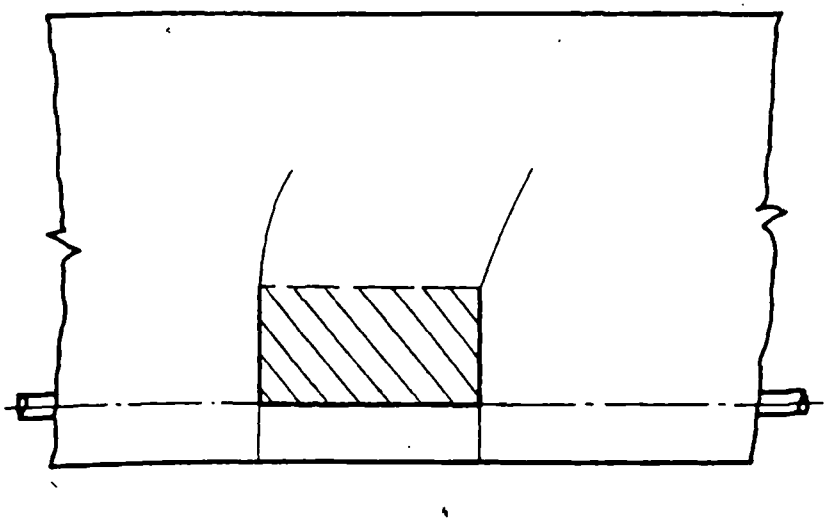

TOOTH ANALYSED BY KANI

FIGURE 2.7

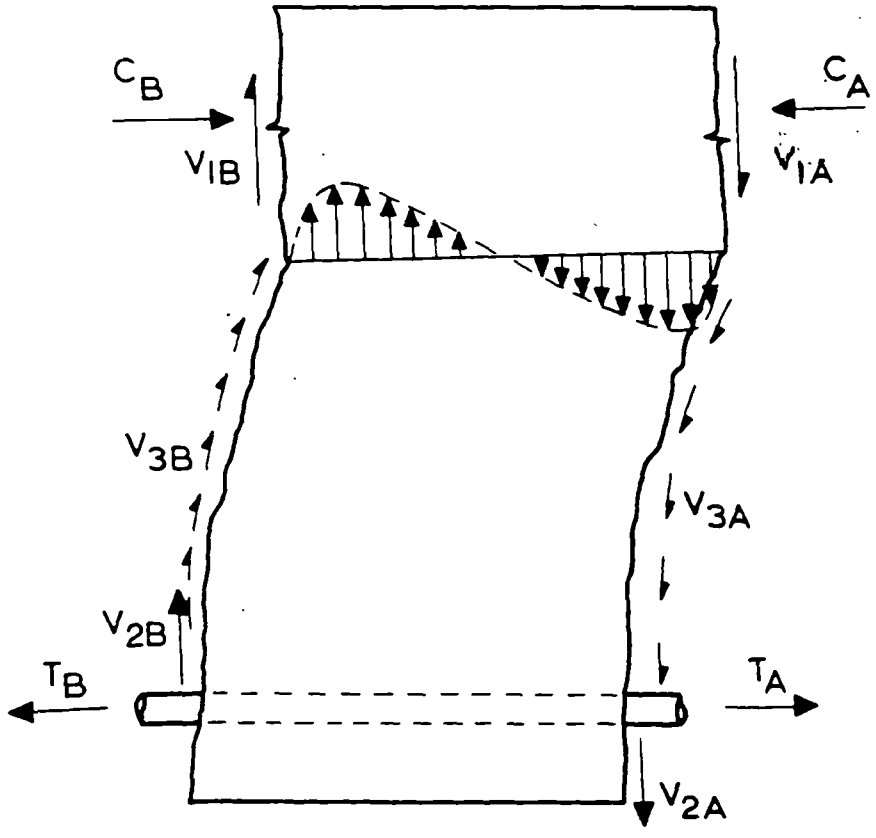

TOOTH ANALYSED BY FENWICK

FIGURE 2.8

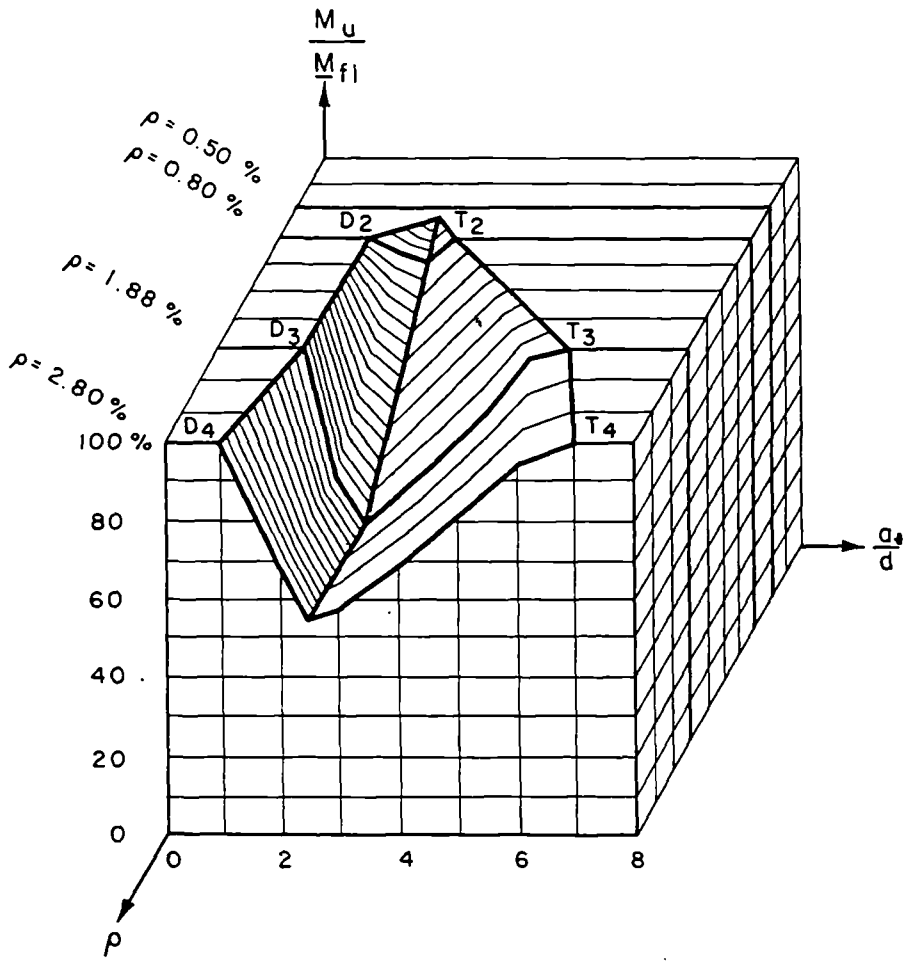

RELATION BETWEEN SHEAR - SPAN
AND
MOMENT CAPACITY FROM KANI'S TESTS

FIGURE 2.9

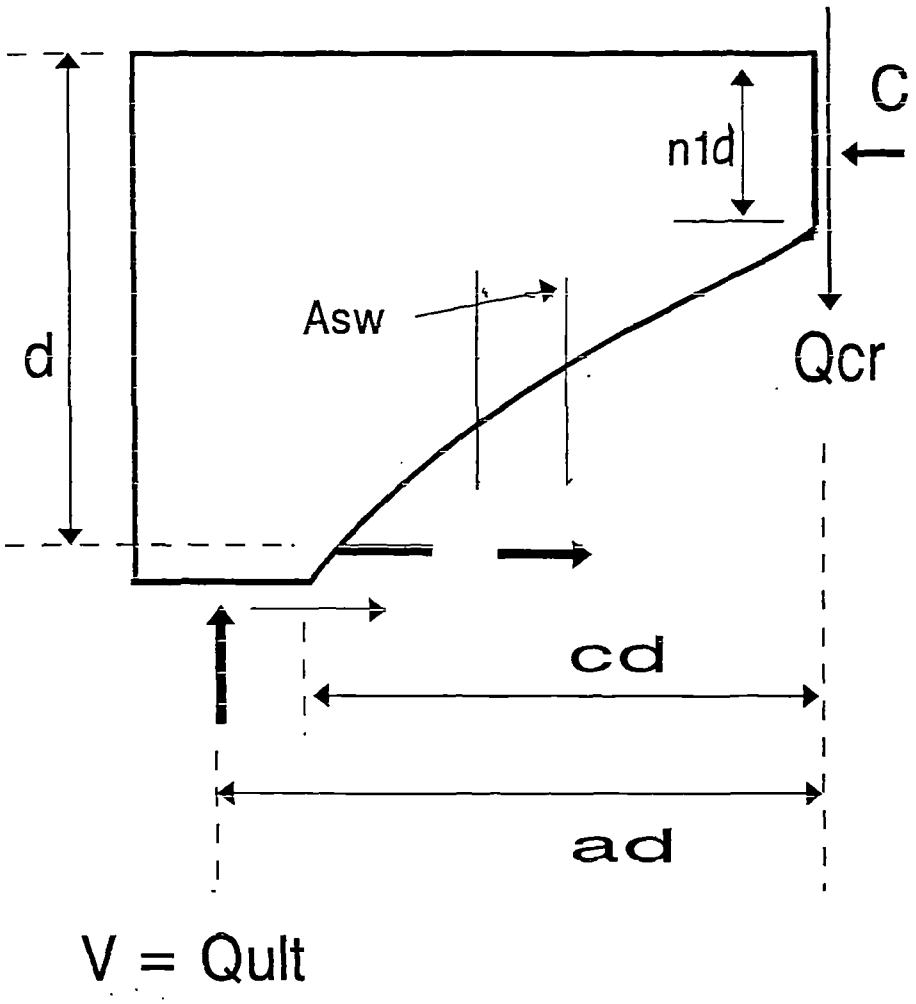

SHEAR-COMPRESSION THEORY

FIGURE 2.10

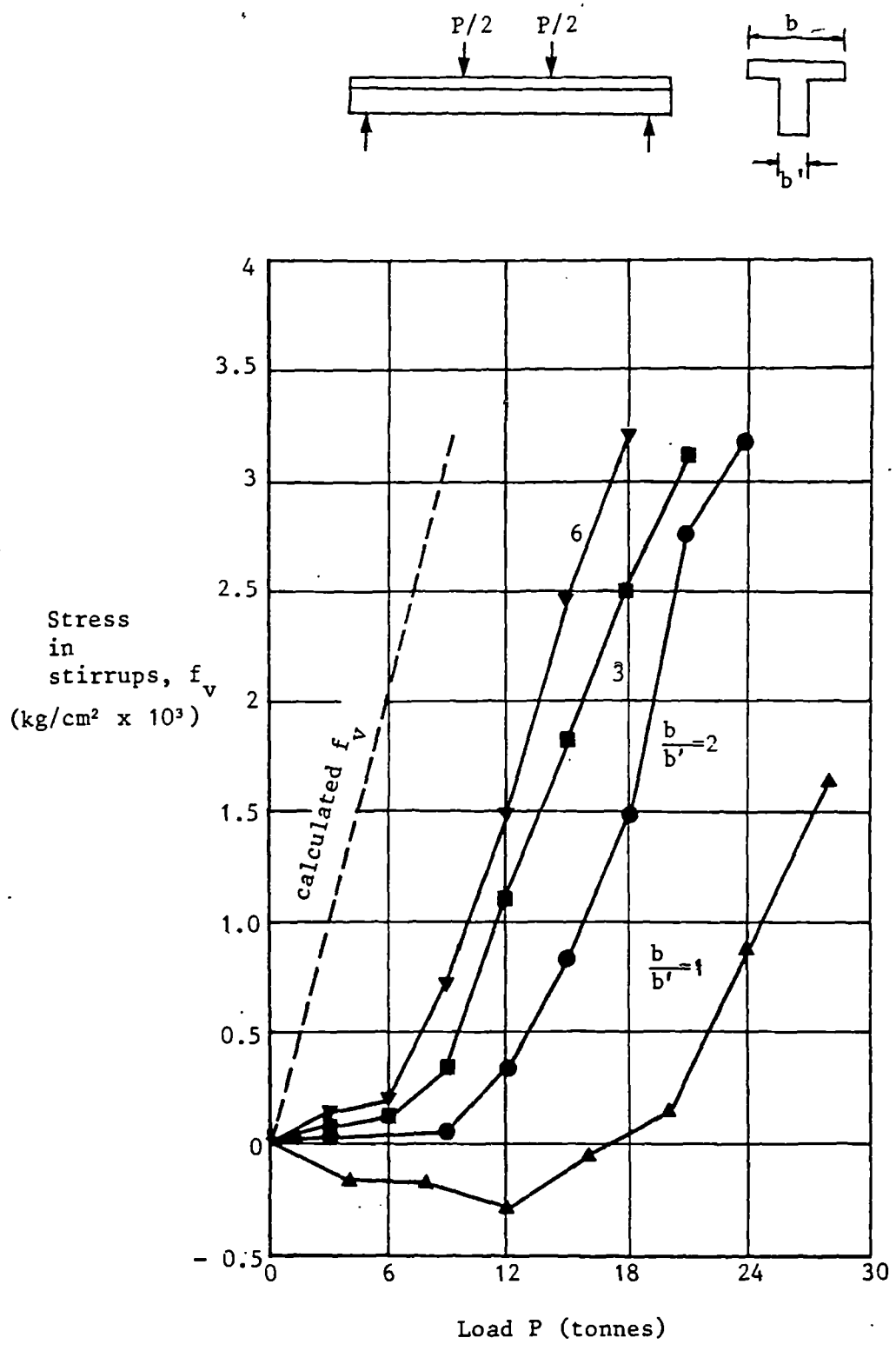

RESULTS FROM LEONHARDT'S TESTS

(1 kg/cm^2 x 10^3 = 100 N/mm^2)

FIGURE 2.11

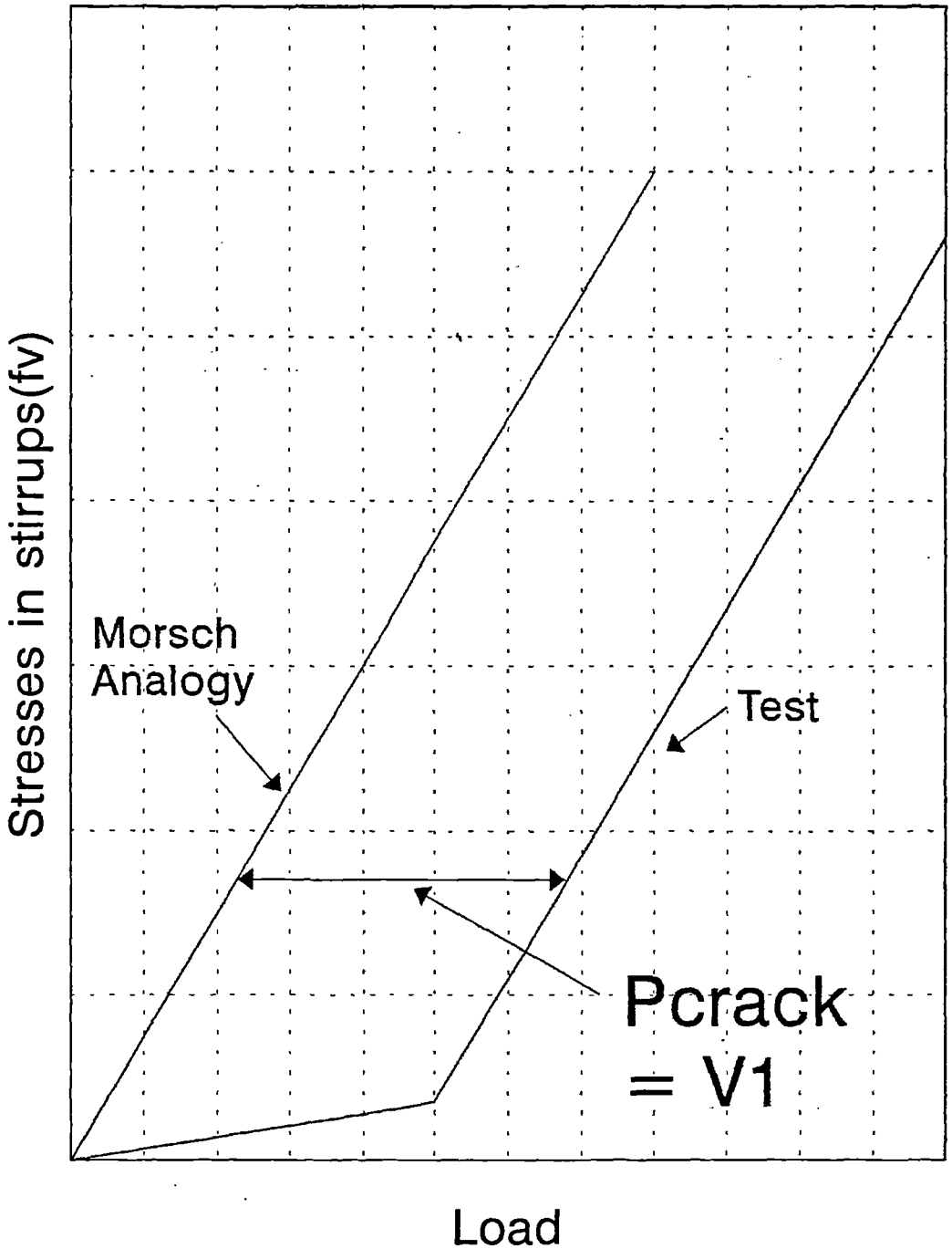

Stresses in links : Comparison between
test results and Morsch truss analogy (Leonhardt)

FIGURE 2.12

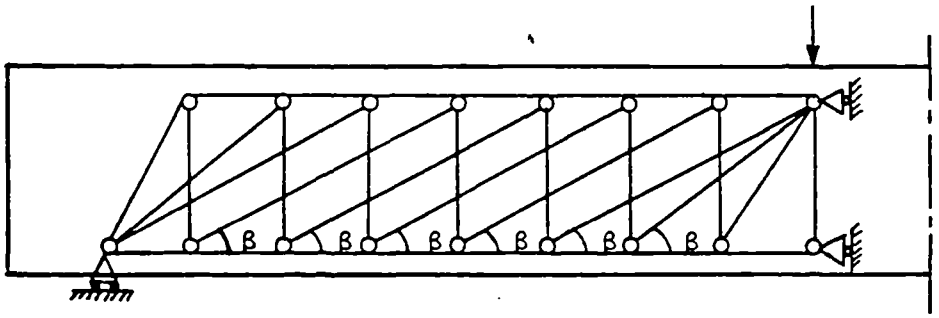

TRUSS PROPOSED BY MOOSECKER

FIGURE 2.13

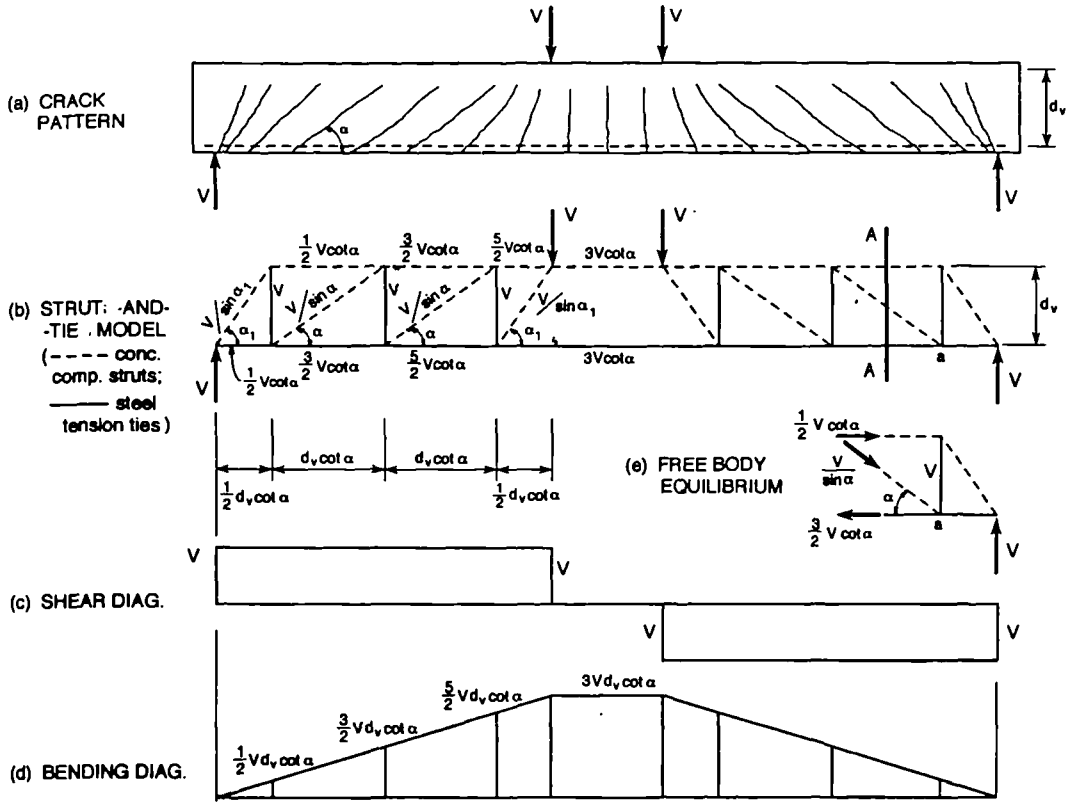

TYPICAL STRUT-AND-TIE MODEL

FIGURE 2.14

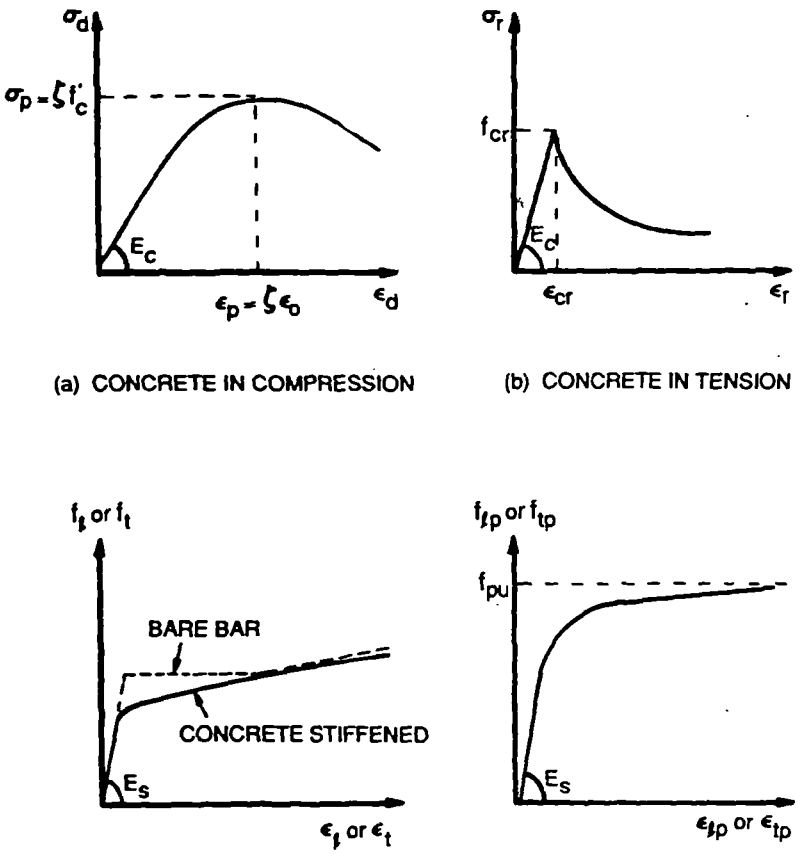

(a) CONCRETE IN COMPRESSION

(b) CONCRETE IN TENSION

(c) MILD STEEL

(d) PRESTRESSING STEEL

STRESS - STRAIN RELATIONSHIP IN MEMBRANE ELEMENTS

FIGURE 2.15

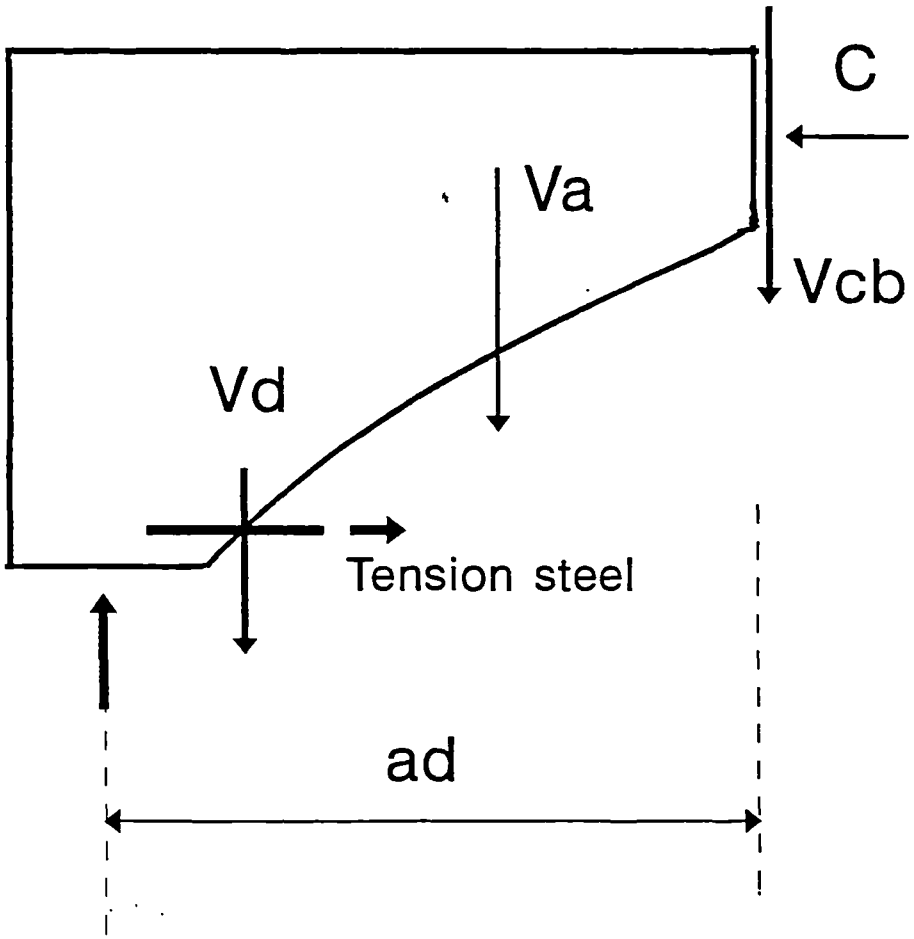

THREE MODES OF SHEAR TRANSFER
IN A BEAM WITHOUT WEB STEEL

FIGURE 2.16

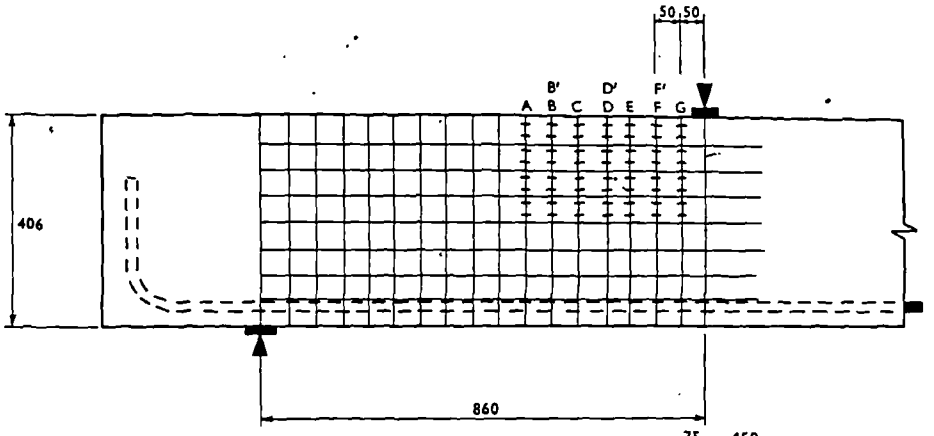

Beam 7

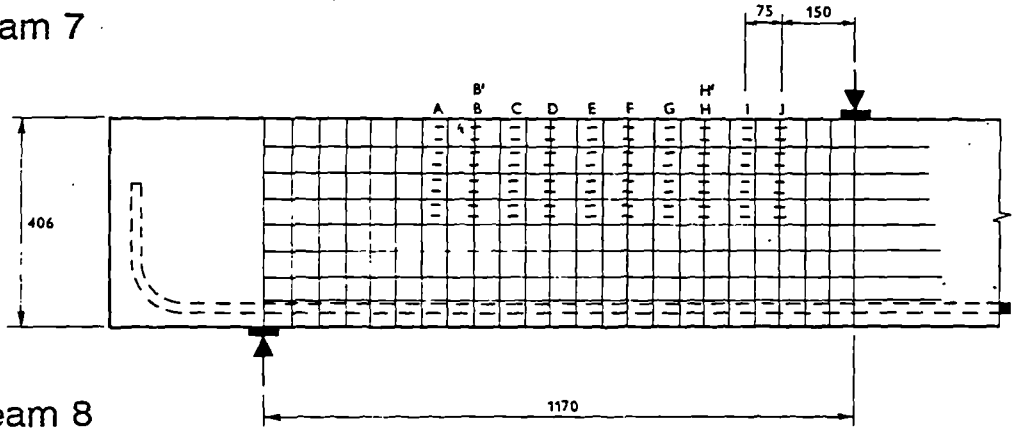

Beam 8

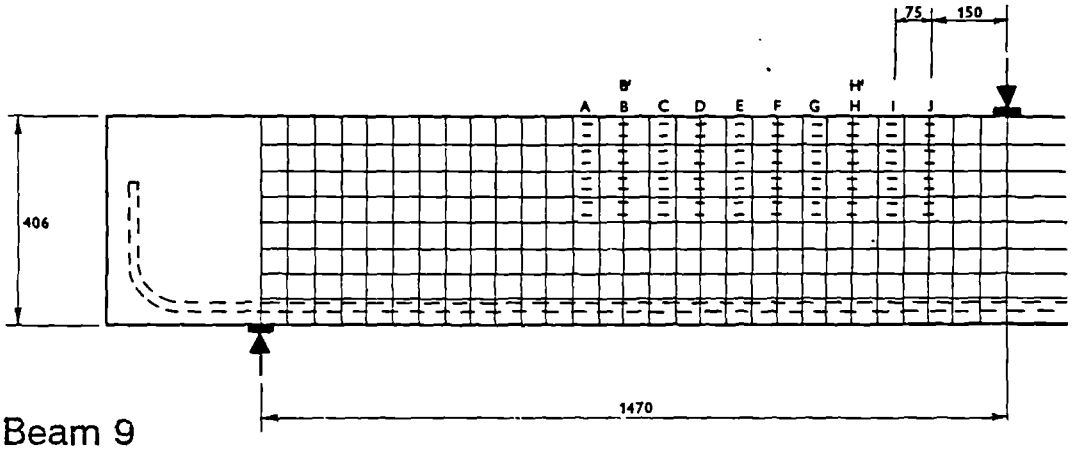

Beam 9

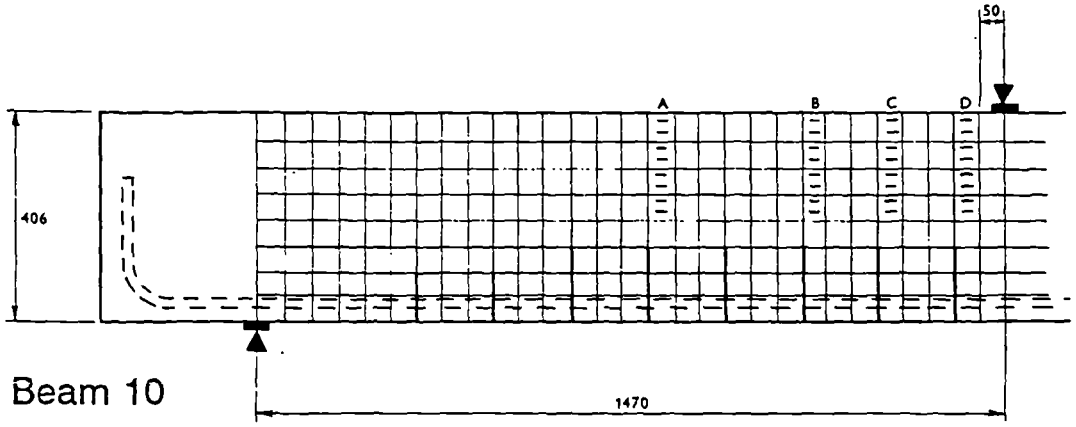

Beam 10

BEAM TEST SPECIMENS (TAYLOR)

FIGURE 2.17

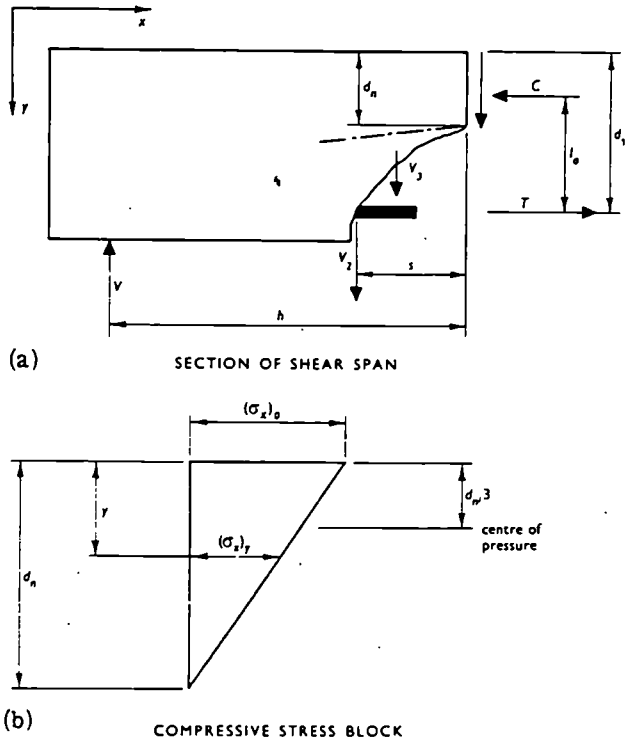

SECTION AND STRAIN PROFILE OF A BEAM CARRYING SHEAR FORCES

FIGURE 2.18

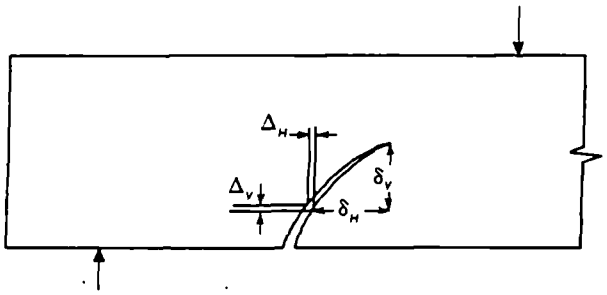

DISLACEMENT PARAMETERS (TAYLOR)

FIGURE 2.19

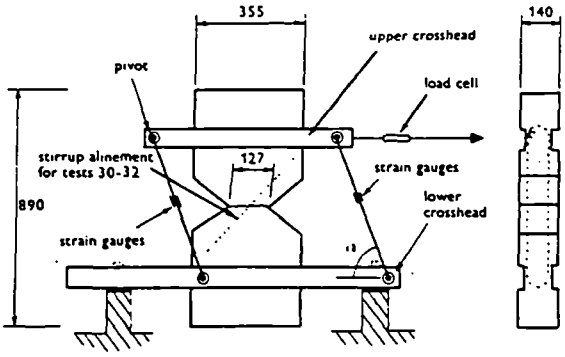

SCHEMATIC ILLUSTRATIONS OF BLOCK TEST (TAYLOR)

FIGURE 2.20

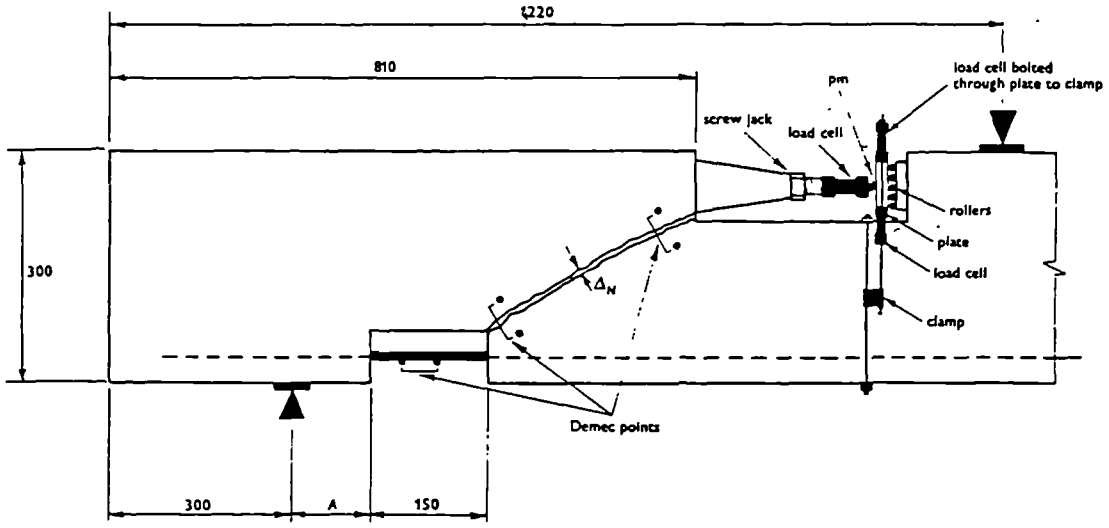

BEAMS WITH PREFORMED CRACKS AND NOTCHES (TAYLOR)

FIGURE 2.21

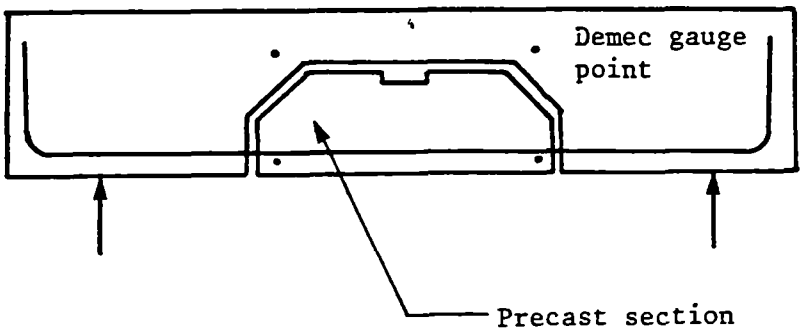

DOWEL TEST SPECIMEN (TAYLOR)

FIGURE 2.22

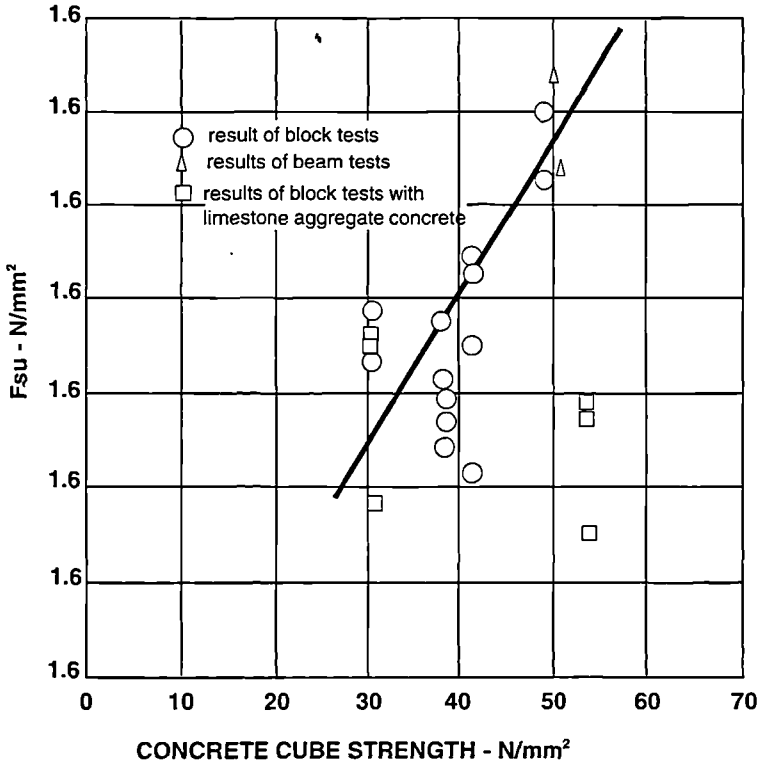

RELATION BETWEEN ULTIMATE SHEAR STRESS AND CONCRETE STENGTH

FIGURE 2.23

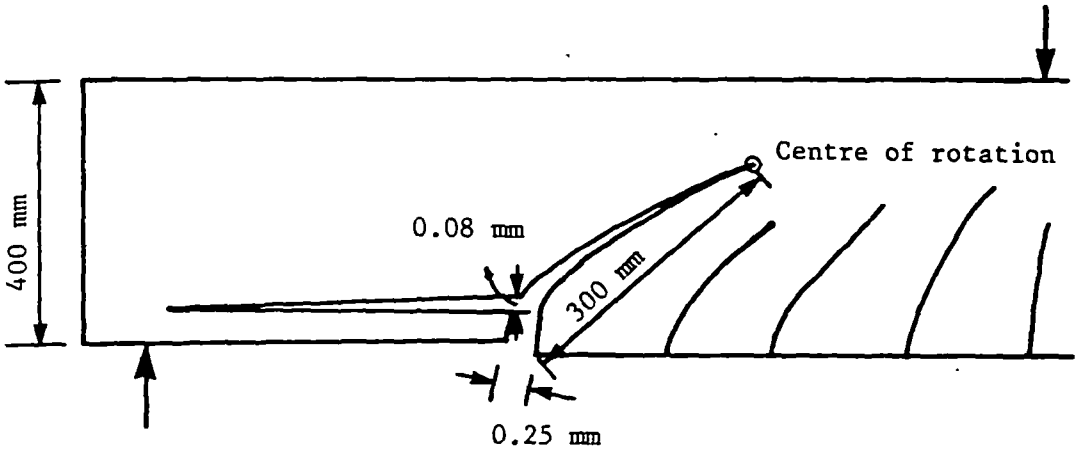

CRITICAL CRACK WIDTHS AT PEAK LOAD (CHANA)

FIGURE 2.24

CHAPTER 3
SHEAR DESIGN AT NORMAL TEMPERATURES

3.1 Introduction

In this chapter, a method for shear design is developed on the basis of an examination of the roles of concrete, the tension steel and the web reinforcement. It is proposed that the web steel should be treated as reinforcement for enhancing the shear resistance of a concrete member and not as an independent component of any analogous truss. It is also proposed to examine the provision of horizontal steel at the centre of the cross-section as an alternative form of shear reinforcement for beams and slabs, with the help of a test programme.

The test programme for beams allows variation in the main parameters; for example, the span of beams, the strength of concrete and the amount of tension steel. Also, some test beams are without any shear reinforcement and some are provided with central bars, some with links and some with the combination of central bar and links. The design rules have been proposed and verified with the help of measurement of stresses in the web steel, using strain gauges fixed on the reinforcement of two of the test beams.

A similar design method is proposed for using central steel to enhance the punching shear resistance of slabs, based on tests on slab specimens allowing for variations in thickness of slabs, the strength of concrete and the amount of central steel.

3.2 Contribution of concrete section to the shear resistance

3.2.1 Analytical estimate of the contribution of the compression block (V_{cb})

It is proposed to use a simplification of the basic shear-compression failure mechanism, developed by Regan in the Institution of Structural Engineers' Shear Study Group report[9]. This approach is based on the consideration of the ultimate state of a beam prior to failure and it treats the beam as a tied arch, with the

tension steel providing the tie.

The resistance of the compression zone concrete (V_{cb}) is equal to the shear force required to produce shear-cracking in the compression zone, under the combined action of shear and flexure. V_{cb} is shown as Q_{cr} in figure 2.10 corresponding to the notation used by Regan[9]. V_{cb} is given by the following equation 3.2.1.

$$V_{cb} = Q_{cr} = (q_{cr})(n_1 d)\, b \quad \ldots \quad 3.2.1$$

q_{cr} = critical average shear stress in compression block

$n_1 d$ = the neutral axis depth which accounts for the action of shear

Regan's value of q_{cr} is $(f_{ck})^{0.67}$[9, p 9] in psi units. This agrees with the term given in equation 3.2.2, which is expressed in N/mm^2. Hsu[17 p 209] has given an expression for q_{cr} as $3.75\sqrt{(f_{ck})}$ in psi units. This expression and the equation 3.2.2 give similar results if f_{cu} is 25 N/mm^2. Hsu's expression gives a value of q_{cr} about 12% lower if f_{cu} is 50 N/mm^2.

$$f_{cr} = 0.167\ (f_{cu})^{2/3} \quad \ldots \quad 3.2.2$$

$n_1 d$ can be expressed in terms of "nd", a reference neutral axis depth which is the depth of compression block before the onset of action of shear. Regan[9, p 31] has given a rule for the reference neutral axis depth factor (n), assuming a fully developed parabolic stress block and an extreme fibre compressive strain of 0.0035 and using a linear strain profile over the depth of the section. Regan's rule is written as follows using the terms ρ and f_{cu} ($f_{ck} = 0.8 f_{cu}$):

$$\frac{n^2}{1-n} = \frac{3}{2}\left(\frac{\rho}{100}\right)\frac{0.0035 E_{st}}{0.8 f_{cu}} = 0.000066\frac{\rho\, E_{st}}{f_{cu}} = \psi$$

This equation is solved to obtain equation 3.2.3a.

$$n = \frac{-\psi + \sqrt{\psi^2 + 4\psi}}{2} \quad \ldots \quad 3.2.3a$$

"n" can also be expressed using the following simplified expression:

$$n = 0.025 \left(\frac{\rho E_{st}}{f_{cu}}\right)^{1/3} \quad \ldots \quad 3.2.3$$

Table 3.2.1 shows that the equations 3.2.3a and 3.2.3 give comparable values of "n" for a range of values of $\varrho E_{st}/f_{cu}$, with a maximum value of "24000" given by E_{st} as 200000 N/mm^2, f_{cu} as 25 N/mm^2 and ϱ as 3.

Table 3.2.1: Values of n obtained from equations 3.2.3a and 3.2.3

$\varrho E_{st}/f_{cu}$	"n" Eq. 3.2.3a	"n" Eq. 3.2.3
4000	0.398	0.397
8000	0.508	0.500
12000	0.577	0.572
16000	0.626	0.630
20000	0.664	0.679
24000	0.694	0.721

A relationship between n and n_1 can be examined using Kani's approximation for the critical capacity of a beam as a tied concrete arch. Kani assumed that the stress trajectories (lines of principal stress) form as shown in figure 3.1 and that they lie within the part contained by the angle S-O-N. He also assumed that the line N-O passes through the flexural neutral plane at 45°, N being the point of its intersection with the vertical plane containing the applied load. Figure 3.1 shows the shear span as "a_1", the distance of the applied load from the support. "a_1" can also be expressed as "ad", "a" being the shear-span ratio. Kani called the unyielding base of the concrete strip adjacent to the last crack as "m".

From geometry, therefore,

$$\frac{y}{y_o} = \frac{n_1 d}{n d} = \frac{d}{ad - m + nd}$$

(Kani used the terms "y" and "y_o" for "n_1d" and "nd" respectively.)

Kani assumed that "m" and the length SO to be generally of a magnitude similar to "nd". With this assumption,

$$n_1 = \frac{n}{a}$$

Kani used this relationship to obtain the ratio of the ultimate bending resistance (M_u) and the theoretical flexural capacity (M_{fl}).

$$\frac{M_u}{M_{fl}} = \frac{n_1}{n} = \frac{1}{a}$$

The critical cross section is located in a region of biaxial compression under the applied load. Kani proposed a 10% higher safety margin compared with the uniaxial flexural compression. Therefore, an equation for n_1 could be written as follows.

$$n_1 = \frac{n}{0.9a} \qquad \ldots \qquad 3.2.4$$

Both Kani and Regan have concluded that the critical condition exists for the shear span ratio in the region of 2.5. This value is used in equation 3.2.4, so that it will apply to this critical condition and, hence, it could serve as an enveloping solution for any other condition. With this assumption, the reduced neutral axis depth (n_1d) becomes 45% of the flexural neutral axis depth (nd). This is in agreement with Taylor's conclusions given in paragraph 2.8 of chapter 2.

Combining equations 3.2.3 and 3.2.4, we get equation 3.2.5 for n_1:

$$n_1 = 0.011 \left(\frac{\rho E_{st}}{f_{cu}}\right)^{1/3} \quad \ldots \quad 3.2.5$$

Equations 3.2.1, 3.2.2 and 3.2.5 are combined and simplified to give equation 3.2.6 which gives an analytical evaluation of the contribution of the compression block to the ultimate shear resistance:

$$V_{cb} = 0.011 \left[\left(\frac{\rho E_{st}}{f_{cu}}\right)^{1/3}\right] [0.167 \ (f_{cu})^{2/3}] \ (bd)$$

$$V_{cb} = 0.00184 \ (\rho \ E_{st} \ f_{cu})^{1/3} \ bd \quad \ldots \quad 3.2.6$$

3.2.2 Rule for the design shear stress v_c

As described in paragraph 2.5.2.4 of chapter 2, Morrell and Chia[23] have shown that the aggregate interlock mechanism enhances both the shear resistance of a beam and the compressive strength of a cube, in a similar manner. In both cases, the resistance mechanism sustains the local shear stresses developed in the interface between aggregate and the cement paste. It is apparent, therefore, that the factors governing the quality of concrete measured in terms of its cube strength should also govern the aggregate interlock contribution. Taylor's block-test and beam-test results (Figure 2.23) also demonstrate an increase in the measured ultimate shear stresses (produced by aggregate interlock) with higher strengths of concrete.

The dowel action contribution is derived from the provision of tension steel and the quality of concrete surrounding the tension steel. Additionally, the aggregate interlock mechanism is also assisted by the resistance provided by the tension steel to widening of cracks, which is related to the amount of tension steel and its elastic modulus.

Swamy et al[25] have concluded, after a detailed test programme, that it would be difficult to separate the contribution of aggregate interlock (V_a) and that of the dowel action (V_d). In their opinion, any use of simplified tests, attempting

to evaluate one of these effects by isolating the other effect, could be misleading. Their test results clearly demonstrated a relationship of the combination (V_a + V_d) with the concrete strength (test range of concrete strength 24 - 69 N/mm^2) and the amount of tension steel (test range 2 - 4 %). Swamy's tests did not use the elastic modulus of steel as a variable.

These contributions, therefore, can be treated as a function of f_{cu} , the percentage of tension steel and the modulus of elasticity of the steel.

$$V_2 = (V_a + V_d) = K(f_{cu})^x (\rho)^y (E_{st})^z$$

It is proposed that the constants x, y and z should each be "1/3", corresponding to the equation 3.2.6. In paragraph 2.5.2.4 of chapter 2, it was shown that the applied shear is carried by two components; V_{cb} (compression zone, 40%) and V_2, the sum of the aggregate interlock and dowel action contributions (60%). Also, the conditions of equilibrium of vertical forces and bending moments were checked as shown in paragraph 2.5.2.1 and they are satisfied with these proportions of V_{cb} and V_2. Therefore, the constant K should be such that the ultimate shear resistance of a concrete section, V_{CU} , given by the sum of the three modes of shear transfer, should be (1/0.4) times the individual value of V_{cb}.

$$V_{cu} = (\frac{1}{0.4}) V_{cb} = \frac{0.00184}{0.4} (\rho E_{st} f_{cu})^{1/3} bd$$

This equation is simplified as follows and the "depth factor" $(400/d)^{0.25}$ is introduced, as discussed in paragraph 2.5.6 of chapter 2:

$$V_{cu} = 0.0046 (\rho E_{st} f_{cu})^{1/3} (\frac{400}{d})^{0.25} bd \quad \ldots \quad 3.2.7$$

The following parameters are introduced in equation 3.2.7 to obtain equation 3.2.8, which is the same as the BS8110 rule for the design shear stress v_c (N/mm^2):

i) partial factor for material strength (γ_m)

ii) E_{st} as 200000 N/mm^2

$$v_c = \frac{0.27}{\gamma_m} (\rho f_{cu})^{1/3} (\frac{400}{d})^{0.25} \quad \ldots \quad 3.2.8$$

where,

ρ ≤ 3

f_{cu} ≤ 40 N/mm^2

(400/d) ≥ 1.0

3.3 Contribution of links to the shear resistance

3.3.1 The beneficial effects of links

The links have a complex role in enhancing the shear carrying capacity of a section. They do not have a limited function as only a direct tension member, which the truss analogy may lead us to believe. As explained earlier in section 2.5 of Chapter 2, the shear resistance of a beam afforded by the three shear transfer modes is shared by the links and the concrete and their shares depend on a number of factors; for example, the size of beam, provision of the reinforcement and the shear-span ratio. However, an increase or decrease in the individual shares of concrete and links in the overall design resistance could be considered as mutually compensating, within a certain range of the design parameters. It is proposed, therefore, that the ultimate shear resistance of a member provided with links, V_{DU}, has two components; V_{CU} , the contribution of concrete and V_{LU} , the enhancement provided by links acting as reinforcement.

The general rule for V_{CU} includes a "depth factor". (Paragraph 2.5.6 of chapter 2) This should be retained when the effect of links is accounted for in the evaluation of the overall resistance of the member. The dowel action strength is improved with provision of links and part of the shear carried by aggregate interlock is transferred to links. This beneficial effect of links depends on the diameter and spacing of links. For beams with different depths and with the same amount of links, therefore, an enhancement in V_{CU} provided by the beneficial effect of links should be treated in the same way as that afforded by the influence of the size of aggregate.

3.3.2 Derivation of a rule

It is proposed to examine the BS8110 rules for enhancement to the shear resistance provided by the links. The Eurocode EC2 "standard method" rules are not separately examined, since they are also based on the "addition principle" and they give provision of links similar in comparison with the BS8110 rules, in general cases within the limitations of the Eurocode.

Although the shear failure is not always caused by yielding of links, it is generally agreed that the strains in links increase with the increase in applied shear, although they may not always reach the yield point. In most cases, the links act in conjunction with the concrete and enhance the overall shear resistance of the section at all stages of loading until the beam fails.

For the sake of convenience, this contribution of links is taken as additional to that of the concrete and it is named as V_L. Initially, V_L is assumed to be a function of the stress developed in links (v_l), the area of cross-section of links (A_{sw}), spacing of links (s), the depth of the beam (d).

$$V_L = v_l \times A_{sw} \times d/s \qquad \ldots \qquad 3.3.1$$

In this section, the validity of the equation 3.3.1 is examined with the use of results of two of the tests carried out by Leonhardt[13]. These beams are named as ET2 and ET3. Figure 2.11 of chapter 2 shows graphs for these beams designated as "b/b' = 2" (for beam ET2) and "b/b' = 3" (for beam ET3). The tests on these beams are selected because these beams are reported to have failed in shear. The details of these tests have been extracted from a translation of the report on Stuttgart Shear Tests, 1961[12].

The beams ET2 and ET3 were 350 mm deep T-shaped beams with an overall length of 3400 mm and a simply supported span of 3000 mm. Two point loads were applied, each at 1050 mm (a_l) from the support.(Figure 2.11) The effective depth (d) was 300 mm and, therefore, the shear span ratio (a_l/d) was 3.5. The flange at the top of each beam was 75 mm deep and 300 mm wide. For

calculation of the ultimate shear resistance of concrete section (V_{CU}), the BS8110 rule requires only the width of the web (b) and this flange has, therefore, been ignored. (b = 150 mm for ET2 and 100 mm for ET3.)

The tension steel at the bottom of the beam was 4T20, giving A_{st} as 1256 mm^2. The BS8110 requires the percentage of steel to be based on the width of the web (b). The percentage of steel (ϱ), therefore, is 2.79 for the beam ET2 and 4.19 for beam ET3.

The limitation on ϱ ($\leq$ 3) given in the BS8110 rule is used for calculating the contribution of concrete (V_{CU}) for the beam ET3. The cube strength of concrete (f_{cu}) was 28.5 N/mm^2 for both the beams. With these parameters, V_{CU} is 56.1 kN for beam ET2 and 38.3 kN for beam ET3.

Nominal top steel was provided at the top for supporting 6 mm diameter single links at 110 mm centres for both beams. The links were provided with small drilled holes for locating pins of the strain gauges and these were accessible from outside the beam through small tubes provided for this purpose.

The stress in links (v_l) at various loading stages was calculated by Leonhardt as an average of stresses in four links in the central part of the shear span of 1050 mm, the first of these links being 375 mm from the support. The contribution of 6 mm diameter links at 110 mm centres (V_L), corresponding to the effective depth of beam (300 mm), is obtained from equation 3.3.1 as follows:

$$V_L = (56 \times 300/110) \times v_l/1000 = 0.153 v_l \text{ kN}$$

The table 3.3.1 gives values of $V_L/(V_{CU})$ at increments in the total applied load (P) of 3 tonnes or increments in the applied shear (V) of 1.5 tonnes. These loads are expressed in kN, using a simplified conversion of 10 kN to a tonne. The self-weight of the beam was a uniformly distributed load of about 5 kN, approximately 2% of the maximum applied load. This load is ignored for the sake of convenience of interpreting the effect of point loads only. The applied shear forces at failure were 131.5 kN for ET2 and 127.5 kN for ET3.

Table 3.3.1 : Details of Leonhardt's tests and results

V kN	V/V_{CU} (ET2)	V_L/V_{CU} (ET2)	V/V_{CU} (ET3)	V_L/V_{CU} (ET3)
30	0.53	0	0.78	0.06
45	0.80	0.01	1.17	0.14
60	1.07	0.10	1.56	0.46
75	1.34	0.23	1.96	0.72
90	1.60	0.41	2.35	1.00
105	1.87	0.76	2.74	1.23
120	2.14	0.87	3.13	1.27

The yield strength was 320 N/mm^2 for links and 340 N/mm^2 for tension steel. The links in both the beams were observed to have reached the yield point of steel, 320 N/mm^2. Although this value differs from the BS8110 characteristic strength of steel as 460 N/mm^2, these results could still be used for assessing the contribution of links at intermediate stages of loading.

Figure 3.2 shows lines representing the relationship between (V_L/V_{CU}) and V/V_{CU} for both the beams, which seem to coincide giving a straight line with a slope less than "1". Figure 3.2 also shows a line drawn through a point on the X-axis where V/V_{CU} value is "1" and the slope of this line is also "1". A rule represented by this new line will correspond to a marginally higher proportion of links, compared with the common relationship deduced from the lines representing beams ET2 and ET3. This rule could be written as follows:

$$\frac{V_L}{V_{CU}} = \frac{V}{V_{CU}} - 1$$

or

$$V = V_{CU} + V_L \qquad \ldots\ldots \quad 3.3.2$$

The ultimate applied shear (V_U) is required to be less than or equal to the ultimate shear resistance V_{DU}. From equation 3.3.2, a rule for V_{DU} can be obtained as follows:

$$V_{DU} = V_{CU} + V_{LU} \quad \ldots\ldots \quad 3.3.3$$

V_{LU} , the ultimate state shear resistance contribution of the links, is obtained by using the yield stress for steel in place of v_l in equation 3.3.1, which is the same as the BS8110 rule.

$$V_{LU} = f_{yv} \times A_{sw} \times d/s \quad \ldots \quad 3.3.4$$

Figure 3.2 also shows that the stress in links starts developing when the applied shear is about $0.5V_{CU}$ and increases gradually, until it is nearly $1.4V_{CU}$, not in direct proportion of $(V-V_{CU})$. This would suggest that, in this range, provision of nominal links could be advantageous for a beam of structural importance. Such provision of links will provide an extra reserve of strength, as a precaution against any marginal and unforeseen increase in the applied shear. BS8110 requires a minimum provision of links corresponding to a value of $(v - v_c)$ of 0.4 N/mm^2, which could enable a beam to sustain an increase in the applied shear of the order of, say $0.4V_C$. This assumption is valid for the common design situations where the BS8110 values for v_c are generally of the order of 1 N/mm^2.

3.3.3 Tests for validating the rules

The rule for contribution of links to the shear resistance of beams has been verified using results of tests on 1400 mm span beams with links. These tests were carried out under a test programme which is fully described in section 3.5. The beams were 200 mm wide and 300 mm deep. They were provided with 3T20 as the tension steel and 2T12 as the nominal top steel. Table 3.3.2 shows the details of tests on these beam types C1, C2 and C3, provided with T6 single links at 200, 150 and 100 mm centres respectively.

Table 3.3.2 shows the ultimate shear resistance as V_{DU} , given by equation 3.3.3 and the applied shear at failure as V_{FU}. Specimens C1, C1a, C2, C2a and C3 failed in shear. In case of the specimen C3a, the compression block concrete had severe cracking suggesting a shear-compression mode of failure. Table 3.3.2

shows that the values of overall ultimate shear resistance provided by the rule are less than V_{FU}, the ultimate applied shear at failure.

Table 3.3.2: 1400 mm span beams with links

Spec No	f_{cu} N/mm^2	V_{CU} kN	V_{LU} kN	$(V_{CU}+V_{LU})$ (kN)	V_{FU} kN
C1	32	61	34.5	95.5	119
C1a					128
C2	41	66	46	112	162
C2a					178
C3	41	66	69	135	185
C3a					187

3.4 Alternative shear reinforcement

3.4.1 Introduction

It is proposed to derive a design rule for estimating an enhancement to the shear resistance using an alternative shear reinforcement in the form of horizontal steel at the centre of a cross-section. It is intended that this rule should be compatible with the rule for V_{CU} given in equation 3.2.7 and that it is suitable for use in conjunction with other similar rules. The derivation of this rule is supported by an adequate number of tests on rectangular beams and slabs, with variation of the principal parameters, concrete strength and the amount of tension steel. While the central bars or a central mesh can be provided on its own for slabs, the beams will require provision of links for practical reasons. It is intended, therefore, to examine the effect of combination of links and central bars for beams.

A rule for V_{BU} , the ultimate state contribution of the central bar, is initially derived on the basis of tests. For the beam tests, rectangular specimens have been used, 200 x 300 mm in cross-section (Figure 3.3). 3 x 3m specimens have been used for tests on flat slabs (Figure 3.4) using the conventional test arrangement for punching shear tests (Figure 3.5). The rules will also be verified

using a computer program ABAQUS in chapter 4.

3.4.2 The ultimate shear resistance contribution of the central bar (V_{BU})

3.4.2.1 Rectangular beams

A bar placed at the centre of a section can be looked upon as performing a combination of two functions. First, as reinforcement enhancing the resistance of surrounding concrete to the progress of a shear crack into the compression block. This is taken as proportional to the tensile strain in concrete which is related to the ultimate shear stress v_{cu} . This part of the ultimate shear resistance provided by the central bar (V_{BU1}) can be expressed in terms of its area of cross-section A_b and a constant K_1:

$$V_{BU1} = K_1 \, v_{cu} \, A_b$$

The central bar and links can provide a combined resistance to the principal tensile stresses in the neutral axis region of the beam. As shown in the sketch, they provide tensile reactive forces F_b (central bar) and F_l (links) across a critical plane represented by the crack. The slope of the crack is assumed to be 1 : 1.5 (paragraph 3.5.2) and the angle between the crack and the horizontal is α, so that $\tan\alpha = 1/1.5$.

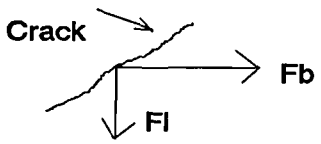

Sketch 3.4 : Reactive forces in the central bar and links

It is proposed to express the contribution to the overall shear resistance provided by the central bar as V_b , which will lead to its ultimate value at failure. V_b will be a quantity directly additional to the overall shear resistance and not a vectorial enhancement. Hence, F_b (the reactive force in the bar) will have the same proportion with V_b as that of the normal stress produced by F_b (σ_b) to its

component stress (σ_n) normal to the crack inclined at an angle α to the line of action of F_b . This relationship between σ_n and σ_b is expressed as follows[42]:

$$\sigma_n = \sigma_b \sin^2 \alpha = \frac{\sigma_b}{1 + 1.5^2} \approx 0.3\sigma_b$$

$$\therefore \quad V_b = 0.3F_b \qquad \ldots \qquad 3.4.1$$

This effect of the central bar could be limited and it could be governed by the tensile strength of concrete, if F_b is not complemented adequately by a component F_l provided by the links. This will be discussed and verified in paragraph 3.5.4.

The second function of the central bar could be to provide an enhancement to the interlocking action against widening of a shear crack. This action would depend on the shear deformation corresponding to the splitting of the crack. The CEB Bulletin no 189[43, p 67] gives the following rule for the ultimate capacity of a dowel bar (V_{BU2}) resisting concrete-to-concrete displacement.

$$V_{BU2} = 1.3 \frac{4A_b}{1000\pi} \sqrt{f_{cc} f_{yv}} \qquad kN$$

(f_{cc} = Ultimate compressive strength of concrete)

A similar rule is adopted in CEB Bulletin No. 203 [32, p 3-45], which specifies a shear displacement of "0.10 x diameter of the bar" along the concrete-to-concrete interface, for mobilisation of such a full dowel action. Such deformation would be too large for normal design conditions. However, a lesser dowel action could be generated to correspond to a smaller shear displacement, in proportion with the area of bar and the tensile strength of concrete surrounding it. The influence of the term f_{yv} (yield strength of steel) could be omitted as the dowel force in question is too small for the steel to yield. This has been confirmed by observation of central bars on completion of the tests which will be reported later in this chapter. The effective dowel action capacity of the central bar, therefore, could be related to the integrity and resistance to cracking of the concrete

surrounding the bar. These characteristics of concrete are influenced by the strength of concrete and the stiffness and amount of the tension steel, which are also the factors controlling v_{cu} , the ultimate shear stress. Hence, the part of the contribution of the central bar providing dowel action could also be expressed in terms of v_{cu} . This could be expressed as follows, using a constant K_2:

$$V_{BU2} = K_2 \, v_{cu} \, A_b$$

The two equations can be combined to give a single constant "K". Also, the term V_{CU} (kN) can be used to replace v_{cu} , the stress, and ϱ_b (the percentage, $100A_b/bd$) can replace the area of the bar A_b to give a convenient rule for V_{BU} , the ultimate contribution of the central bar.

$$V_{BU} = K \, V_{CU} \, \rho_b \qquad kN \qquad \ldots \qquad 3.4.2$$

3.4.2.2 Flat slabs

For flat slabs, ΣA_b is taken as the sum of the area of bars of the central mesh, A_b being the area of each bar with a spacing s_b , effective at the centre of an inclined surface where the punching failure occurs. According to BS8110, this surface is represented by the inclined face of a notional truncated cone or pyramid. This pyramid has one base with a perimeter u_o , representing the column or the loaded area. The other base is enclosed by the shear perimeter "u", at a distance of 1.5d from the face of the column or the loaded area. Although the mesh is placed at the centre of the overall depth and not the effective depth, the bars are assumed to be spaced over a length $(u + u_o)/2$. This assumption represents a reduction of about 4% in the number of bars, which is considered to be marginally on the safe side.

$$\sum A_b = A_b \frac{(u + u_0)}{2s_b} = \frac{\rho_b \, d \, (u + u_o)}{200}$$

(ϱ_b is the percentage area of the bars, $100A_b/s_bd$).

$$\therefore \; V_{BU} = (CONSTANT) \; (\sum A_b) \; (v_{cu})$$

$$= (CONSTANT)\ \left(\frac{\rho_b d\ (u + u_0)}{200}\right)\left(\frac{V_{cu}}{ud}\right)$$

$$= K\,\rho_b\,\frac{(u + u_0)}{u}\,V_{cu} \quad kN \quad \ldots \quad 3.4.3$$

3.4.2.3 Consideration of the depth factor

The general rule for V_{CU} includes a "depth factor". (Paragraph 2.5.6; Chapter 2.) This should be retained when the effect of central bars is accounted for in the evaluation of the overall shear resistance. The central steel would share the shear carried by concrete through aggregate interlock and this beneficial effect should depend on the diameter and amount of the central bar. Beams and slabs with different depths could have the same size and amount of central steel. An enhancement in V_{CU} given by the central bars, therefore, should be treated in the same way as that afforded by the influence of the size of aggregate.

3.5 Test programme for beams

3.5.1 Test specimens and procedure

Tests were carried out on 200 x 300 mm size simply supported beams loaded at mid-span. Each specimen type had two test beams; for example, for specimen type A1, beam numbers were A1 and A1a, etc. 1400 mm and 2100 mm spans were chosen to have a variation in the shear span ratio; 2.6 for the 1400 mm span and 4.0 for the 2100 mm span. Specimen series A, B, C, D and E, with a span of 1400 mm, were tested at the BCA laboratory. Specimen types F1 to F5, with span of 2100 mm, were tested at Imperial College. Specimen types F6 and F7, also with 2100 mm span, were tested at the University of Dundee, as a part of the validation exercise for the computer analysis described in chapter 4.

Three different amounts of tension steel were chosen; 2T20 (1.2%), 3T20 (1.8%) and 3T25 (2.8%). For beams with T20 bars as the tension steel, the effective depth (d) was 265 mm and it was 262 mm for beams with T25 bars, the

cover being 25 mm for all beams. For all specimen types, the top steel was 2T12.

For specimen types F6 and F7, 2T20 central bars were placed on the vertical centre line of the beam, each at 30 mm on either side of the centre of the beam. Additionally, specimen type F7 had links. Beam F6a was provided with strain gauges (Figure 3.22) to measure the stresses in central bars at 200 mm on each side of the mid-span and the stresses in the tension steel at mid-span. Beam F7a was provided with similar strain gauges and additional gauges for measuring strains in links at 200 mm on each side of the mid-span.

Some of the specimens were cast using ready-mixed concrete and, in some cases, site-mixed concrete was used and, in all cases, the maximum size of aggregate was 20 mm. Ordinary Portland Cement (OPC) was used. The tests were carried out over a period of four years, depending on the availability of test facilities. As a result, the concrete strengths of specimen types provided a variation of the main parameter f_{cu} , which was considered to be an advantage. The tables 3.5.1 and 3.5.2 show the values of f_{cu} for the specimens, which are average values of the cube strength test results of three air-cured cubes placed alongside the specimens. Water-cured cubes were also tested for the purposes of cross-checking and these strengths were approximately 5 to 10 % higher than those of the air-cured cubes. Also, tensile splitting strengths of 100 mm diameter cylinders cured by the side of the specimens were obtained for some 1400 mm span beam specimens. These tensile strengths were consistently of the order of 7 to 10 % of the compressive strength f_{cu} .

The characteristic strength f_{yv} is taken as 460 N/mm^2 for all steel excepting the links for specimen type F7. The links used in beams F7 and F7a were made with plain bars. Tests were carried out on five specimens representing the steel in these links and the average value of f_{yv} was 342 N/mm^2. Similar tests for the 20 mm diameter central and tension steel gave an average value of f_{yv} as 436 N/mm^2. Although this test result for f_{yv} was marginally lower than 460 N/mm^2, the difference was not considered to be significant for the consideration of shear carrying capacity of beams F6, F6a, F7 and F7a. The average value of E_{st} given by tests on 20 mm diameter bars was 199 kN/mm^2. This test result confirmed the

acceptability of the value of E_{st} as 200 kN/mm^2, as implied in the BS8110 rule. (paragraph 3.2.2)

The load was applied over 200 mm width, centrally over a 75 mm wide steel plate bedded on the top surface of the beam with a thin layer of mortar. The load increment was 15 kN. The values of V_{FU} shown in the tables are half of the recorded applied loads at failure plus an allowance for the self-weight of the specimens. The test frame used for 1400 mm span beams is shown in photograph 1. A similar arrangement was used for the 2100 mm span beams (photograph 7), with the addition of a pair of transducers positioned at mid-span to measure deflections. For all specimens, the span was measured between the centres of roller bearing supports under plates similar to the top plate. 100 mm overhang was provided at each support and the overall length of specimens, therefore, was 200 mm in excess of the span.

The following rule for V_{CU} is obtained from equation 3.2.8 (BS8110 rule) for the design concrete shear stress v_c , but excluding the partial factor γ_m .

$$V_{CU} = 0.27\ (\rho f_{cu})^{1/3}\ [\frac{400}{d}]^{1/4}\ \frac{bd}{1000} \qquad kN$$

In calculating V_{CU} , the actual values of f_{cu} (N/mm^2) are used, even where f_{cu} exceeds the limiting BS8110 value of 40 N/mm^2. This is considered as acceptable for an even interpretation of all the test results.

Cracks were marked when they appeared at each stage and the cracks at failure are shown in figures 3.6 to 3.14 for specimen types F1 to F7. Also, the photographs 2 to 9 show the cracks in other beams. The mid-span deflections for specimen types F1 to F7 are plotted in figures 3.15 to 3.20, to show their response to the applied load.

3.5.2 Beams with central bars only

The values of V_{FU}/V_{CU} are plotted against the percentage of horizontal web steel (ρ_b) in figure 3.21. This graph shows a line representing a rule for the

ultimate shear resistance V_{DU} , giving relationship between ϱ_b and the ratio V_{DU}/V_{CU}, which follows the trend given by the relationship between V_{FU}/V_{CU} and ϱ_b . This rule is only an indication of the contribution provided by the central steel on its own and a rule for contribution of web steel to the shear resistance of beams, provided jointly by links and the central bar, will be verified later in paragraph 3.5.4. The standard deviation for values of V_{DU}/V_{FU} is 0.1 as shown under the tables 3.5.1(a) and 3.5.1(b), which is considered as acceptable. The mean and standard deviation for all values of V_{DU}/V_{FU} shown in table 3.5.1 are 0.95 (< 1)and 0.12 respectively, which are also satisfactory. The rule is written as follows:

$$V_{DU} = V_{CU} + V_{BU} = (1 + 0.4\varrho_b)V_{CU} \leq 1.4V_{CU} \quad \ldots\ldots \qquad 3.5.1$$

All specimens were observed to have failed in shear. Specimens with central bars were able to sustain loads well after the appearance of initial cracks and the cracks did not widen significantly until failure. This was noticeably different to the specimens without web reinforcement, where the distress was clearly visible as the failure approached.

For 2100 mm span beams, when the load reached approximately 90% of the failure load, the tip of the predominant shear crack joined a flatter crack rising upwards towards the mid-span in the compression zone. (Figure 3.6) The failure was triggered when this junction appeared to split, demonstrating the action of excessive tensile stresses in the neutral axis region.

For 2100 mm span specimens, the inclined crack started generally at a distance greater than 200 mm from the support. In case of the 1400 mm span specimens, the crack started at a distance of about 150 mm from the support. In both cases, the predominant crack had a slope of approximately 1:1.5 and the failure was observed to be associated with the worsening of this predominant crack.

Table 3.5.1 : Beams without web reinforcement and beams with central bars (a) 1400 mm span beams

Spec No	A_{st}	Centre steel(ϱ_b)	f_{cu}	V_{FU} kN	V_{CU} kN	V_{FU}/V_{CU}	V_{DU} kN	V_{DU}/V_{FU}
A1	2T20	(0)	28	55	51	1.08	51	0.93
A1a				63		1.24		0.81
A2	"	2Y8(0.19)	36	67	55	1.21	59	0.89
A2a	[Test was abandoned; Test load application was faulty.]							-
B1	3T20	0	27	58	58	1.01	58	1.00
B1a				60		1.04		0.97
B2	"	2T10	27	65	58	1.13	64	0.98
B2a		(0.29)		68		1.18		0.94
B3	"	1T16	28	81	58	1.39	67	o.83
B3a		(0.38)		88		1.51		0.76
B4	"	1T20	33	101	62	1.64	76	0.75
B4a		(0.59)		110		1.78		0.69
B5	"	1T25	33	90	62	1.46	85	0.94
B5a		(0.93)		96		1.56		0.89
E1	3T25	0	28	72	67	1.07	67	0.93
E1a				75		1.11		0.89
E2	"	2T10	34	80	72	1.11	80	1.00
E2a		(0.30)		92		1.28		0.87
E3	"	2T12	34	90	72	1.25	84	0.93
E3a		(0.43)		84		1.17		1.00
E4	"	1T16	35	75	73	1.03	84	1.12
E4a		(0.38)		88		1.21		0.95
						Mean V_{DU}/V_{FU} :		0.91
						Standard deviation :		0.10

Table 3.5.1 (continued):
(b) 2100 mm span beams

Spec No	A_{st}	Centre steel(ϱ_b)	f_{cu}	V_{FU} kN	V_{CU} kN	V_{FU}/V_{CU}	V_{DU} kN	V_{DU}/V_{FU}
F1	3T20	0	43	69	67	1.03	67	0.97
F1a				75		1.11		0.89
F2	"	1T12	44	80	68	1.18	74	0.93
F2a		(0.21)		82		1.21		0.90
F3	"	1T16	46	76	69	1.10	79	1.04
F3a		(0.38)		82		1.19		0.96
F4	"	1T20	44	86	68	1.27	84	0.98
F4a		(0.59)		79		1.17		1.06
F5	"	1T25	43	82	67	1.22	92	1.12
F5a		(0.93)		80		1.19		1.15
F6	"	2T20	34	75	62	1.18	87*	1.16
F6a		(1.18)		72		1.16		1.21

(* V_{DU} for specimen type F6 is limited to $1.4V_{CU}$)

Mean V_{DU}/V_{FU} : 1.03
Standard deviation : 0.10

For specimen types B5, F5 and F6, with larger amount of central bars and without links, the test results are close to or less than the values of V_{DU} . It was observed in paragraph 3.4.2.1 above, that the effectiveness of the horizontal web steel could be restricted if it is not adequately complemented by a vertical component. This will be discussed in paragraph 3.5.4.

3.5.3 Beams with links and central bars

Table 3.5.2 shows the results of tests carried out on 1400 mm span specimen series D. Table 3.5.2 also shows details extracted from table 3.3.2 for test on beam C1, a beam with links only, for easy comparison with specimens type D. V_{LU} , the contribution of links to the ultimate shear resistance, is calculated as "A_{sw} x d x f_{yv}/s". (Equation 3.3.4)

These beams had the same cross-section as the other beams, 200 x 300 mm. The amount of longitudinal steel was 2T12 at top and 3T20 at bottom. The links were T6 single links at 200 centres. Table 3.5.2 shows f_{cu} , the amount of central steel and the corresponding estimates of the ultimate shear resistance (V_{DU} = $V_{CU}+V_{BU}+V_{LU}$). The mean value of V_{DU}/V_{FU} is 0.82 (<1.0) and the standard deviation is 0.11, which demonstrate that the rules are satisfactory.

Table 3.5.2: Beams with links and central bars

Spec No	Centre steel(ϱ_b)	f_{cu} N/mm^2	V_{FU}	V_{CU} kN	V_{BU} kN	V_{LU}	V_{DU}	V_{DU}/V_{FU}
C1	(0)	32	119	61	-	34.5	95.5	0.80
C1a			128					0.75
D1	2T10	32	132	61	7	34.5	102.5	0.78
D1a	(0.29)		141					0.72
D2	1Y16	28	146	58	9	34.5	101.5	0.69
D2a	(0.38)		154					0.66
D3	1Y20	26	130	57	14	34.5	105.5	0.81
D3a	(0.59)		134					0.79
D4	1Y25	26	134	57	21	34.5	112.5	0.84
D4a	(0.93)		133					0.85
					*	*		
F7	2T20	34	110	62	25	25.5	112.5	1.02
F7a	(1.18)		104					1.09

(* V_{BU} for F7 and F7a is limited to $0.4V_{CU}$
and V_{LU} is calculated with f_{yv} = 342 N/mm^2)

Mean V_{DU}/V_{FU} : 0.82
Standard deviation : 0.11

The tension reinforcement for beams F7 and F7a was chosen to be 3T20, same as the tension steel for beam types B, C and D, to achieve an equitable comparison of the effectiveness of web steel. With this amount of tension steel, the applied load was expected to be close to the limits of flexural load-carrying capacity of the beam and its ultimate shear resistance. This was confirmed by the test. Severe cracking was noticed in the compression zone as well as at the tension steel level, when the failure approached. (Figures 3.13 and 3.14). Both beams

failed as a result of worsening of the main shear crack on the left hand side. The overall shear resistance (V_{DU}), obtained as a sum of V_{CU} , V_{BU} and V_{LU} , was close to the failure loads for these beams. It is possible that the provision of strain gauges in beam F7a could have caused some local weakness. This could be the reason for the marginal difference in failure loads of beams F7 and F7a, which were subjected to the critical shear-compression type of failure.

Figure 3.20 shows the mid-span deflections which follow a smooth curve. At failure, the excessive cracking and deterioration in the compression block concrete appears to have caused strains in the tension steel (e_t) which correspond to tensile stresses in excess of the yield stress, shown as ** in table 3.5.5 under paragraph 3.5.4. Table 3.5.5 shows that the strain in the tension steel "e_t" increases gradually with the applied load. This is also demonstrated in figure 3.23, by the graph representing values of "e_t/100" ranging numerically from 0 to 27.72 on the Y-axis, plotted against the applied shear on the X-axis.

3.5.4 Strains in web reinforcement

Tables 3.5.3, 3.5.4 and 3.5.5 show micro-strain measurements e_b, e_t and e_l for central bars, tension steel and links respectively, obtained from the tests on specimens F6a and F7a. The readings refer to locations of gauges as shown in figure 3.22. The corresponding stresses, v_b (for central bars), v_t (tension steel) and v_l (links), are calculated using the modulus of elasticity of steel as 200 kN/mm^2. It is observed that higher stress is developed in the lower central bar. The stress in the central steel is the average of stresses in the two bars, based on strains given by gauges 5 and 7 on the left hand side (LHS) and 6 and 8 on the right hand side (RHS). Also, the stress in the link on each side is the average of stresses in two legs, based on strains given by LHS gauges 1 and 2 and the RHS gauges 3 and 4. The stress in the tension steel at various stages of the loading is obtained from the readings given by the strain gauge 9.

From tables 3.5.3 and 3.5.5 and figure 3.23, it can be seen that the central bars in beam F7a are able to develop stresses which are larger than those developed in the central bars in beam F6a. This effect is clearly attributable to the

provision of links in beam F7a, which enables the beam to sustain the component of principal tensile stresses in the direction perpendicular to the central bars, as shown in the sketch 3.4. At the ultimate state of failure, the rule suggested in paragraph 3.4.2.1, equation 3.4.1, is verified as follows, using values for stresses from the LHS gauges (beam F7a) given in table 3.5.5:

$$V_{BU} = (0.3\ v_b\ A_b)/1000 = 0.3 \times 152 \times 628/1000 = 29\ kN$$

V_{BU} is given as 25 kN in table 3.5.2, which is its maximum value, $0.4V_{CU}$. Without this limit, V_{BU} will be $0.4x\varrho_b xV_{CU}$ or 32 kN. The rule given by equation 3.4.1 is, therefore, considered as acceptable.

The contribution of links is deduced from the measured stresses as follows:

$$V_{LU} = \frac{v_l\ A_{sw}\ d}{s} = 186\ x\ \frac{75}{1000} = 14kN$$

The contribution of links is shown as 25.5 kN in table 3.5.2. However, as discussed in paragraph 3.3.1, the tension in links forms only a part of the contribution of links. The links also provide enhancement in V_{CU} , by sharing the aggregate interlock and dowel action contributions, which is implied in the empirical rule but it could not be measured. The lower stress in the links in beam F7a is also due to their interaction with the large amount of central bars, which will be discussed in paragraph 3.5.5 and in chapter 4.

The sum of V_{CU} , V_{BU} and V_{LU} give the estimated overall shear resistance (V_{DU}) which is validated by the test result for beam F7a. (Table 3.5.2)

Table 3.5.3: Stresses and strains in the central bars and the tension steel for beam F6a

V kN	e_b	v_b (N/mm^2) LHS	RHS	e_t	s_t (N/mm^2)
9.8	(-2+69)/2	6.7		223	44.6
	(-7+54)/2		4.7		
19.6	(-11+117)/2	10.6		392	78.4
	(-20+88)/2		6.8		
29.5	(-7+192)/2	18.5		593	118.6
	(-23+136)/2		11.3		
39.3	(20+328)/2	34.8		900	180.0
	(-6+265)/2		25.9		
52.5	(59+489)/2	54.8		1267	253.4
	(29+416)/2		44.5		
61.3	(102+631)/2	73.3		1562	312.4
	(80+527)/2		60.7		
71.1	(159+780)/2	93.9		1846	369.2
	(172+658)/2		83.0		

Table 3.5.4: Stresses and strains in the links for beam F7a

V kN	Left Hand Side e_l	v_l (N/mm^2)	Right Hand Side e_l	v_l (N/mm^2)
9.8	(-21-8)/2	-2.9	(19+26)/2	1.1
19.6	(-33-12)/2	-4.5	(30+38)/2	1.8
29.5	(-48-16)/2	-6.4	(44+50)/2	2.8
39.3	(0+0)/2	0	(94+86)/2	9.4
52.5	(110+81)/2	19.1	(172+178)/2	25.3
61.3	(181+181)/2	36.2	(257+252)/2	43.8
71.1	(250+300)/2	55.0	(345+347)/2	64.5
81.0	(348+406)/2	75.4	(465+488)/2	87.1
90.2	(587+669)/2	125.6	(593+681)/2	126.2
100	(802+883)/2	168.5	(898+1021)/2	158.1
103	(882+973)/2	185.5	(857+1197)/2	183.0

Table 3.5.5: Stresses and strains in the central bars and the tension steel for beam F7a

V kN	e_b	v_b (N/mm^2) LHS	RHS	e_t	v_t (N/mm^2)
9.8	(2+74)/2	7.6		240	48.0
	(5+88)/2		9.3		
19.6	(-4+123)/2	11.9		416	83.2
	(0+145)/2		14.5		
29.5	(-6+180)/2	17.4		602	120.4
	(1+211)/2		21.2		
39.3	(19+318)/2	38.7		874	174.8
	(34+343)/2		37.7		
52.5	(42+503)/2	54.5		1205	241.0
	(66+512)/2		57.8		
61.3	(73+655)/2	72.8		1492	298.4
	(78+654)/2		73.2		
71.1	(110+797)/2	90.7		1751	350.2
	(107+795)/2		90.2		
81.0	(144+918)/2	106.2		1955	391.0
	(160+906)/2		106.6		
90.2	(175+1104)/2	127.9		2316	**
	(183+1037)/2		122.0		
100	(186+1277)/2	146.3		2572	**
	(251+1216)/2		146.7		
103	(174+1342)/2	151.6		2717	**
	(298+1318)/2		161.6		

[** indicates stresses in excess of the yield stress. (paragraph 3.5.3)]

Table 3.5.6 shows the ratios of contributions of the web steel to the ultimate shear resistance of concrete, at the LHS location of the strain gauges for beam F7a; (V_b/V_{CU}) for the central bars and (V_l/V_{CU}) for the links. V_w/V_{CU} is the sum of these two ratios. Figure 3.24 shows these ratios plotted on Y-axis, with V/V_{CU} on the X-axis.

Table 3.5.6: Change in the contribution of web steel with the increase in applied load for beam F7a

V kN	V/V_{CU}	V_b/V_{CU}	V_l/V_{CU}	V_W/V_{CU}
9.8	0.16	0.02	0	0.02
19.6	0.31	0.04	-0.01	0.03
29.5	0.47	0.05	-0.01	0.04
39.3	0.63	0.12	0	0.12
52.5	0.84	0.16	0.03	0.19
61.3	0.98	0.22	0.04	0.26
71.1	1.14	0.27	0.07	0.34
81.0	1.30	0.32	0.09	0.41
90.2	1.45	0.39	0.15	0.54
100	1.61	0.44	0.21	0.65
103	1.65	0.46	0.22	0.68

In the case of beam F7a, v_l is the stress measured in one link and it could represent the links spaced at 200 mm over the length 265 mm, almost on its own. The stress in the next link nearer to the support could be lower. (This will be discussed in the finite element analysis in paragraph 4.4.3 of chapter 4.) This reduction in stresses, however, is not considered to be significant.

Table 3.5.4 shows that the links do not reach the yield stress. The lower stresses in links in beam F7a indicate that there could be an interaction between the central steel and the links. This interaction is believed to depend on the proportion of the two provisions of web reinforcement. Further study is required to determine the optimum combination of links and central bars. However, a rule can be deduced from figure 3.24, related to the ultimate condition of the beam. The following rule is proposed:

$$\frac{V_W}{V_{CU}} = \frac{V}{V_{CU}} - 1$$

or

$$V = V_{CU} + V_W$$

The ultimate applied shear is required to be less than V_{DU}, the ultimate shear resistance of the section. The combined effect of web steel V_W is replaced by a sum of the ultimate state contributions of central bars and links, given by the rules for V_{BU} and V_{LU} subject to their limitations.

$$\therefore \quad V_{DU} = V_{CU} + V_{WU} = V_{CU} + V_{BU} + V_{LU} \quad \ldots \quad 3.5.2$$

$$V_{BU} = 0.4\ \rho_b\ V_{CU} \leq 0.4\ V_{CU} \quad \ldots \quad 3.5.3$$

Also, the contribution of links is given by equation 3.3.4.

$$V_{LU} = \frac{A_{sw}\ f_{yv}\ d}{s}$$

3.5.5 Recommendation for beams with links and central bars

The test results for specimens D1, D2 and D3 (Table 3.5.2) show that the shear at failure (V_{FU}) exceeds the estimated ultimate capacity of the section (V_{DU}). V_{DU} is the sum of the ultimate state contributions V_{BU} , V_{LU} and V_{CU} . These test results also show that the contribution of the central bars does not increase in direct proportion with the area of the central bar. This is due to the interaction between central bars and links. The stresses developed in the individual web steel could vary and the links could develop smaller stresses in conjunction with a larger central bar. However, the estimates of the ultimate shear resistance V_{DU} , as an addition of V_{CU} and the combination of contributions V_{LU} and V_{BU} , are quite satisfactory. It is recommended, therefore, that a central bar with an area $\leq$ 1% of the area of cross-section should be provided in beams with links to provide V_{BU} not exceeding $0.4V_{CU}$, as an enhancement to the shear resistance additional to that provided by the links.

Figure 3.24 shows the combined shear resistance of central bar and links (V_b + V_l) in the region where $V < 1.4V_{CU}$. This is similar to the contribution of links discussed earlier in this chapter, justifying the BS8110 rule for minimum amount of links [$(v - v_c) \geq 0.4$ N/mm^2]. This requirement applies approximately to

the range $0.5V_{CU} < V < 1.4V_{CU}$ and it could be met by an adequate combination of central bar and links with minimum spacing only, corresponding to the beam depth and the diameter of longitudinal steel.

3.6 Test programme for flat slabs

3.6.1 Test specimens and procedure

Fifteen 3 x 3m specimens were tested using a procedure similar to the earlier test programme as described in Reference**[44]**. The details of specimens were as follows:

Specimens 1 to 5 :
Overall depth 150 mm (d = 120 mm); bottom steel T6@160 and top (tension) steel T10@80 (ϱ = 0.81).
Specimens 6 to 9 :
Overall depth 200 mm (d = 165 mm); bottom steel T8@160 and top (tension) steel T16@160 (ϱ = 0.76).
Specimens 10 to 15 :
Overall depth 250 mm (d = 210 mm); bottom steel T8@175 and top (tension) steel T20@175 (ϱ = 0.85).

Conventionally, a slab specimen for punching shear tests is simply supported at the nominal line of contraflexure. This line is assumed to be at 0.2L from the column centre, where L is the span (Figure 3.4). The test specimens were 3 x 3 m. All specimens were cast in timber moulds and cured under polythene for seven days. They were then lifted and positioned on the test rig until testing, about 14 days later.

Table 3.6.1 shows the values of f_{cu} and the amount of central bars. f_{cu} was the average of the results of three tests on air-cured cubes, which were carried out at the time of the test on the corresponding specimen. The cubes were cured in the same way as the test specimens were cured.

The test arrangement is shown in figure 3.5 and it is also illustrated in photograph 10. The load was applied by means of hydraulic jacks at eight locations on the circumference of a circle of diameter 2.4 m, acting through load cells and prestressing cables. The hydraulic jacks were linked to a common supply so that the force on each cable was the same. The load was applied in equal increments of approximately 50 kN. The loads were recorded at eight loading points.

V_{FU} (kN) was the failure load as observed plus the self-weight of the specimen. V_{CU} was calculated using the following rule which is derived from the BS8110 rule[28] for design shear resistance, excluding the partial factor γ_m:

$$V_{CU} = 0.27\ \rho^{1/3}\ f_{cu}^{1/3}\ \left(\frac{400}{d}\right)^{1/4}\ \frac{ud}{1000} \quad kN$$

In calculating V_{CU} , the actual values of f_{cu} were used even where f_{cu} exceeded 40 N/mm^2 for the same reasons as for the beam tests. V_{BU} is given by the equation 3.6.2 which is derived from equation 3.4.3, using ϱ_{bu} in place of ϱ_b . ϱ_{bu} is named as the "Horizontal steel factor" and it represents the effect of horizontal steel in terms of ϱ_b , u (the shear perimeter) and u_0 (the perimeter of column or the loaded area).

$$V_{BU} = K\ \rho_b\ \frac{(u + u_0)}{u}\ V_{CU} \quad kN \qquad \ldots \quad 3.4.3$$

$$\rho_{bu} = \frac{\rho_b\ (u + u_0)}{u} \qquad \ldots \quad 3.6.1$$

$$\therefore\ V_{BU} = K\ \rho_{bu}\ V_{CU} \quad kN \qquad \ldots \quad 3.6.2$$

Table 3.6.1 gives the test results and the ultimate shear resistance V_{DU} . ($V_{DU} = V_{CU} + V_{BU}$; The rule for V_{BU} is given by equation 3.6.3 in the next paragraph.)

Table 3.6.1: Results of tests on slab specimens

Spec No.	f_{cu}	Central Steel (ϱ_{bu})	V_{CU} kN	V_{FU} kN	V_{FU} / V_{CU}	V_{DU} kN	V_{DU}/V_{FU}
1	44	- (0)	438	489	1.12	438	0.90
2	37	T6@160 (0.225)	414	502	1.21	451	0.90
3	23	T8@160 (0.400)	353	448	1.27	409	0.91
4	38	T10@160 (0.624)	418	556	1.33	522	0.94
5	46	T10@80 (1.249)	445	575	1.29	605	1.05
6	47	- (0)	656	938	1.43	656	0.70
7	47	T8@160 (0.275)	656	883	1.35	728	0.82
8	29	T12@160 (0.620)	558	811	1.45	696	0.86
9	29	T16@160 (1.102)	558	853	1.53	804	0.94
10	44	- (0)	919	1356	1.47	919	0.68
11	35	T10@175 (0.297)	852	1278	1.50	953	0.67
12	37	T12@175 (0.427)	868	1467	1.69	1016	0.69
13	33	T16@175 (0.760)	835	1190	1.42	1089	0.92
14	46	T20@175 (1.187)	933	1354	1.45	1376	1.02
15	23	T25@175 (1.854)	741	1210	1.63	1186	0.98
					Mean V_{DU}/V_{FU}:		0.86
					Standard deviation :		0.12

The standard deviation for all the values of V_{DU}/V_{FU} is influenced particularly by the high failure loads for 250 mm thick specimens 10, 11 and 12. The standard deviation for 150 mm and 200 mm thick slabs are 0.06 and 0.09 respectively. The mean V_{DU}/V_{FU} is 0.86 which is well below 1.00, and the rule is considered to be satisfactory.

The specimens failed in a punching shear failure mode, with the crack

patterns similar to those observed in the earlier test programme[38]. Photographs 11 and 13 show crack-patterns for 150 mm and 200 mm thick specimens without central steel. Photographs 12, 14 and 15 show crack-patterns for slabs with central mesh and of various depths, 150 mm, 200 mm and 250 mm. Although the crack-patterns do not appear distinctly different, it was noted that the failure of slabs with central steel was less brittle than for slabs without any central bars.

3.6.2 Conclusions from the flat slab tests

Values of V_{FU}/V_{CU} (table 3.6.1) are plotted against ρ_{bu} in figure 3.25. From figure 3.25, the constant "K" used in equation 3.6.2 is derived using the lower bound of the test data. The maximum contribution of the central mesh (V_{BU}) appears to have a limit similar to the limit observed earlier for beams. The following rule is deduced from the test results:

$$V_{BU} = 0.4\ \rho_{bu}\ V_{CU} \quad \ldots \quad 3.6.3$$

$$V_{BU} \leq 0.003\ d\ V_{CU}$$ (d is the effective depth in mm)

or

$$V_{BU} \leq 0.6\ V_{CU}$$ whichever is the lesser.

For slabs, the limit on V_{BU} ($0.6V_{CU}$) is higher than that for the beams ($0.4V_{CU}$). This could be attributable to the punching type of shear failure in slabs which allows the central mesh to provide a better dowel resistance at the centre of the crack compared with that of the central bars for beams. Also, it seems that the effectiveness of the central mesh as a dowel increases with the larger crack surface for deeper slabs, up to the maximum limit of $0.6V_{CU}$.

The central mesh could be used on its own for all flat slabs including those with depth less than 200 mm. Also, a suitable central mesh could be provided to give $(v - v_c) \geq 0.4$ N/mm^2, instead of links. If the applied shear V_U is large and the shear resistance of the slab cannot be sufficiently enhanced by the central bars, links could be used together with the central bars, up to a limit "$V_U \leq 2V_C$"[38].

3.7 General Conclusions and recommendations

The ultimate applied shear should be less than or equal to the ultimate shear resistance (V_{DU}) which is expressed as the sum of the contributions of concrete (V_{CU}), links (V_{LU}) and the cental steel (V_{BU}). The rules for contributions of concrete (V_{CU}), links (V_{LU}) and the central bar (V_{BU}) for beams have been derived in this chapter, on the basis of test results. The rule for V_{BU} for slabs is also derived in the same way. The other rules for flat slabs, for contributions to the punching shear resistance provided by concrete section and the links, are available in the codes of practice.

The rules for V_{BU} could be used in conjunction with any design method allowing for the contribution of concrete as additional to that of the web reinforcement, provided that the corresponding limits of application and the values of depth factors etc. are used. The partial factor for obtaining the design value V_B should be the same as the factor applicable to the contribution of the concrete section, V_C , according to the design method in use. For example, when following the BS8110 design method, this partial factor for calculating V_B should be 1.25.

For flat slabs, a central mesh could serve on its own as shear reinforcement, especially for slabs with an overall depth less than 200 mm. The central bars are not expected to be used on their own in beams, where some provision of links is necessary for forming the reinforcement cages. However, the central bars could provide an effective supplement to the contribution of links and they could assist in avoiding congestion of steel. For beams, a rule for estimating the combined effect of central bars and links is given in this chapter, subject to the limitations on the contribution of the central bars. Further research is necessary for determining the optimum combination of central bars and links.

In addition to their contribution to the shear resistance of the section, the central bars could afford some ductility and reduce the undesirable brittleness of shear failure. Specimens with central bars were able to sustain loads well after the appearance of initial cracks and the cracks did not widen significantly until failure. This was noticeably different to the specimens without web reinforcement, where

the distress was clearly visible as the failure approached.

The ductility provided by the central bars could be an important consideration in the design against accidental loading. The enhanced ductility provided by the central bars and their location protected by the surrounding concrete could be considerably advantageous for design including fire exposure conditions.

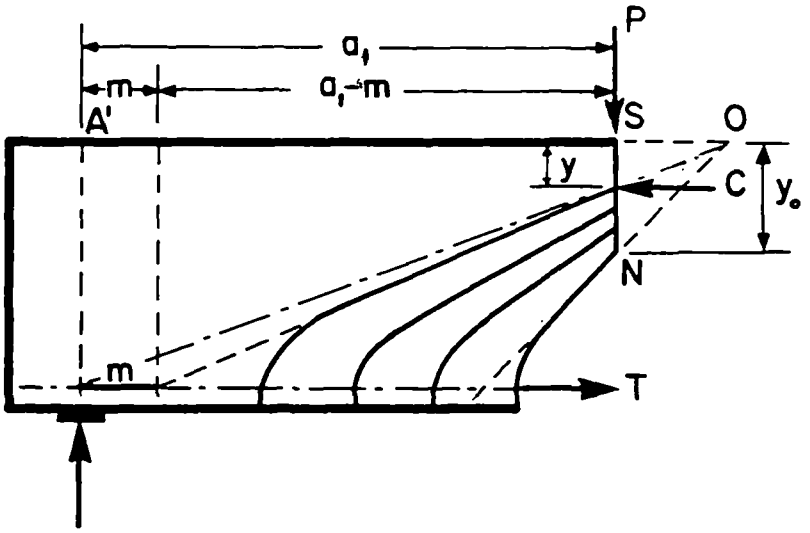

CONDITIONS PRIOR TO DIAGONAL FAILURE

(Note: y_0= nd, compression block corresponding to flexural failure
y = n_1d, post cracking depth of the compression block

FIGURE 3.1

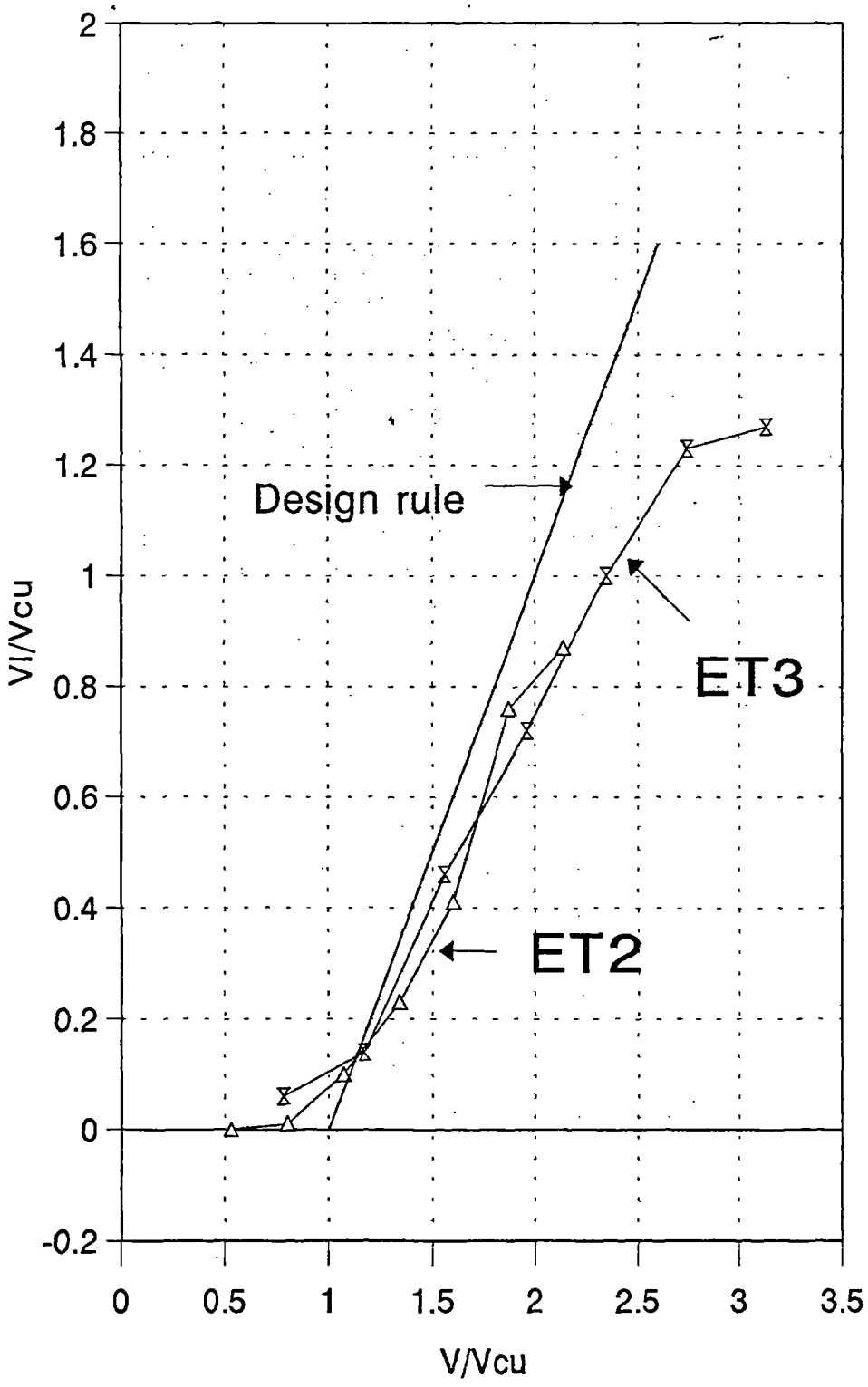

Contribution of links (Leonhardt's tests)

FIGURE 3.2

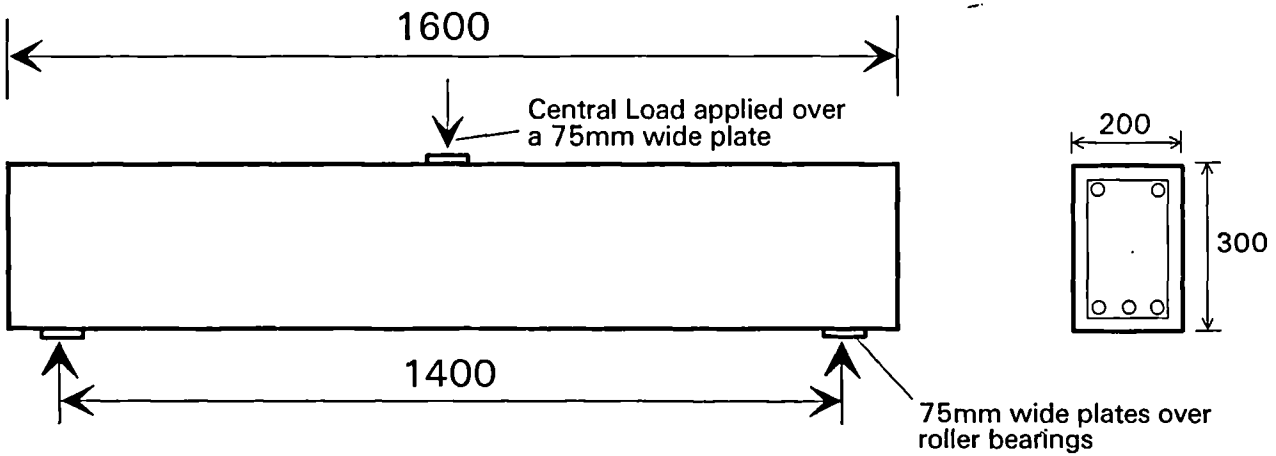

Details of Specimen for tests on beams

FIGURE 3.3

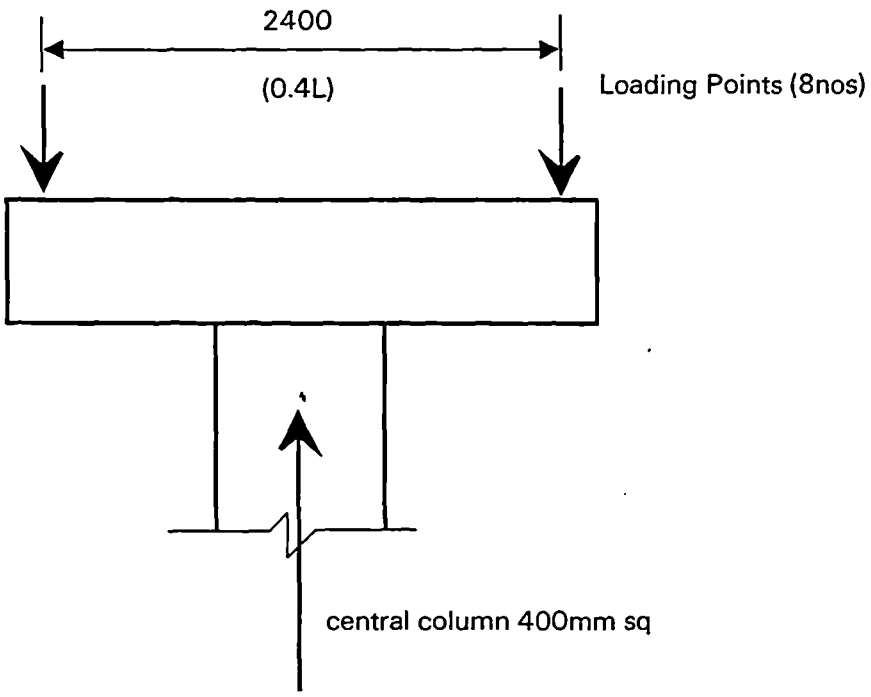

Specimen for punching shear test on slabs

FIGURE 3.4

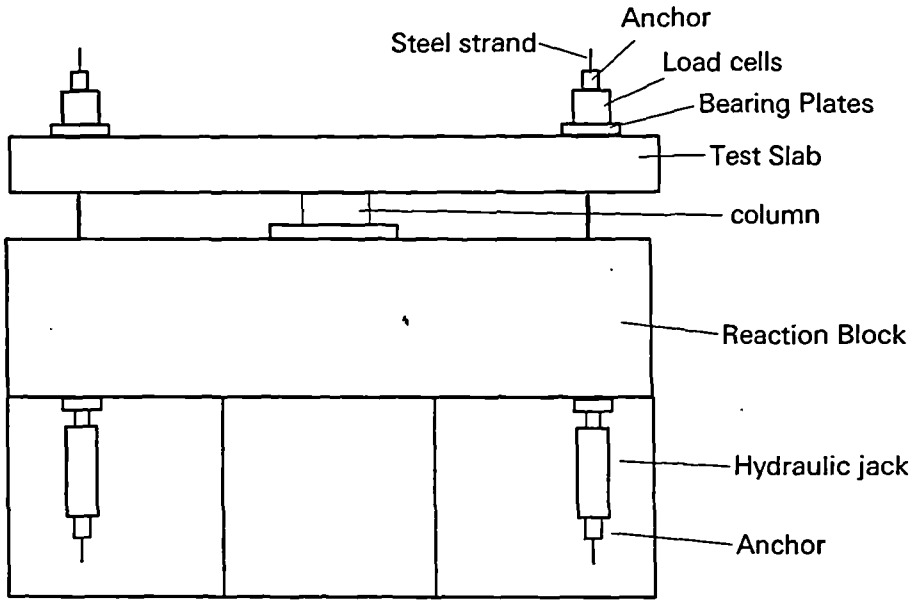

Arrangement for slab tests

FIGURE 3.5

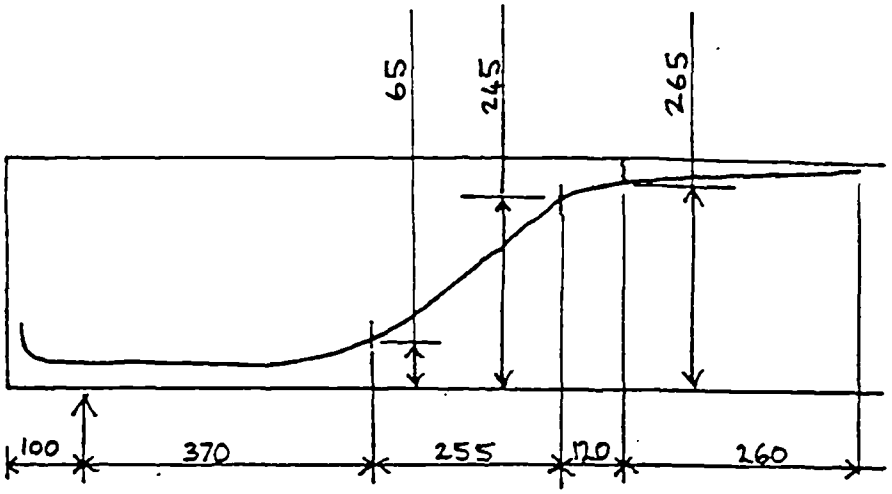

Beam F1

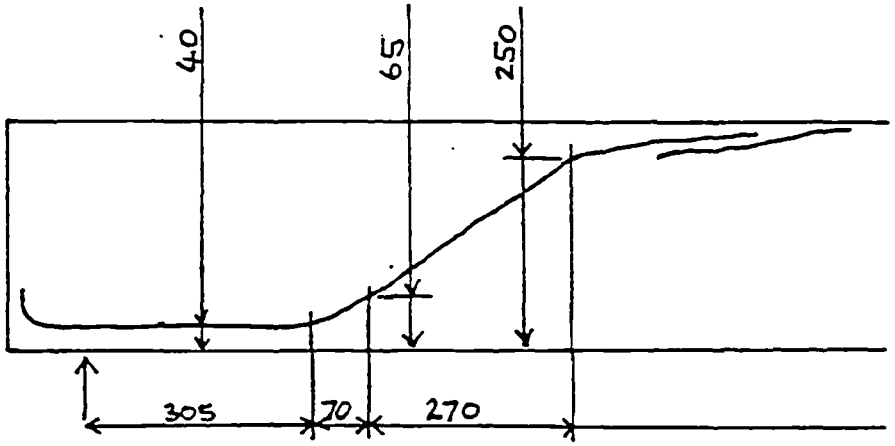

Beam F1a

Beams F1 and F1a Diagonal crack geometry at failure

FIGURE 3.6

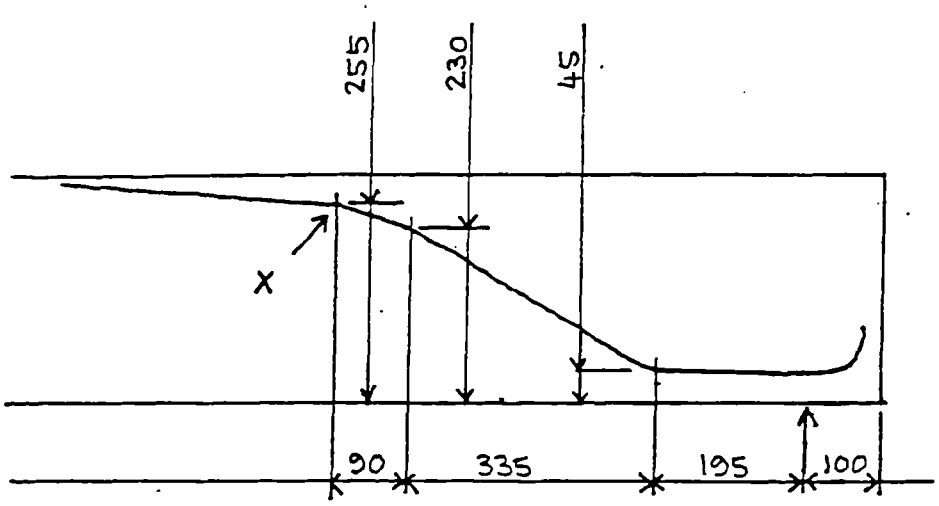

Beam F2

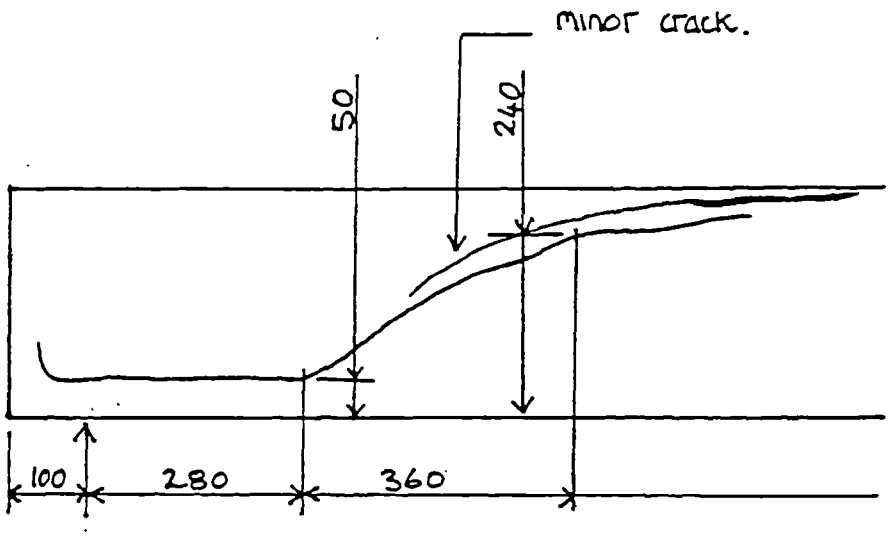

Beam F2a

Beams F2 and F2 Diagonal crack geometry at failure

FIGURE 3.7

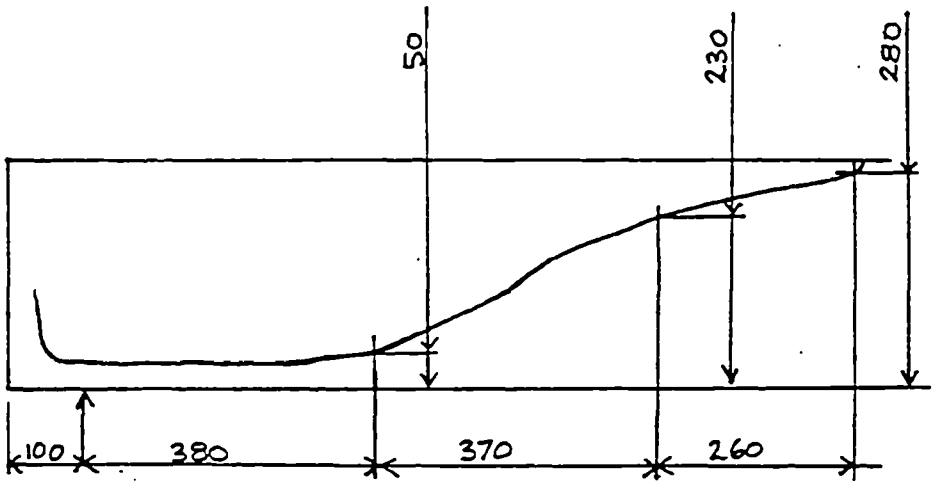

Beam F3a

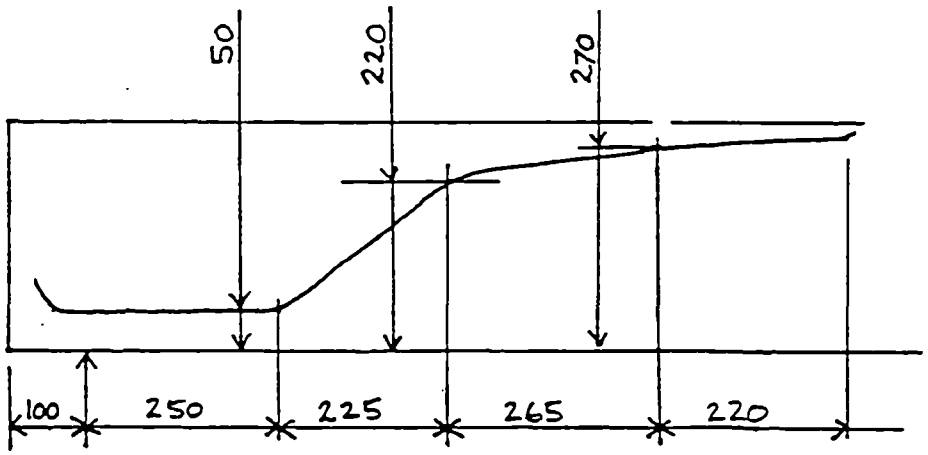

Beam F3

Beams F3 and F3a Diagonal crack geometry at failure

FIGURE 3.8

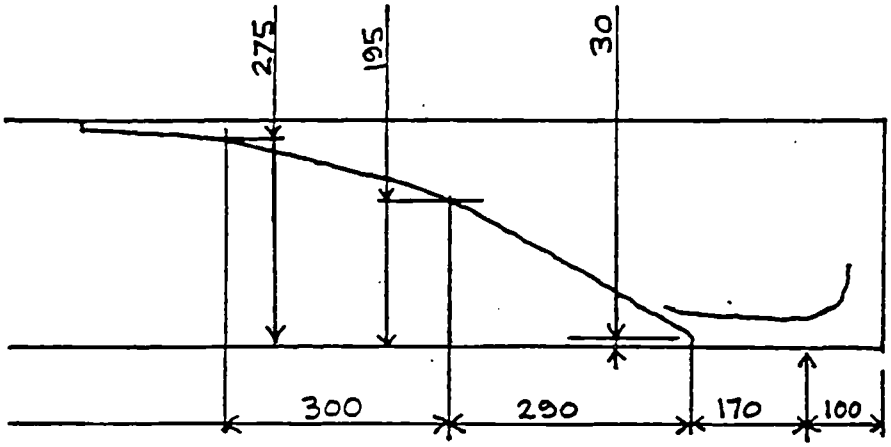

Beam F4

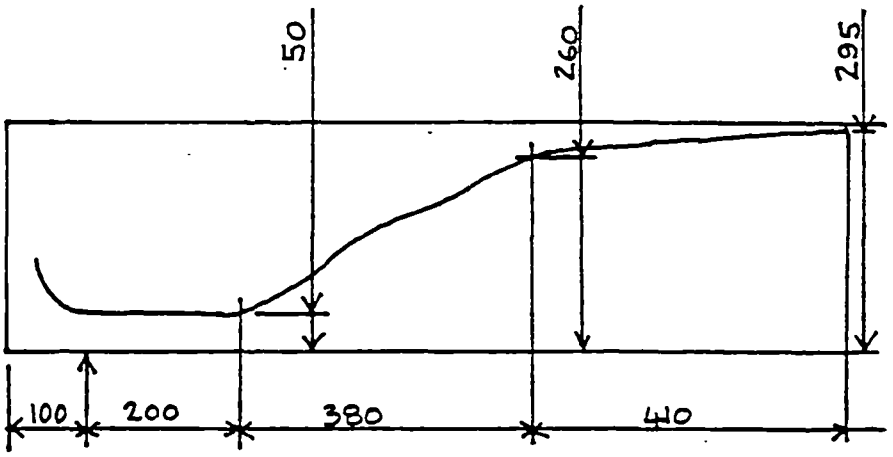

Beam F4a

Beams F4 and F4a Diagonal crack geometry at failure

FIGURE 3.9

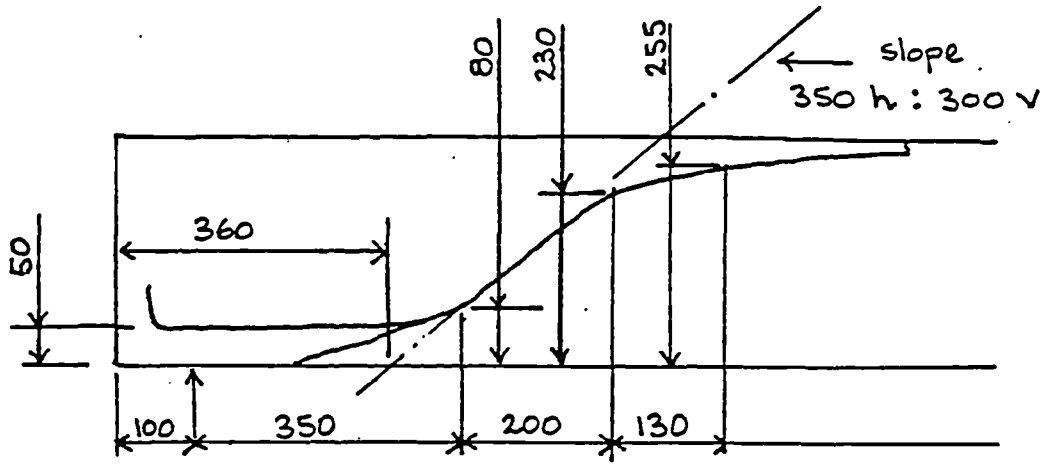

Beam F5

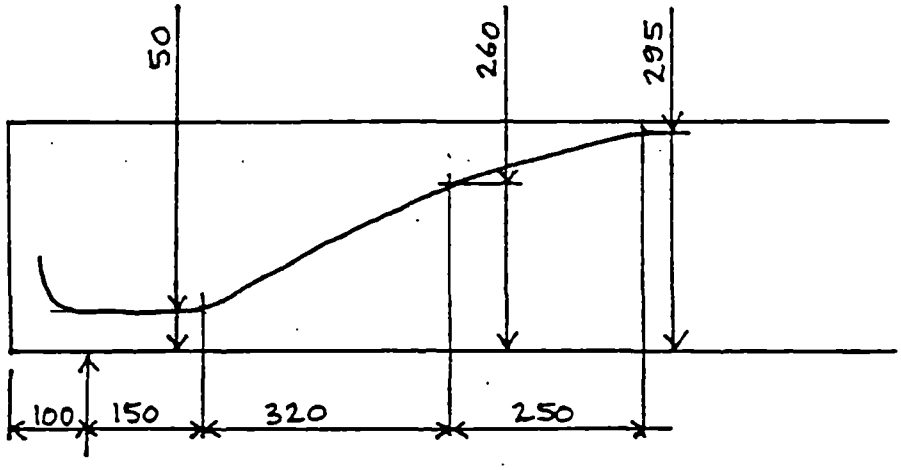

Beam F5a

Beams F5 and F5a Diagonal crack geometry at failure

FIGURE 3.10

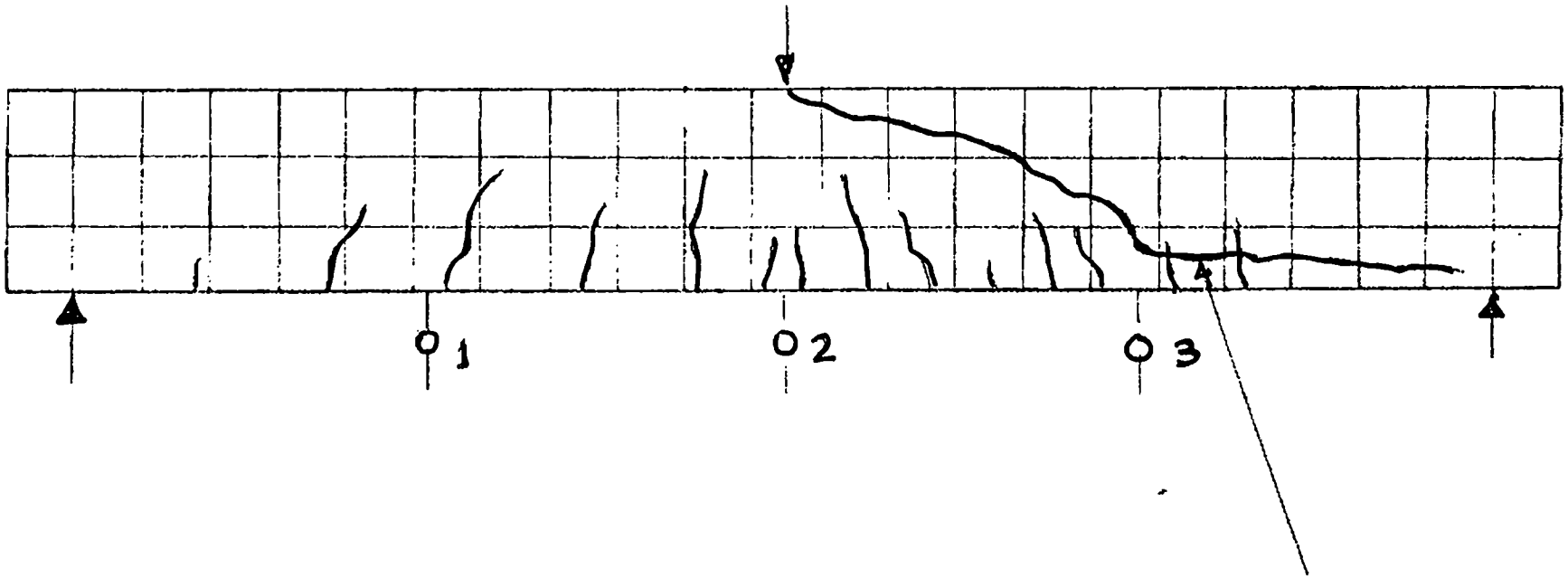

Beam F6 : Diagonal Crack geometry at failure

FIGURE 3.11

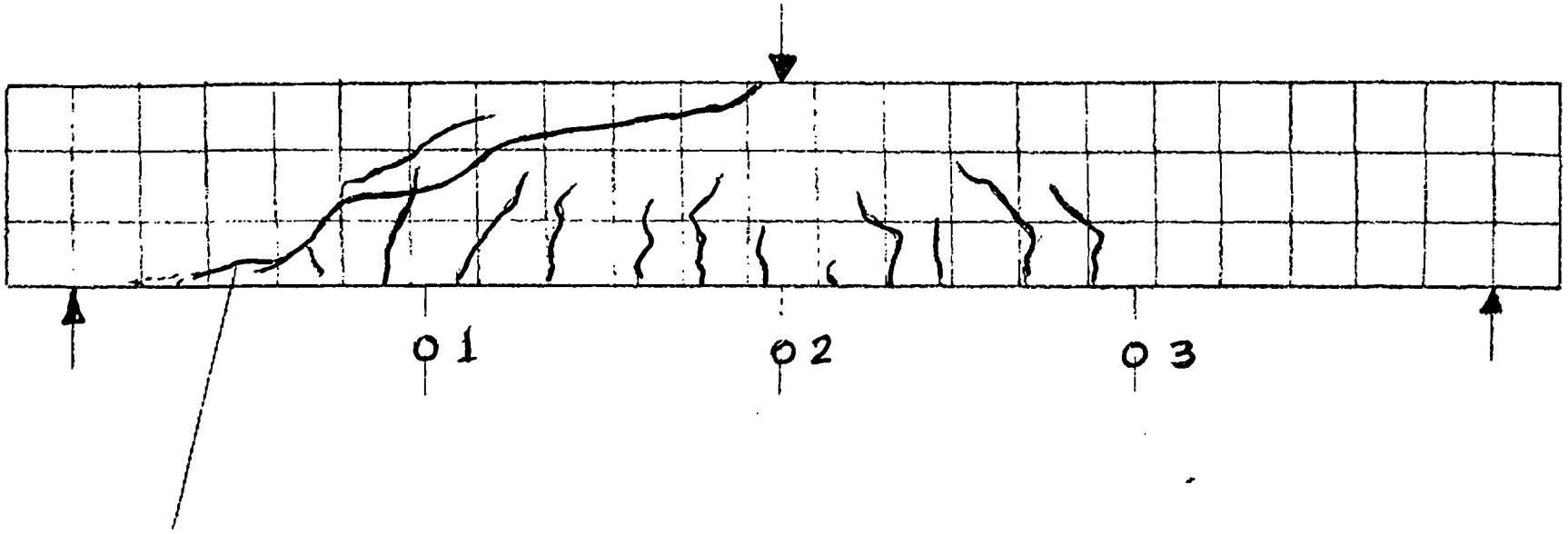

Beam F6a: Diagonal Crack geometry at failure

FIGURE 3.12

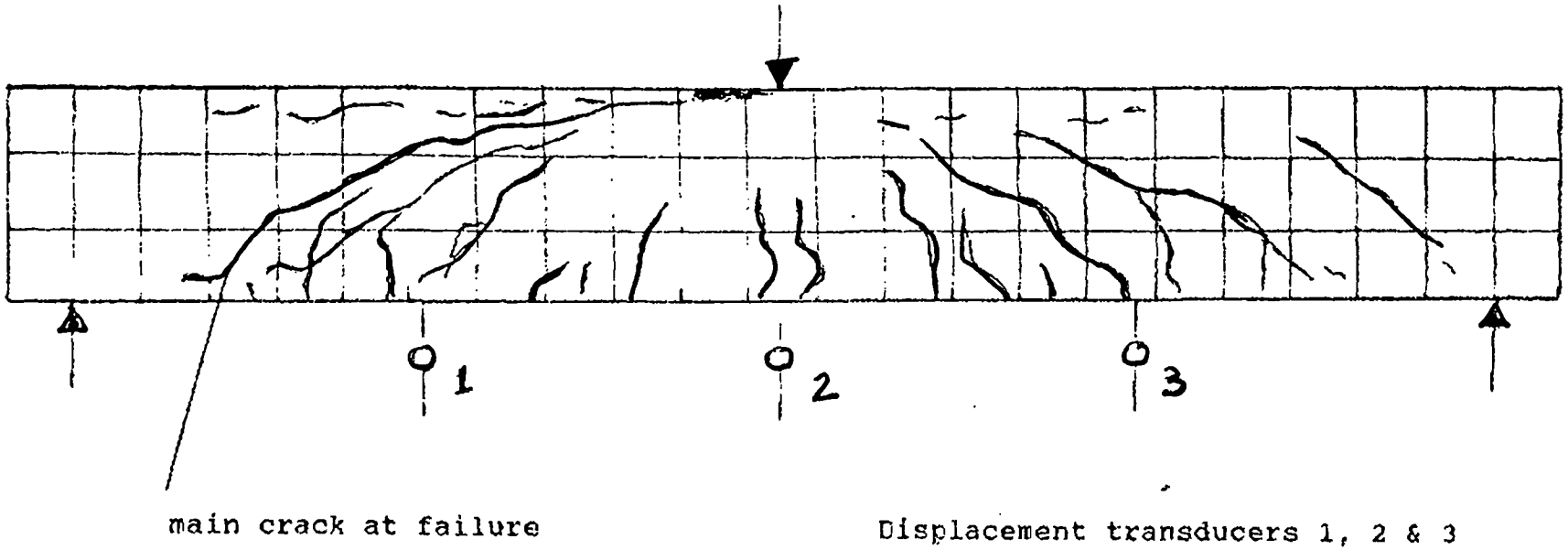

Beam F7 : Diagonal Crack geometry at failure

FIGURE 3.13

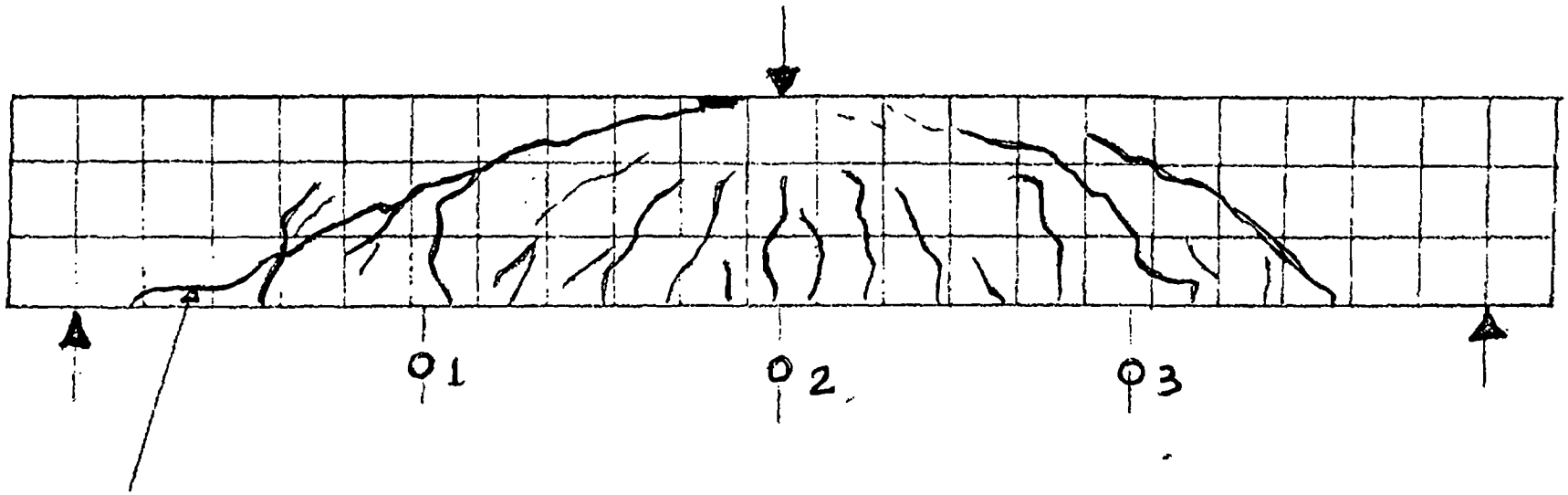

Beam F7a: Diagonal Crack geometry at failure

FIGURE 3.14

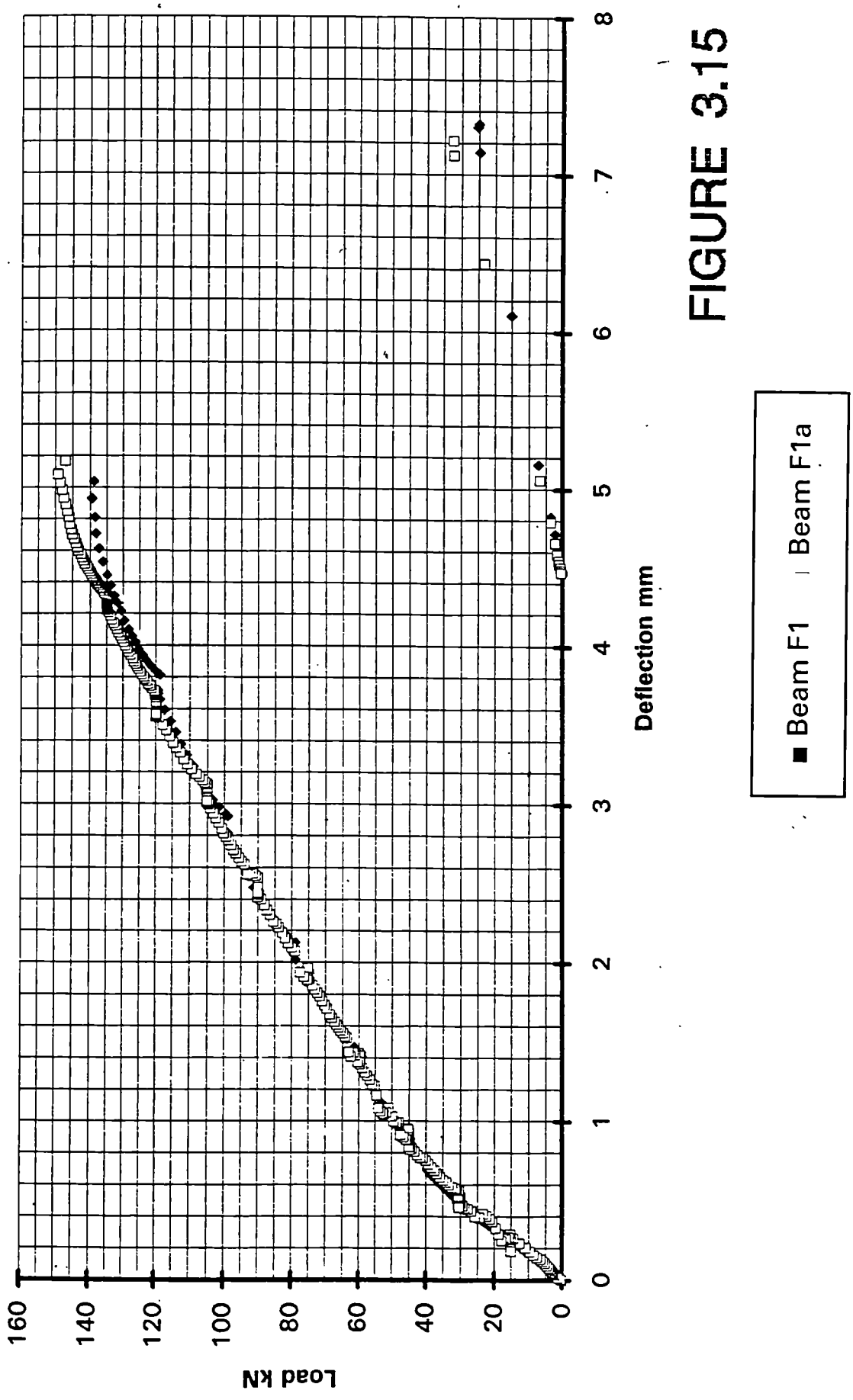
Load kN
0
20
40
60
80
100
120
140
160
0
1
2
3
4
5
6
7
8
Deflection mm
Beam F1
Beam F1a

FIGURE 3.15

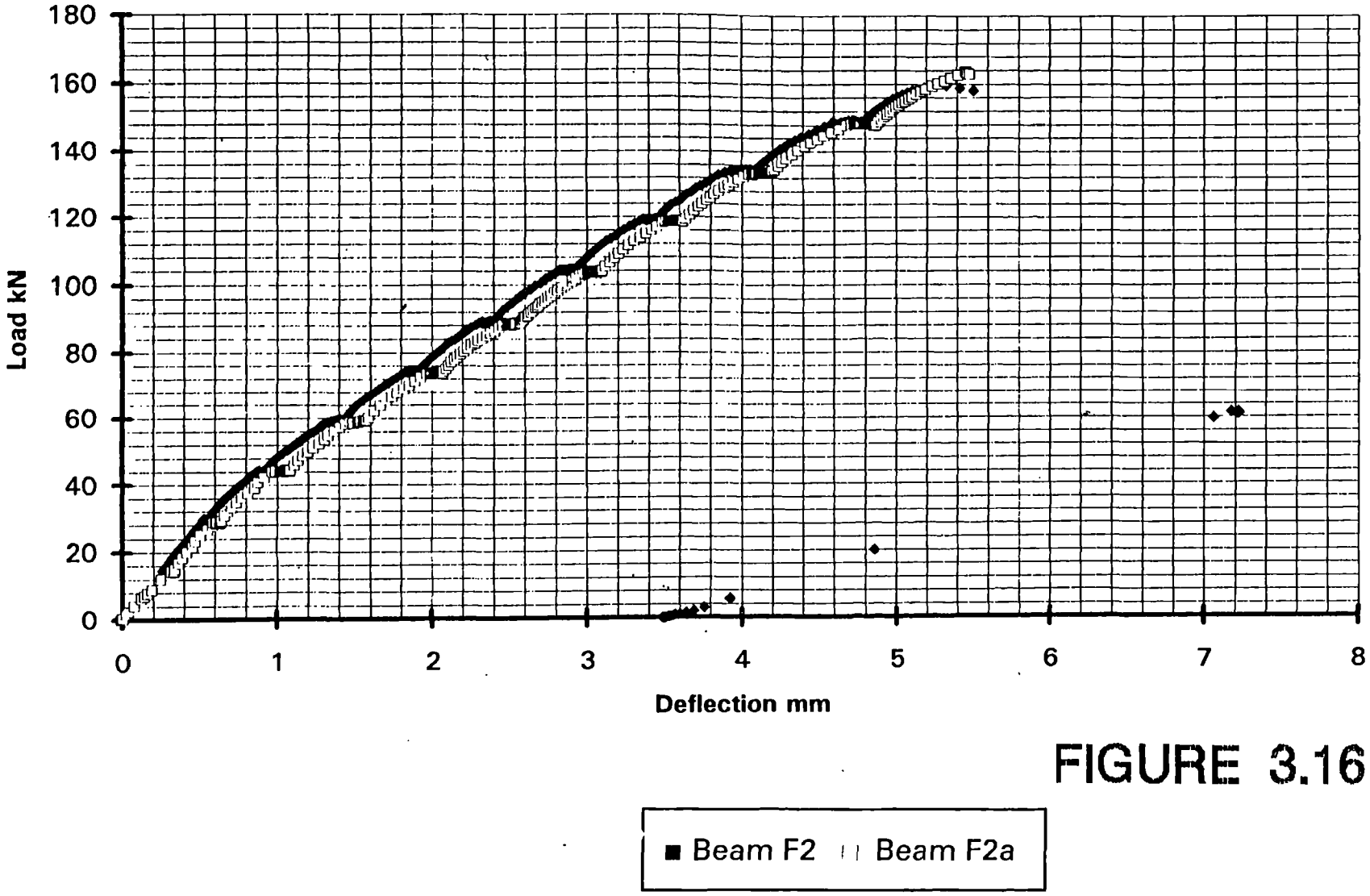
180
160
140
120
100
80
60
40
20
0
Load kN
0
1
2
3
4
5
6
7
8
Deflection mm
Beam F2
Beam F2a

FIGURE 3.16

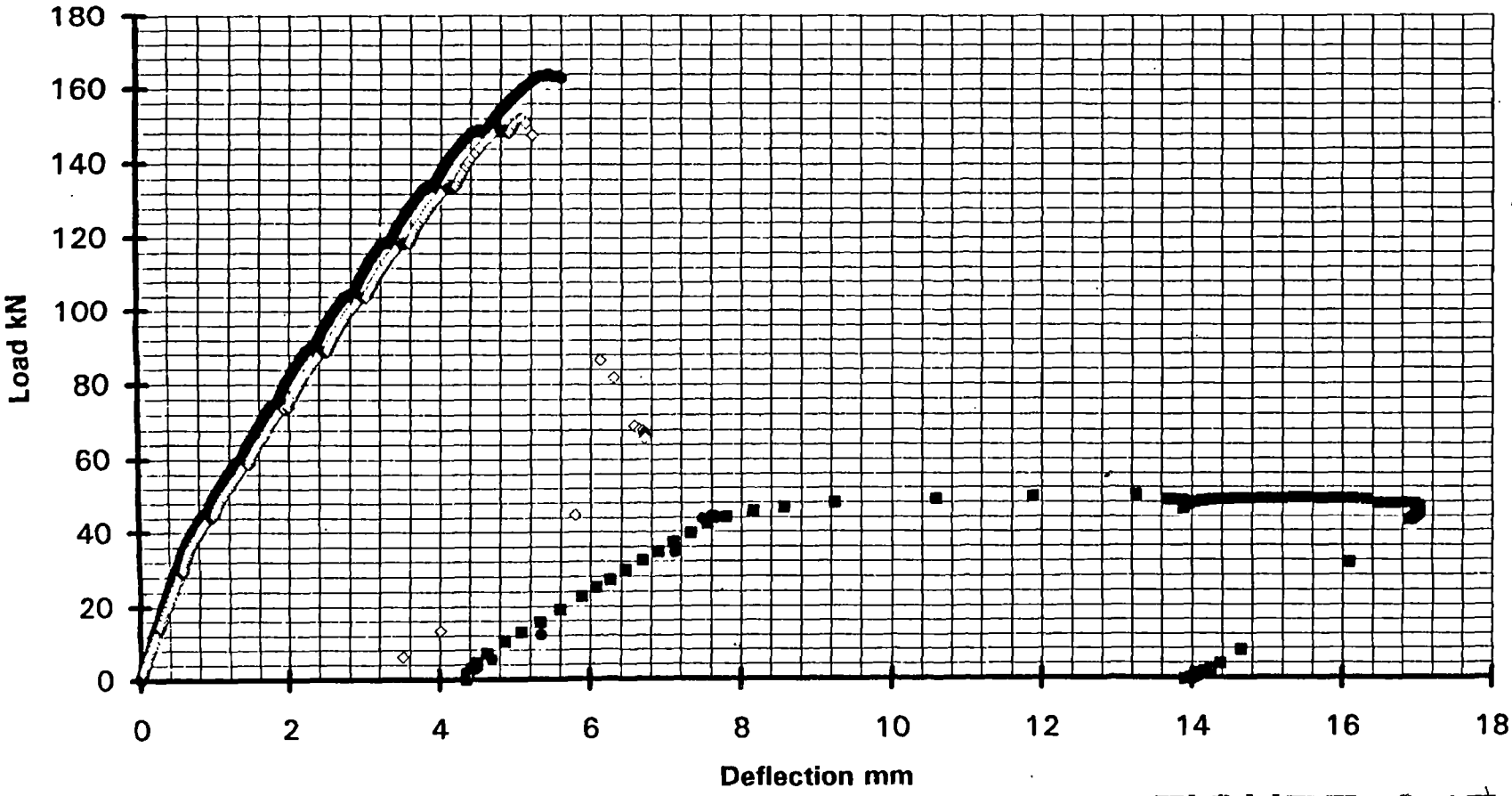
180
160
140
120
100
80
60
40
20
0
Load kN
0
2
4
6
8
10
12
14
16
18
Deflection mm
● Beam 3a ■ Beam 3a ◇ Beam3

FIGURE 3.17

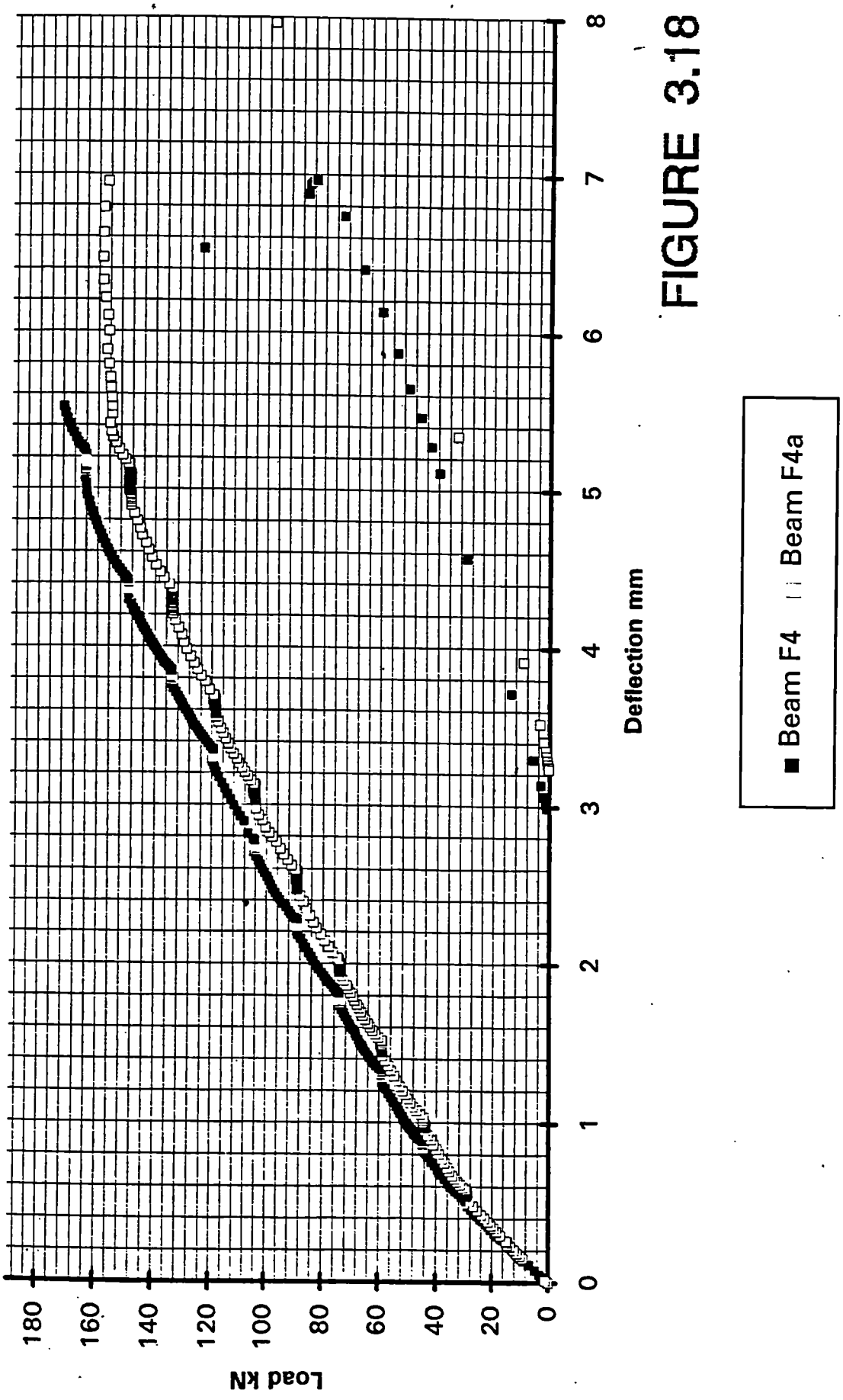
Load kN
0
20
40
60
80
100
120
140
160
180
0
1
2
3
4
5
6
7
8
Deflection mm
Beam F4
Beam F4a

FIGURE 3.18

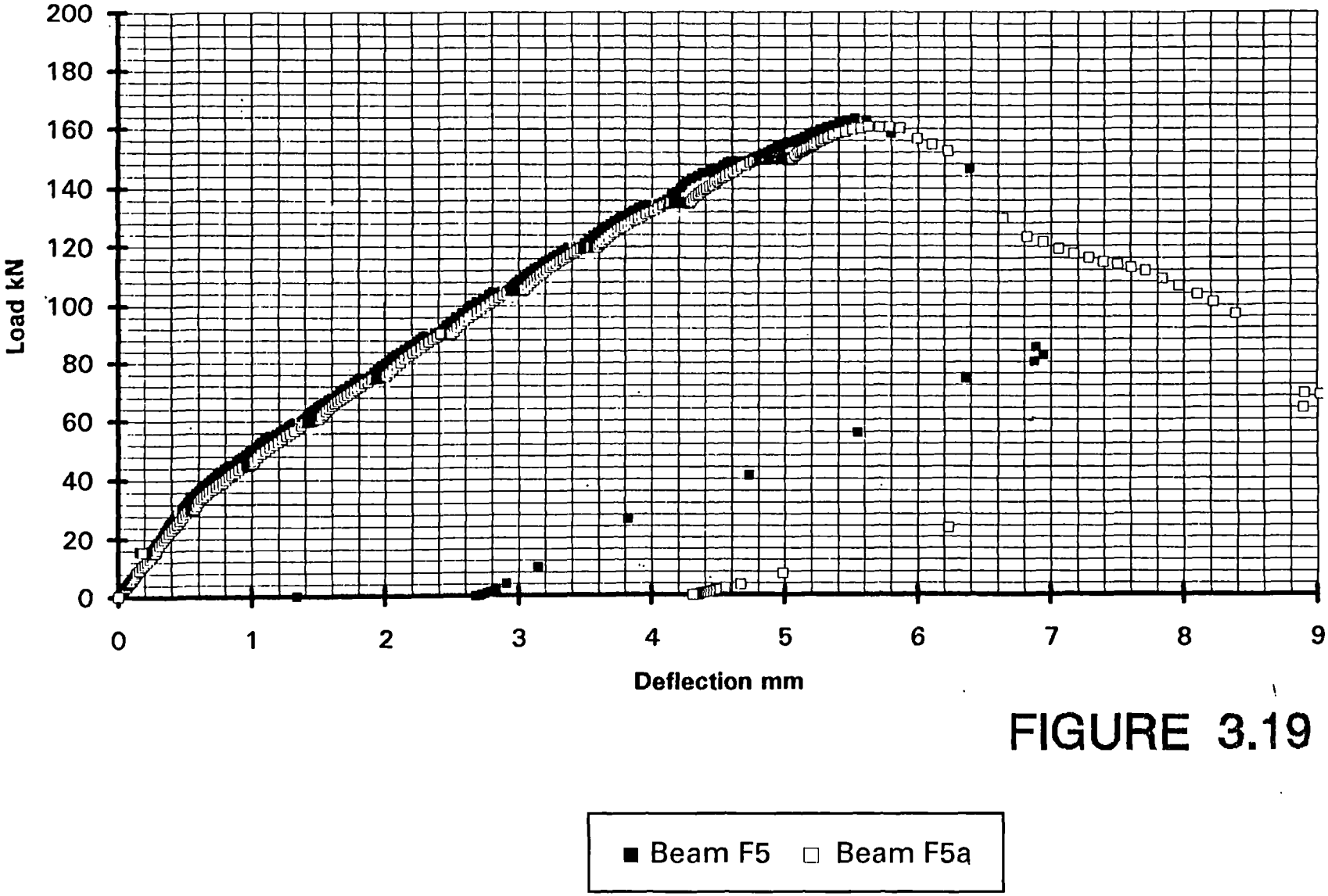
Load kN
200
180
160
140
120
100
80
60
40
20
0
0
1
2
3
4
5
6
7
8
9
Deflection mm
Beam F5
Beam F5a

FIGURE 3.19

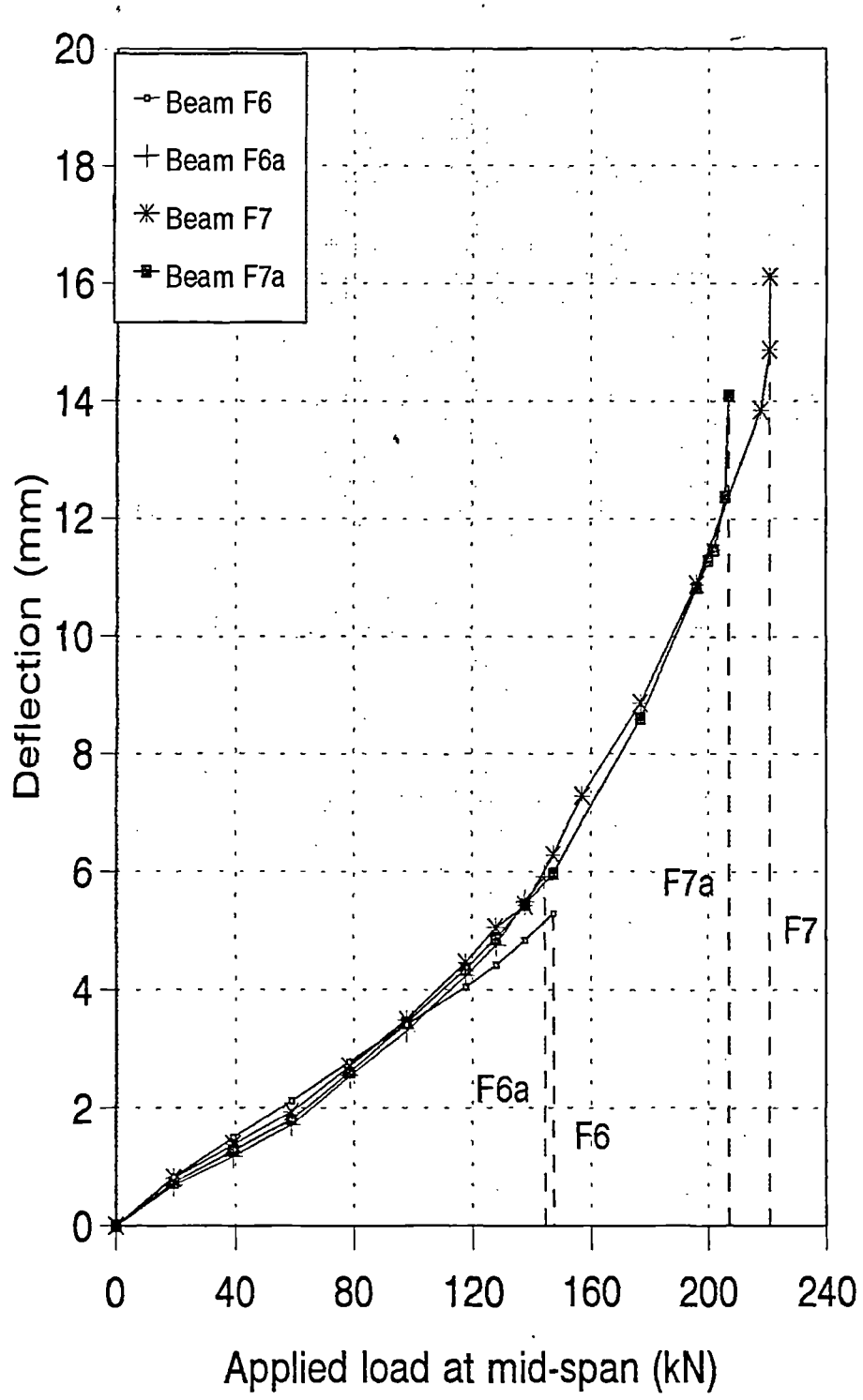

Mid-span deflections in beams

FIGURE 3.20

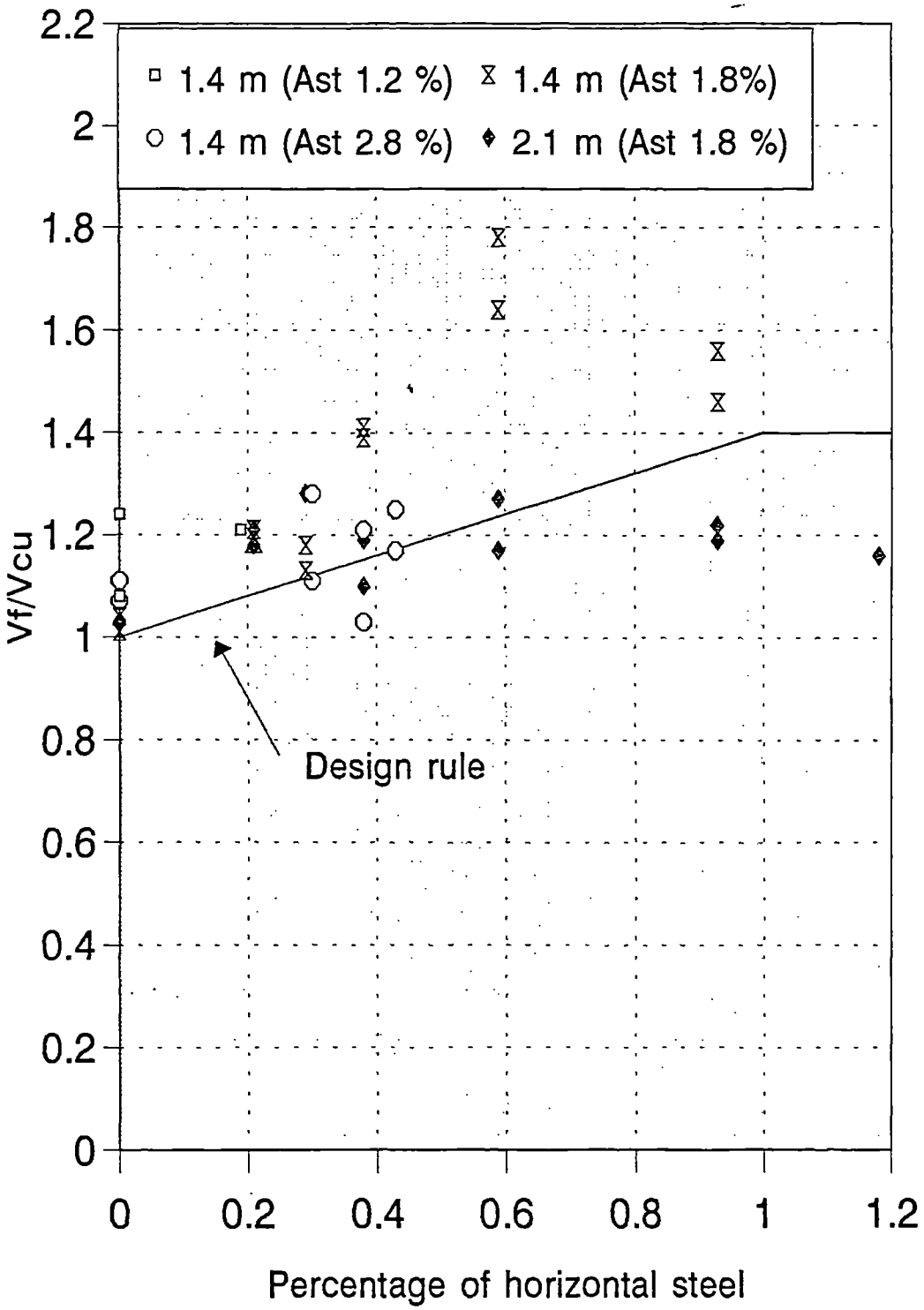

Design rule for contribution of central bar
Rectangular beams

FIGURE 3.21

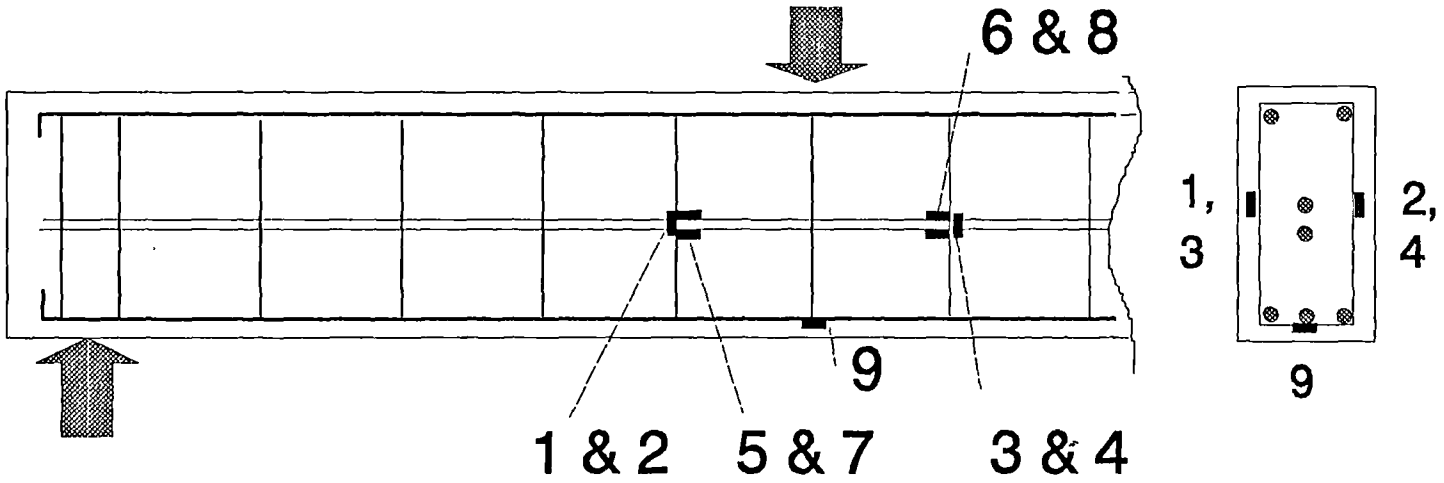

(5 to 8 for central bars and 9 for tension steel for F6a & F7a)
(1 to 4 for links , additional for F7a only)

Positions of strain gauges for beams F6a and F7a

FIGURE 3.22

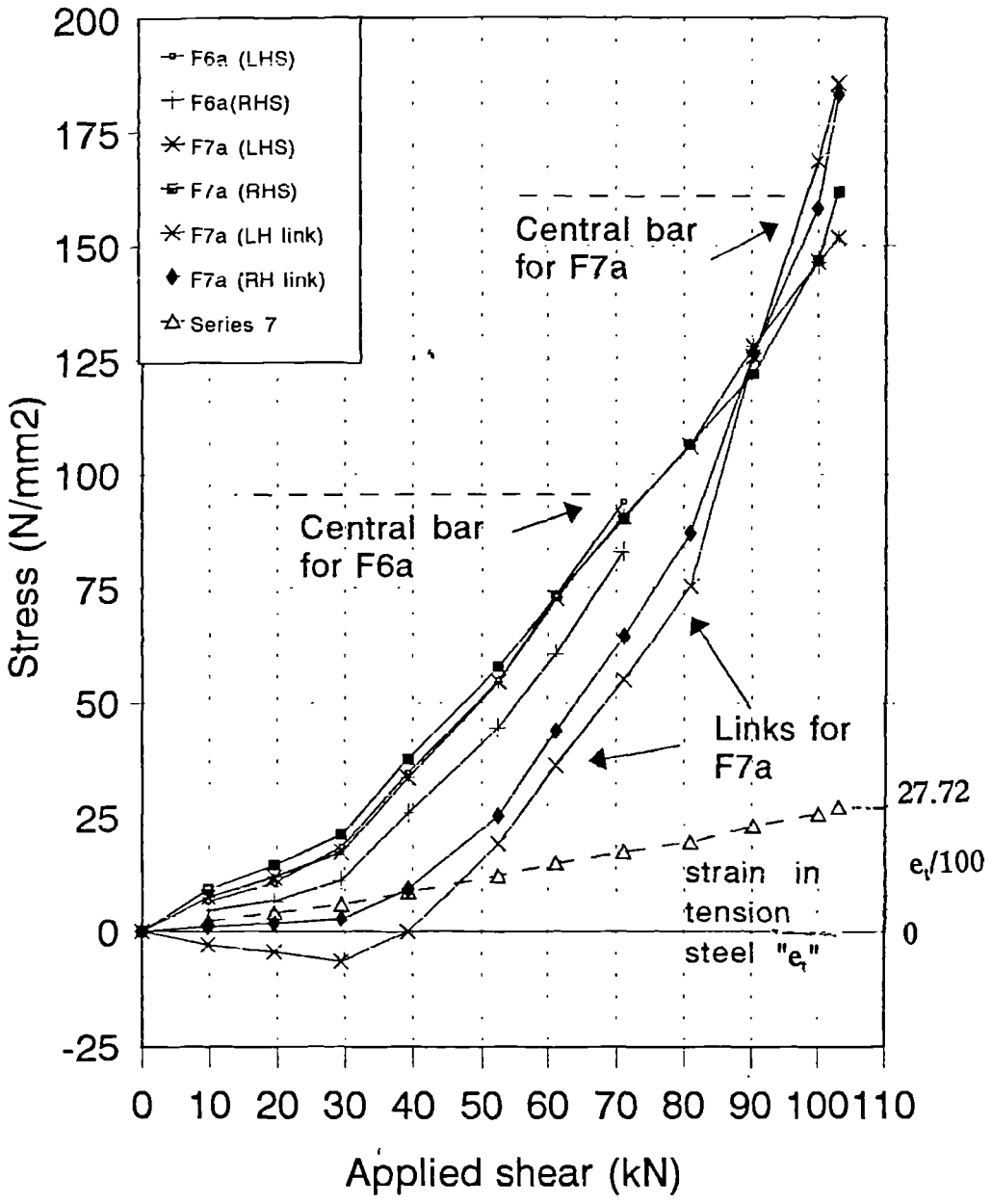

Stresses in web steel

FIGURE 3.23

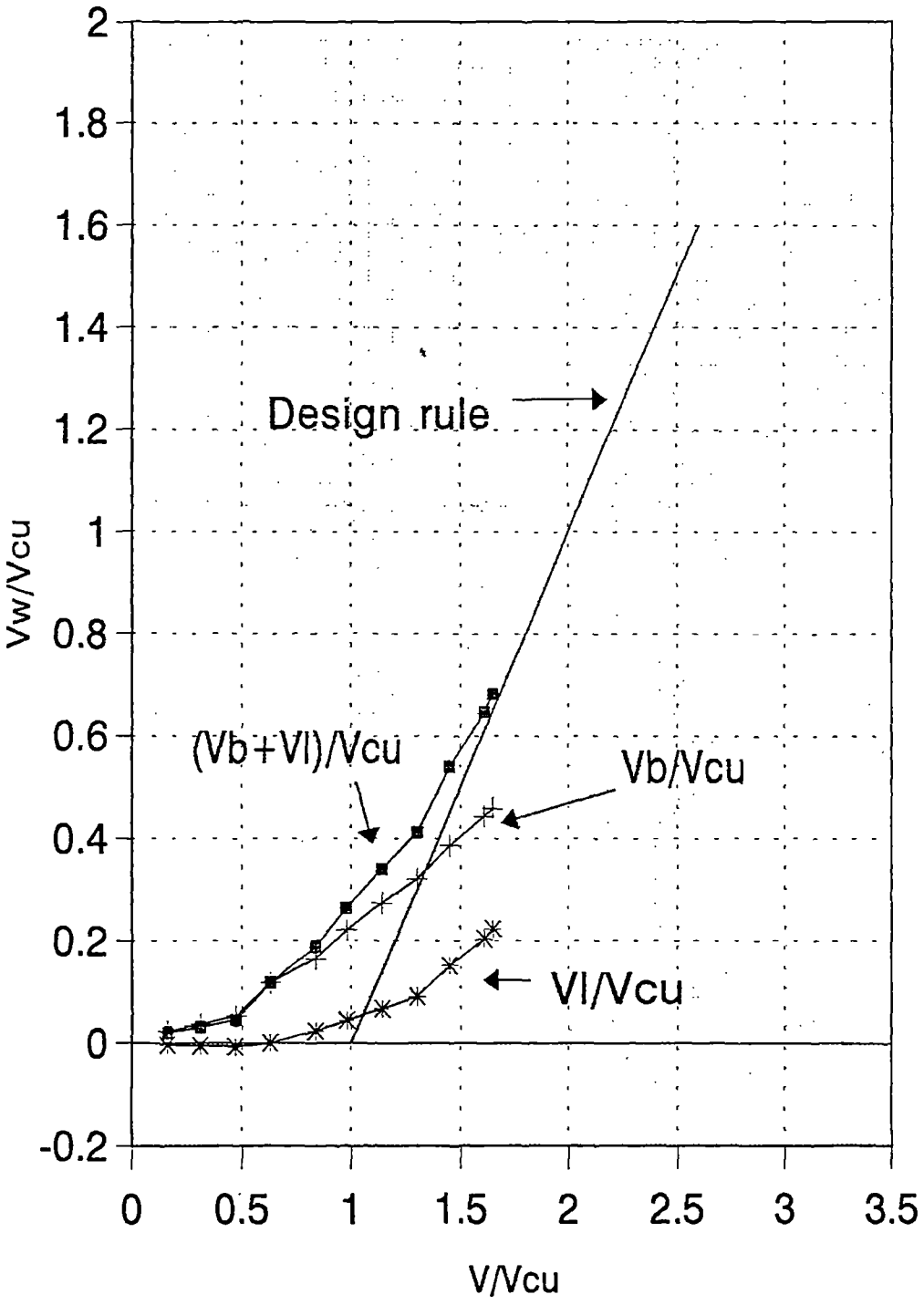

Combined contribution of
central bars and links (Beam F7a)

FIGURE 3.24

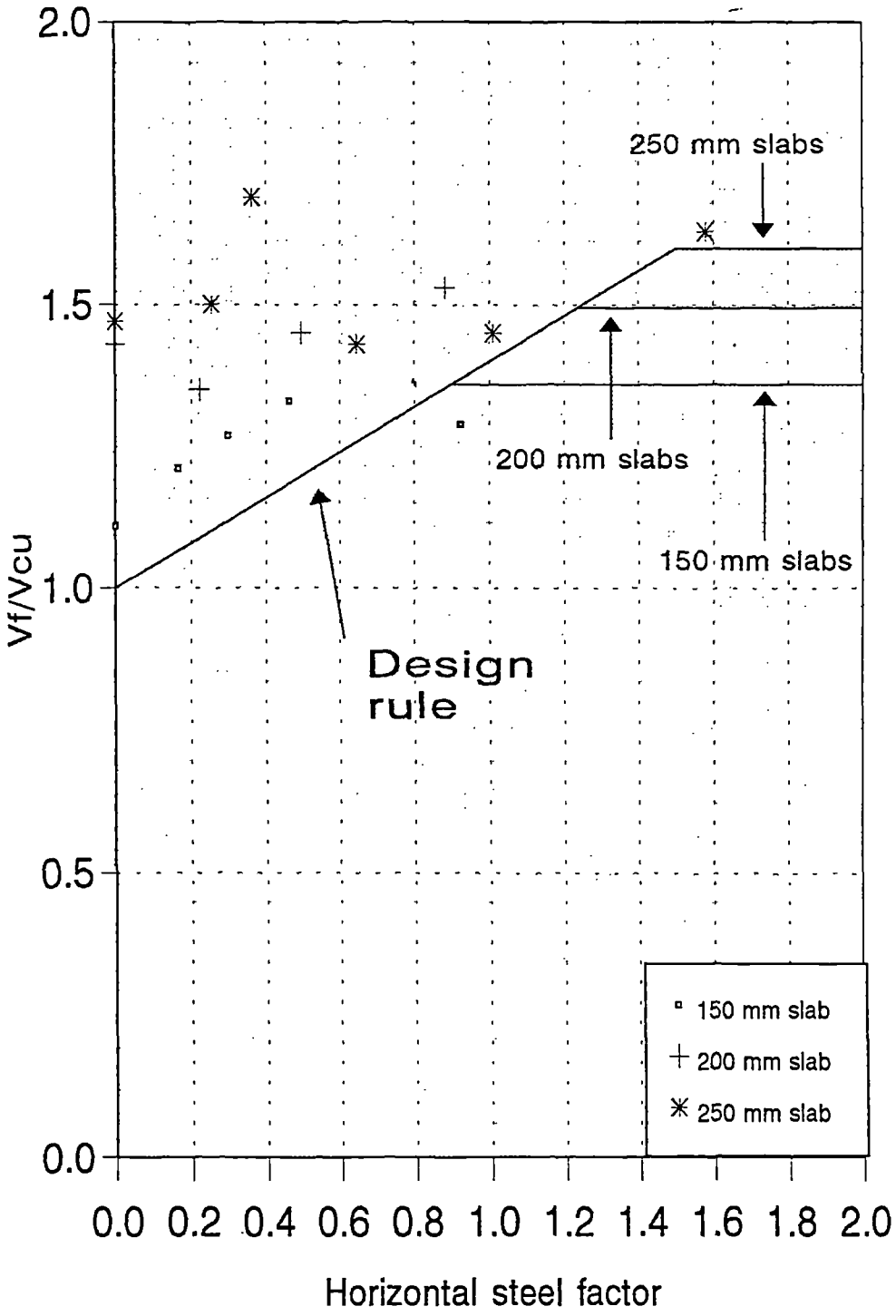

Design rule for contribution of central mesh
Punching Shear for flat slabs

FIGURE 3.25

CHAPTER 4
ANALYTICAL EXAMINATION OF THE PROPOSED RULES

4.1 Introduction

The design rules, which were proposed in chapter 3, have been supported by test data. This is in accordance with Bobrowski's plan, as quoted in paragraph 2.8 of chapter 2, which recommends that the design rules should be based on a sufficient number of tests. In addition to the support of the test data, it was decided to examine the design rules using a non-linear finite element program. ABAQUS[45] computer program was available at the University of Dundee and the examination of design rules was carried out as a "Joint Study" in collaboration with the University of Dundee.

ABAQUS analysis has been used to examine the relationship of shear resistance with the main parameters; for example, the dimensions of a member, the amount and properties of the reinforcement and the strength of concrete. The influence of these main parameters on the shear resistance of members has been studied to see whether there is a common trend between the estimates of load-carrying capacity given by ABAQUS and the design rules. The computer program assumes an idealised behaviour of a reinforced concrete member model based on the assumptions made in the program and the input properties of materials. All these properties of materials are not used in the general design rules which have to be suitable for practical design of reinforced concrete members. Also, the design rules are mainly based on tests and, therefore, they can be assumed to account for the variability and local weakness in the internal structure of the concrete as it is cast. For this reason, a comparison between the empirical design method and the computer analysis is used for examining only the common trends and correlation between the two methods.

4.2 Brief description of the computer program

4.2.1 Program operation[39]

The program is based on analyzing a member, divided into a number of finite elements. Initially, a fraction of a chosen magnitude of load is applied to the member and it is increased stage by stage. At each stage, the program checks if equilibrium can be achieved with the use of specified strengths and properties of the constituent materials. This depends on the ability of individual elements of the member to reach an equilibrium condition between the actions and reactions, without exceeding the assumed strength and properties of materials. The operation proceeds to the next stage if the solution is successful or "convergence" can be achieved. At every stage, the program is able to judge if a convergent solution is possible and it is able to adjust the rate of increase in the applied load between the stages accordingly. In this way, a solution finally converges to give the ultimate load carrying capacity of a member, within a range of tolerances which could be chosen as the default values defined within ABAQUS.

4.3 The input for the program for beams

4.3.1 General

The applied load was chosen to be the ultimate capacity of each specimen estimated according to the rules derived in chapter 3 and a percentage of this load was selected for application in a certain number of incremental stages. The tolerances mentioned above for a successful convergent solution were all default values defined within ABAQUS.

There is a wide range of options under the following headings for input information, to suit the nature of the problem:

i) Types of elements
ii) Properties of materials
iii) Support conditions

iv) Load increments

v) Number of iterations for convergence of solution

The text of input file for beam A2 is shown in Appendix B, modified for the sake of clarity, as an example of input data for beams. Appendix B also includes some explanatory notes on the terms used in the ABAQUS input.

4.3.2 Type of elements

The elements can be chosen from the following standard types:

i) Continuum Plane Stress elements with four or more nodes (CPS4, CPS.. etc.);

ii) Solid "brick" type of three dimensional elements; and

iii) Plate elements.

Initially, some trial runs were made for beams with CPS4 elements. The results were not satisfactory and, therefore, solid elements were used as shown in figure 4.1. These elements are described as "3-D Solid 20-Node Quadratic Brick, Reduced Integration Elements". For beam specimens, only half the beam was modelled as shown in figure 4.2 for 1400 mm span beam and figure 4.3 for 2100 span beam. The directions 1, 2 and 3 shown in these figures correspond to X-axis, Y-axis and Z-axis respectively.

The node numbers are at the corners and at centre points of the edges of elements as shown in figure 4.1. Node 1 is the front bottom left hand corner of the specimen. In this row, the elements are 50 mm deep (distance between node 1 and node 2001) and 75 mm high (distance between node 1 and node 43) and the element numbers increase towards the mid-span to element 10 for the 1400 mm span beam and to element 13 for the 2100 mm span beam. (Figures 4.5 and 4.6.) The elements 101 (100 mm deep) and 201 (50 mm deep) are adjacent to the element 1 making up the 200 mm width of cross-section. The 300 mm height is made of elements with 75 mm height, for example, elements 1, 11, 21 and 31 for the 1400 mm span beam.

Element 1 is 62.5 mm long and the next element 2 over the support is 75 mm long, a dimension same as the width of the steel bearing plate. The element next to the centre of the span is 37.5 mm long, half the width of the plate under the applied load. These dimensions of the elements are necessary for specifying the applied load and the reaction at the support as uniformly distributed load.

The remaining length of the beam is shared by other elements as shown by the coordinates from the left hand face of the beam in figures 4.5 and 4.6. (These figures are meant for showing the output with clarity and they are diagrammatic and not-to-scale.)

4.3.3 Properties of concrete

i) Stress-strain relationship

The non-linear stress-strain curve for concrete is modelled on the basis of properties compatible with BS8110. A curve is constructed to represent the relationship between the stress (y-axis) and the strain (x-axis). The basic boundary conditions are as follows:

a). at $x = 0, y = 0$

b) at $x = 0, dy/dx = E$ (the modulus of elasticity of concrete)

For each specimen type, the limiting longitudinal stress is taken as $0.67f_{cu}$ corresponding to the strain at peak stress (N) of $2.4(\sqrt{f_{cu}}) \times 10^{-4}$. In case of the test specimens, f_{cu} represents the actual strength of cubes, tested at the time of each test, at about 28 days from casting. The elastic modulus of concrete, therefore, is derived from table 7.2 of BS8110: Part 2[28], so that the mean value of "E" in terms of f_{cu} at 28 days is $(20000 + 200f_{cu})$ N/mm^2, for $60 > f_{cu} > 20$ N/mm^2. It is noted that BS8110: Part 1 gives a parabolic curve for the non-linear stress-strain relationship, but the corresponding modulus of elasticity is given as $5.5\sqrt{f_{cu}}$ (kN/mm^2). It is decided, therefore, to use the BS8110: Part 2 rule for the modulus of elasticity and construct a curve which will be similar to the BS8110: Part 1 curve, as closely as possible. The following equation is proposed for such a curve:

$$y = A x^3 + B x^2 + E x$$

Differentiating,

$$\frac{dy}{dx} = 3A x^2 + 2B x + E$$

The constants A and B are evaluated using two more conditions.

c) The relationship between the peak stress and the corresponding strain

$$\therefore \quad at \quad x = N = 2.4 \times 10^{-4} \sqrt{f_{cu}}, \qquad y = 0.67 f_{cu}$$

d) The slope (dy/dx) is zero at the strain at peak stress.

$$\therefore \quad for \quad x = N = 2.4 \times 10^{-4} \sqrt{f_{cu}}, \qquad \frac{dy}{dx} = 0$$

These conditions give the values of A and B as follows:

$$\therefore \quad A = \frac{(EN - 1.34 f_{cu})}{N^3} \qquad B = \frac{2.01 f_{cu}}{N^2} - \frac{2E}{N}$$

ABAQUS requires the part of stress-strain input in the elastic range, which is assumed to correspond to the range of stress from 0 up to 5N/mm^2. For beam A2, the actual upper limit is 4.82 N/mm^2 (stress) and 0.000177 (strain). This limit is chosen as a convenient point on the non-linear relationship graph, plotted for a series of values up to the maximum $0.67f_{cu}$, 24.12 N/mm^2 for the beam A2. For stresses higher than 4.82 N/mm^2, ABAQUS requires only the difference between the total strains and the elastic strain. ABAQUS adds these input values of strains to the limiting elastic strain to obtain the total strains, up to the highest limit corresponding to the stress $0.67f_{cu}$. Figure 4.4 shows the curve corresponding to the total strain and, also, the ABAQUS input curve. ABAQUS requires that the input should include the horizontal part of curve at the peak stress. The curve is, therefore, extended up to the strain value of 0.0035, same as the BS8110: Part 1 curve.

ii) Failure ratios

"*FAILURE RATIOS" option is used to define the shape of the failure surface, as a function of predefined field variables. Sketch 4.3 (not-to-scale) shows the yield and failure surfaces in plane stress as follows:

i) Lines "wx" and line "yz" represent the crack detection surface and the compression surface respectively.

ii) Points "w" and "y" show the uniaxial tension and compression respectively.

ii) Points "v" and "z" show the biaxial tension and compression respectively.

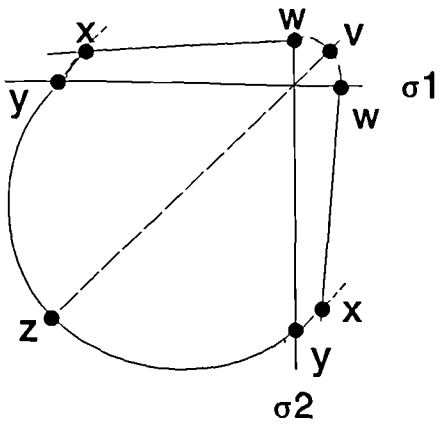

Sketch 4.3
Failure Ratios

As defined within ABAQUS, the following four values are entered in the input file:

a) The ratio of the ultimate biaxial compressive stress to the ultimate uniaxial compressive stress = 1.16

b) The absolute value of the ratio of uniaxial tensile stress at failure to the ultimate uniaxial compressive stress = 0.12

c) The ratio of the magnitude of a principal component of

plastic strain at ultimate stress in biaxial compression to
the plastic strain at ultimate stress in uniaxial compression = 1.28

d) The ratio of the principal tensile stress at cracking
(in-plane stress, when the other non-zero principal stress
component is at the ultimate compressive stress value),
to the tensile cracking stress under uniaxial tension = 0.33

iii) Tension stiffening ratio

This ratio enables ABAQUS to account for post-cracking behaviour of reinforced concrete. When a section cracks, it undergoes a discontinuity in the distribution of stresses and the cracks affect the material stiffness associated with the integration point. In a zone where cracks are present, the uncracked concrete between the cracks has a capacity to carry a certain proportion of the tensile force. This proportion of the tensile force depends on a number of parameters, mainly related to the properties of the constituents of the section and, also, the density and distribution of reinforcement in the section. This phenomenon is called the tension stiffening effect.

The program provides a range of input for the tension stiffening effect. The input defines the retained tensile stress normal to a crack as a function of the strain in a direction normal to the crack. ABAQUS Manual[39] recommends introduction of a "reasonable" amount of tension stiffening, appropriate to the density and distribution of steel, strength of concrete, etc., to simulate an interaction between the reinforcement crossing the crack and the concrete. This interaction allows "smearing" of cracking over the finite volume associated with an integration point.

For all beams, the TYPE=STRAIN option is chosen, which is appropriate for structural members with reinforcement. This input requires two pairs of parameters. The first pair, for example (1.0, 0.0), relates to the number of field-variable dependencies included in the definition of compressive yield stress, in addition to temperature. The values chosen are the default values. The analysis would otherwise be carried out assuming that the post-cracking behaviour depends only on temperature.

The second pair of parameters, for example (0.0, $3.1x10^{-3}$), defines the total strain at which the tensile stress normal to a crack will be zero. This strain is a multiple of the strain at which concrete cracks, called "the strain at failure". The ABAQUS manual quotes a "typical" value of this strain as 10^{-4}. However, this is taken as only an indication since the actual value of this strain, for normal grade concrete, is 3×10^{-4}. The ABAQUS manual recommends that the total strain (for zero tensile stress across a crack) should be 10 times this strain as a starting point or 3×10^{-3}. It is also suggested that a calibration should be done to arrive at an optimum value for a beam, with regard to the density and distribution of steel, strength of concrete, etc. The values chosen after some initial trial runs were within a narrow range of 3.1×10^{-3} to 3.5×10^{-3}. For example, this value for specimen type B was 3.4×10^{-3}.

iv) Shear retention

The shear retention input is used to describe the reduction of shear modulus associated with the crack surfaces. This is taken as a function of the tensile strain across the crack. The shear stiffness of open cracks is assumed to reduce linearly to zero as the crack widens and the tensile strain is, say, 0.0075 or 0.009. The shear retention input values were chosen to be within a narrow range, between (1.0, 0.0075, 1.0, 0.0075) and (1.0, 0.009, 1.0, 0.009), after some initial trials.

4.3.4 Properties of reinforcement

The reinforcement was incorporated as "SINGLE" bars at specified positions defined within the elements. The bars had to be entered over the full dimensions of the elements and, therefore, the longitudinal bars appear to be without any end cover. Also, the links appear to be made of four separate bars placed between the faces of the beam as shown in figure 4.7.

4.3.5 Convergence criteria control

The control parameters are defined within ABAQUS as the criteria for convergence of a solution. The "GLOBAL" option was chosen for this exercise.

Under this option, the control criterion is represented by the ratio of the largest residual forces and bending moments to the corresponding initial values. The default value of this ratio is 5×10^{-3} and this is adopted for the analyses of all beams.

4.4 The output from the program for beams

The beam model and the typical output are shown in figure 4.5 (Beam B3 and stresses in central bar for 1400 span beams), figure 4.6 (Beam F3 and stresses in central bar for 2100 mm span beams) and figure 4.7 (Beam D1 and stresses in links). The sketches are meant for showing the data clearly and, therefore, they are diagrammatic and not-to-scale.

4.4.1 Beams without web reinforcement

Values of V_{AU}, the ABAQUS estimate of ultimate shear resistance, are compared with the values of V_{FU} (the failure loads of the two specimens) and V_{DU} (the ultimate shear resistance given by the design rule). The details of test specimens are extracted from table 3.5.1, chapter 3.

Table 4.1: Beams without web reinforcement

Spec No	f_{cu} N/mm^2	ϱ	V_{DU} kN	V_{AU} kN	V_{AU}/V_{DU}	V_{FU} kN (1)	(2)
A1	28	1.18	51	59	1.16	55	63
B1	27	1.78	58	75	1.30	58	60
E1	28	2.80	67	104	1.55	72	75
F1	43	1.78	67	75	1.12	69	75

i) For beams without any web steel and with a shear span ratio of 2.6, ABAQUS estimates (V_{AU}) exceed the design rule estimates (V_{DU}) and this difference increases with the increase in the amount of tension steel. This is shown by the ratio of V_{AU}/V_{DU} , which is 1.16, 1.3 and 1.55 for beam A1,

B1 and E1 respectively. It seems that the program is sensitive to the effect of tension steel on the shear resistance and it overestimates this effect in comparison with the BS8110 rule. The BS8110 rule results are supported by the test data while the ABAQUS estimates are not.

ii) For beam F1, the shear span ratio (a) is 4. The ratio V_{AU}/V_{DU} is 1.12 for beam F1 which is less than the ratio 1.3 for beam B1, a beam with the same amount of tension steel but "a" equal to 2.6. ABAQUS analysis seems to confirm that the design rule has an extra reserve for values of "a" closer to 2.5, which was also observed in paragraph 2.7.2(iv) of chapter 2.

4.4.2 Beams with central bars as web reinforcement

Table 4.2 shows V_{CU} and V_{DU} obtained from tables 3.5.1 of chapter 3. F_{AB} is the maximum reactive force in the central bar (kN), given by the product of ABAQUS estimate of the maximum stress (Figures 4.5 and 4.6) and $0.001A_b$, A_b being the area of the bar in mm^2. Table 4.2 shows that the estimate of the reactive force in the central bar increases with the applied shear, showing the effectiveness of these bars and that the central bars are equally effective for shear span ratios of 2.6 and 4.

Table 4.2 includes results of two additional analyses, for beams B33 and B34, which had the section properties and the concrete strength same as beam B3. The horizontal web steel was placed at 100 mm and at 200 mm from the top surface for beams B33 and B34 respectively. The estimated values of V_{AU} for beams B33 and B34 are within $\pm$ 8% of the estimate for beam B3 (79 kN). It seems that there is no real advantage in providing the web steel away from the centre of the section.

The mean value V_{AU}/V_{DU} is 1.19, as shown in table 4.2 and it has a reasonable standard deviation of 0.13. This suggests that the ABAQUS estimates of shear resistance (V_{AU}) are about 20 % higher than those given by the design rule for V_{DU}. This could be attributed to the indeterminate local weakness of the internal structure of concrete, which is accommodated in the empirical rules supported by the test results. On the other hand, ABAQUS assumes an idealised

and theoretical behaviour of concrete in accordance with the input and, as a result, provides higher overall estimates of shear resistance.

In the case of beam E1 with 2.8% tension steel, the ABAQUS estimate of shear resistance of concrete seemed to be much larger, compared with those for beams B1 and F1 with 1.78% tension steel. This is clearly shown in table 4.1, in the column "V_{AU} /V_{DU}". This effect of higher amount of tension steel appears to result in a lower mobilisation of V_{BU} , contribution of the central bars to the shear resistance of beams E2, E3 and E4. However, the reduction in V_{BU} is compensated by the overestimate of the shear resistance contribution of concrete. The overall ABAQUS estimates of V_{AU} for beams E2, E3 and E4 are of the right order and, similar to those for beams B2, B3 etc, they are nearly 20 % higher than V_{DU}.

Table 4.2: Beams with central bars

Spec No	Stress (N/mm^2)	A_b mm^2	F_{AB} (kN)	V_{DU} (kN)	V_{AU} (kN)	V_{AU}/V_{DU}	V_{FU} (kN) (1)	(2)
A2	87	100	8.7	59	63	1.07	67	-
B2	48	156	7.5	64	78	1.22	65	68
B3	47	201	9.5	67	79	1.20	81	88
B33	-42	201	- 8.5	"	77	1.15	-	-
B34	111	201	22.3	"	85	1.27	-	-
B4	55	314	17.1	76	89	1.17	101	110
B5	46	490	22.7	85	90	1.06	90	96
E2	24	156	3.7	80	97	1.20	80	92
E3	24	226	5.4	84	102	1.21	84	90
E4	26	201	5.1	84	102	1.22	75	88
F2	87	113	9.9	74	102	1.39	80	82
F3	94	201	18.9	79	116	1.47	76	82
F4	58	314	18.3	84	93	1.11	79	86
F5	45	490	22.2	92	85	0.92	80	82
F6*	69	618	* 42.6	87 *	100	1.15	75	72
				Mean V_{AU}/V_{DU} :		1.19		
				Standard deviation :		0.13		

(* Specimen type F6: V_{DU} (87 kN) was limited to $1.4V_{CU}$. F_{AB} is based on the average of the maximum stresses developed in the two central bars.)

4.4.3 Beams with central bars and links

Table 4.3 shows the details for beam types C1, D2, D3, D4 and F7 which are taken from table 3.5.2 of chapter 3. Also, the details for beam types C2 and C3 are extracted from table 3.3.2 of chapter 3.

F_{AB} is the maximum force in the central bar, corresponding to the maximum stress in the bar extracted from ABAQUS results. v_l is the maximum stress in links in N/mm^2, as shown in figure 4.7.

Table 4.3: Beams with central bars & links

Spec No	Stress (N/mm^2)	A_b mm^2	F_{AB} (kN)	v_l (N/mm^2)	V_{DU}	V_{AU} (kN)	V_{AU}/V_{DU} (kN)	V_{FU} (kN) (1)	(2)
C1	-	-	-	101	96	115	1.20	119	128
C2	-	-	-	117	112	143	1.27	162	178
C3	-	-	-	130	135	152	1.12	185	187
D1	74	156	11.5	114	103	122	1.19	132	141
D2	78	201	15.7	117	102	116	1.14	146	154
D3	47	314	14.8	94	106	99	0.94	130	134
D4	42	490	20.6	94	113	97	0.87	134	133
F7	60	618	37.1	122	113	90	0.80	110	104
						Mean V_{AU}/V_{DU} :	1.07		
						Standard deviation:	0.16		

The mean value of V_{AU}/V_{DU} is 1.07 with a marginally large standard deviation of 1.16. Hence, separate examinations are proposed for the estimates given by the design rule and ABAQUS, for different provisions of web steel.

ABAQUS estimates of V_{AU} for beams with links (C1, C2 and C3) are about 20% higher than the estimates of V_{DU} given by the empirical rule. This could be the effect of ABAQUS overestimating the contribution of concrete (V_{CU}) which has an additive effect on the overall shear resistance of the section. All ABAQUS estimates are, however, well below the test results. The ABAQUS estimate for C3 does not fully reflect the increase in amount of links. This is attributable to the

increased flexural stresses and the shear-compression type of failure.

ABAQUS predictions of stresses in links v_l are low, ranging from 101 N/mm^2 (beam C1) to 130 N/mm^2 (beam C3). ABAQUS also appears to evaluate the contribution of links as "reinforcement" for assisting concrete to resist the principal tensile stresses in the neutral axis region and not as the tension member of a truss. This is evident from figure 4.7 which shows that the stresses in links are maximum in the element near the applied load and at the top and the stresses reduce for elements nearer to the support and the bottom of the beam.

The ABAQUS estimates for beams D1 and D2 exceed the design rule estimates of V_{DU} by 14% and 19% but the ABAQUS estimates for beams D3, D4 and F7 are lower than V_{DU} . The design rule estimates (V_{DU}), however, are supported by the test data. The ABAQUS estimates show that the contribution of the central bar does not increase in direct proportion to the increase in its area or the percentage ϱ_b and the central bars and the links interact as shown in the sketch 3.4 in paragraph 3.4.2.1 (Chapter 3). The ABAQUS estimate of the force in the central bar (and hence its corresponding contribution to the shear resistance) is influenced by its combination with the forces in links. However, an interaction between the links and central bars is noticeable. F_{AB} increases from 11.5 kN for D1 with 2T10 bars to 20.6 kN for D4 with 1T25 bar and the corresponding values of v_l decrease from 114 N/mm^2 to 94 N/mm^2. The value of v_l (122 N/mm^2) for beam F7 does not follow this trend which could be due to the difference between the shear-span ratio for specimen types D and F.

Further study is required to determine the optimum combination of links and the central bars. However, the proposal given in chapter 3, for combined provision of links and central bars, could serve as a safe solution. For rectangular beams with links, it was proposed that the central bar area should be less than or equal to 1%, to obtain its contribution not exceeding $0.4V_{CU}$. The remainder of the contribution from the web reinforcement should be obtained by providing links, subject to the minimum amount of links required for practical reasons.

4.5 Analysis of slab specimens

4.5.1 Choice of elements

Initial trial runs were carried out using three-dimensional shell elements, S8R, with eight nodes and reduced integration. The reinforcement was specified in accordance with the ABAQUS format for shells. These trial analyses, however, were found unsatisfactory. The predicted failure loads were very low and they seemed to relate to the flexural properties only, ignoring the punching shear resistance of the specimens. This led to the choice of three-dimensional "brick" type elements, C3D20, similar to the type of elements chosen for beams.

Since the loading applied to the 3 x 3 m square specimens was symmetrical, it was possible to model only one quarter of the area of the specimen. The area of the model was 1.5 x 1.5 m, divided into 25 elements. (Figure 4.8) The load on the model was a quarter of the estimated failure load, applied at three points on the quarter circumference of a circle with a diameter 2.4 m. Two point loads at the edge and one in the middle were equivalent to 1/16th and 1/8th of the estimated applied load respectively. Vertical reaction was provided uniformly over a quarter of the area of the 400 mm square column. The conditions along the X-axis and the Y-axis sides of the model were specified to account for the symmetry of the actual slab specimen represented by the model. The idealized finite element mesh, plan dimensions of the elements, the load and the support are shown in figure 4.8.

4.5.2 Details of specimens and the reinforcement

Table 4.4 shows the groups of specimens (paragraph 3.6.1 and table 3.6.1 of chapter 3); 150 mm thick slabs (Specimens 1 to 5), 200 mm thick slabs (Specimens 6 to 9) and 250 mm thick slabs (Specimens 10 to 15).

The reinforcement was specified in the form of individual bars at the top, bottom and centre of the cross-section for the three types of slab specimens, 150 mm, 200 mm and 250 mm in depth. This was an apparently rigorous exercise, but

it enabled a clear description of the number and positions of the bars. The reinforcement specification consisted of three typical meshes made of bars at 80 mm, 160 mm and 175 mm centres.

4.5.3 Tension stiffening

The description of "Tension stiffening" was the same as applied to the beam specimens. The range of strain, for the gradual reduction of the tensile stress to zero after the onset of cracking, was between 3.45×10^{-3} and 3.52×10^{-3}. The input values were 3.45×10^{-3} for specimen 1, 3.52×10^{-3} for specimen 2 and 3.5×10^{-3} for all other specimens.

4.5.4 Shear-retention

The option of shear-retention is not used in the analysis of slabs. The retention of shear stiffness across the cracks is not considered to be significant for the assessment of load-carrying capacity of thin slabs.

4.5.5 Convergence criteria control

The default value of the ratio was adopted as 5×10^{-3} (or 0.5%), under the "GLOBAL" convergence criterion for the analyses of all beams. (paragraph 4.3.5) For the beam specimens, the convergence of solutions was possible with this control parameter. For slab specimens, however, the trial runs showed that convergence of solutions could not be achieved with this criterion.

ABAQUS manual[39] suggests that the default convergence criterion is rather strict by engineering standards. It is recommended that the value of this parameter should be increased, if it is found necessary to do so. Accordingly, this control criterion was relaxed for the slab specimens. The convergence of a solution was assumed to be acceptable if the check of equilibrium of forces was achieved with a tolerance of 2.5% to 2.75% of the applied load. Such tolerance is well within the limits which are generally acceptable for rigorous structural analyses.

4.5.6 The output from the program for slabs

Table 4.4 shows the failure loads (V_{FU} from table 3.6.1 in chapter 3), the stresses in the central bars (v_b) and ABAQUS estimates of shear resistance capacity of slabs (V_{AU}). F_{AB} is obtained as follows, using the terms effective area of bars A_{be} , u (shear perimeter) and u_o (perimeter of the column or loaded area):

$$F_{AB} = (A_{be} \times v_b) /1000 \qquad \text{kN}$$

$$A_{be} = \frac{A_b \ (u + u_0)}{2 \ s_b}$$

The ratios of the design rule estimates of V_{BU} to F_{AB} show a wide range. The empirical rule for punching shear capacity of flat slabs assumes a failure surface, as described in chapter 3. This surface is represented by the inclined face of a notional truncated cone or pyramid, with one base as the column area or the loaded area and the other base enclosed by the shear perimeter (u) at a distance of 1.5d from the face of the column or the loaded area. Also, it was observed in paragraph 3.6.2 that central mesh provides a better dowel resistance for slabs compared with that afforded by the central bars in beams. This dowel action of the central steel was attributed to the punching type of failure of flat slabs, which does not feature in the computer analysis. ABAQUS analysis is based on failure, which occurs when the elements are not able to reach the condition of equilibrium. ABAQUS estimates of stresses in the central bars, therefore, may not correspond to the empirical rule values of V_{BU}. However, the table 4.4 shows an increase in F_{AB} with the increase in the applied load, which demonstrates the effectiveness of the central bars. Table 4.4 also shows that the high ABAQUS estimates of F_{AB} correspond to the ABAQUS estimates of V_{AU} for slabs 5, 8, 9 and 12, which are much larger than the test results.

Table 4.4 : Analysis of slab specimens

Spec No.	Central steel	A_{be} (mm^2)	V_{BU} kN	V_{DU} kN	V_{FU} kN	V_{AU} kN	v_b N/mm^2	F_{AB} kN	V_{BU}/F_{AB}
1	0	-	-	438	489	413	0	0	0
2	T6@160	410	37	451	502	520	385	158	0.23
3	T8@160	729	56	409	448	462	346	252	0.22
4	T10@160	1139	104	522	556	513	270	308	0.34
5	T10@80	2278	160	605	575	652	415	945	0.17
6	0	-	-	656	938	1056	0	0	0
7	T8@160	814	72	728	883	678	68	56	1.28
8	T12@160	1831	138	696	811	1002	398	729	0.19
9	T16@160	3255	246	804	853	1124	460	1497	0.16
10	0	-	-	919	1356	956	0	0	0
11	T10@175	1284	86	953	1278	928	59	76	1.33
12	T12@175	1848	148	1016	1467	1698	421	779	0.19
13	T16@175	3286	254	1089	1190	1066	112	368	0.69
14	T20@175	5134	443	1376	1354	1277	91	469	0.94
15	T25@175	8022	445	1208	1210	1237	127	1022	0.44

4.6 Conclusions

The general design rules are based on test results and, also, they use the "addition" principle which does not feature in the computer analysis. However, there is a general correspondence between the estimates of shear resistance given by ABAQUS and the design rules proposed in the previous chapter.

It is recommended that the central bars should be located at the centre of the beams or slabs. This location will make the bar equally effective near the mid-span and at the support and provide it with similar protection from fire in both situations. It is shown in paragraph 4.4.2 and table 4.2, that the shear

resistance contribution of the bar changes marginally (by about 10%) if its central position is changed and it is placed at 1/3 or 2/3 height from the top of the beam.

The total contribution of the central bars was attributed to the strengthening of central core of the section for resisting the tensile stresses as well as the enhancement through dowel action of the central bars. The dowel action was considered to be particularly significant for resistance against punching shear in slabs. The computer analysis is not able to account for the dowel action, but it has provided variations in the reactive tensile force generated in the bar for each case. This reactive force corresponds to the increase in shear resistance attributable to the central steel and this is considered to confirm the effectiveness of the central steel as shear reinforcement.

ABAQUS analysis has shown that further study is required to determine the optimum combination of links and the central bars. In the meantime, however, the proposal for combined provision of links and central bars, as given in chapter 3, could serve as a safe solution.

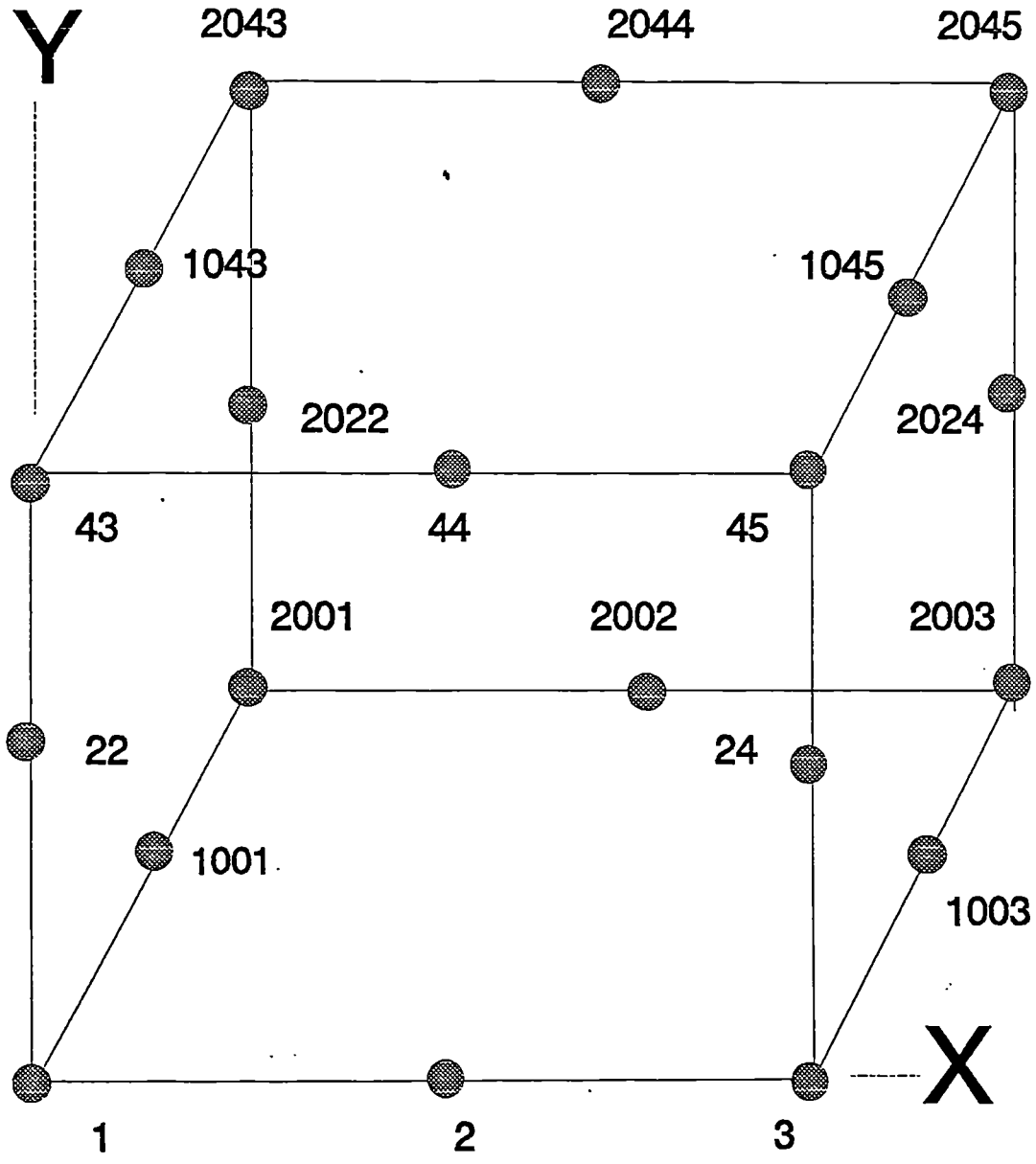

TYPICAL ELEMENT

(C 3D 20 R)

FIGURE 4.1

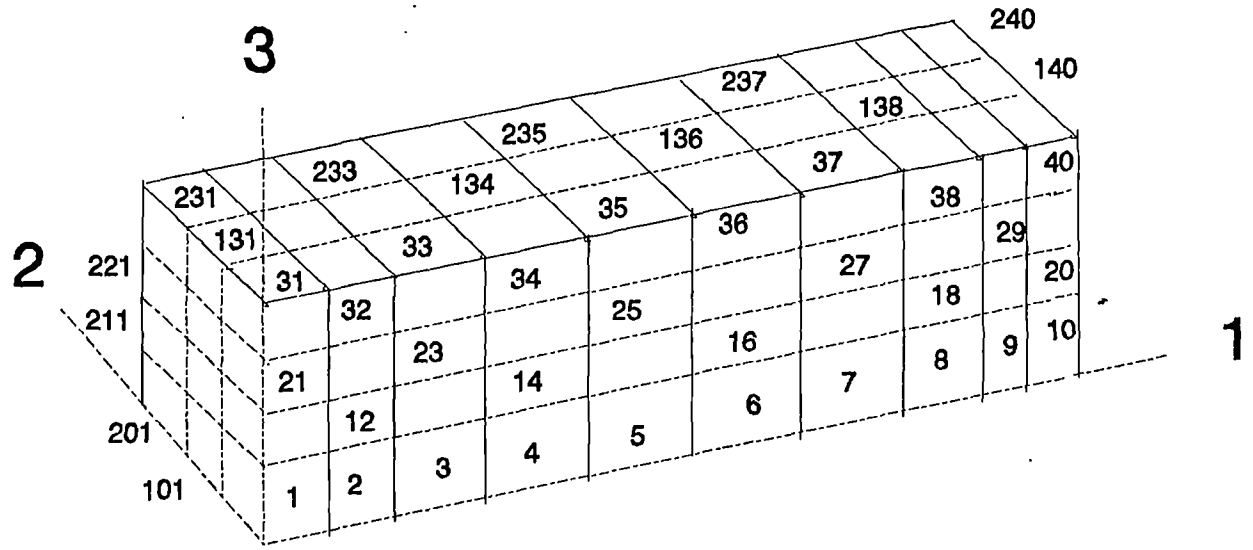

TYPICAL ELEMENT DEATAIL - 1400 MM SPAN BEAMS

FIGURE 4.2

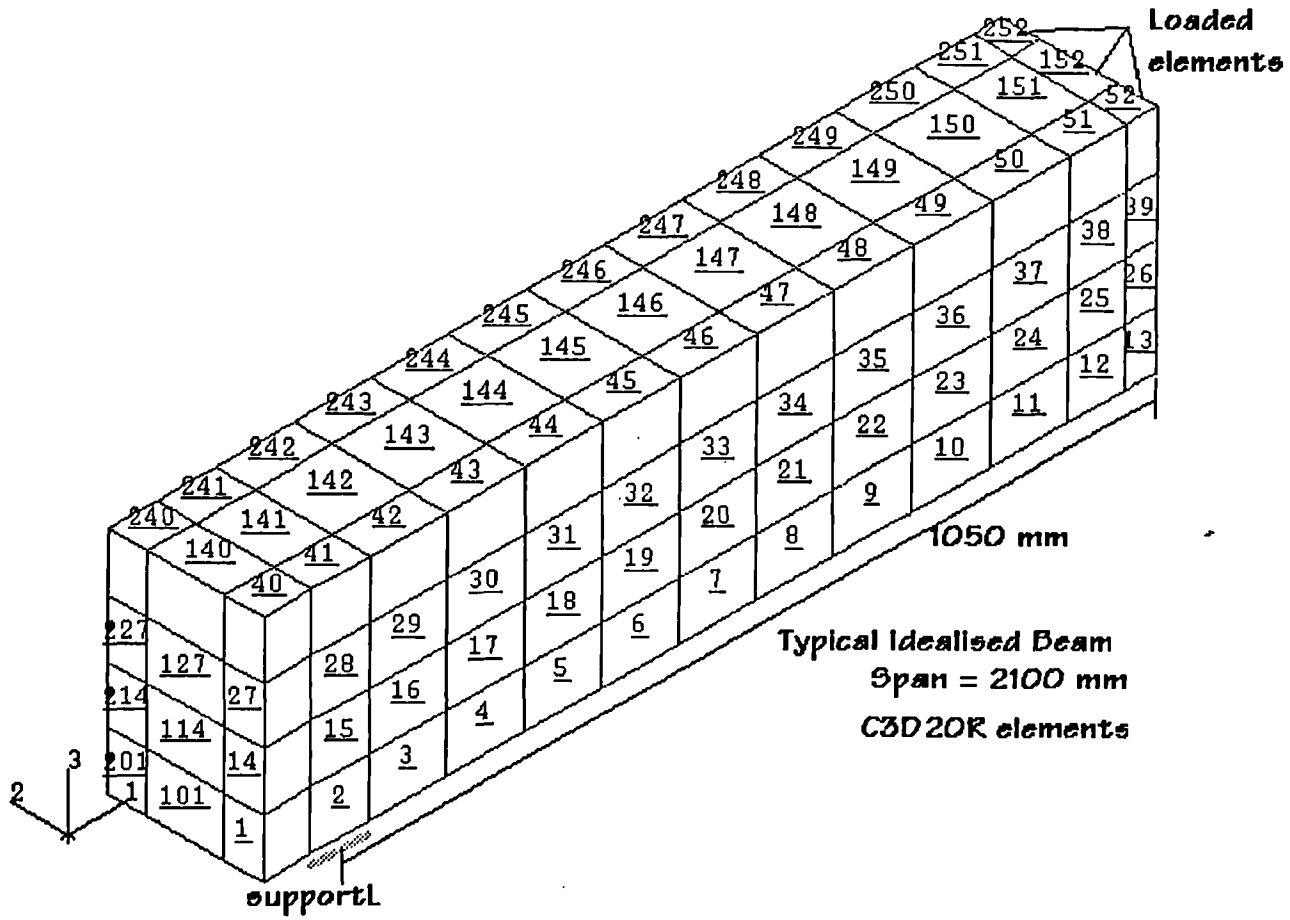

TYPICAL ELEMENT DETAIL - 2100 MM SPAN BEAMS

FIGURE 4.3

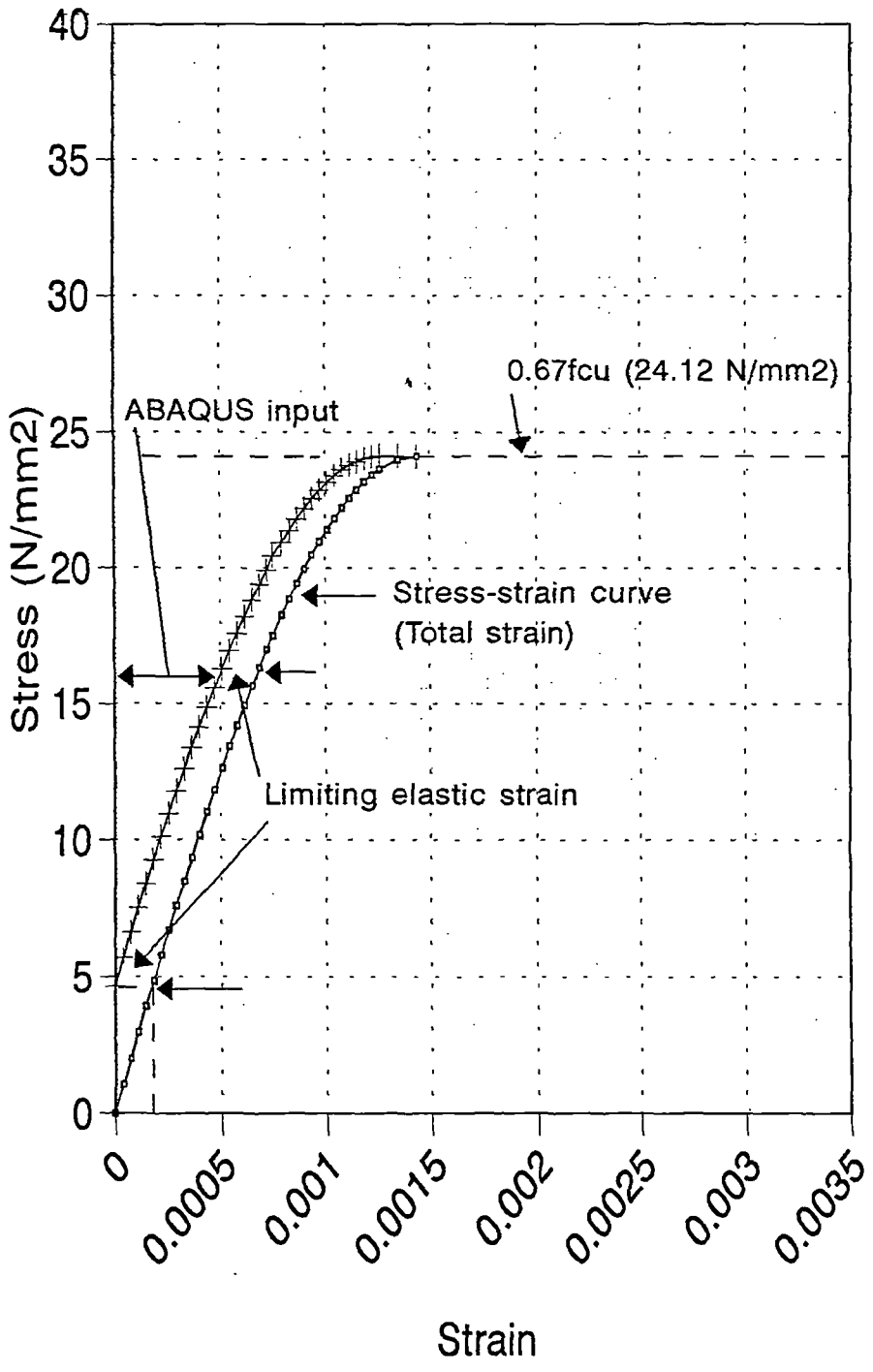

Stress-strain relationship for concrete
Beam A2 (fcu = 36 N/mm2)

FIGURE 4.4

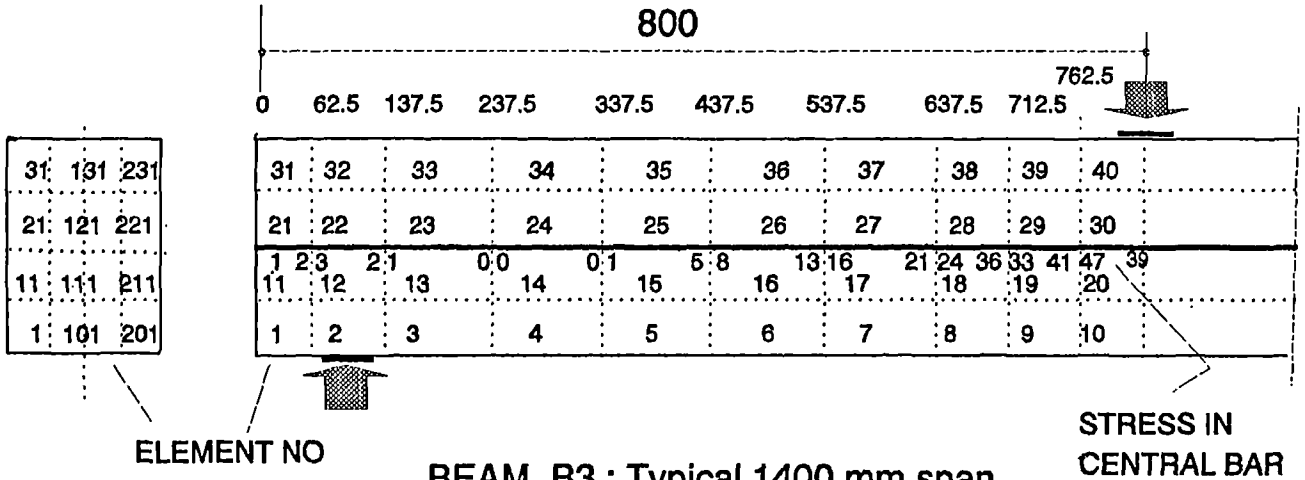

BEAM B3 : Typical 1400 mm span

CRITICAL STRESS IN CENTRAL BAR IN EACH ELEMENT (N/mm2)

B3	2	3	1	0	5	13	21	36	41	47
D1	3	4	2	11	31	38	51	63	74	70
D2	2	4	2	21	29	35	48	59	52	78
D3	2	3	2	7	17	23	34	43	47	45
D4	2	3	2	7	16	23	31	38	42	40

FIGURE 4.5

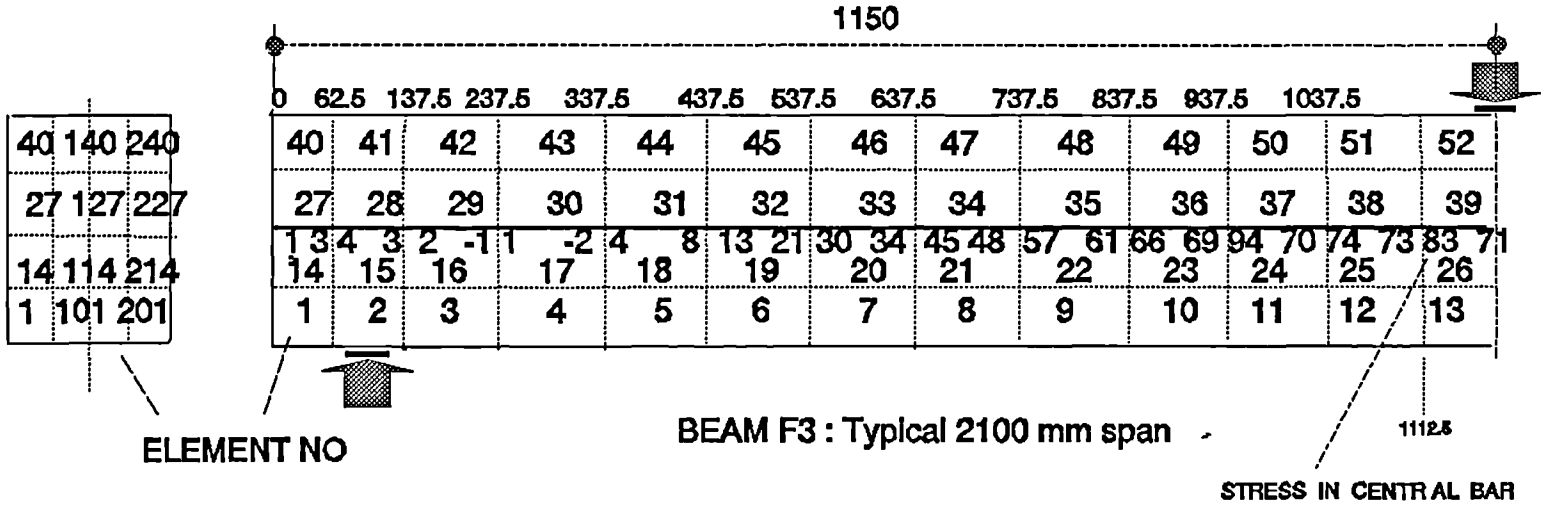

CRITICAL STRESS IN CENTRAL BAR IN EACH ELEMENT (N/mm2)

F3	3	4	2	1	8	21	34	48	61	69	94	74	83
F6	2	3	2	2	12	14	24	30	35	44	50	57	69
F7	2	2	2	0	7	11	18	25	29	37	43	50	60

(For beam F7, the stress is the average of the maximum stresses in the two bars.)

FIGURE 4.6

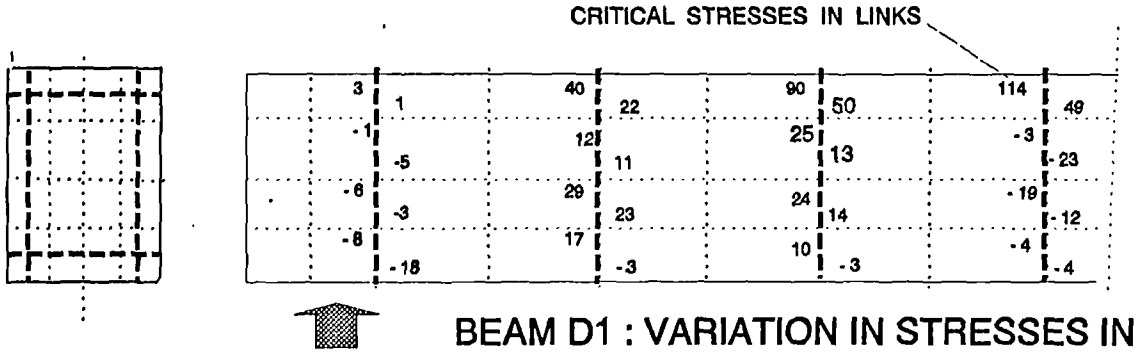

BEAM D1 : VARIATION IN STRESSES IN LINKS

CRITICAL STRESSES IN LINKS FOR SPECIMEN SERIES C & D AND BEAM F 7

C1	C2	C3	D1	D2	D3	D4	F7
101	117	130	114	117	94	94	122
- 23	- 11	-12	- 23	- 26	- 18	- 19	39
- 11	- 30	- 30	- 19	- 8	- 17	- 18	3
- 2	- 24	- 23	- 4	4	- 4	- 4	5

FIGURE 4.7

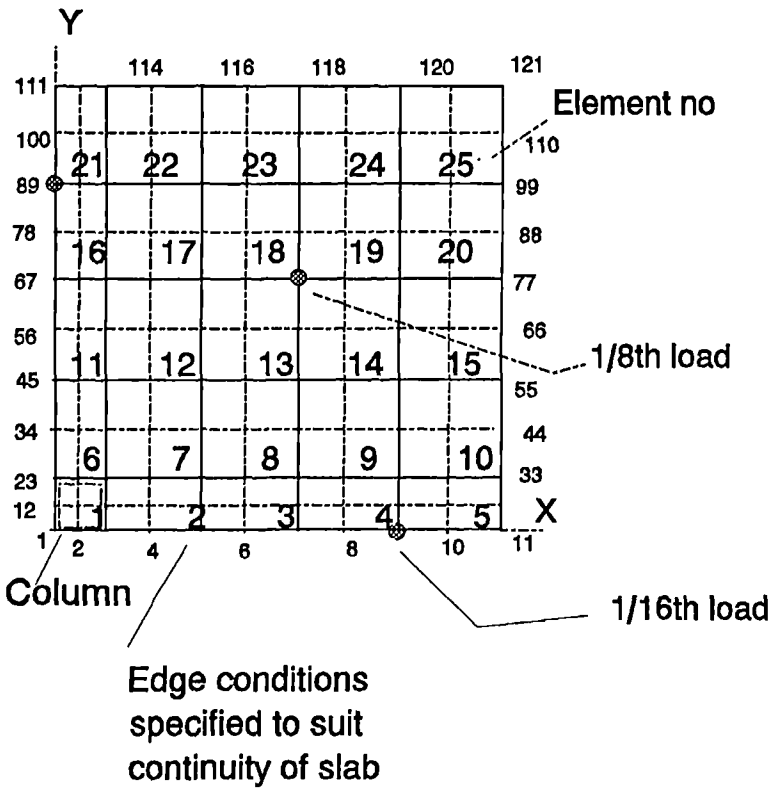

Finite element idealization for quarter-slab

FIGURE 4.8

CHAPTER 5
ADOPTION OF DESIGN RULES TO FIRE EXPOSURE CONDITIONS

5.1 Review of research related to fire exposure conditions

5.1.1 Properties of materials at high temperatures

i) Concrete

Hertz[46] has identified the factors concerning the reduction in strength of a heated concrete member as follows:

a) Temperature level;
b) Loads acting on the member; and
c) Aggregates used. (Concrete made with calcareous or lightweight aggregate is more vulnerable to the action of fire than the silicious aggregate concrete.)

Initially, the effect of heat on concrete is to cause evaporation of free moisture. If the fire continues to heat the concrete, the heat may cause release of water which is chemically bound in the hydrated calcium silicates. This may occur at temperatures in excess of about 150^0 C. This loss of water weakens the concrete and causes reduction in its strength, as the hydrated cement paste shrinks and the aggregate and the reinforcement bars tend to expand. In certain cases, the pressure generated by conversion of moisture into steam may be too high for the surface layer of concrete to resist and it may spall.

Temperatures above 300^0 C result in micro-cracking which will pierce the matrix. This causes further reduction in the compressive strength, tensile strength and the modulus of elasticity. Above 400^0 C, the crystals of calcium hydroxide begin to decompose and convert into calcium oxide and water. This process is at its highest intensity at 535^0 C. In addition to this weakening effect, further loss of strength could result during the cooling period. During this period, the calcium oxide begins to react with atmospheric moisture and expands, causing widening of

cracks already present. The minimum strength could be reached one week into the cooling period and the reduction in the strength could be of the order of 20%.

At about 575^0 C, volume expansion of 1% could take place as a result of change in the structure of quartz. Following this stage, if the concrete contains limestone aggregate, chemical reactions result in the release of carbon dioxide from the limestone at about 650^0 C. At 715^0 C, the rate of decomposition of remaining calcium silicates is intense and maximum. At temperatures in excess of 700^0 C, the quartz aggregates may decompose and certain aggregates made from burnt clay may melt at 1150^0 C.

According to Hertz, the reduction in strength does not depend on the water-cement ratio or the initial compressive strength. The reduction depends significantly on the amount of calcium hydroxide crystals in the matrix. The decrepitation in strength could be lessened by adding Pozzuolana to the Ordinary Portland Cement. This Pozzuolana should contain Aluminium Oxide, sufficient to react with the calcium hydroxide and produce heat-resistant crystals, thus improving the heat-resistance of concrete. This effect has been experimentally proved in Danish laboratories, using Danish mo-clay powder as Pozzuolana and burnt mo-clay as aggregate to produce improved heat-resistance of concrete up to 1150^0 C.

Such means of modifications to the properties of concrete may not be practicable for use in normal construction. Also, the design rules for reduction in strength of concrete are generally based on fire exposure tests on specimens made with concrete with ingredients which are commonly available.

ii) Reinforcement

EC2 Part 1.2[29] provides data for reduced strength of reinforcing steel as a function of the temperature. The reduction in strength corresponds to various conditions of using and specifying the strength of steel.

5.1.2 Development of the German Code of Practice

The German code of practice DIN 1045 (1959 Edition) gave a recommendation to the effect that the bent-up bars should share a larger proportion of shear when used in combination with links. The fire resistance recommendations in DIN 4102 (Part 4) were, therefore, based on tests on specimens conforming to this recommendation. When this recommendation was not carried forward in the revised code DIN 1045[47], there were concerns about the safety of reinforced concrete elements exposed to fire, provided with two-legged links only. It was suggested that the inclined bars, placed inside the concrete section, would have better protection from fire than that available to the links located nearer to the surface.

A test-programme was carried out as reported by Krampf[48] using beams with vertical links, generally conforming to DIN1045 (1972) and DIN 4102. The main conclusions were as follows:

i) The two-span beams were found to be more susceptible to shear failure than single-span beams. This is attributed to rapid deterioration in the compression zone, a principal contributor to the shear resistance, while the tension reinforcement could remain effective for a comparatively longer time, providing the flexural resistance. The single-span beams underwent a flexural-tensile failure, failure of the bottom steel. In only one case, where the web was 80 mm thick, web-failure was observed to have initiated a flexural-compression failure. The links reached a temperature of 680^0 C but did not fail.

ii) The specimens designed for class F180 (180 minutes exposure) and subjected to uniformly distributed loading fared better than those subjected to concentrated loading. For periods of exposure of 90 minutes, the type of loading did not seem to have any influence.

iii) The effect of varied shear span ratio was not conclusive. However, where the shear span ratio was 1.5 and beams were designed for class F180, the beams fared better than those with higher values of the shear span ratio.

iv) F90 specimens with high shear stresses (about 3 N/mm^2) failed earlier than

those with lower design shear stresses. F180 specimens were all in higher range and, therefore, a comparison was not possible. In such cases, the failures seemed to be due to decrepitation of concrete and not due to fracturing of links. In some cases where the design shear stresses were lower, failure of links was noted. The general conclusion was that the stresses expected in the links in accordance with the design based on modified truss analogy (reduced shear coverage **[13]**) were not in fact attained at any stage up to failure of the beam.

v) Three different grades of concrete were used, with cylinder strengths of 25, 35 and 45 N/mm^2. However, there was no relative difference in performance of specimens in fire conditions on this account.

vi) The overall conclusion was to accept the provisions as adequate for classes up to F90 and make recommendations for additional measures for higher classes F120 and F180.

The observations of specimens were made subject to some limitations imposed by practical difficulties, which could be valid for any other test programme. The main points were identified as follows:

i) It is not practicable to measure the strains in links and the main bars using "electrical resistance strain gauges". Such strain gauges are not suitable for use at variable and high temperatures, unless some expensive measures are available; for example, welded connections with the steel, which require a very high level of expertise.

ii) Cracks can be detected from outside the fire chamber only after they become visible. The width of a crack, however, can only be estimated roughly.

iii) A horizontal crack at the tension steel level in a normal test could mean the start of dowel splitting. In fire exposure tests, this could generally (but not always) be the indication of spalling at the corners or the peeling of the bottom layer of concrete outside the links, under very high temperatures.

iv) There are practical limits on the duration of a fire test, which may inhibit detailed investigation; for example, risk of damaging the instrumentation may require an earlier termination of a test. The failure conditions,

therefore, may not be identical for all tests.

v) If the web steel recovers after cooling and shows no signs of distress, the conclusion that the failure was due to decrepitation of concrete compressive block could be generally justified. But, if the links do show signs of yielding or fracture, the primary cause could not be clearly identified.

In view of these limitations, Krampf commented that the inferences drawn regarding the mechanism of failure from results of such tests could be "at best very tentative, if indeed justified at all". This comment, however, could apply to the usefulness of tests for validation of basic principles. The results of such fire exposure tests could provide a comparative assessment of the load-carrying capacity of specimens of different dimensions and provided with different reinforcement. The indicators provided by Krampf's test programme were valuable for the testing carried out under this project.

5.1.3 Fire tests carried out by Lin et al[49]

Lin has reported tests on beams exposed to two different types of fire; "Short Duration High Density Fire" and the standard fire ASTM Designation: E119, specified by the American Society of Testing and Materials, Philadelphia, Pa. This chapter includes an examination of Lin's tests on beams exposed to ASTM type of fire, since the time-temperature relationship under this type of fire is similar to that of the standard test fire used in tests reported in this project. The details of test beams 1, 2, 3 and 4 and the results of these tests will be discussed later in section 5.7.

The span-to-depth ratio for beams 1, 2 and 3 was 12. The provision of tension steel and links was such that Lin did not expect any beam to fail in shear under the action of loads which were uniformly placed on the span. Accordingly, the beams were observed to have failed in bending under exposure to fire. The test periods ranged from 206 minutes to 248 minutes, in agreement with the authors' estimates based on consideration of flexure.

5.2 Recommendations in the codes of practice

5.2.1 General recommendations

The current practice could be generally seen to adopt one of the routes discussed below but each route concentrates mainly on the influence of high temperatures on flexural capacity of members.

i) Prescriptive method

Both BS8110[29] and Eurocode EC2 Part 1.2[30] give the minimum cover to steel and the member dimensions appropriate to achieve the required fire resistance rating. BS8110: Part 1 gives covers related to the minimum dimensions of members. BS8110: Part 2 allows a reduction in cover where the width of a member is greater than the prescribed minimum. EC2 tables give "trade-off" combinations of cover and member dimensions.

For example, BS8110: Part 1: 1985 requires a minimum width of 200 mm for reinforced concrete beams and a 20 mm minimum cover is required to all steel including links. A 200 mm wide beam with 25 mm cover to the longitudinal steel could be used to meet a specified period of fire resistance of less than 90 minutes.

Using the current draft of Eurocode EC2 part 1.2, a 200 mm wide beam would require a minimum clear cover to the longitudinal steel of 35 mm and 55 mm for fire resistance periods of 90 and 120 minutes respectively. Also, 10 mm must be added to these minimum covers to obtain the minimum clear distance between the corner bar and the side of the beam, for beams with a single layer of longitudinal steel.

Both codes provide prescriptive guidance for protection against the effects of spalling. At present, the reasons for spalling are not clearly understood and there is no general agreement on any definite and quantified prevention measures against spalling. EC2 recommends minimum member dimensions and BS8110 recommends measures which give added protection to the concrete surface. A

supplementing mesh is also recommended in both codes when the covers are large; for example, covers in excess of 45 mm in accordance with BS8110.

ii) Simple calculations method

BS8110: Part 2 recommends a method related to structural elements in flexure, where failure is governed by yielding of the main tensile reinforcement. This code gives limited guidance and refers to a joint report prepared by the Institution of Structural Engineers (IStructE) and the Concrete Society[50].

EC2 Part 1.2 gives a more detailed guidance including temperature profiles and change in concrete and steel properties due to elevated temperatures. From the present draft of EC2, it seems that this information is generally similar to that in the reference[50], with minor differences. For example, in case of ribbed members, EC2 tends to be more conservative.

These methods could provide more economical sections compared with the prescriptive provisions. Advantage could be taken of the support conditions and the resulting reduction in the mid-span bending moment. Such reduction would depend on the capacity of the member to sustain negative moment and the provision of top reinforcement at the support.

BS8110 allows reduction in partial factors under conditions of fire exposure. γ_m is reduced from 1.5 to 1.3 for concrete and from 1.15 to 1.0 for steel. Similarly, γ_f is reduced from 1.4 to 1.05 for dead load and from 1.6 to 1.0 for imposed loads. The latest EC2 Part 1.2 allows reduction of γ_m from 1.5 for concrete and from 1.15 for steel to 1.00 for both materials. The combined effect of all actions is reduced by using combination factors appropriate for accounting for fire as an accidental action. This could be simplified by applying an overall reduction factor for reducing the effect of actions under fire exposure conditions, compared with the effect accounted for in the cold design. This factor could be 0.6 for all cases except for certain categories of structures (warehouses, department stores, etc) where the factor could be 0.7.

iii) Detailed calculations methods

These methods are based on fundamental principles. Computer programs similar to SOSMEF[51] could be adopted for flexural design of reinforced concrete elements, accounting for non-linear variations in material properties at elevated temperatures.

5.2.2 EC2 guidance on evaluation of shear carrying capacity

The guidance given in the current Eurocode EC2 Part 1.2 is summarised as follows:

i) The shear carrying capacity may be calculated in accordance with the normal temperature design rules using reduced material properties.

ii) When using the simplified calculation method, the normal temperature design rules may be applied directly to a reduced cross-section.

iii) When using the simplified calculation method, the actual shear behaviour of the concrete at elevated temperatures should be considered if the shear capacity relies on tensile strength of concrete.
(The information giving reduction in the tensile strength at high temperatures is not available in the current draft. It is understood that this information will be included in the final draft of the code.)

The rules proposed in this chapter generally accord with the principles implied in the EC2 guidance. In addition to the reduction in strength of concrete with increase in temperature, the proposed rules also account for the loss of stiffness of the tension steel or reduction in its modulus of elasticity.

5.3 Shear resistance of beams at elevated temperatures

i) Ultimate shear resistance of concrete (V_{cT})

Equation 3.2.7 (Chapter 3) can be rewritten as Equation 5.1 to give V_{cT} (kN), for application at elevated temperatures. The terms used below have the

same meaning as in chapter 3, unless shown differently in some cases.

$$V_{cT} = 0.0046 \left(\frac{100\ A_{st}}{b_T d_T}\ E_T\ f_{cT}\right)^{1/3} \left(\frac{400}{d_T}\right)^{0.25} \frac{b_T d_T}{1000} \quad .. \quad 5.1$$

f_{cT} = Concrete strength at T° C (paragraphs 5.4.1 and 5.4.2)

E_T = E_{st} of tension steel at T° C " "

b_T = width of the beam at T° C " "

d_T = depth of the beam at T° C " "

ii) Contributions of links(V_{IT})

$V_{IT} = A_{sw} \times d_T \times f_{yT} / s$ ... 5.2

(f_{yT} = characteristic strength of links at T° C)

iii) Contribution of central bars (V_{bT})

At temperature T° C, the contribution of the central bar should correspond to the strength of concrete at the centre of the section (f_{cTm}). The rule for V_{bT} , therefore, is obtained by modifying the equation 3.5.3 (Chapter 3), replacing V_{CU} by V_{cT} modified accordingly. A_b is the area of cross-section of the central bar.

$$V_{bT} = 0.4\ (V_{cT})\ \left[\frac{f_{cTm}}{f_{cT}}\right]^{1/3} \frac{100 A_b}{b_T\ d_T} \quad kN \quad ... \quad 5.3$$

5.4 Proposed design method for rectangular beams

5.4.1 General Procedure

The procedure for calculating the load carrying capacity of beams is generally based on the method described by Wade**[46]**.

i) Check for resistance to bending

a) Ignore concrete layer with temperature in excess of 750^0 C. (This step provides b_T and d_T.) However, the concrete is considered as adequate for

providing bond for the reinforcement present in this layer.

b) Calculate the revised moment of resistance using the residual section and the reduced stresses in the tension steel and concrete.

ii) Check for resistance to shear

Use the equations 5.1, 5.2 and 5.3 to evaluate V_{cT}, V_{IT} and V_{bT} respectively. The overall shear resistance (V_{dT}) is given by equation 5.4.

$$V_{dT} = V_{cT} + V_{IT} + V_{bT} \quad .... \quad 5.4$$

For calculating V_{cT} , the concrete strength f_{cT} is based on eleven values corresponding to the temperature contours as shown in figure 5.6 for a typical specimen D2; $f_{cT}1$, the maximum value at the centre reducing to $f_{cT}11$, the minimum at the temperature contour 750° and nine values at contours spaced equally between these two locations. The sum of the products given by multiplying the area of the strip by its average concrete strength [$(f_{cT}1 + f_{cT}2)/2$, etc] is divided by the total area of the beam to obtain the concrete strength f_{cT}. (The area of strip outside the 750° contour is included with its average concrete strength as zero.)

For calculating V_{bT}, the concrete strength is f_{cTm} or $f_{cT}1$ as mentioned above. V_{IT} is calculated using f_{yT} as the steel strength corresponding to the temperature at the link.

5.4.2 Derivation of temperatures in the cross-section

The application of the rules 5.1 to 5.4 requires estimates of temperatures developed within the cross-section of a beam at the end of a certain fire exposure period. The rise in temperature in a concrete section, as a response to the external high temperatures, depends on a large number of factors. These factors include the moisture content in the concrete and the chemical composition of the aggregate and cement. Also, the development of temperature in a beam depends on the heating conditions and the heat transfer characteristics of the environment. However, these factors cannot be conveniently evaluated for the purposes of

developing a general design rule. It is decided, therefore, to use data based on tests; for example, the graphs prepared by Wade[52] for beams exposed to fire on three sides. These graphs, the test results reported by Lin[49] and the data obtained from tests described in section 5.5 are used for constructing equations to give temperature profiles in beams.

The temperature contours are assumed to be parallel to the vertical faces and the soffit of the beam exposed to fire on these three faces, as shown in figure 5.6. This is in agreement with the figures given by Lin for contours of temperatures at 1200 °F, 1000 °F etc, which are based on interpolation of temperatures measured at various locations of thermocouples.

The temperature (T° C) at a point located at a distance of "x" mm from the face of the beam is assumed to be governed by the following factors:

i) the ambient high temperature which is a function of the fire exposure time (t, in minutes) ;

ii) b, the width of the cross-section (mm); and

iii) r, the ratio of the overall height to the width of the beam.

The following cubic equation is proposed:

$$T = (D - Ax + Bx^2 - Cx^3) / r^{0.25}$$

The values of D, A, B, and C are obtained by solving a number of simultaneous equations constructed to represent, as closely as possible, the trends given in Wade's charts and to accord with Lin's measurements and the data obtained from the tests described in section 5.5.

$$D = 475\, r^{7/12} - (b - 105\, t^{1/3})$$

$$A = 3.33 \left(3 + 0.0033t + \frac{(100-t)}{b}\right)$$

$$B = 0.085 \qquad C = 0.000221$$

Figures 5.1 to 5.5 are based on the above equation for "r = 1.5" and they illustrate the plots of temperature distribution in beams with various widths, for 30, 60, 90, 120, 180 and 240 minutes exposure periods. The temperature distribution for intermediate values of beam widths and exposure periods may be obtained by interpolation. The application of this rule should be limited to beam widths (mm) within the range $300 > b > 100$ and values of "r" within the range $1 < r < 3$. For beams with "r $\leq$ 1.5", the temperature distribution for "r = 1.5" should apply.

For slabs, the temperature profiles are shown in figure 5.7, based on the following rule and the values of constants:

$$T = (D - Ax + Bx^2 - Cx^3)$$

$$D = 300 + \frac{2t}{3} + 105(t)^{1/3}$$

$$A = 3.75\ (3 + 0.0033t + \frac{100-t}{650})$$

$$B = 0.0715 \qquad C = 0.00014$$

5.4.3 Properties of materials at high temperatures (EC2 part 1.2[29])

a) f_{cT}: (Characteristic strength of concrete at T°C)

$f_{cT}/f_{cu} = K_c$

$K_c = 1.0$ for $T \leq 100$

$K_c = (1.067 - 0.00067T)$ for $100 \leq T \leq 400$

$K_c = (1.44 - 0.0016T)$ for $400 \leq T \leq 900$

$K_c = 0$ for $900 \leq T$

b) f_{yT}: (Characteristic strength of steel at T°C)

$f_{yT}/f_{yv} = K_s$

$K_s = 1.0$ for $T \leq 350$

$K_s = (1.899 - 0.00257T)$ for $350 \leq T \leq 700$

$K_s = (0.24 - 0.0002T)$ for $700 \leq T \leq 1200$

$K_s = 0$ for $1200 \leq T$

c) E_T: (Modulus of elasticity of steel at T°C)

$E_T/E_{st} = K_e$

$K_e = 1.0$ for $T \leq 100$

$K_e = (1.10 - 0.001T)$ for $100 \leq T \leq 500$

$K_e = (2.05 - 0.0029T)$ for $500 \leq T \leq 600$

$K_e = (1.39 - 0.0018T)$ for $600 \leq T \leq 700$

$K_e = (0.41 - 0.0004T)$ for $700 \leq T \leq 800$

$K_e = (0.27 - 0.000225T)$ for $800 \leq T \leq 1200$

$K_e = 0$ for $1200 \leq T$

5.4.4 Shear carrying capacity of beams at high temperatures

Equations given above have been set in a LOTUS spread-sheet program, as shown in the next section, to obtain the load-carrying capacity of rectangular beams subjected to fire exposure. At mid-span, the flange of a beam enhances the compression chord and, hence, its flexural resistance. At the support, the flange protects the tension steel from fire acting on the soffit of the flange and the beam. For demonstrating the application of this program and for estimating the load-carrying capacity of the test specimens, however, only a rectangular section is considered, with fire exposure on three sides and a protected top face.

A similar program could be written for evaluating the punching shear capacity of flat slabs, with modifications of the rules given in chapter 3. The tests for validation of such rules, however, could not be accommodated in this project.

5.5 LOTUS Spreadsheet program

5.5.1 General notes

i) The section dimensions (b, d, & r), f_{cu} , minimum cover, E_{st} , f_{yv} and the provision of reinforcement (tension steel, links and central bars) are entered

in cells near the top of the page. The program calculates the actual areas of steel, links, etc.

ii) The required fire exposure time is entered as an input, for estimating the safe ultimate load carrying capacity of the beam. If it is necessary to evaluate the safe fire exposure period for a given ultimate load, "trial and error" procedure should be used.

iii) The program evaluates the temperatures in the beam exposed to fire at the soffit and the two sides. The strength of materials corresponding to the temperatures are estimated and used for calculating the shear resistance capacity. The safe ultimate centrally applied load is twice the estimated ultimate shear resistance, V_{dT} .

iv) A "trial and error" procedure should be used for assessing the effect of change in provisions; for example, the cover, the central bar, links, the tension steel, section width, etc.

5.5.2 Examples of LOTUS Spread-sheet

The following two pages show typical LOTUS Spread-sheet calculations; one for the load-carrying capacity of beams D201 and D202 tested at Veseli, which will be described in section 5.6 and the other page for beam no 1 of the beams tested by Lin, which will described in section 5.8.

Shear resistance of beams : D201 and D202

b =	200 mm				
d =	265 mm	Min cover to			
r =	1.5	tension steel =	25	mm	
h =	300 mm	Est =	200000	N/mm2	
		fyv =	460	N/mm2	
Tension steel	3	20 mm dia	Ast =	942	mm2
Central bar :	1	16 mm dia	Ab =	201	mm2
Links :		6 mm dia	Asw =	57	mm2
Spacing of links (s):		200 mm			

	D201		D202	
Compressive strength at the start fcu (N/mm2)	38.50		38.40	
	bT	dT	bT	dT
At max temperature	186.60	265	190.84	265
fcT (average for the section)		21.27		22.56
Temp at the central bar		383.40		357.72
fcT at the central bar		31.19		31.77
Temp at location of links =		628.85		608.35
Revised stress in links =		130.12		154.35

Temp. at tension steel (C) =	550	C	528	C	
Stress in the tension steel	223.89	N/mm2	249.14	N/mm2	
Reduced Est	91273	N/mm2	103663	N/mm2	

	t (minutes)	VcT	VbT	VlT	VdT
D201	107.0	39.0	7.2	9.7	55.9
D202	94.0	42.1	7.5	11.6	61.2

	Applied load (Wt)		Estimated load (West)		West/Wt
D201	120	kN	111.9	kN	0.93
D202	120	kN	122.4	kN	1.02

Flexural capacity of beams tested by Lin : Beam 1

b =	229 mm		fcu (compressive strength at the start) =	34.83	N/mm2
d =	447 mm		Min cover to		
r =	2.328		tension steel =	48	mm
h =	533 mm		Est =	200000	N/mm2
			fyv =	510	N/mm2
Tension steel	4	25.4 mm dia	Ast =	2027	mm2

Fire exposure period :			220	minutes
	bT		dT	
Revised dimensions	164.29		447	mm

Temp. at tension steel (C) =	647	C
Stress in the tension steel	120.73	N/mm2
Revised Est	45152	N/mm2

Corresponding flexural strength		
Concrete comp. =	352.88	kN
Tension in steel =	244.69	kN

Estimated Momemt of Resistance : **98.42** kNM

Ultimate BM : **98.00** kNM

Fire exposure period : 220 minutes

5.6 Fire exposure tests on beams

5.6.1 Details of specimens

A test programme comprising 10 tests under fire exposure conditions was undertaken for validation of the design method. The specimens were cast at the City University, using Thames gravel as coarse aggregate. There were two beams of each type; 200 x 300 mm in cross-section, 1600 mm overall length and 1400 mm supported span. The types of specimens were similar to the specimen types in the test programme on beams described earlier in chapter 3. Types B1, B3, B4, C1 and D2 were chosen to represent various combinations of the web reinforcement.

All specimens were provided with thermocouples, as shown in figure 5.9 and photograph 16, to obtain the temperature distribution in the beams. The thermocouples were "PTFE insulated K type twisted cables". The ends of the thermocouples were precisely located by placing them in 20x30 mm miniature columns 300 mm long, cast in the formwork prior to concreting the beam itself. The strength of the mortar used for these columns was 30 N/mm^2. Thermocouples were also placed in links for beams type D2, but they are not shown in figure 5.9 for the sake of clarity.

Three 100 mm size cubes were cast and stored by the side of each specimen for ascertaining the concrete strength at the time of testing. The concrete strength f_{cu} was the average cube strength of these air-cured cubes. The specimens were wet-cured for the first four days and they were kept dry for a period of three months before starting the test-programme of four weeks for the ten beams.

The yield strengths of reinforcement, obtained from tests on 300 mm long segments, were 444 N/mm^2, 476 N/mm^2, 504 N/mm^2 and 532 N/mm^2 for 6 mm, 12 mm, 16 mm and 20 mm diameter bars respectively. However, the characteristic strength of steel (f_{yv}) is taken as 460 N/mm^2 for all reinforcement used in the test specimens.

The specimens were transported to the Pavus Institute Laboratory at Veseli near Prague, Czech Republic and the tests were carried out at this laboratory. The test results and the data were compiled in conjunction with the Klokner Institute, Czech Technical University, Prague.

Table 5.1: Details of beam specimens

Spec No	f_{cu} N/mm^2	Top steel	Tension steel	Centre steel	Links
B101	39.6	2T12	3T20	-	-
B102	39.5				
B301	34.4	"	"	1T16	-
B302	34.0				
B401	42.9	"	"	1T20	-
B402	41.5				
C101	42.3	"	"	-	T6@200
C102	42.9				
D201	38.5	"	"	1T16	T6@200
D202	38.4				

5.6.2 Test Procedure

The load was applied at mid-span and it was kept constant during each test. The deflections were measured at mid-span and at quarter-span points, using "Linear Voltage Deflection Transducers". Only the mid-span deflections are reported in this section.

The beam was placed centrally at the roof level of the furnace. The walls of the furnace were constructed with bricks as shown in photographs 17. The roof was made with precast slabs with insulation at the top, as shown in photographs 17 and 19. The gaps between the slab-insulation and the beam were carefully packed with insulation to protect the instrumentation above the slabs and to allow the beam to deflect freely under the load.

It was decided that the test should be terminated when the specimen attained a deflection of 0.10 x span or it was judged as incapable of sustaining the applied load or it showed signs of instability, whichever occurred earlier.

5.6.3 Estimates of load-carrying capacity of the specimens

The estimates of load-carrying capacity of specimens were calculated to correspond to the duration of tests, as shown in the previous section. For the purposes of these analyses, f_{cu} is taken as the cube strength of concrete used in the specimen. The effective distances (x) from the surface of the beam were as follows:

a)	For links:	x = 25 - (6/2)	= 22 mm
b)	For tension steel (20 mm dia bars):	x = 25 + (20/2)	= 35 mm

Figure 5.8 illustrates the estimated shear resistance contributions of the components of specimen type D2, with links and a central bar. Time (minutes) is marked on the X-axis. V_{cT}, V_{bT}, V_{lT} and V_{dT} (total shear resistance, $V_{cT}+V_{bT}+V_{lT}$) are marked in kN on the Y-axis. Table 5.2 shows the estimates of load-carrying capacity of specimens.

5.7 Observations on fire tests

5.7.1 Test results

Test results are shown in table 5.2, using the following symbols:

W_t : The centrally applied test load (kN). W_t is twice the applied shear. For all beams, except beam B101, W_t was calculated to be 60% of the load carrying capacity of the beams at normal temperature using a notional value of f_{cu} of 30 N/mm^2.

W_{est} Estimated load-carrying capacity corresponding to the duration of the test (t_t in minutes) [LOTUS Spreadsheet pages in section 5.5);

δ_m : The mid-span deflection (mm)

Table 5.2 : Test results and the estimated load-carrying capacity of specimens

Spec no	t_t minutes	W_t kN	W_{est} kN	W_{est}/W_t	δ_m mm
B101 *	126	56	70	1.25	10
B102	113	70	76	1.08	10
B301	128	80	78	0.98	12
B302	101	"	92	1.15	12
B401	102	90	107	1.19	12
B402 **	56	"	128	1.42	6
C101	111	110	97	0.88	7
C102	101	"	105	0.95	12
D201	107	120	112	0.93	11
D202	94	"	122	1.02	11

Mean value (excluding beams B101 & B402) = 1.02
Standard deviation " " = 0.10
(General comments on table 5.2 are given in section 5.9: Conclusions.)

Notes on table 5.2

i)* The test on specimen B101 was a trial test and it was witnessed by the writer. This was useful in taking some additional measures for the other tests; for example, additional insulation was provided on the top of the beam for the subsequent tests to protect the instruments from heat from the furnace, using a 60 mm thick layer of mineral wool ORSIL (75 kg/m^3). This test was stopped after a period of 126 minutes (t_t) due to reasons explained in paragraph 5.7.2.

ii)** Beam B402 failed earlier than expected and the temperatures in concrete were low as shown in figure 5.15, corresponding to the short fire exposure period. There could have been some local weakness near the support, resulting in severe spalling as shown in figure 5.27. This spalling could have exposed the tension steel to fire and caused a rapid reduction in its strength and modulus of elasticity and, hence, an early failure of the beam.

5.7.2 Test on Beam 101

The test on beam B101 was treated as a trial test and it was decided to have the initial load as 50 kN. After 15 minutes of fire exposure, some minor spalling, 2-3 mm deep and about 20-30 mm in size, appeared on the side of the beam as shown in figure 5.22. After 30 minutes, a fine crack developed at mid-span at the level of the bottom steel. Wet patches were seen on the top of the beam and water vapours were escaping. After 50 minutes, the cracks had extended towards the support, the spalling increased and some spalling appeared on the soffit of the beam as well. At 60 minutes, another crack developed 35 mm above the first crack. Thereafter, the lower crack widened and some more horizontal cracks developed in the upper region at about 90 minutes. At 105 minutes, the second crack above the tension steel level became some 3 mm wide over a length of 200 mm near each support. At 115 minutes this crack was about 5 mm wide.

At about 120 minutes, the load cell became very hot and it was decided to increase the load to 56 kN, with an intention to accelerate the failure. At this stage, the beam must have been close to failure and it did fail soon afterwards, following some excessive spalling between the two lower-most cracks, exposing the bottom steel. The test was terminated at 126 minutes.

5.7.3 Tests on beams B102, B301, C101, C102, D201 and D202

The ratio W_{est}/W_t is close to 1.00 for beams B102, B301, C101, C102, D201 and D202. Beams D201 and D202 have 16ϕ central bars and they show an increase in the shear resistance capacity over beams C101 and C102, which is attributable to the central bars. The stages of cracking in the beams were observed and noted as shown in figures 5.23, 5.24, 5.28, 5.29, 5.30 and 5.31. Observations made at various stages of behaviour of the test specimens are listed below. The first three stages resembled the observations made for beam B101. The beams reached these stages at intervals of time roughly proportional to the durations of the tests and they finally failed in shear.

i) An initial crack, approximately 0.5 mm wide, developed at a level

immediately under the tension steel.

ii) The second crack developed just above the tension steel and was similar in width, 0.5 mm.

iii) The first crack widened and minor cracks developed in the mid-span region in the lower third of the height of the beam.

iv) Cracks, inclined at an angle of approximately 30° to 45° to the horizontal, started at the tension steel level at the support and rose upwards towards the mid-span. Their width increased to about 1 mm.

v) Some more horizontal and parallel cracks developed over the depth of the beam. The tension steel appeared to lose bond and the concrete suffered severe spalling, leading to the failure of the beam in shear.

5.7.4 Tests on beam B302 and B401

The stages of cracking were similar to those described in paragraph 5.7.3. These beams, however, suffered substantial cracking and spalling near the tension steel as shown in figures 5.25 and 5.26. Although these beams developed diagonal cracking at failure, it could be deduced that the failure was accelerated due to exposure of a large length of the tension steel to fire. The estimated loads (W_{est}), therefore, are 15% and 19% higher than the actual failure loads for beams B302 and beam B401 respectively.

5.7.5 Furnace temperatures

The furnace temperatures were recorded, monitored and controlled to follow the standard fire curve in accordance with BS476: Part 20**[47]**. Temperatures were measured at three points in the furnace. The average values and the corresponding values given by the standard time-temperature curve are shown in table 5.3.

Table 5.3 : Furnace temperatures in ° C

Time (minutes)	Standard Curve	Average of the readings
15	727	706
30	830	780
45	890	852
60	933	893
75	967	923
90	994	945
105	1017	965
120	1037	983

5.7.6 Temperatures in beams

Figures 5.10 to 5.17 show estimated temperatures obtained from the rule in paragraph 5.4.2 as smooth lines:

- firm lines (————) for estimates at 50 mm and
- dotted lines (- - -) for those at 100 mm from the face of the beam.

The figures show comparisons of empirical rule estimates with the records of thermocouple 10 (outer) and thermocouple 3 (inner), at locations TA, TB and TC. For beams B301 and B302, the readings at 100 mm from the face of the beam refer to thermocouple 4, since the readings for thermocouple 3 were not available.

The data exclude some readings which showed sudden, erratic and abrupt changes. This may be attributable to a possible shorting of a PTFE coated wire and the record showing temperature at a location other than the end of the thermocouple. This is evident in figures 5.12, 5.13 and 5.14 where the erratic readings were too numerous to be excluded. The temperature readings at 50 mm from the face of the beam show a good correspondence with the estimated temperatures, for beams B101, C101, C102, D201 and D202. Also, figures 5.12 (beam B301), 5.18 (beam D201) and 5.20 (beam D202) show some correspondence between the estimated and the measured temperatures at the centre of the beam.

The readings for the thermocouple 10 show a scatter and exaggerated fluctuations as shown in figure 5.12 (beam B301) and figure 5.13 (beam B302). It is possible that these fluctuations in readings are caused by displacement of the thermocouple due to local cracking or spalling.

The increase in temperature at the centre of the beam, given by TA3, TB3 and TC3, seemed slower than expected in accordance with the empirical rule given in paragraph 5.4.2. The influence of moisture in the beams was a common feature and vapours were seen escaping from the top of the beams during the tests. Also, some of the thermocouples at 100 mm from the face of the beam recorded no rise in temperature above 100° C during the first 60 or 70 minutes of the test. This is attributed to the local moisture surrounding the thermocouple, influencing its response to the rise in temperature until the moisture evaporated through the cracks. The empirical rule has disregarded the delay in temperature rise due to moisture and, therefore, this rule could result in safe design provision for beams exposed to high temperatures.

5.7.7 Temperatures in beams with links (Beams D201 and D202)

Figures 5.18 and 5.20 show the readings from the thermocouples placed at 100 mm from the face for beams D201 and D202. Readings from the thermocouples placed at the location of links and at 50 mm from the face of the beam are shown in separate figures 5.19 (D201) and 5.21 (D202), for the sake of clarity of their comparison with the estimated temperatures.

The readings TA(L) and TC(L) are typical measurements of temperatures in links at locations TA and TC, as shown in figures 5.19 and 5.21. The links reached marginally lower temperatures compared with the empirical rule estimates represented by the smooth dotted lines in these figures. Also, both the figures show that the temperature in links drop abruptly below the line representing the temperature at 50 mm from the face after about 60 or 80 minutes. This would appear to be the effect of shorting of a PTFE coated wire at a point inside the beam. As a consequence, the record of temperature may well relate to this point and not to the end of the thermocouple placed at the location of the link.

The empirical rule given in paragraph 5.4.2 is partly derived from Wade's graphs which are based on the results of tests on plain concrete and not on reinforced concrete specimens. The links form a cage of steel which is continuous between the hottest part of the beam and the comparatively cooler part of the beam remote from the fire. It is possible that the steel cage could conduct the heat away from the hotter region to the cooler one. More research is necessary for assessment of temperature profiles in concrete beams with longitudinal steel and links.

5.8 Flexural capacity of beams

Lin's beams 1, 2, 3 and 4 had a span of 6100 mm and a cantilever of 1524 mm, representing the end-span condition of a continuous beam. The links were 10 mm diameter at 146 mm centres at the end supporting the cantilever and at 215 mm centres at the simply supported end. The beams failed in flexure at a location within the span, closer to the free-end support, as expected by Lin.

Beams 1, 2 and 3 were 229 mm wide and 533 mm deep. Beam 4 was 254 wide and 610 mm deep. The effective depth (d) was measured from the top of the beam to the centroid of the group of 25.4 mm diameter bars; 4 for beams 1, 2 and 3 (A_{st} = 2027 mm^2) and 5 for beam 4 (A_{st} = 2534 mm^2). Table 5.4 shows the other details of test beams.

The beams were loaded with six point loads uniformly spaced within the span (Sketch 5.8); 44 kN for beams 1, 2 and 3 and 71 kN for beam 4. These loads were kept constant during the fire test. Initially, the loads at the tip of the cantilever were applied to generate a negative moment of 59% of the strength of the beam at the support; for example, 114 kN for beams 1, 2 and 3. This cantilever load was increased during the test, for maintaining the cantilever end of the beam at a constant elevation. The maximum value of the load on the cantilever was reached after 60 minutes for beams 1, 2 and 3 and after 90 minutes for beam 4. This maximum value of load was kept unchanged until the end of each test.

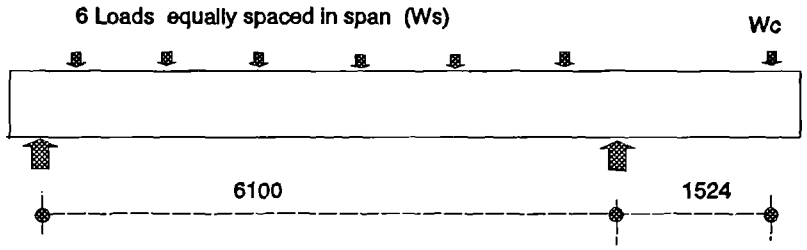

Sketch 5.8: Loading on beams tested by Lin

Table 5.4 : Details of beams tested by Lin

Beam no	cover mm	d mm	f_{cu} N/mm^2	* W_s kN	* W_c kN
1	48	447	34.83	264	164
2	"	"	38.71	"	"
3	67	428	37.07	"	"
4	48	529	42.84	426	252

(* W_s is the total load on the span and W_c is the load at the tip of the cantilever.)

Table 5.5: Comparison between estimated flexural capacity and results of Lin's tests

Beam No	test duration "t" (minutes)	Maximum applied Bending Moment in the span (kNm)	Estimated Moment of Resistance (kNm)
1	220	98	98.42
2	206	"	112.92
3	243	"	102.87
4	248	163	143.00

It is observed that the beams 1 and 2 had the same provisions except for the marginal difference in the concrete strength. Beam 3 shows an increase in the duration time of the test (243 minutes) compared with beams 1 and 2, which is attributable to its larger cover. Beam 4 was larger in cross-section and it was tested to study the effect of shear stress on the fire endurance of beams. All beams developed similar flexural cracks in the positive moment region closer to the free-end support. The failure in all cases was flexural as expected by Lin and there was no shear failure. The LOTUS Spread-sheet calculations for the assessment of flexural capacity of the beams have been shown in section 5.5. Table 5.5 shows good correspondence between these estimates and the test results.

One of the differences observed between the Veseli tests and Lin's tests was the effect of moisture. Lin's test on beam 1 was carried out after 298 days from the date of casting the beam and the other beams were tested after some 360 days from the date of casting. The Veseli tests were carried out when the specimens were 90 to 120 days old. Also, the beams tested by Lin were cured under damp burlap for seven days and, immediately after removal of the formwork, the beams were transported to a chamber for " moisture conditioning". This chamber was provided with controls to maintain the temperature at 20-25 °C and the relative humidity at 30-40%. The Veseli specimens were cured normally but moisture conditioning was not provided.

5.9 Conclusions

The beam B101 was tested as a trial beam for establishing a satisfactory test procedure. The centrally applied load for each of the other beams was approximately 60% of its shear resistance capacity at room temperature. Beam B402 failed earlier than expected as explained above. Beams B302 and B401 appeared to have suffered from excessive spalling at the tension steel level and the estimated loads for these beams were 15-19% higher than the applied test loads. The estimated loads for all other beams, corresponding to the duration of the tests, were close to the applied loads.

The mean value of W_{est}/W_t, excluding the results for beams B101 and beam

B402, is 1.02 with a standard deviation of 0.1. The proposed method, therefore, could be considered as satisfactory, subject to its limitations, for design against shear under fire exposure conditions. It is also observed that the method could be used for estimating the flexural capacity of beams as demonstrated in section 5.8 with the help of Lin's tests.

The prescriptive rules in BS8110 and EC2 Part 1.2 are not based on consideration of design against shear. These rules would appear to be restrictive, as described earlier in section 5.2.1. They do not allow the freedom of choice of dimensions of beams. They are not related to the load carrying capacity of the beams and the strength of materials used in construction. The method described in this report could lead to a more direct way for designing reinforced concrete beams exposed to fire.

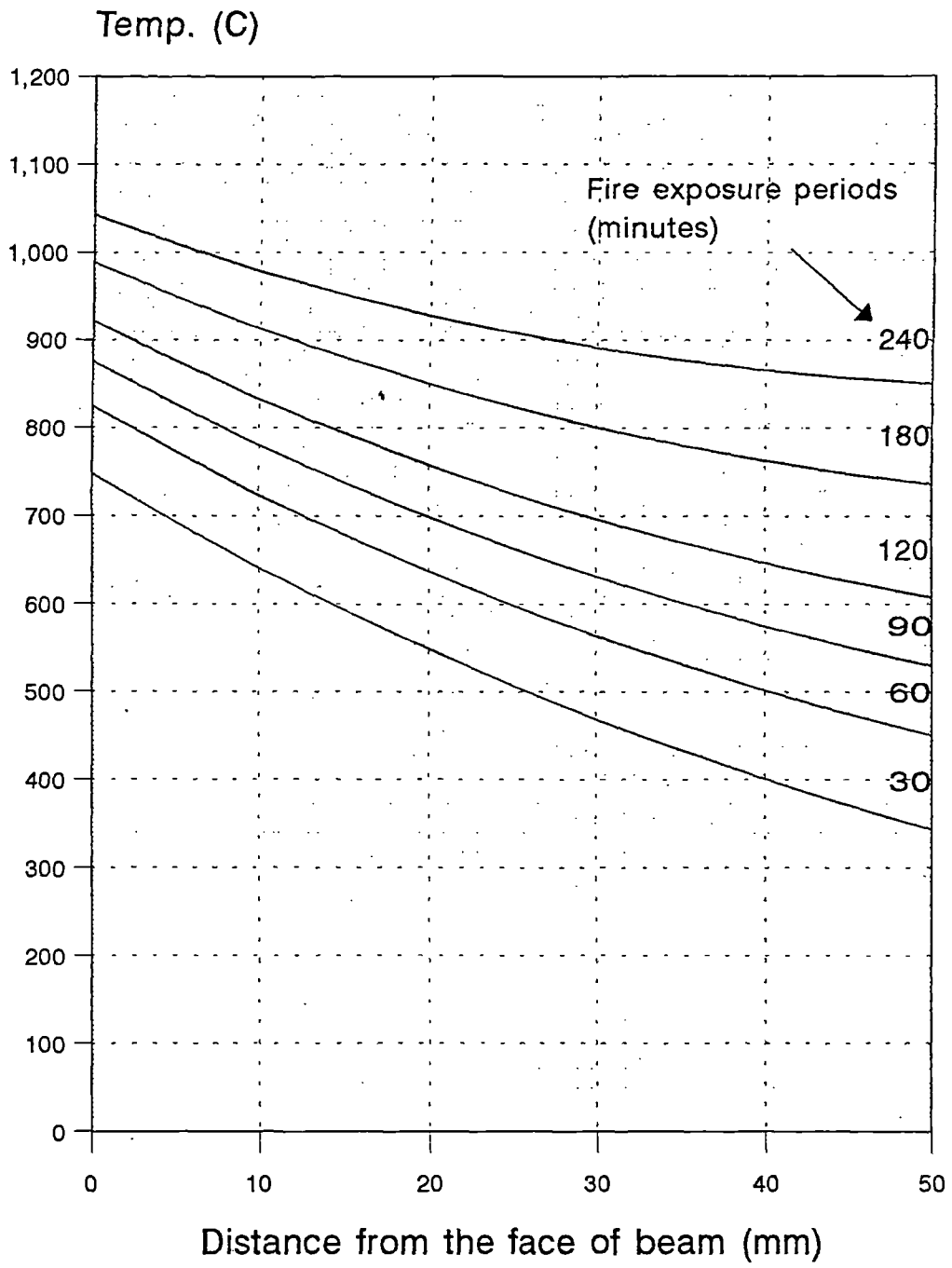

Temperature profile in beams
b = 100 mm ; r = 1.5

FIGURE 5.1

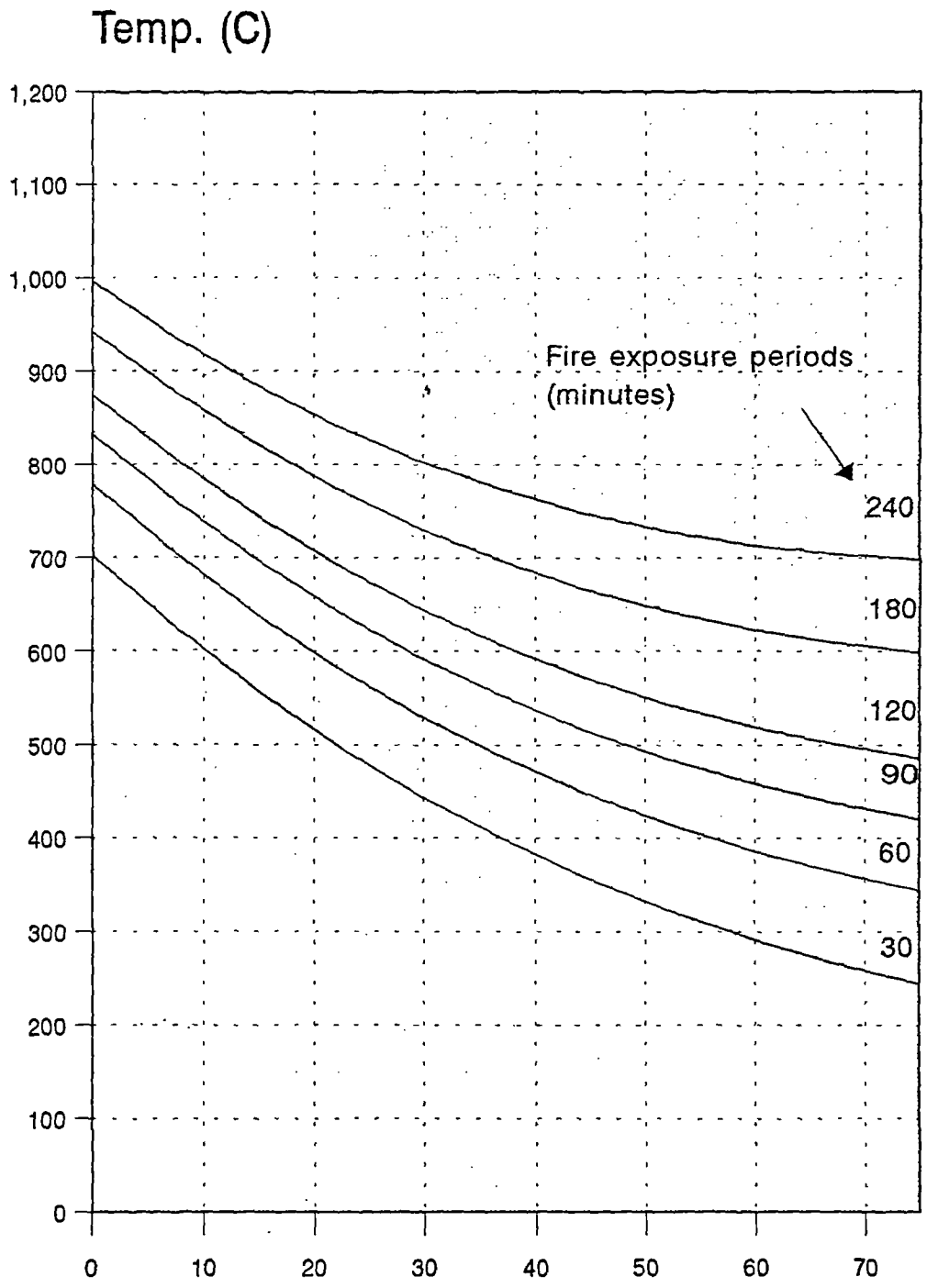

Temperature profile in beams
b = 150 mm ; r = 1.5

FIGURE 5.2

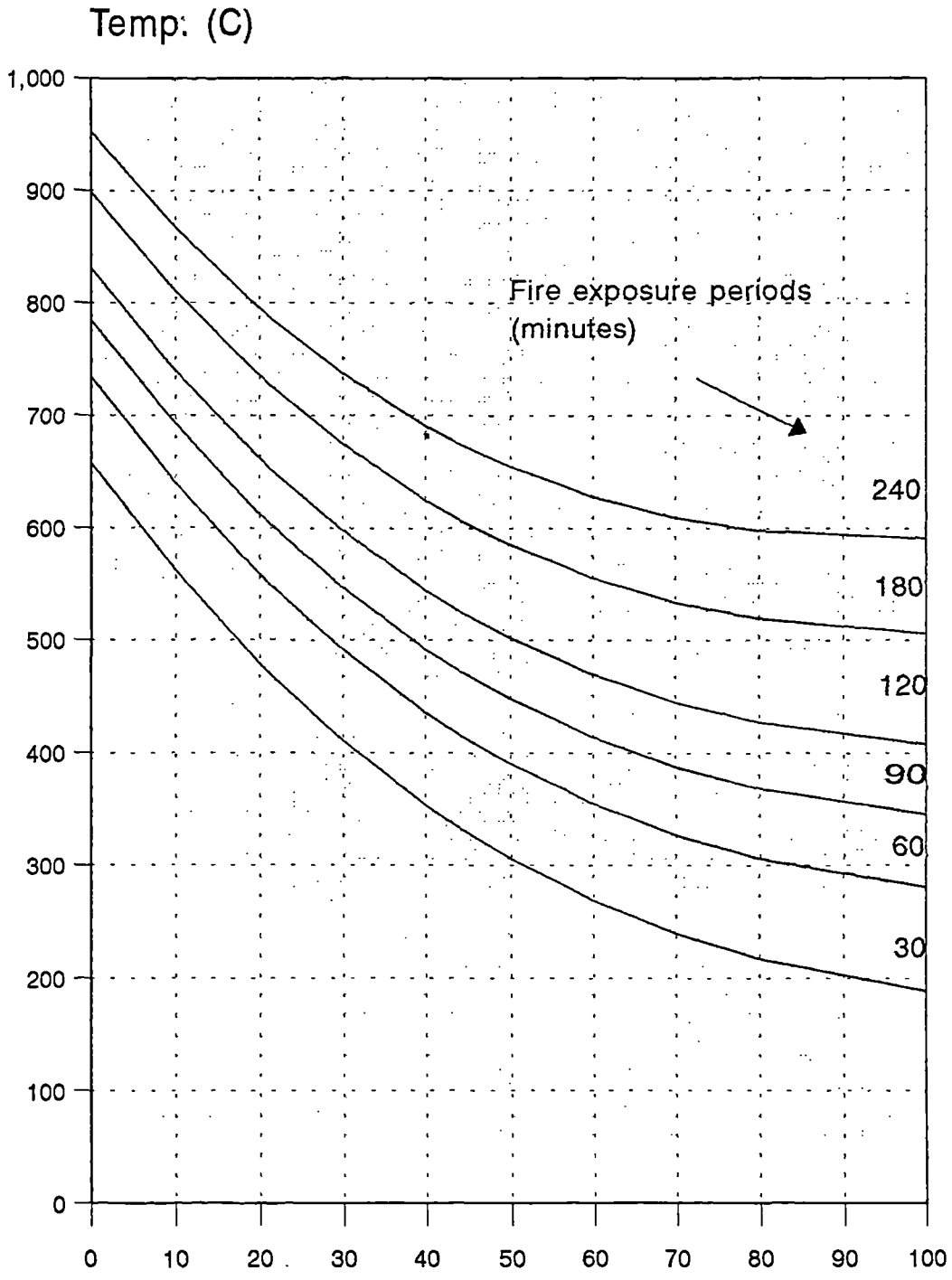

Temperature profile in beams
b = 200 mm ; r = 1.5

FIGURE 5.3

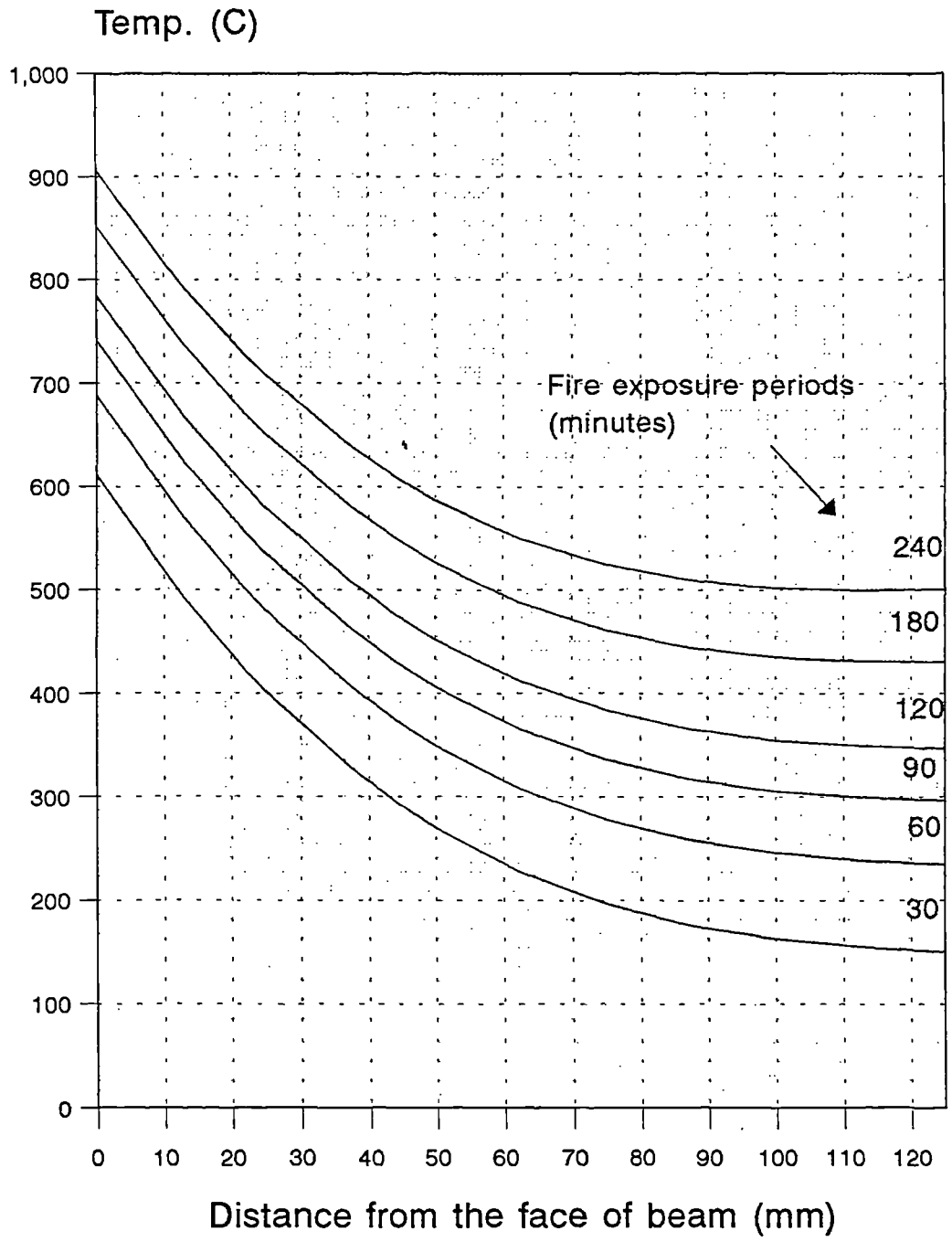

Temperature profile in beams
b = 250 mm ; r = 1.5

FIGURE 5.4

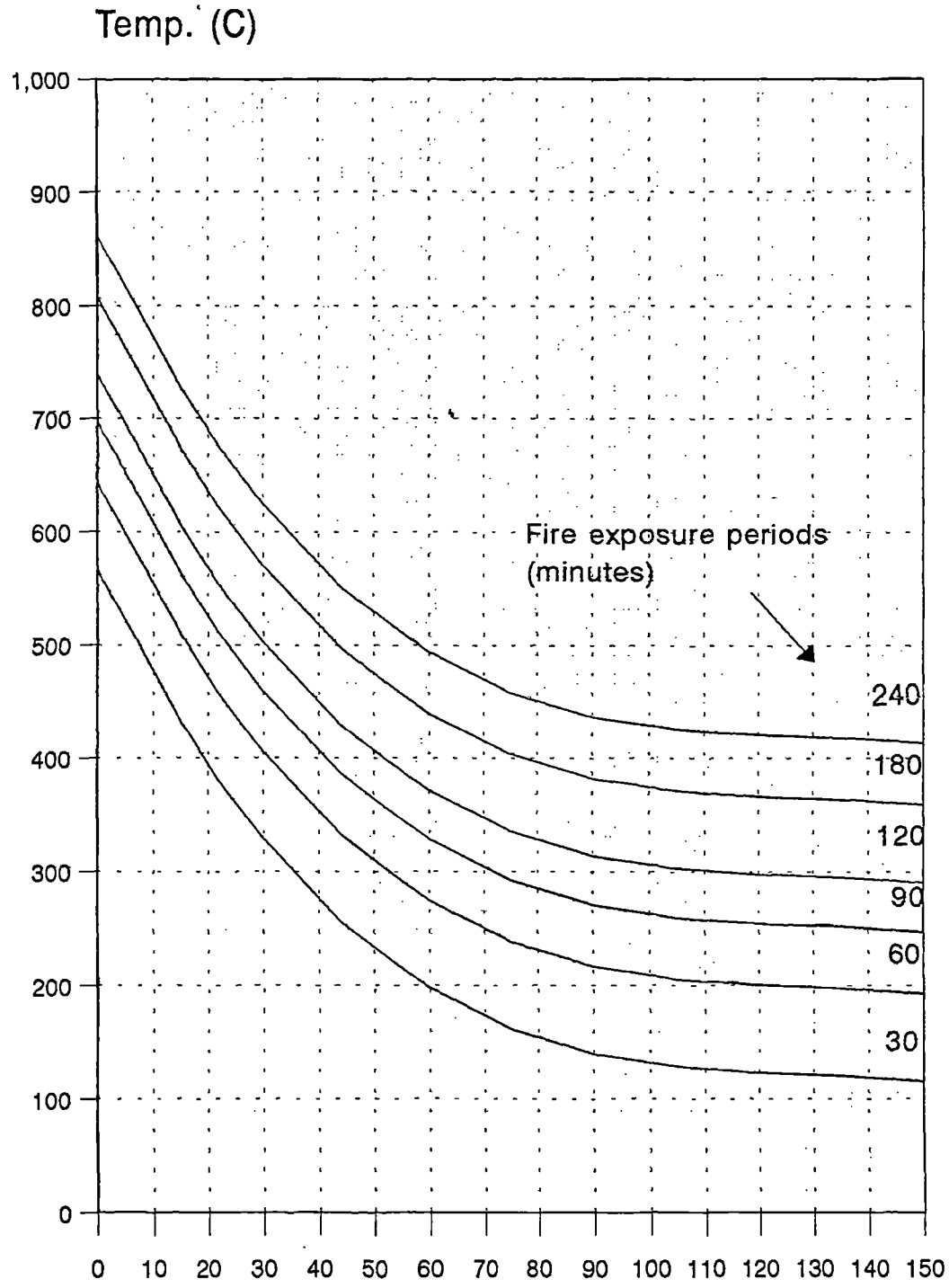

Temperature profile in beams
b = 300 mm ; r = 1.5

FIGURE 5.5

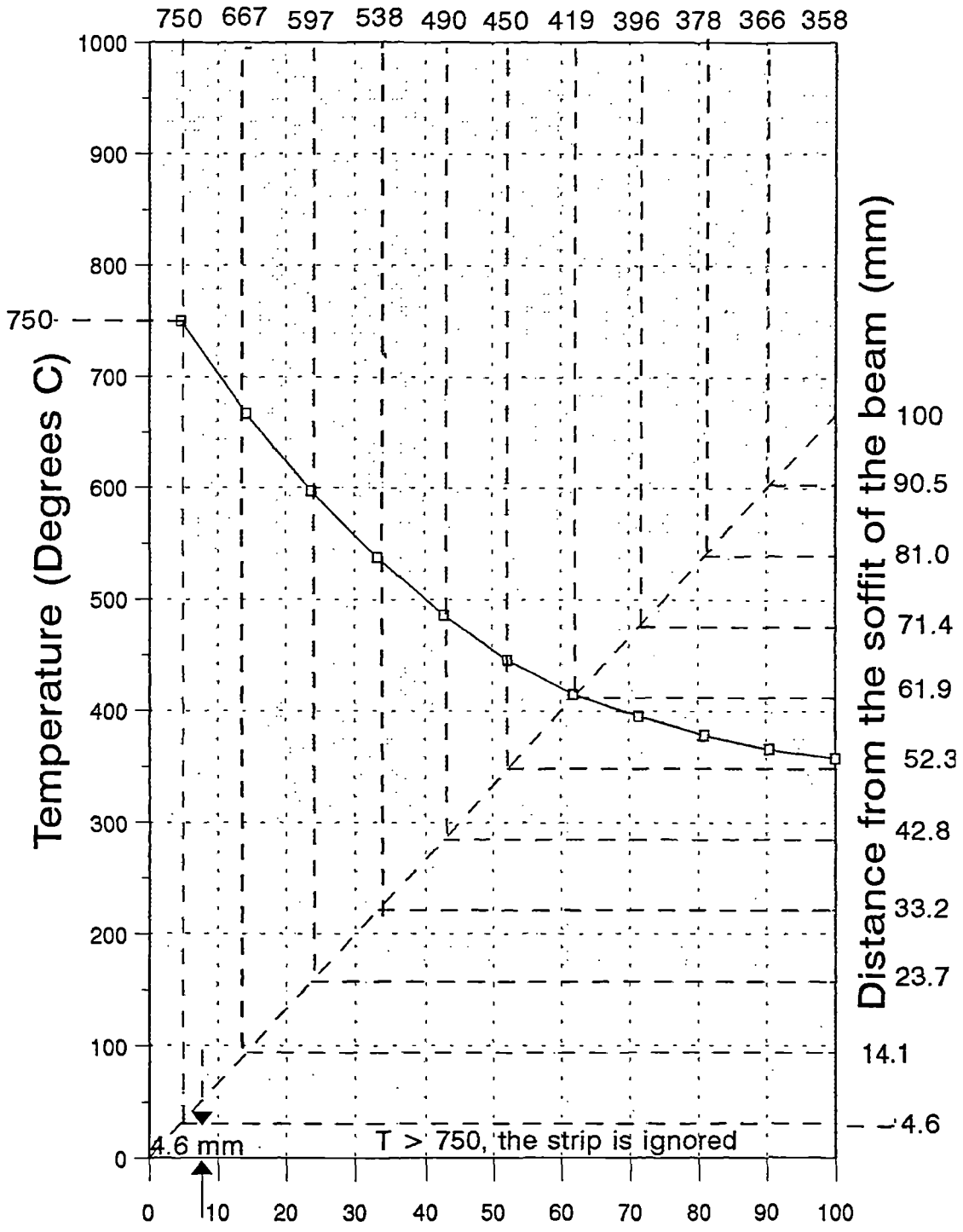

Temperature contours in Beam D202
at t = 94 minutes

FIGURE 5.6

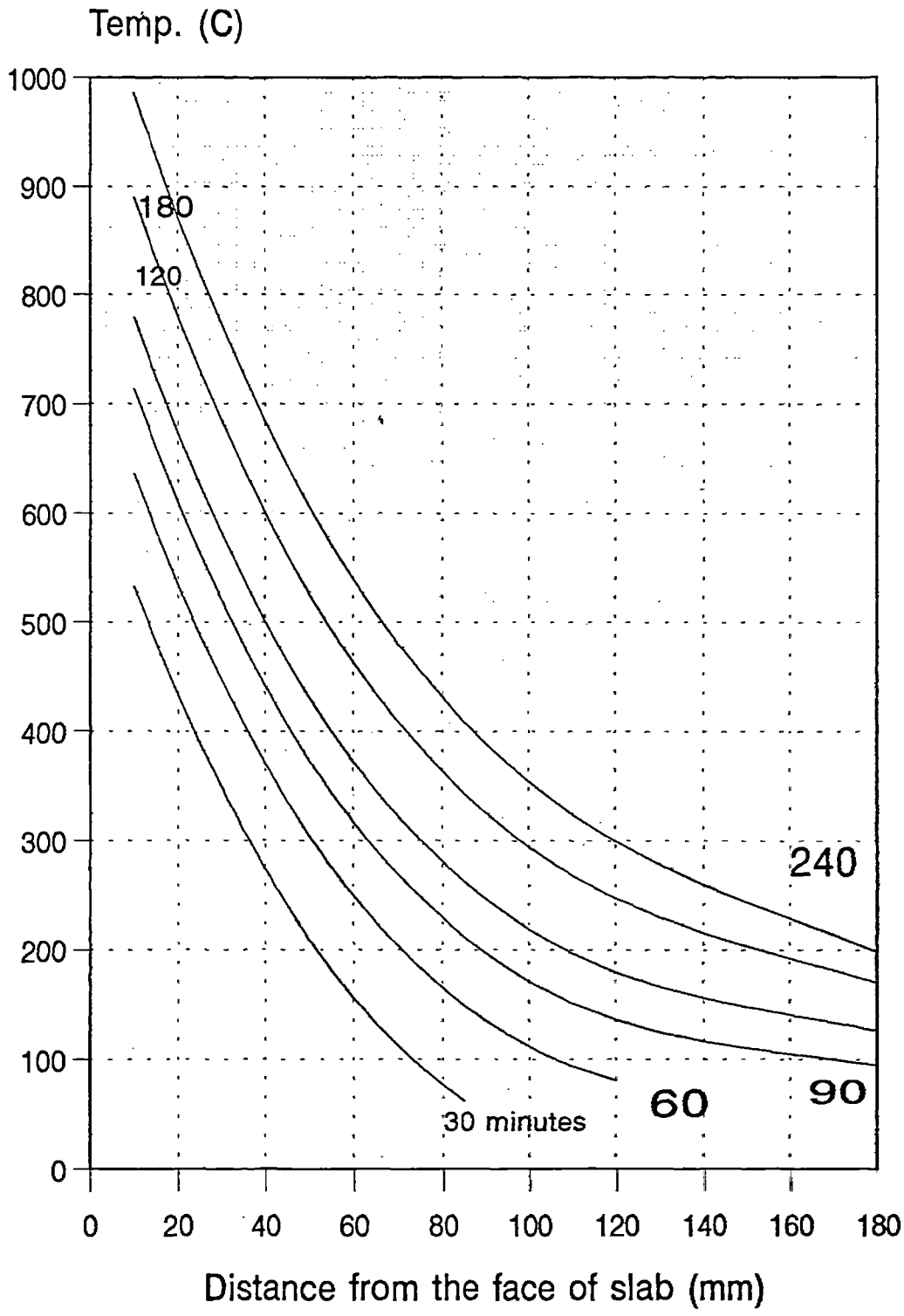

Temperature profiles in slabs
for different fire exposure periods

FIGURE 5.7

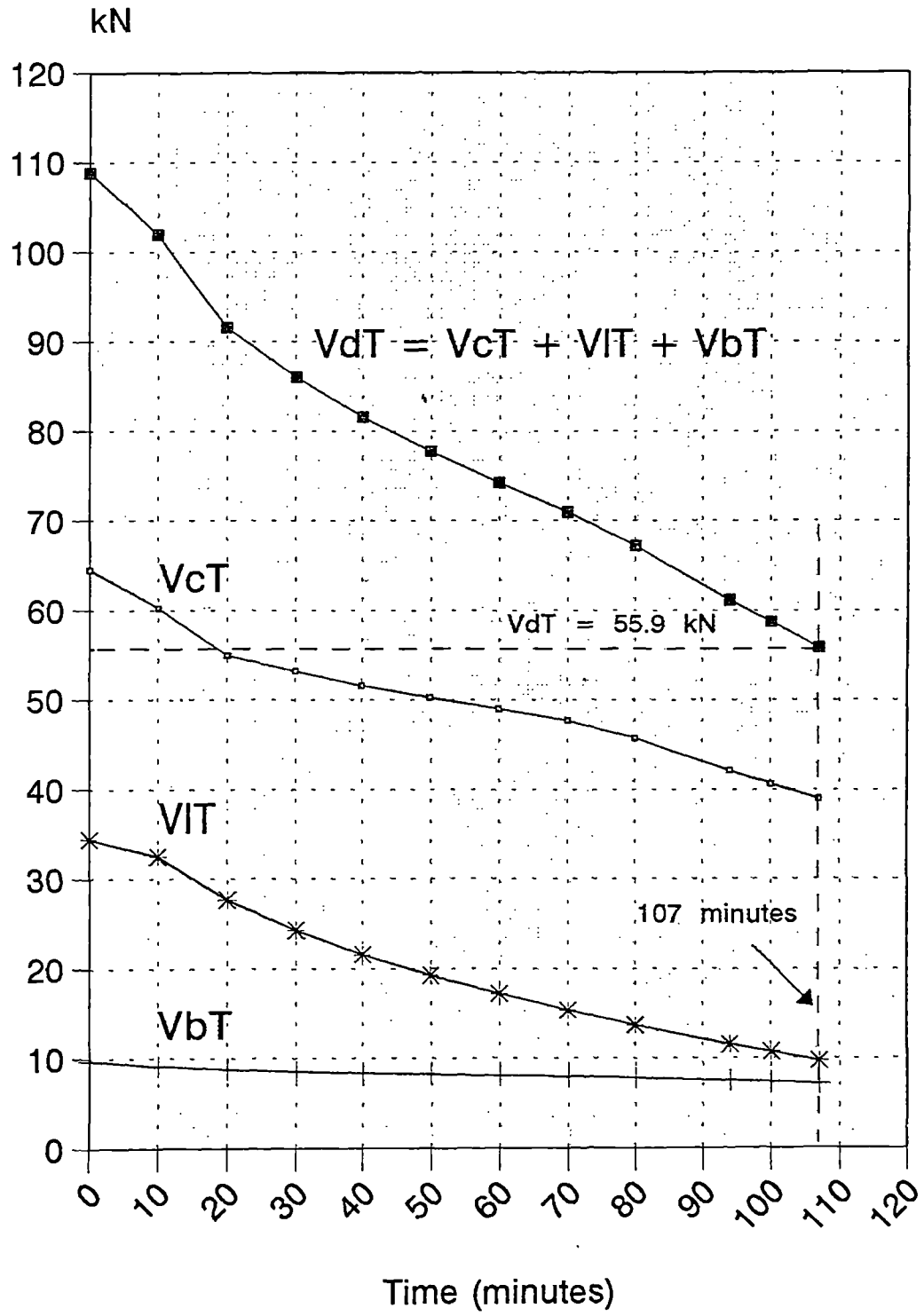

Changes in estimated shear resistance
Typical beam specimen D201

FIGURE 5.8

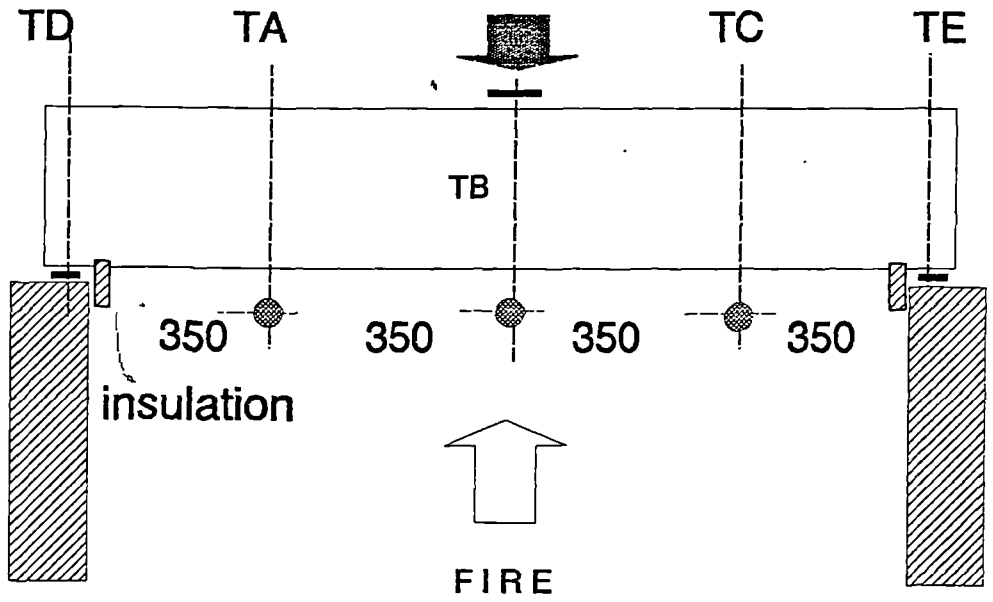

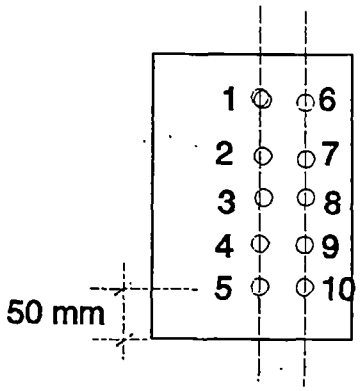

GROUP OF THERMOCOUPLES AT A, B & C
NO 1 TO 5 ON THE CENTRE LINE,
NO 6 TO 10 AT 50 MM FROM FACE OF
THE BEAM AND ALL AT 50 MM C / C

Schematic test arrangement and positions of thermocouples

FIGURE 5.9

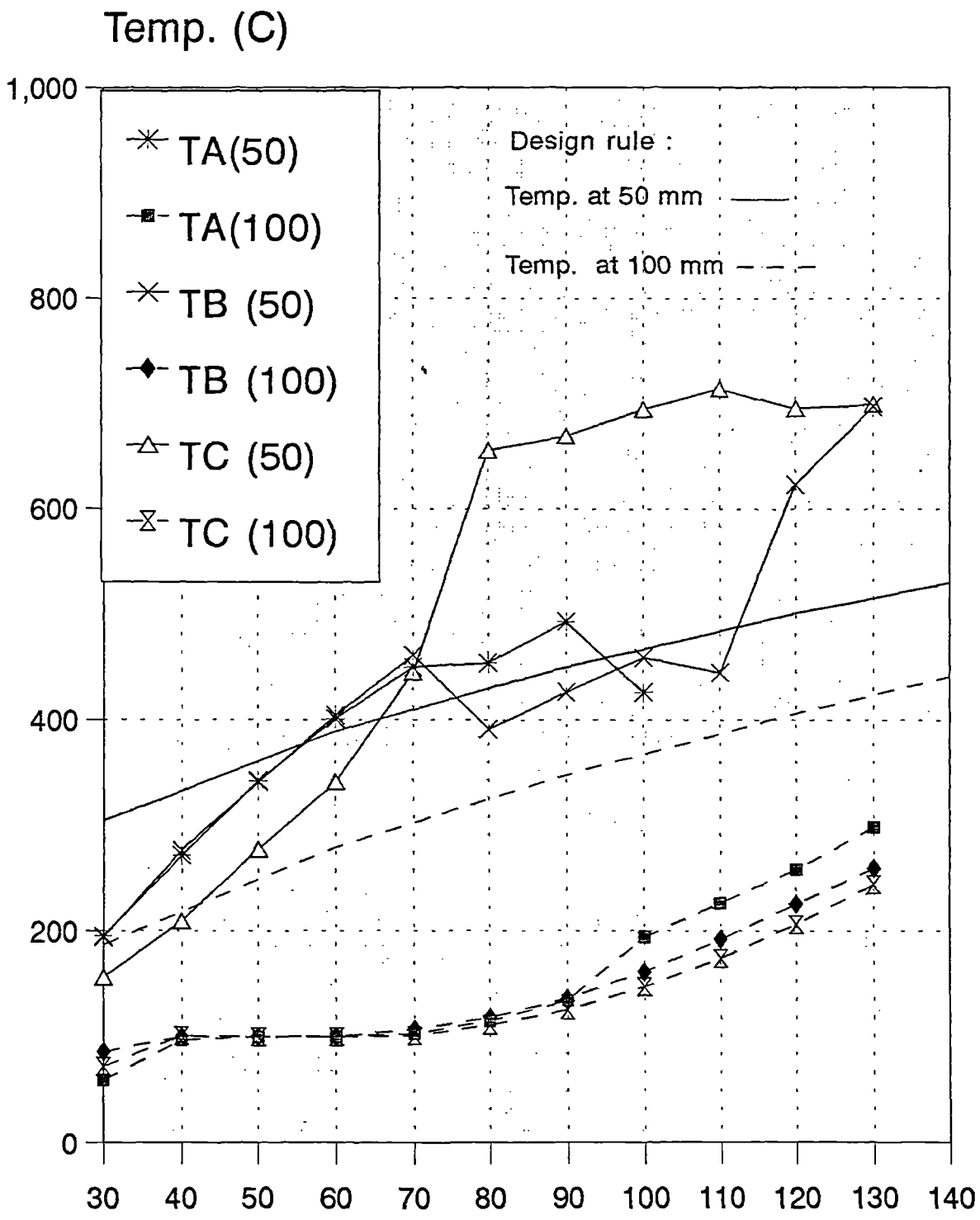

Temperatures in beam B101
Design rule and test results

FIGURE 5.10

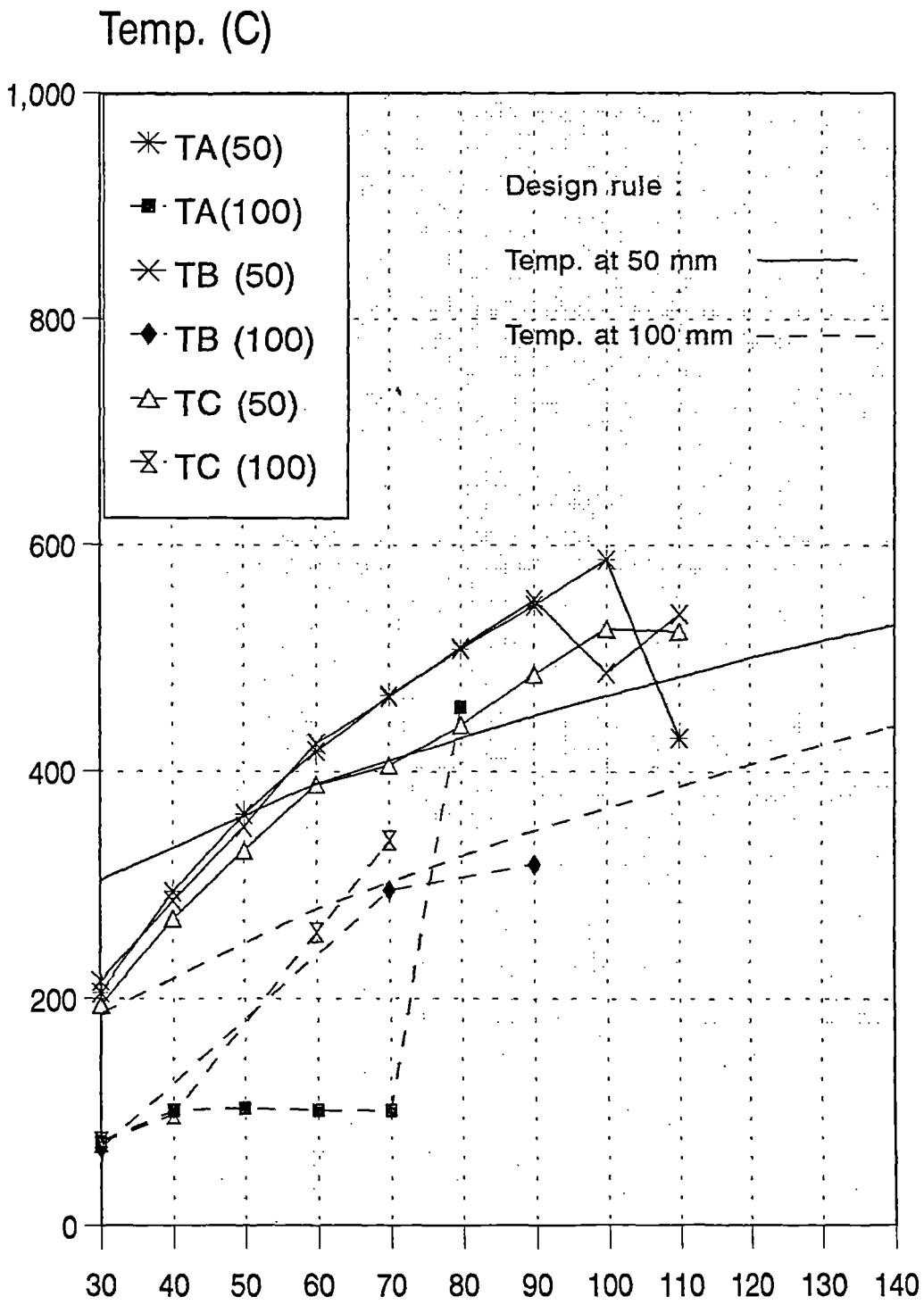

Temperatures in beam B102
Design rule and test results

FIGURE 5.11

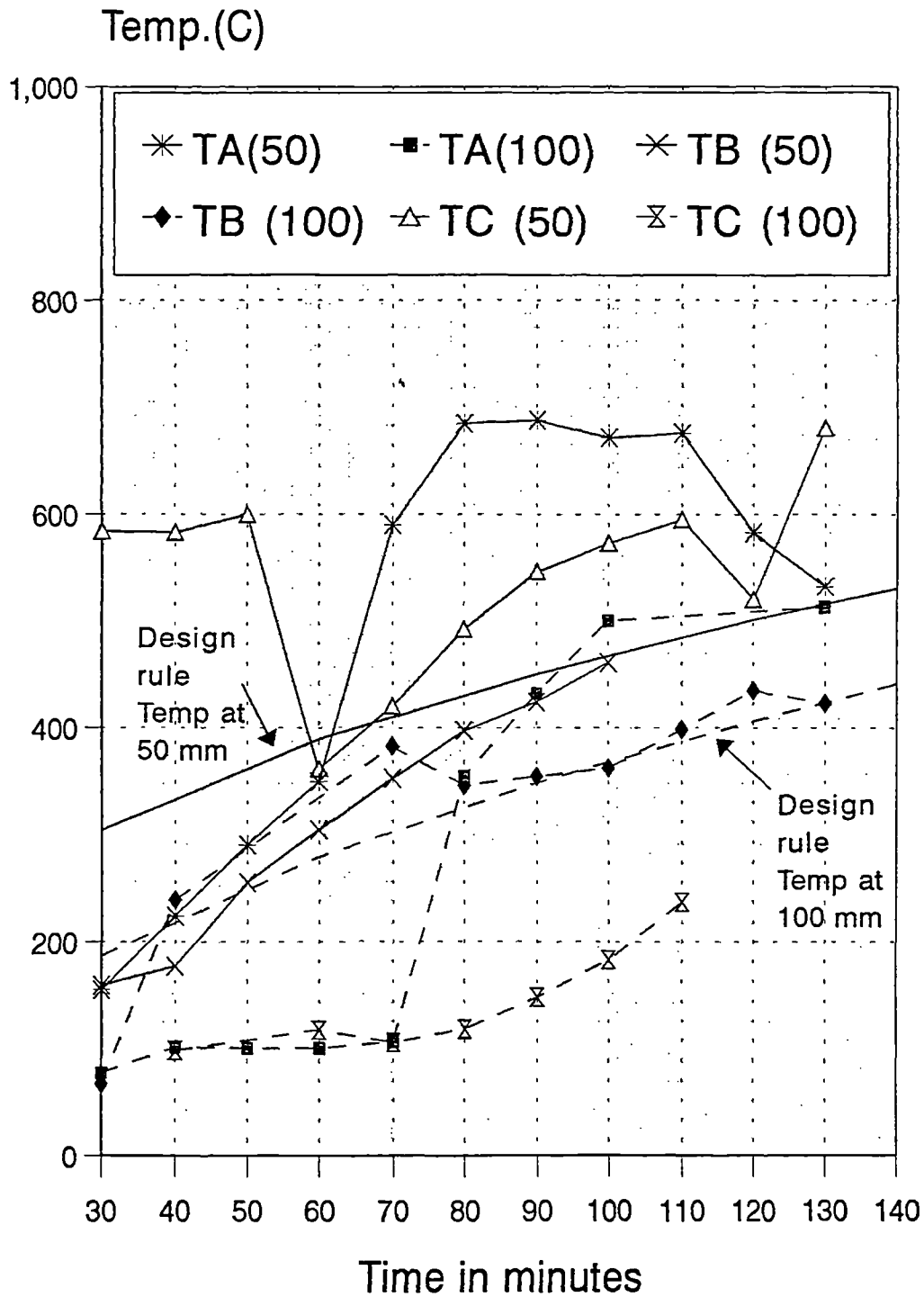

Temperatures in beam B301
Design rule and test results

FIGURE 5.12

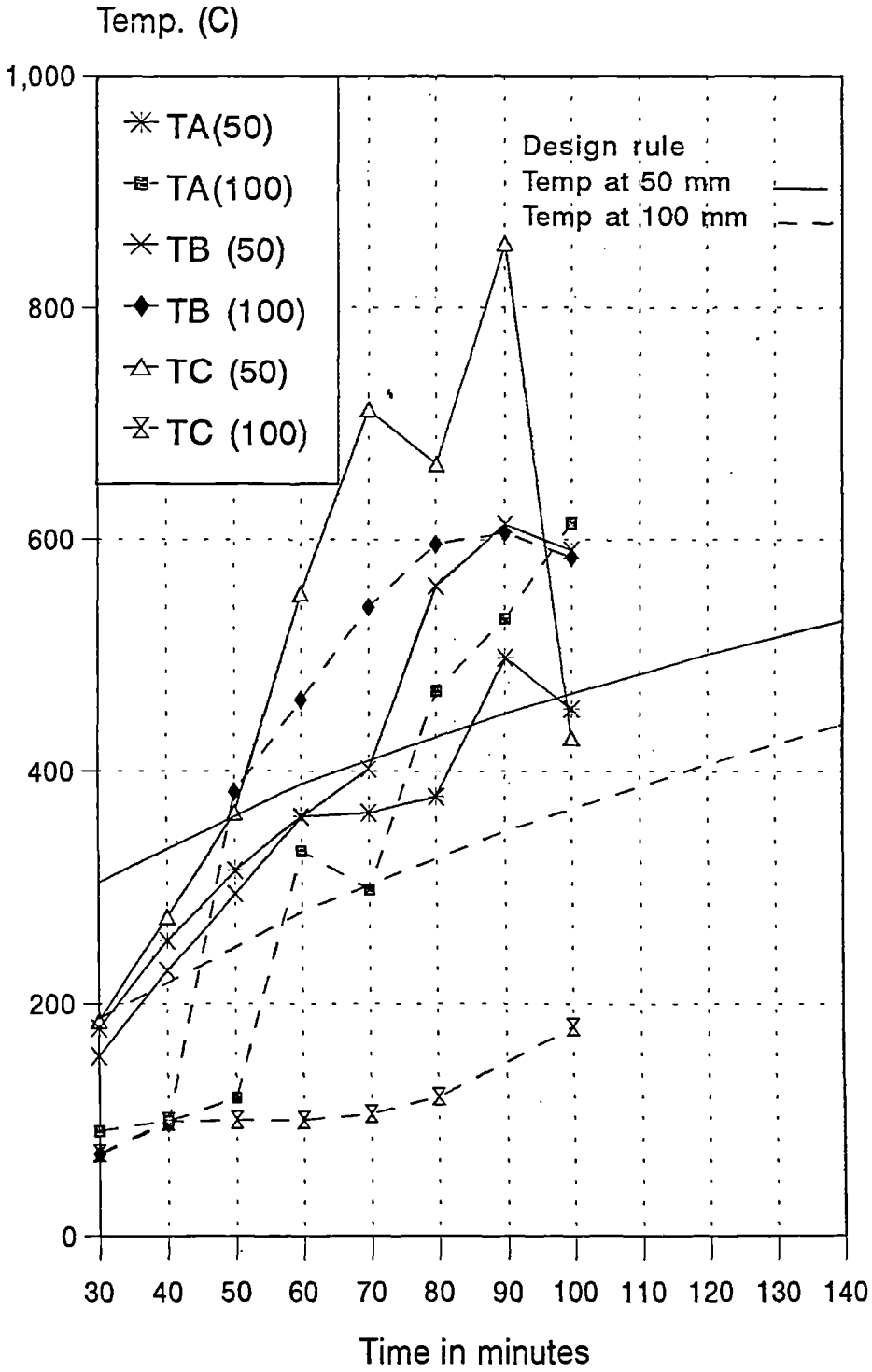

Temperatures in beam B302
Design rule and test results

FIGURE 5.13

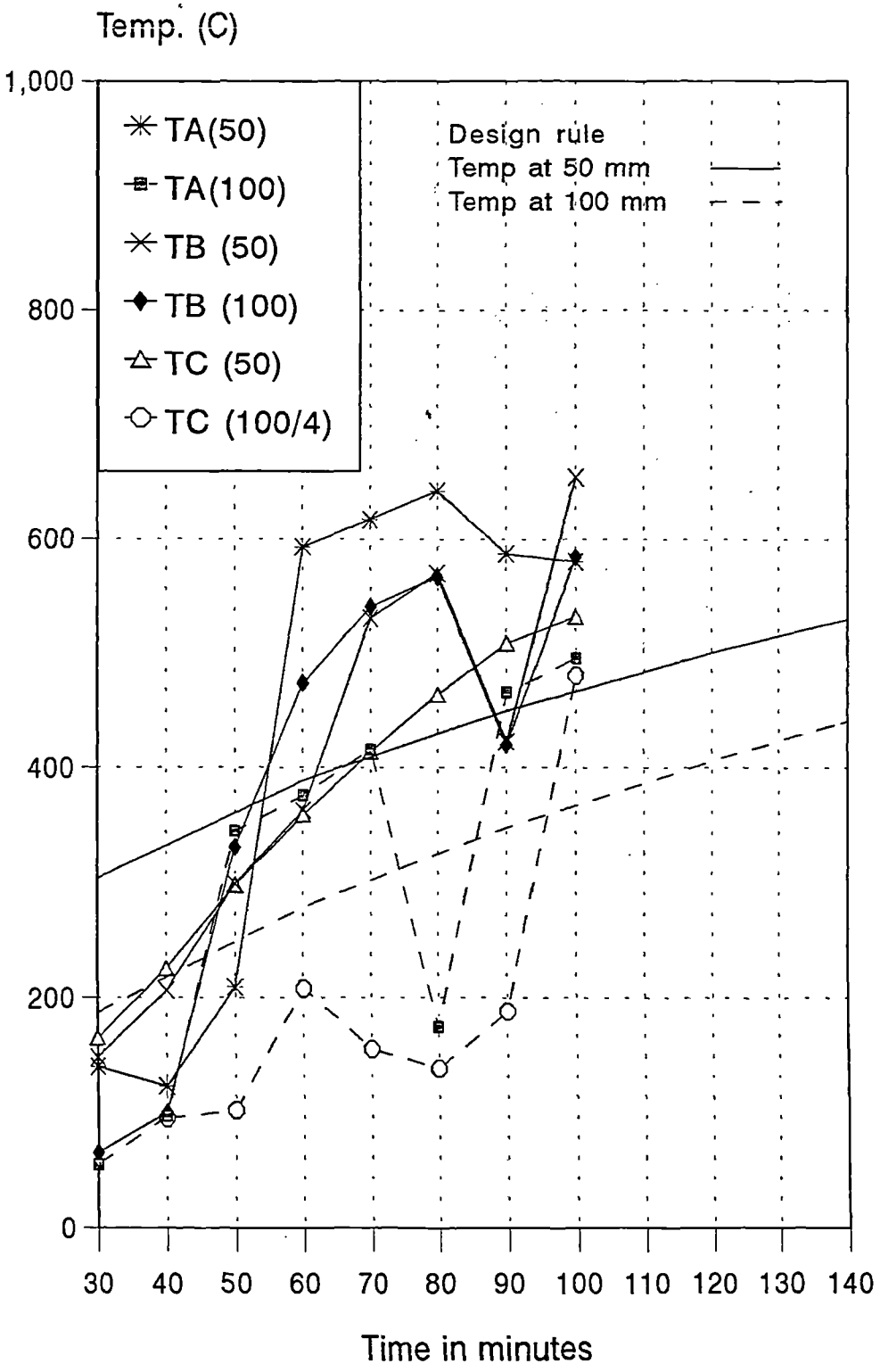

Temperatures in beam B401
Design rule and test results

FIGURE 5.14

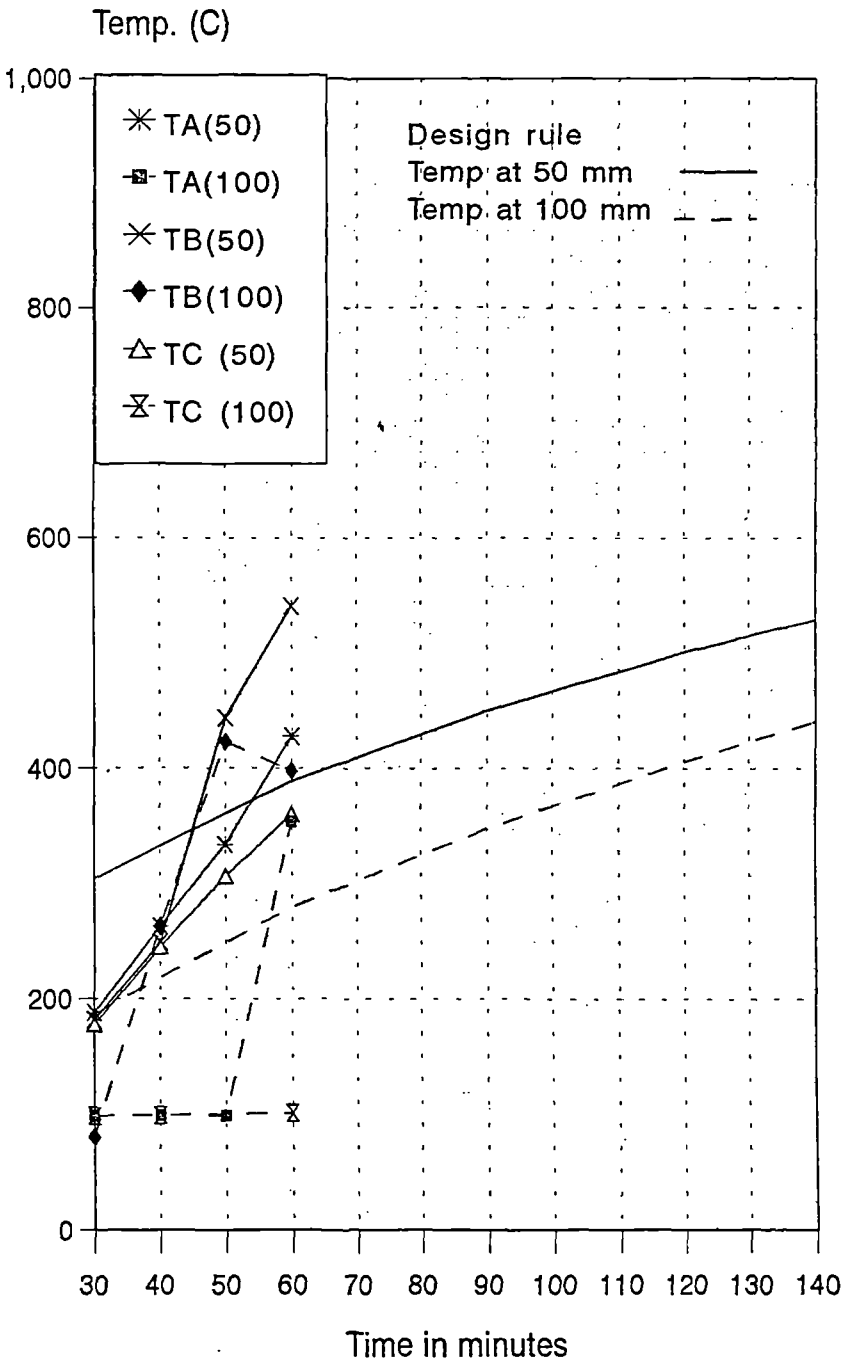

Temperatures in Beam 402
Design rule and test results

FIGURE 5.15

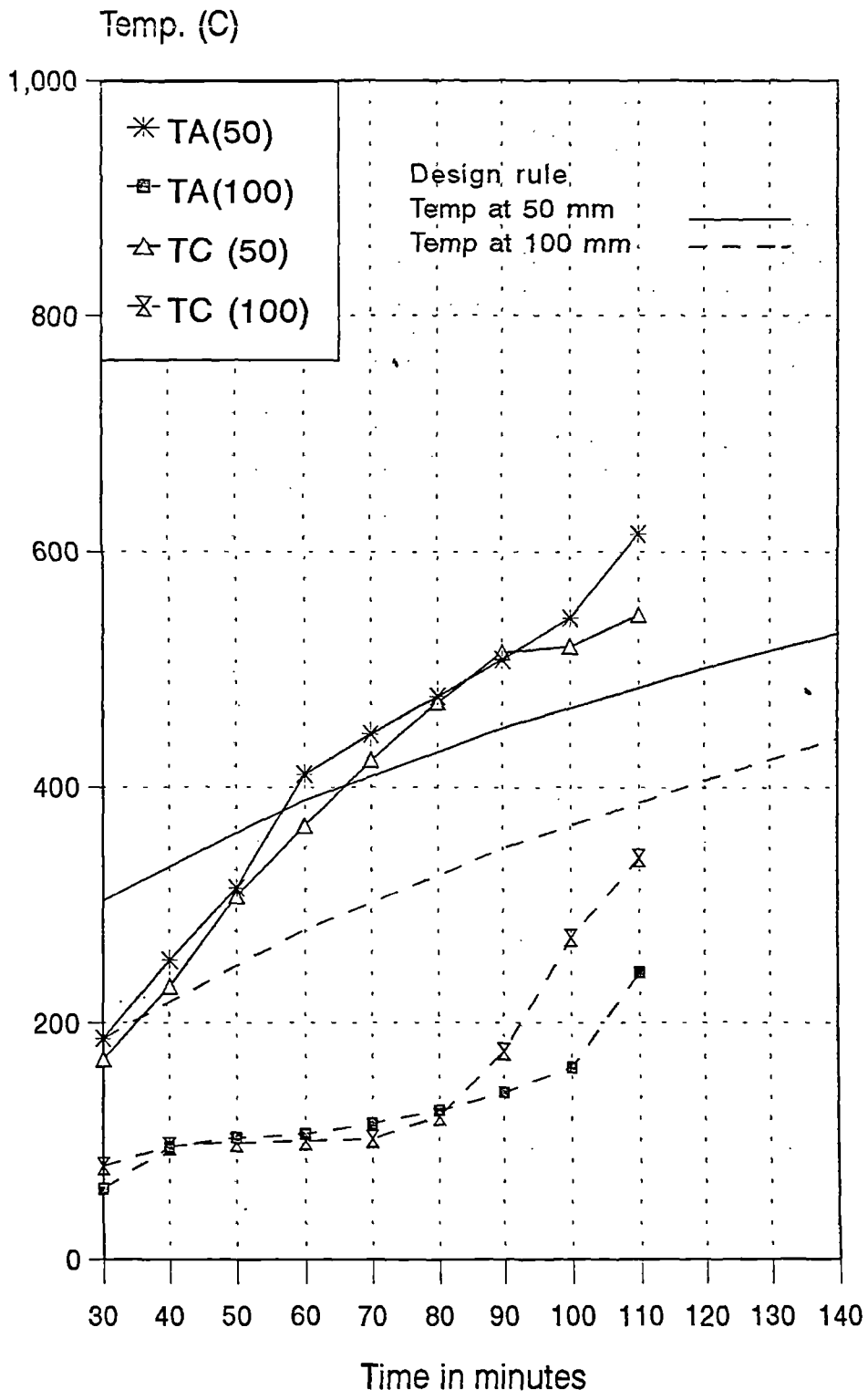

Temperatures in beam C101
Design rule and test results

FIGURE 5.16

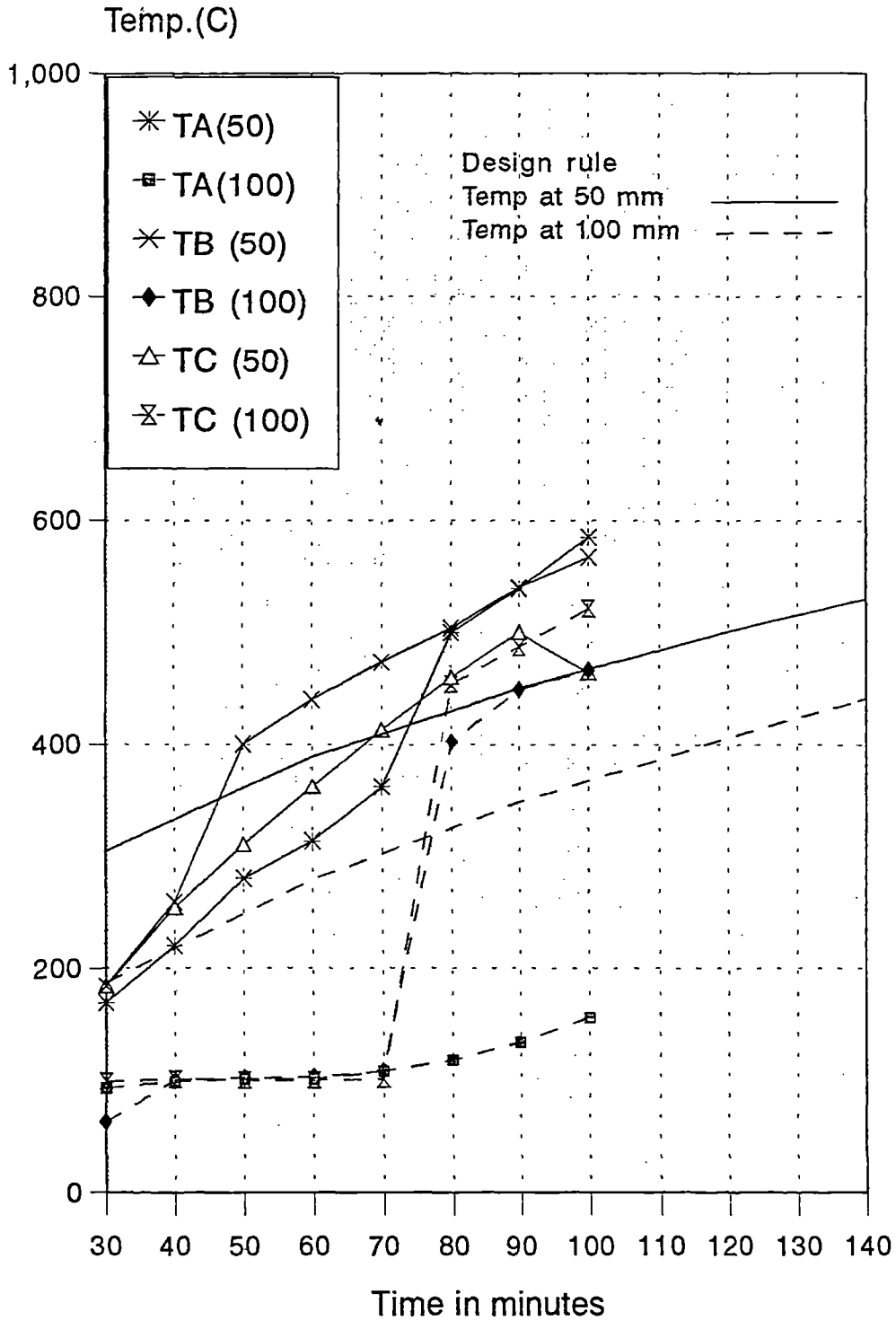

Temperatures in beam C102
Design rule and test results

FIGURE 5.17

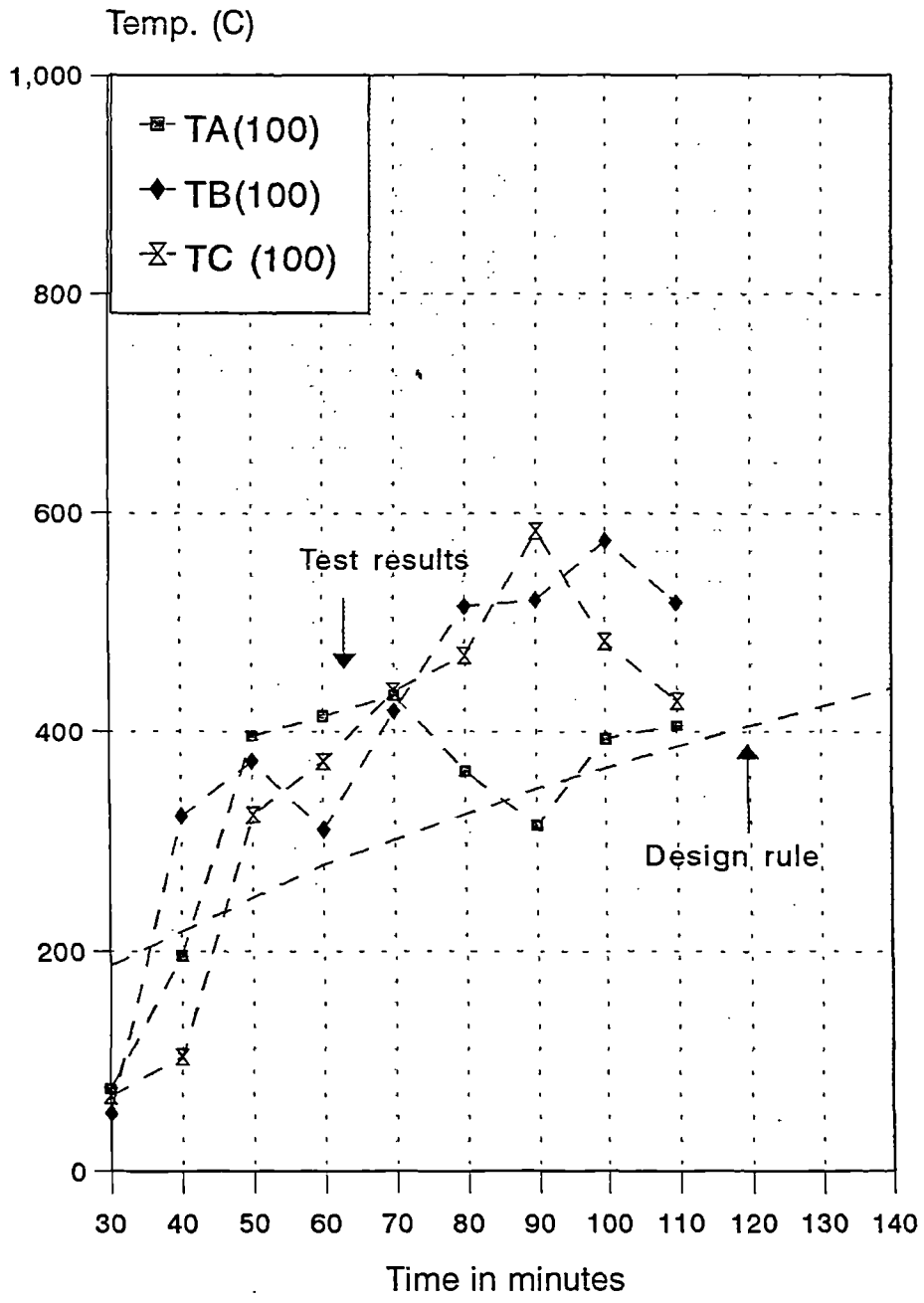

Temperatures in beam D201
at the centre of the beam

FIGURE 5.18

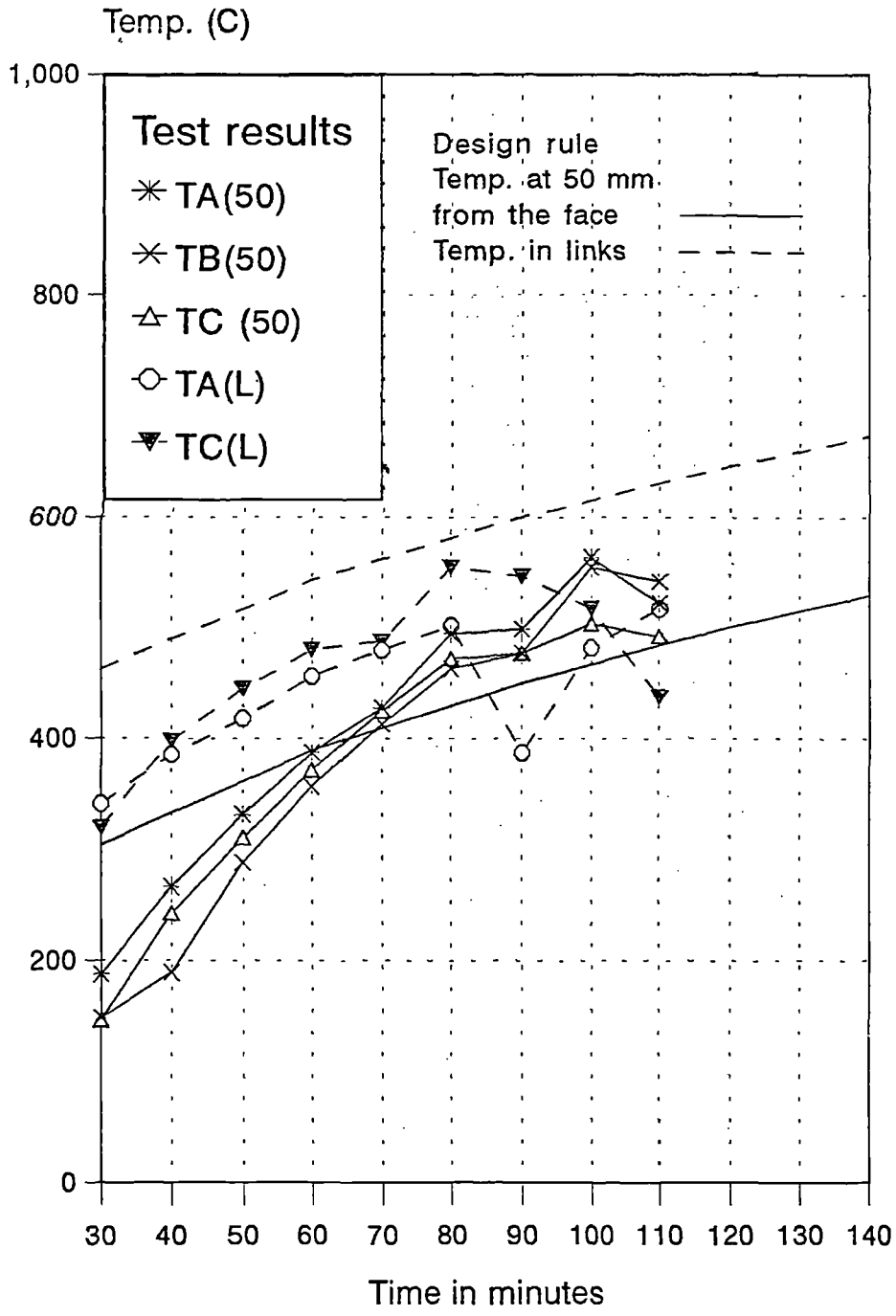

Temperatures at 50 mm from the face and in links : Beam D201

FIGURE 5.19

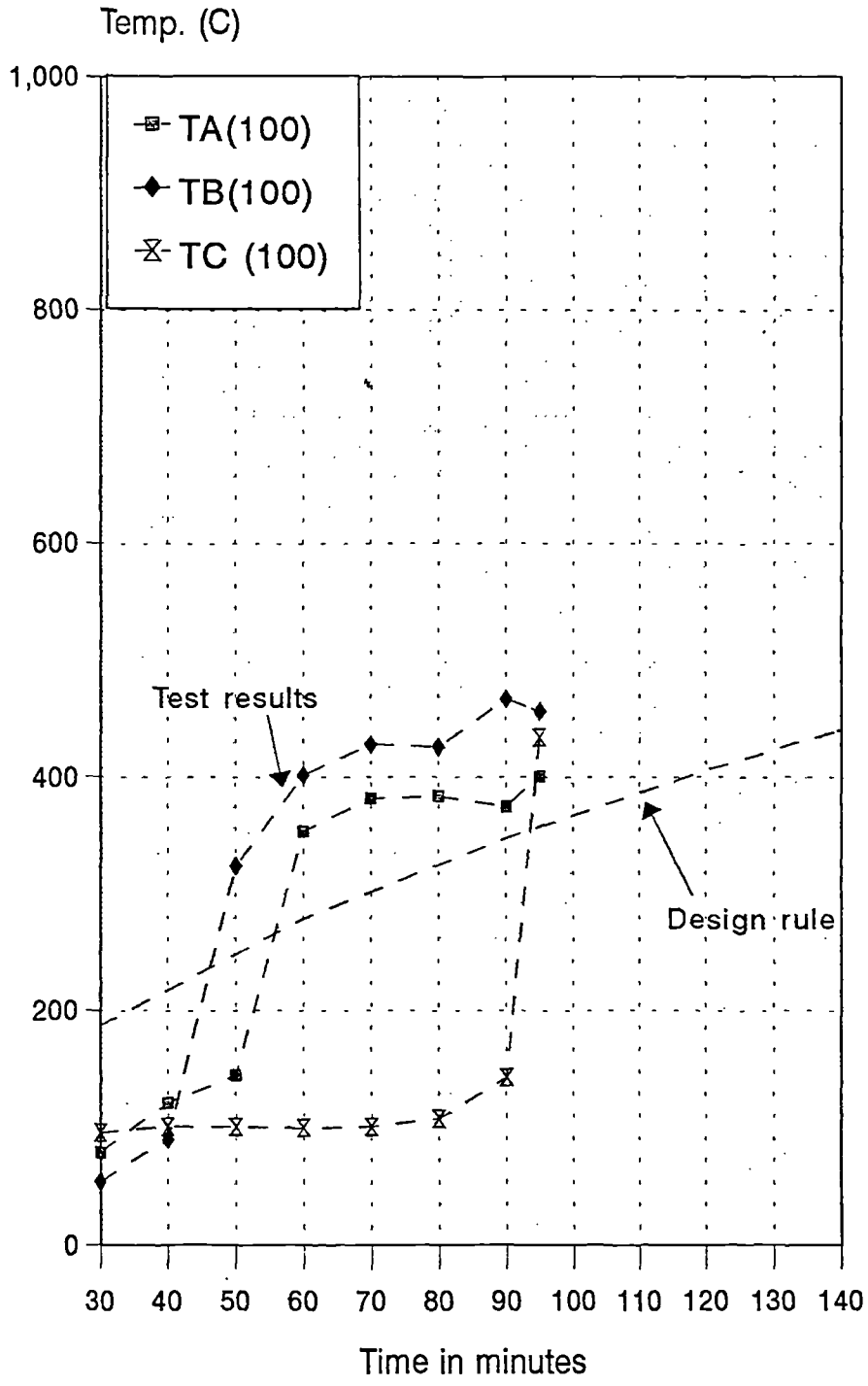

Temperatures in beam D202
at the centre of the beam

FIGURE 5.20

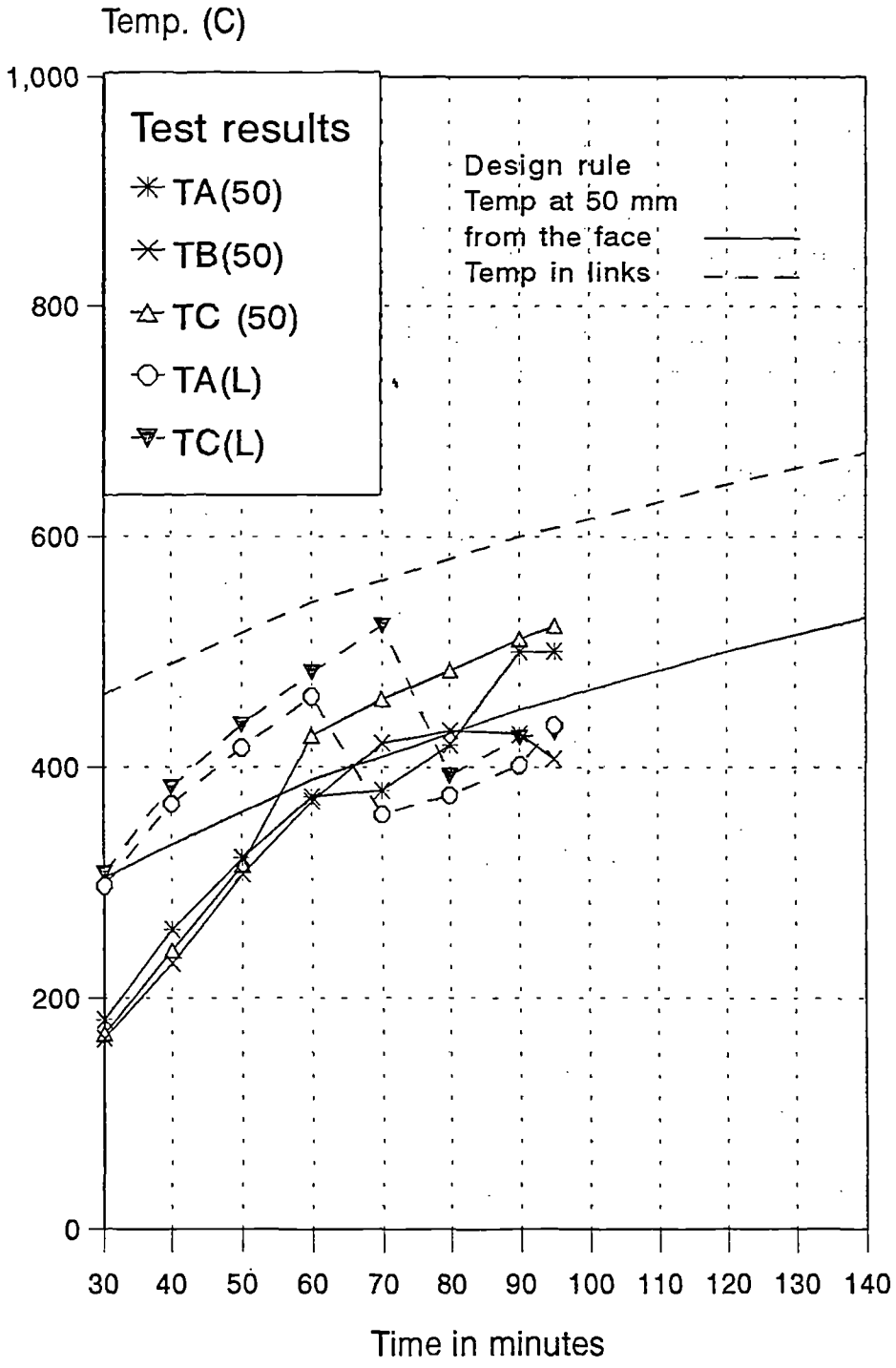

Temperatures at 50 mm from the face
and in links : Beam D202

FIGURE 5.21

i) After 15 minutes

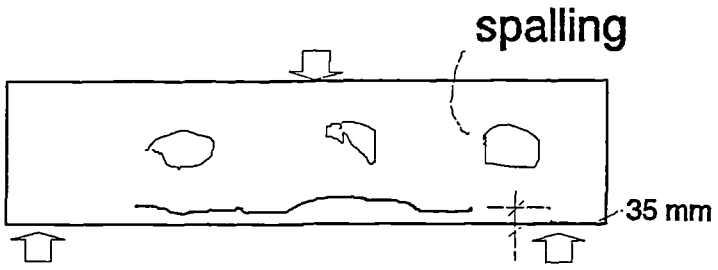

ii) After 50 minutes

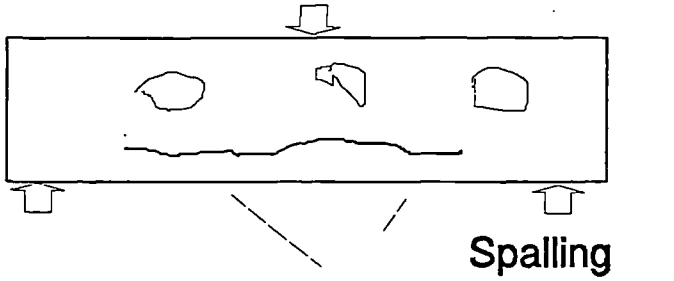

iii) After 65 minutes

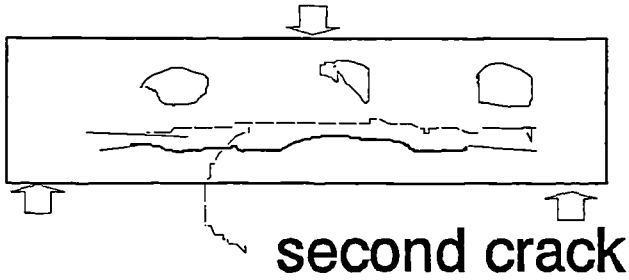

iv) After 130 minutes

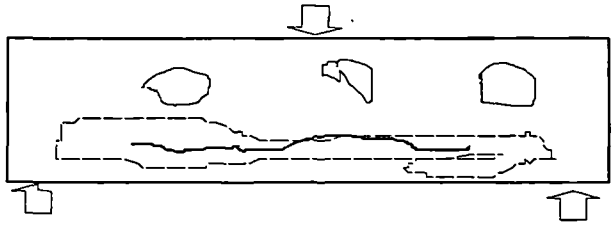

Observations of test on Beam B101

FIGURE 5.22

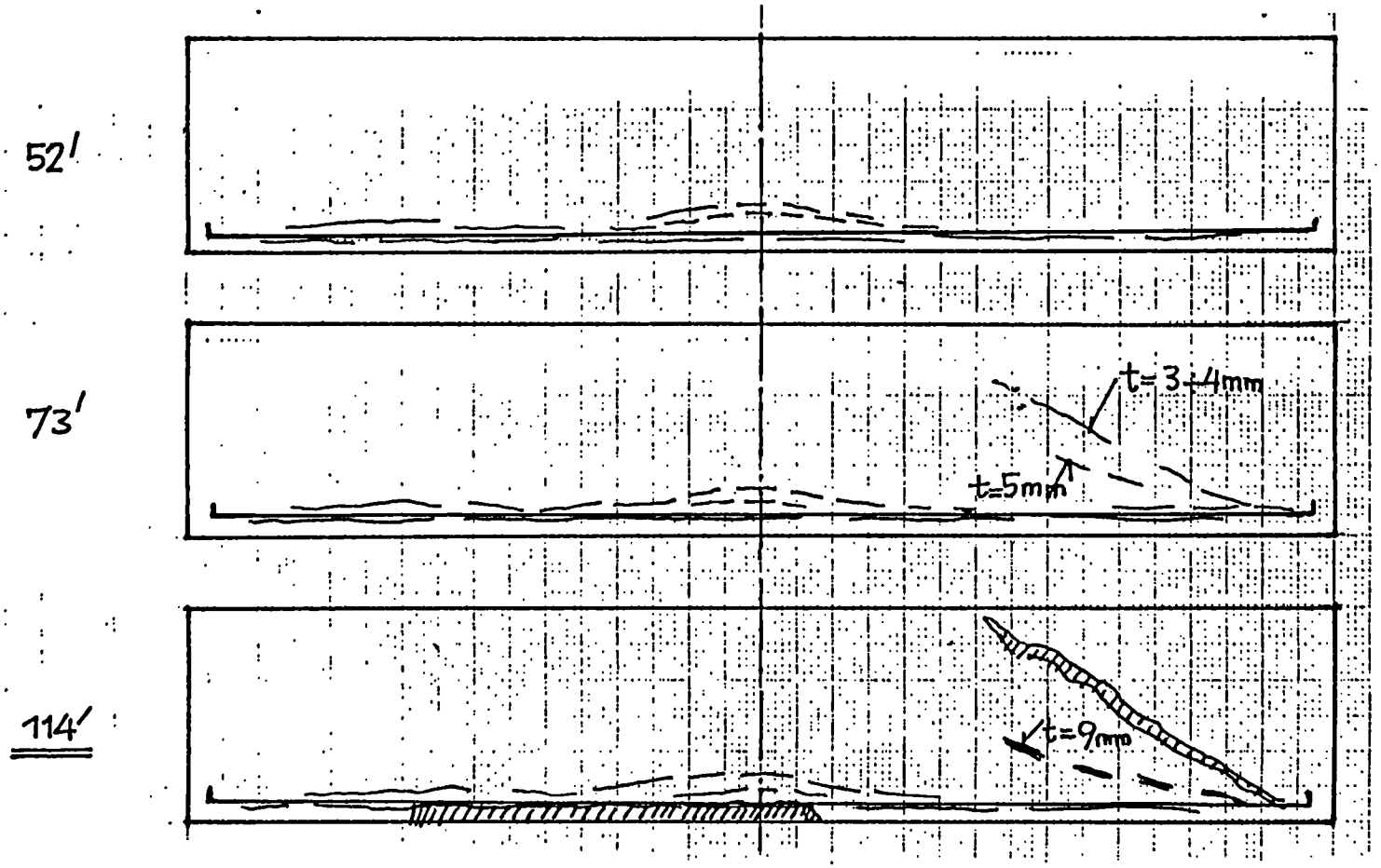

Observations of test on beam B102

FIGURE 5.23

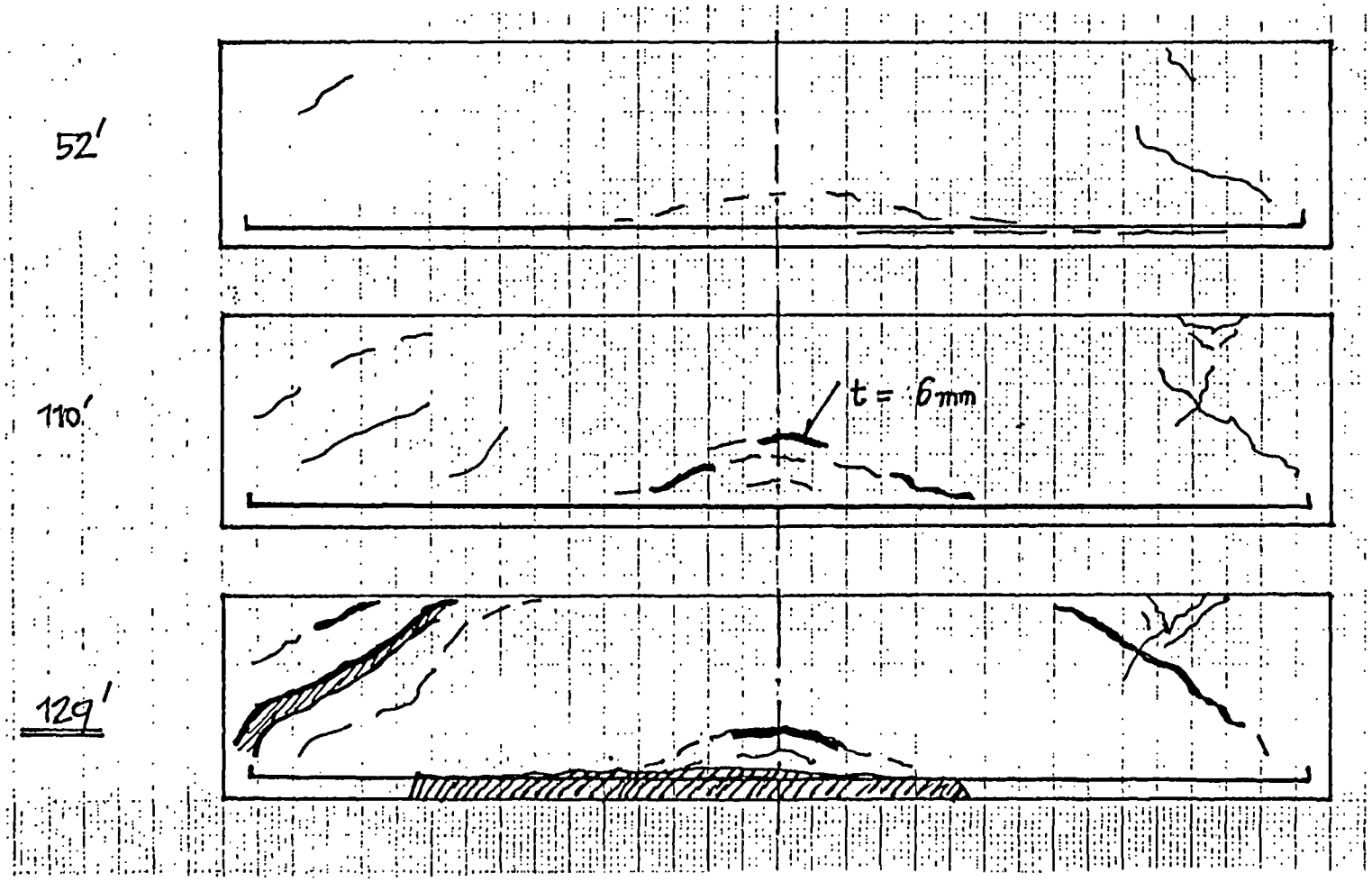

Observations of test on beam B301

FIGURE 5.24

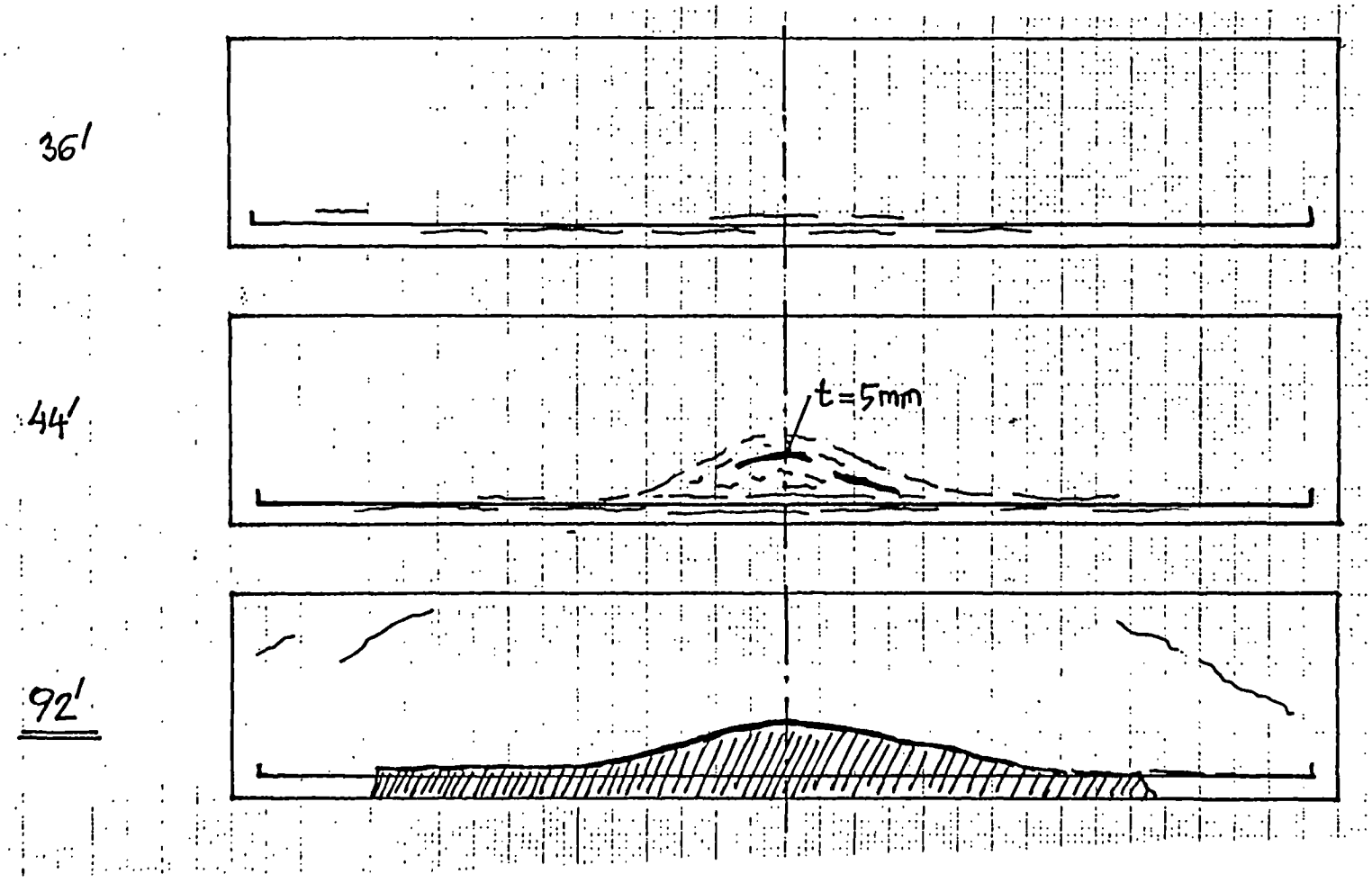

Observations of test on beam B302

FIGURE 5.25

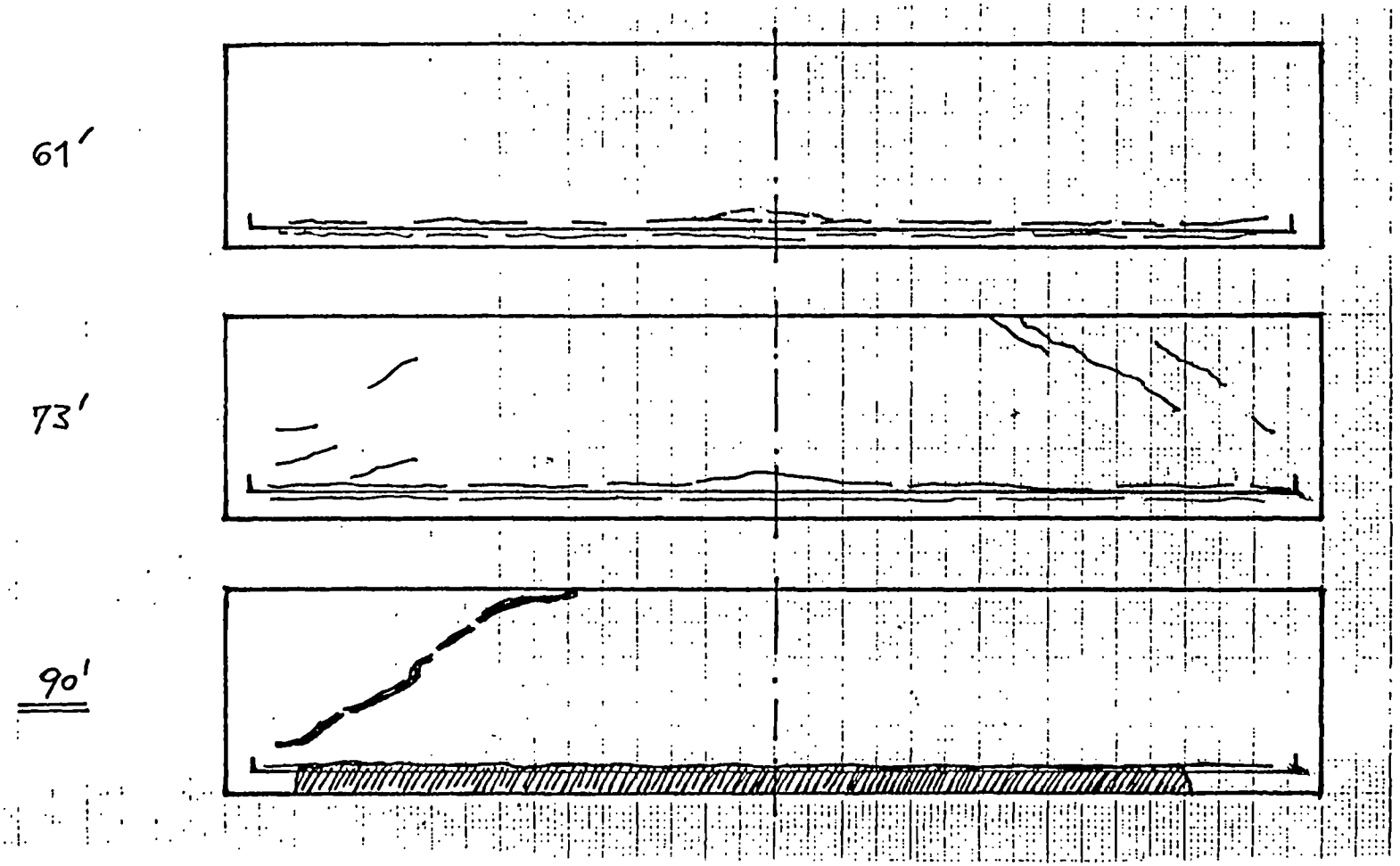

Observations of test on beam B401 FIGURE 5.26

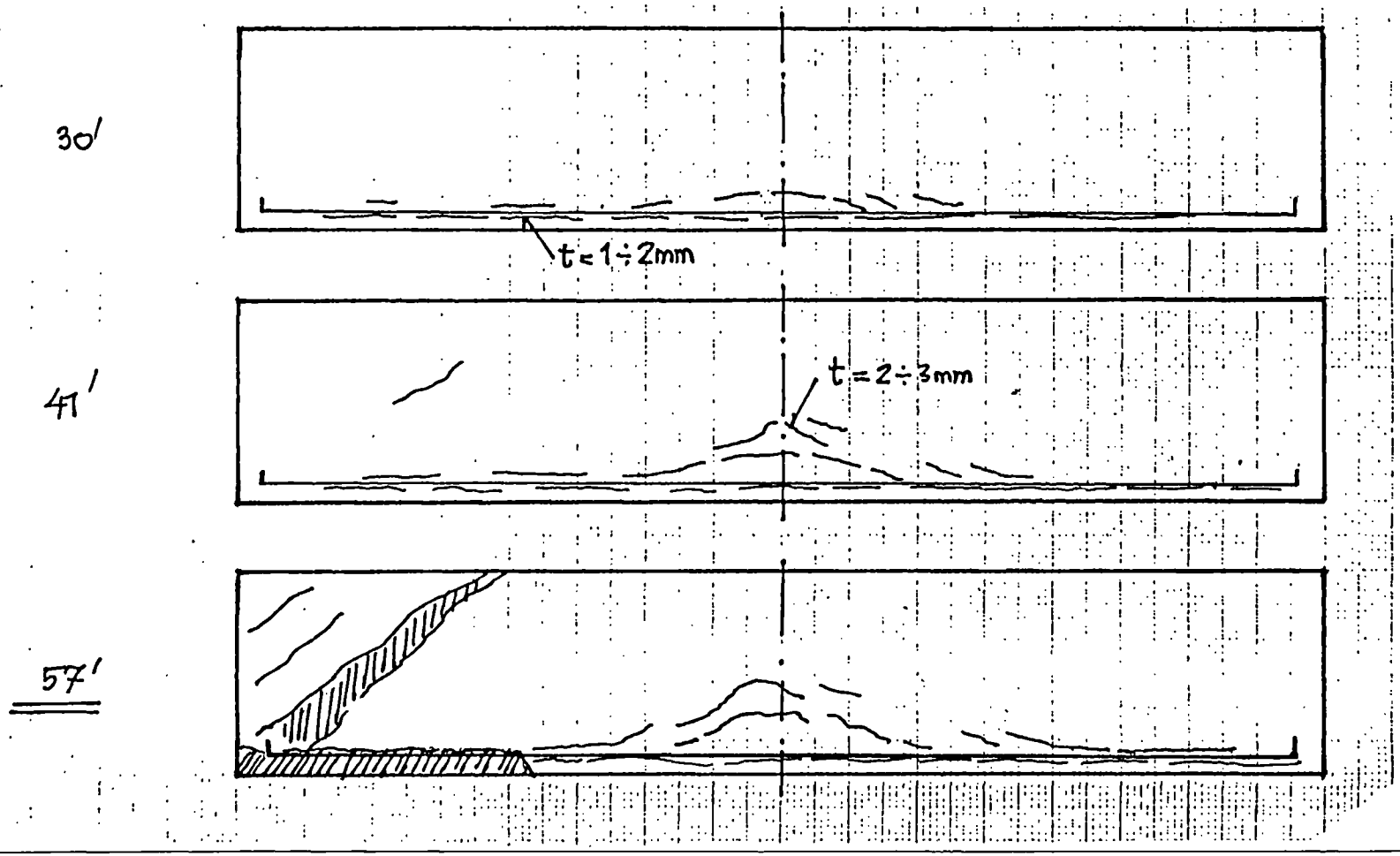

Observations of test on beam B402 FIGURE 5.27

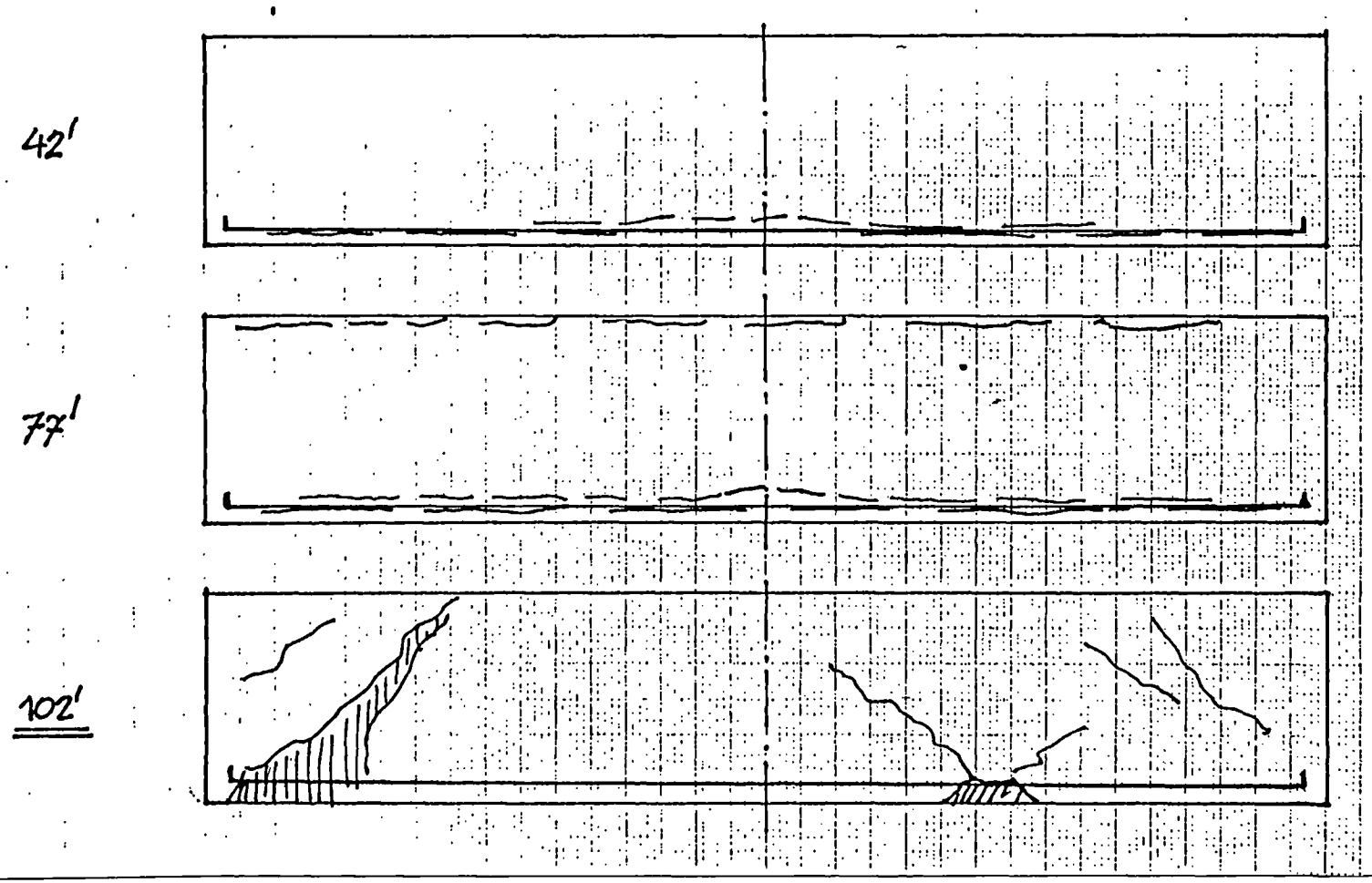

Observations of test on beam C101

FIGURE 5.28

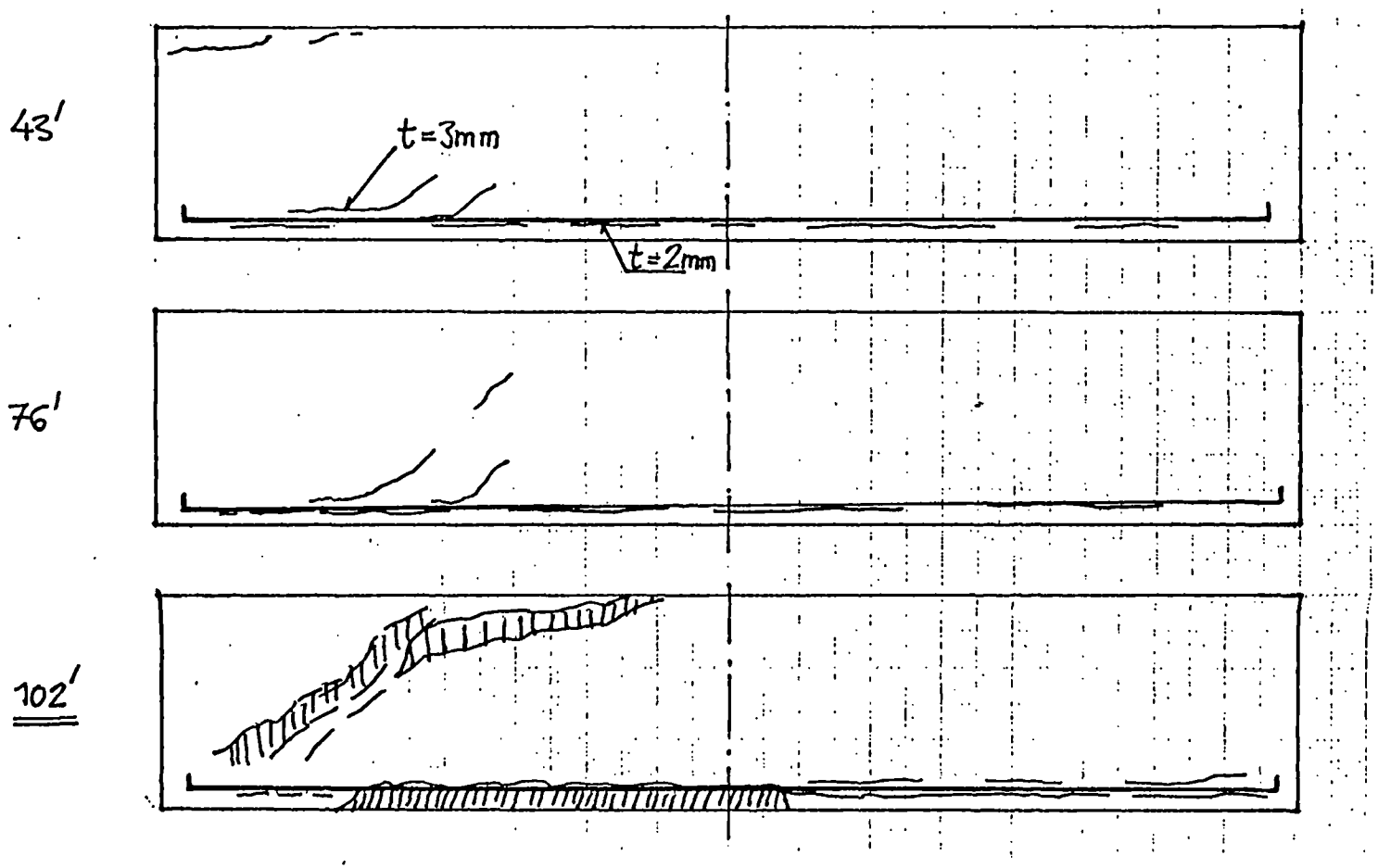

Observations of test on beam C102 FIGURE 5.29

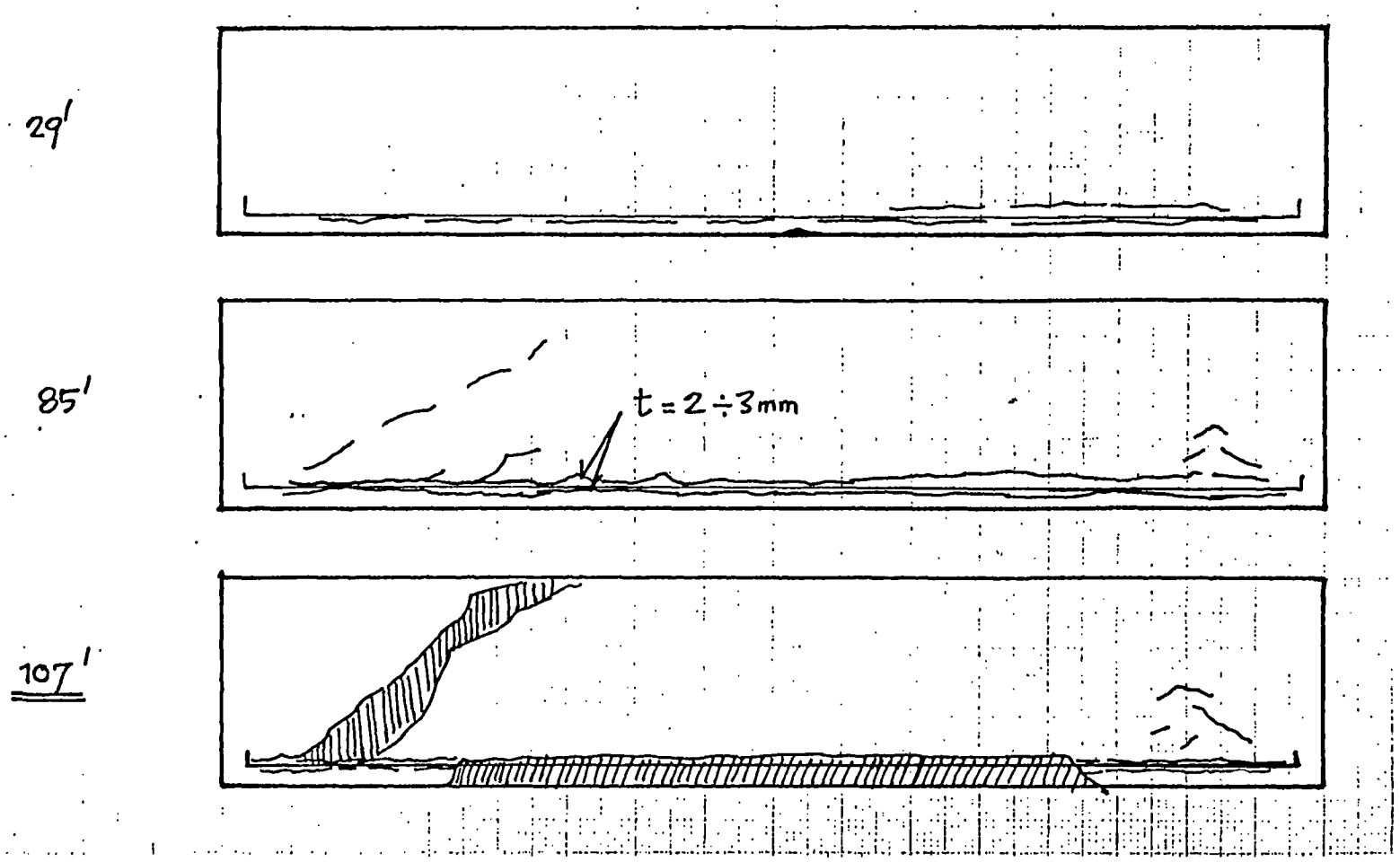

Observations of test on beam D201

FIGURE 5.30

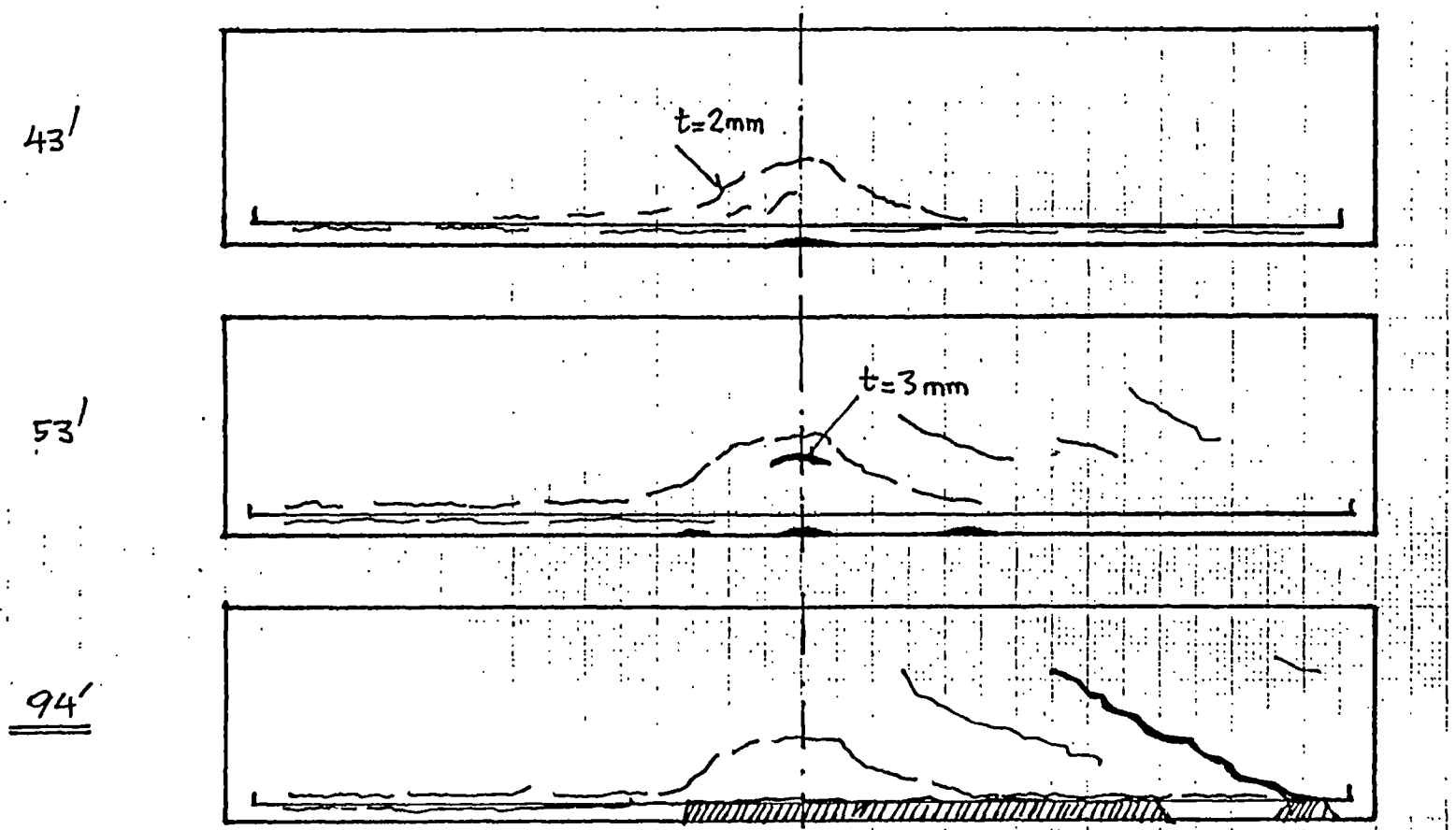

Observations of test on beam D202

FIGURE 5.31

CHAPTER 6
GENERAL CONCLUSIONS

In chapter 1, it was observed that the design of a reinforced concrete member against shear should account for the roles of its constituents; concrete, the tension steel and the web steel. Previous research was reviewed in chapter 2, to examine the individual, combined and interchanging influence of these constituents on shear resistance. The overall shear-carrying capacity of a section was described as a combination of contributions of the compression block, the dowel action of tension steel and the aggregate interlock. These individual contributions were examined, especially with the help of Taylor's work**[20, 21, 22]**. The contribution of compression block was identified to be 40% of the total shear resistance. However, it was proposed that the actual contribution of each mechanism should not be considered separately, since the influence of the constituents of the section (concrete, the tension steel and the web steel) could change and the increase or decrease in the individual contributions could be compensated.

The BS8110 rule for the design concrete shear stress (v_c) was found to correspond to the following basic derivation of the ultimate shear resistance of a section without any web steel. (Equation 3.2.7, Chapter 3)

$$V_{cu} = 0.0046\ (\rho\ E_{st}\ f_{cu})^{1/3}\ \left(\frac{400}{d}\right)^{0.25}\ \frac{bd}{1000} \quad kN$$

In paragraph 2.7.2 of chapter 2, it was observed that the limit of 40 N/mm^2 on the use of f_{cu} in the BS8110 rule could be increased to 60 N/mm^2. This observation was supported by the results of tests reported in this project and also the tests carried out by Kim and Park**[34]** and Clarke**[35]**.

On the basis of previous research, it was deduced that the links have a complex role in enhancing the shear carrying capacity of a section. They do not have a limited function as only a direct tension member, which the truss analogy may lead us to believe. However, the rule for the ultimate stage contribution of links to the shear resistance was shown to be similar to the current rules in BS8110 and EC2.

$$V_{LU} = \frac{A_{sw}\, f_{yv}\, d}{1000\, s} \quad kN$$

The "addition" principle was shown to be a valid proposition through interpretation of results of tests done under this project and also on the basis of Stuttgart tests[12].

$$V_{DU} = V_{CU} + V_{LU}$$

In section 3.5 of chapter 3, design rules were developed for an alternative form of shear reinforcement as horizontal bars at the centre of the section. Following rules were proposed for V_{BU} (kN), the ultimate stage contribution of the central steel, both for beams and for flat slabs, based on the results of a test programme. These rules were examined using a non-linear finite element program in chapter 4.

For beams,

$$V_{DU} = V_{CU} + V_{LU} + V_{BU}$$

$$V_{BU} = 0.4\, \rho_b\, V_{CU} \leq 0.4\, V_{CU}$$

For slabs, the following rules for V_{BU} were proposed.

$$V_{BU} = 0.4\, \rho_{bu}\, V_{CU}$$

where

$$\rho_{bu} = \frac{(u + u_0)}{u}\, \rho_b$$

$$V_{BU} \leq 0.003\, d\, V_{CU}$$ or

$$V_{BU} \leq 0.6\, V_{CU}$$ whichever is the lesser.

Rules for estimating the combined effect of central bars and links were given in chapter 3, subject to their limitations. For beams with links, it was recommended that a central bar with an area less than or equal to 1% of the area of cross-section should be provided to obtain $V_{BU} \leq 0.4V_{CU}$ as an enhancement to the shear resistance additional to that provided by the links. Further research is necessary for determining the optimum combination of central bars and links.

For slabs, the limit on V_{BU} ($0.6V_{CU}$) is higher than that for the beams ($0.4V_{CU}$). This could be attributable to the punching type of shear failure in slabs which allows the central mesh to provide a better dowel resistance at the centre of the crack compared with that of the central bars for beams. Also, it seems that the effectiveness of the central mesh as a dowel increases with the larger crack surface for deeper slabs, up to the maximum limit of $0.6V_{CU}$.

In addition to their contribution to the shear resistance of the section, the central bars could afford some ductility and reduce the undesirable brittleness of shear failure. In paragraphs 3.5.2 and 3.6.1 of chapter 3, it was noted that the specimens with central bars were able to sustain loads well after the appearance of initial cracks and the cracks did not widen significantly until failure. This was noticeably different to the specimens without web reinforcement, where the distress was clearly visible as the failure approached. The ductility provided by the central bars could be an important consideration in the design against accidental loading.

In principle, the proposed design rules agree with the normal temperature design methods given in the current codes of practice. These rules were adapted for evaluating shear resistance of beams under elevated temperature conditions in chapter 5. The modified rules allowed for the change in strength and properties of concrete, the tension steel and the web reinforcement under fire exposure conditions. It was observed that the rule could be used for estimating the flexural capacity of beams as demonstrated in section 5.7 of chapter 5.

Chapter 5 gave details of fire exposure tests on beam specimens similar to those used in the test programme described in chapter 3. Beams were tested at

high temperatures following the standard time-temperature curve, for validation of the design rules and demonstration of the effectiveness of central bar in beams exposed to fire. It was observed from the test results that the temperatures in links were marginally lower than estimated. It was noted that the empirical rule used for estimating the temperature profiles was based on data derived from tests on plain concrete. The increase in temperature in links may be less than that predicted by the empirical rule since the rule could not allow for any conduction of heat by the steel cage from the hotter to the comparatively cooler part of the beam. More research is necessary based on tests on concrete members provided with longitudinal bars and links.

It is proposed that further research should be carried out for developing a computer program to include shear design of reinforced concrete members under elevated temperatures. Consideration could be given for using ABAQUS, with suitable modifications for these purposes. It is also proposed that a test programme should be carried out for validation of the rule suggested in chapter 5 for evaluating the punching shear capacity of flat slabs at high temperatures.

APPENDIX A
REFERENCES

REFERENCES

1 Stanley C C, Highlights in the history of concrete, British Cement Association Publication, London, 1986.

2 Mörsch E, Concrete-steel construction, Technical Report, Engineering News Publishing Co., New York, 1909 (Translation of the 3rd German Edition).

3 Mörsch E, Der Eisen-Betonbau, Verlag von Konrad Witter, Stuttgart, 1922.

4 Talbot A N, Tests on reinforced concrete beams, University of Illinois, Engineering Experiment Station Bulletins 4, 8, 12, 14, 28 & 29; 1906-1909.

5 Richard F E, An investigation of web stresses in reinforced concrete beams, Bulletin No. 166, University of Illinois, Engineering Experiment Station 1907.

6 Kani G N J, Huggins M W and Wittkopp R R, Kani on shear in reinforced concrete, Department of Civil Engineering, University of Toronto, 1979.

7 Kani G N J, Basic facts concerning shear failure, ACI Journal, Vol 63 No. 6, June 1966.

8 Fenwick R C, The shear strength of reinforced concrete beams, Thesis for the degree of Doctor of Philosophy in Engineering. University of Canterbury, New Zealand, 1966.

9 Shear Study Group Report: The Institution of Structural Engineers, London, January 1969.

10 Placas and Regan, Shear failure of reinforced concrete, ACI Journal Vol No. 68-67, October 1971.

11 Zsutty T C, Shear strength prediction for separate categories of simple beam tests, ACI Journal, Proceedings Vol 68 No. 2, February 1972.

12 Leonhardt F and Walther R, The Stuttgart Shear Tests (1961), A translation of articles which appeared in "Beton und Stahlbetonbau" (Vol 56, No 12, 1961 and Vol 57, Nos 2, 3 6, 7 and 8, 1962) by Amerongen CV for the Cement and Concrete Association Library, Number 111, UDC 624.012.45:620.176.

13 Leonhardt F, Reducing the shear reinforcement in reinforced concrete beams and slabs, Magazine of Concrete Research, Vol 17, No. 53 : December 1965.

14 Moosecker W, Zur Bemessung der Schubbewehrung von Stahlbetonbalken mit moglichst gleichmassiger Zuverlassigkeit. Deutscher Ausscuss fur Stahlbeton, Heft 307, Berlin, 1979.

15 Collins M P, Towards a rational theory for reinforced concrete members in shear, Journal of the Structural Division, ASCE, Vol 104, April 1978.

16 Vecchio F and Collins M P, The response of reinforced concrete to in-plane shear and normal stresses, Technical Report Publication No. 82-03, Department of Civil Engineering, University of Toronto, March 1982.

17 Hsu T C H, Unified theory of reinforced concrete CRC Press Inc., Boca Raton, Florida, USA 1003, 1993.

18 Schlaich J, Schafer K and Jennewein M, Toward a consistent design of structural concrete, PCI Journal, Vol 32 No. 3, May/June 1987.

19 Canadian Standards Association, Rexdale, Design of Concrete Structures for Building (CA N3-A23.3-M54), 1984.

20 Walraven J C and Reinhardt H'W, Theory and experiments on the mechanical behaviour of cracks in plain and reinforced concrete subjected to shear loading, Concrete Mechanics, Part A (Heron) Vol 26 (No 1A), 1981, pp 1-68.

21 Taylor H P J, Further tests to determine shear stresses in reinforced concrete beams, Cement and Concrete Association, TRA 438, February 1970.

22 Taylor H P J, Investigation of the forces carried across cracks in reinforced concrete beams in shear by interlock of aggregate, Cement and Concrete Association, 42.447, November 1970.

23 Taylor H P J, Fundamental behaviour in bending and shear of reinforced concrete, Thesis for the degree of Doctor of Philosophy in Civil Engineering, City University, London 1971.

24 Morrell P J B and Chia C H, A method of determining the contribution of aggregate interlock forces to the shear resistance of singly reinforced concrete beams, pp 855-861, Proceedings, Institution of Civil Engineers, Part 2, September 1980.

25 Chana P S, Analysis and experimental studies of shear failures in reinforced concrete beams, Proceedings, Institution of Civil Engineers, Part 2, December 1983.

26 Swamy R N and Andriopoulos, Contribution of aggregate interlock and dowel forces to the shear resistance of reinforced beams with web reinforcement, ACI Journal Special Publication SP42-6, 1974.

27 American Concrete Institute (ASCE-ACI Committee 426), The Shear Strength of Reinforced Concrete Members, ACI 426-74 (Re-Approved 1980), Detroit, 1974.

28 British Standards Institution : CP110 : Part 1 : 1972, Code of Practice for Structural Use of Concrete, November 1972.

29 British Standards Institution, BS8110 : Structural Use of Concrete,
Part 1 : 1985 : Code of practice for design and construction.
Part 2 : 1985 : Code of practice for special circumstances.

30 Eurocode 2: Design of concrete structures
BSI Publication DD ENV 1992-1-1 : 1992
Part 1 : General rules and rules for buildings.
Part 1.2 : Structural fire design.

31 CEB Comite Euro-International Du Beton :
Model Code for concrete structures, Paris, April 1978.

32 CEB Comite Euro-International Du Beton :
Model Code for concrete structures, Final Draft of 1990 version (Chapters 1 - 3); Bulletin D'Information No. 203, Paris, July 1991.

33 ACI Committee 318, Building code requirements for reinforced concrete (ACI 318-89), American Concrete Institute, Detroit, USA 1989

34 MacGregor J G, Challenge and changes in the design of concrete structures, Concrete International, Design and Construction, Vol 6 No. 2, February 1984.

35 Chana P S, Some aspects of modelling the behaviour of reinforced concrete under shear loading, Cement and Concrete Association, Technical Report 543, July 1981.

36 Bazant Z P and Sun H H, Size effect in diagonal shear failure: Influence of aggregate size and stirrups, ACI Materials Journal, Vol no 84-M27, July-August 1987.

37 Blackman J S, Smith G M and Young L, Stress distribution affects ultimate tensile strength, ACI Journal, Proceedings Vol 555, No 6, December 1958

38 Kim J K and Park Y D, Shear strength of reinforced concrete beams without web reinforcement, Magazine of Concrete Research, Vol 46, No. 166, March 1994.

39 Clarke J L, Shear capacity of high strength concrete beams, Concrete Journal of the Concrete Society, Vol 21 No. 3, March 1987.

40 Regan P E, Research on shear: a benefit to humanity or a waste of time?, Structural Engineer, Vol 71, No 19, October 1993.

41 Bobrowski Jan, Origin of Safety in Concrete Structures, Thesis for the degree of Doctor of Philosophy, University of Surrey, 1982.

42 Heyman J, Elements of stress analysis, Cambridge University Press, Cambridge, 1982.

43 *CEB Comite Euro-International Du Beton, CEB-FIP Model Code 1990 Supplementary Documents; Bulletin D'Information No. 189, July 1988.*

44 Chana P S & Desai S B: Design of shear reinforcement against punching, Structural Engineer, Vol 70, No. 9, May 1992.

45 ABAQUS Manual Version 5.2, Hibbitt, Karlsson and Sorensen (UK) Ltd, Warrington, Cheshire, UK.

46 Hertz K, Analyses of concrete structures exposed to fire, PhD Thesis, Technical University of Denmark, DK-2800 Lyngby 1992.

47 Concrete and reinforced concrete, design and construction, German Code of Practice DIN 1045, January 1972.

48 Krampf L, Investigation on shear behaviour of reinforced concrete beams exposed to fire, Draft Report on tests carried out under Professor Kordina, University of Brunswick, Germany, March 1978.

49 *Lin T D, Ellingwood B and Piet O, Flexural and shear behaviour of* reinforced concrete beams during fire tests, NBS-GCR-87-536, US Department of Commerce, National Institute for Science and Technology, Centre for Fire Research, Gaithersburg, MD, USA, December 1988.

50 Joint Committee of the Institution of Structural Engineers and the Concrete Society, Design and Detailing of concrete structures for fire resistance, April 1978.

51 Computer Programme, SOSMEF (Strength of Structural Members Exposed to Fire), City University, London, December 1992.

52 Wade C, Method for fire engineering design of structural concrete beams and floor systems, Technical Recommendation 8, C1/SfB/HQ4 (K), New Zealand, February 1991.

53 British Standards Institution, BS476: Fire tests on building materials and structures: Part 20: Method of determination of the fire resistance of elements of construction (General principles), 1987.

APPENDIX B
ABAQUS INPUT FILE

ABAQUS INPUT FILE

```
*HEADING
TEST BEAM : SPAN=1400 : SOLID ELEMENTS : BEAM A2
*NODE, SYSTEM=R
1, 0, 0,0                          .....(Node numbers and x, y & z co-ordinates)
169, 0, 0, 300
3, 62.5, 0, 0
171, 62.5, 0, 300
5, 137.5, 0, 0
173, 137.5, 0, 300
15, 637.5, 0, 0
183, 637.5, 0, 300
17, 712.5, 0, 0
185, 712.5, 0, 300
19, 762.5, 0, 0
187, 762.5, 0, 300
21, 800, 0, 0
189, 800, 0, 300
1001, 0, 25, 0
1169, 0, 25, 300
1003, 62.5, 25, 0
1171, 62.5, 25, 300
1005, 137.5, 25, 0
1173, 137.5, 25, 300
1015, 637.5, 25, 0
1183, 637.5, 25, 300
1017, 712.5, 25, 0
1185, 712.5, 25, 300
1019, 762.5, 25, 0
1187, 762.5, 25, 300
1021, 800, 25, 0
1189, 800, 25, 300
2001, 0, 50, 0
2169, 0, 50, 300
2003, 62.5, 50, 0
2171, 62.5, 50, 300
2005, 137.5, 50, 0
2173, 137.5, 50, 300
2015, 637.5, 50, 0
2183, 637.5, 50, 300
2017, 712.5, 50, 0
2185, 712.5, 50, 300
2019, 762.5, 50, 0
2187, 762.5, 50, 300
2021, 800, 50, 0
2189, 800, 50, 300
3001, 0, 100, 0
3169, 0, 100, 300
3003, 62.5, 100, 0
```

3171, 62.5, 100, 300
3005, 137.5, 100, 0
3173, 137.5, 100, 300
3015, 637.5, 100, 0
3183, 637.5, 100, 300
3017, 712.5, 100, 0
3185, 712.5, 100, 300
3019, 762.5, 100, 0
3187, 762.5, 100, 300
3021, 800, 100, 0
3189, 800, 100, 300
4001, 0, 150, 0
4169, 0, 150, 300
4003, 62.5, 150, 0
4171, 62.5, 150, 300
4005, 137.5, 150, 0
4173, 137.5, 150, 300
4015, 637.5, 150, 0
4183, 637.5, 150, 300
4017, 712.5, 150, 0
4185, 712.5, 150, 300
4019, 762.5, 150, 0
4187, 762.5, 150, 300
4021, 800, 150, 0
4189, 800, 150, 300
5001, 0, 175, 0
5169, 0, 175, 300
5003, 62.5, 175, 0
5171, 62.5, 175, 300
5005, 137.5, 175, 0
5173, 137.5, 175, 300
5015, 637.5, 175, 0
5183, 637.5, 175, 300
5017, 712.5, 175, 0
5185, 712.5, 175, 300
5019, 762.5, 175, 0
5187, 762.5, 175, 300
5021, 800, 175, 0
5189, 800, 175, 300
6001, 0, 200, 0
6169, 0, 200, 300
6003, 62.5, 200, 0
6171, 62.5, 200, 300
6005, 137.5, 200, 0
6173, 137.5, 200, 300
6015, 637.5, 200, 0
6183, 637.5, 200, 300
6017, 712,5, 200, 0
6185, 712.5, 200, 300
6019, 762.5, 200, 0

```
6187, 762.5, 200, 300
6021, 800, 200, 0
6189, 800, 200, 300
*NGEN, NSET-N1
1, 169, 21                          .....(Nodes 1 to 169 in increments of 21)

*NGEN, NSET=N3
  3, 171, 21
*NGEN, NSET=N5
  5, 173, 21
*NGEN, NSET=N15
 15, 183, 21
*NGEN, NSET=N17
 17, 185, 21
*NGEN, NSET-N19
 19, 187, 21
*NGEN, NSET=N21
 21, 169, 21

*NFILL N1, N3, 2, 1   .....(Filling in the nodes between two sets)
N3, N5, 2, 1
N5, N15, 10, 1
N15, N17, 2, 1
N17, N19, 2, 1
N19, N21, 2, 1

*NGEN, NSET=N1001
1001, 1169, 21
*NGEN, NSET=N1003
1003, 1171, 21
*NGEN, NSET=N1005
1005, 1173, 21
*NGEN, NSET=N1005
1015, 1183, 21
*NGEN, NSET=N1017
1017, 1185, 21
*NGEN, NSET=N1019
1019, 1187, 21
*NGEN, NSET=N1021
1021, 1189, 21

*NFILL
N1001, N1003, 2, 1
N1003, N1005, 2, 1
N1005, N1015,10, 1
N1015, N1017, 2, 1
N1017, N1019, 2, 1
N1019, N1021, 2, 1
```

```
*NGEN, NSET=N2001
2001, 2169, 21
*NGEN, NSET=2003
2003, 2171, 21
*NGEN, NSET=N2005
2005, 2173, 21
*NGEN, NSET=N2015
2015, 2183, 21
*NGEN, NSET=N2017
2017, 2185, 21
*NGEN, NSET=N2019
2019, 2187, 21
*NGEN, NSET=N2021
2021, 2189, 21

*NFILL
N2001, N2003, 2, 1
N2003, N2005, 2, 1
N2005, N2015, 10, 1
N2015, N2017, 2, 1
N2017, N2019, 2, 1
N2019, N2021, 2,1

*NGEN, NSET=N3001
3001, 3169, 21
*NGEN, NSET=N3003
3003, 3171, 21
*NGEN, NSET=N3005
3005, 3173, 21
*NGEN, NSET=N3015
3015, 3183, 21
*NGEN, NSET=N3017
3017, 3185, 21
*NGEN, NSET=N3019
3019, 3187, 21
*NGEN, NSET=N3021
3021, 3189, 21

*NFILL
N3001, N3003, 2, 1
N3003, N3005, 2, 1
N3005, N3015, 10, 1
N3015, N3017, 2, 1
N3017, N3019, 2, 1
N3019, N3021, 2, 1

*NGEN, NSET=N4001
4001, 4169, 21
*NGEN, NSET=N4003
4003, 4171, 21
```

```
*NGEN, NSET=N4005
4005, 4173, 21
*NGEN, NSET=N4015
4015, 4183, 21
*NGEN, NSET=N4017
4017, 4185, 21
*NGEN, NSET=N4019
4019, 4187, 21
*NGEN, NSET=N4021
4021, 4189, 21

*NFILL
N4001, N4003, 2, 1
N4003, N4005, 2, 1
N4005, N4015, 10, 1
N4015, N4017, 2, 1
N4017, N4019, 2, 1
N4019, N4021, 2, 1

*NGEN, NSET=N5001
5001, 5169, 21
*NGEN, NSET=N5003
5003, 5171, 21
*NGEN, NSET=N5005
5005, 5173, 21
*NGEN, NSET=N5015
5015, 5183, 21
*NGEN, NSET=N5017
5017, 5185, 21
*NGEN, NSET=N5019
5019, 5187, 21
*NGEN, NSET=N5021
5021, 5189, 21

*NFILL
N5001, N5003, 2, 1
N5003, N5005, 2, 1
N5005, N5015, 10, 1
N5015, N5017, 2, 1
N5017, N5019, 2, 1
N5019, N5021, 2, 1

*NGEN, NSET=N6001
6001, 6169, 21
*NGEN, NSET=6003
6003, 6071, 21
*NGEN, NSET=N6005
6005, 6173, 21
*NGEN, NSET=N6015
6015, 6183, 21
```

```
*NGEN, NSET=N6017
6017, 6185, 21
*NGEN, NSET=N6019
6019, 6187, 21
*NGEN, NSET=N6021
6021, 6189, 21

*NFILL
N6001, N6003, 2, 1
N6003, N6005, 2, 1
N6005, N6015, 10, 1
N6015, N6017, 2, 1
M6017, N6019, 2, 1
N6019, N6021, 2, 1

*NSET, NSET=NSUP
5, 1005, 2005, 3005, 4005, 6005
**ELEMENT DEFINITION                    ...(** means a comment or a statement
*ELEMENT,TYPE=C3D2OR, ELSET=ALL      ....(*  means a command)
1, 1, 3, 2003, 2001, 43, 45, 2045, 2043, 2, 1003, 2002
1001, 44, 1045, 2044, 1043, 22, 24, 2024, 2022
*ELGEN, ELSET=ALL
1, 10, 2, 1, 3, 2000, 100, 4, 42, 10
*SOLID SECTION, MATERIAL=CON, ELSET=ALL
*MATERIAL, NAME=CON
*ELASTIC
27200.0, 0.2                            .....(Elastic modules and Poisson's ratio)
*CONCRETE
 4.82, 0.0                              .....(Stress-strain relationship; units: n,mm)
 5.71, 3.864E-5
 6.62, 7.464E-5
 7.52, 1.106E-4
 8.40, 1.466E-4
 9.27, 1.826E-4
10.13, 2.186E-4
10.96, 2.546E-4
11.78, 2.906E-4
12.58, 3.266E-4
13.36, 3.626E-4
14.13, 3.986E-4
14.87, 4.346E-4
15.58, 4.706E-4
16.28, 5.066E-4
16.95, 5.426E-4
17.60, 5.786E-4
18.22, 6.146E-4
18.82, 6.506E-4
19.38, 6.866E-4
19.93, 7.226E-4
20.44, 7.506E-4
```

```
20.92, 7.946E-4
21.37, 8.306E-4
21.79, 8.666E-4
22.18, 9.026E-4
22.54, 9.386E-4
22.86, 9.746E-4
23.15, 1.010E-3
23.40, 1.046E-3
23.62, 1.082E-3
23.79, 1.118E-3
23.93, 1.154E-3
24.03, 1.190E-3
24.09, 1.226E-3
24.12, 1.262E-3
24.00, 0.0035

*FAILURE RATIOS
1.16, 0.12, 1.28, 0.33
*TENSION STIFFENING
1.0, 3.35E-3
*SHEAR RETENTION
1.0, 0.0075, 1.0, 0.0075                    .....   (ABAQUS requirement for
                                                     definition of shear retention)
*ELSET, ELSET=LOWER1, GENERATE                      [Details of reinforcement :
1, 10, 1                                            lower (tension steel)
*ELSET, ELSET=LOWER2, GENERATE                      central (central bar0
101, 110, 1                                         upper (nominal top steel)]
*ELSET, ELSET=LOWER3, GENERATE
201, 210, 1
*ELSET, ELSET=CENTRAL2, GENERATE
111, 120, 1
*ELSET, ELSET=UPPER1, GENERATE
 31,  40, 1
*ELSET,ELSET=UPPER2, GENERATE               .....   (Not used as there are
131, 140, 1                                          only two top bars)
*ELSET,ELSET=UPPER3, GENERATE
231, 240, 1
**REBAR DEFINITION
*REBAR, ELEMENT=CONTINUUM, MATERIAL=MAIN,
GEOMETRY=ISOPARAMETRIC, SINGLE
LOWER1, 314.0, 0.7, 0.46, 1          ....     (Area of bar and its location as a
LOWER3, 314.0, 0.3, 0.46, 1                   fraction of the element dimensions,
                                              from the left bottom corner)
*REBAR, ELEMENT=CONTINUUM, MATERIAL=CS,
GEOMETRY=ISOPARAMETRIC, SINGLE
CENTRAL2, 101.0, 0.50, 1.0, 1
*REBAR,ELEMENT=CONTINUUM, MATERIAL=TOP,
GEOMETRY=ISOPARAMETRIC, SINGLE
UPPER1,113.0, 0.7, 0.59, 1
UPPER3,113.0, 0.3, 0.59, 1
```

```
*MATERIAL,NAME=MAIN                (Properties of reinforcement)
*ELASTIC
200000.0
*PLASTIC
460.0
*MATERIAL, NAME=CS                 (CS = Central Steel)
*ELASTIC
200000.0
*PLASTIC
460.0
*MATERIAL, NAME=TOP
*ELASTIC
200000.0
*PLASTIC
460.0
*DRAW, ELNUM
*DRAW, NODENUM
*RESTART, WRITE, FREQ=5    (Frequency for reporting the status)
*BOUNDARY                          .....(Support)
  N21, 1                           .....(Support nodes)
N1021, 1
N2021, 1
N3021, 1
N4021, 1
N5021, 1
N6021, 1
NSUP, 3                      .....  ("3" is the direction in which restraint
                                     is defined
*STEP, INC=60                .....  (Maximum increment)
*STATIC, RIKS                .....  (RIKS is the method for solving
                                     non-linear algorithms)
0.025, 1.0, 1E-9, 2.0                .....  (IE-9: Reduced increment
                                       2.0 : Limit set on the maximum load
                                             as a multiple of the applied
                                             load for the analysis to stop)
*CONTROLS, PARAMETERS=LINE SEARCH
4
*DLOAD
 40, P2, 7.95
140, P2, 7.95
240, P2, 7.95
  2, P1, 3.98
102, P1, 3.98
202, P1, 3.98
*EL PRINT, FREQ=55                   ....        (Reporting outputs)
S                                    ....        Stress
*EL PRINT, FREQ=55
E                                    ....        Strain
```

```
*EL PRINT, FREQ=55
SP1, SP3                    .....   (Principal stresses (-ve)
                                     Min (-ve) compression - SP1
                                     Max (+ve) tension - SP3

*EL PRINT, FREQ=55
CRACK
*EL PRINT, FREQ=55
CONF                        .....   Report if crushing occurs
*EL PRINT, REBAR, FREQ=55
COORD,S                     .....   Location
*NODE PRINT, FREQ=55
U                           .....   Deflection
RF                          .....   Reactive forces
*END STEP
```

APPENDIX C

PHOTOGRAPHS

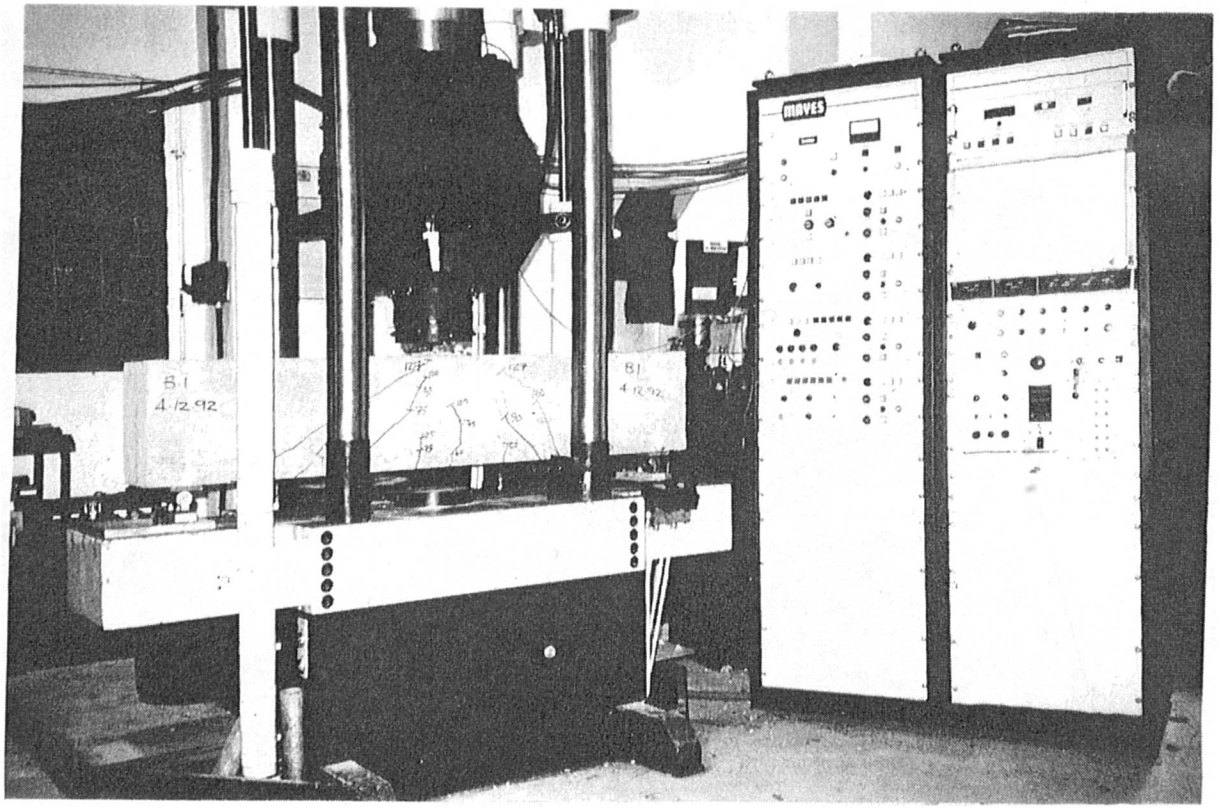

1 TEST ARRANGEMENT FOR 1400 MM SPAN BEAMS

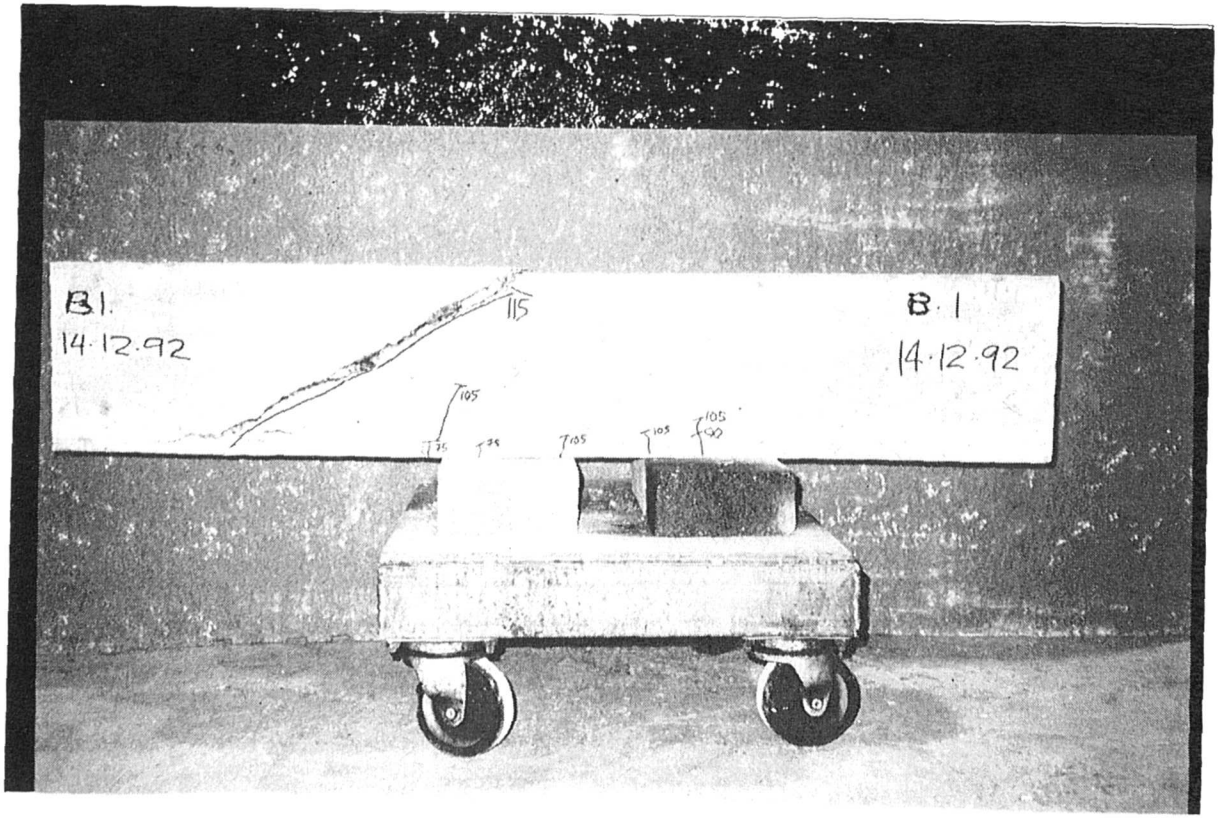

2 BEAM B1 - 3T20 @ BOTTOM & NO CENTRAL BAR

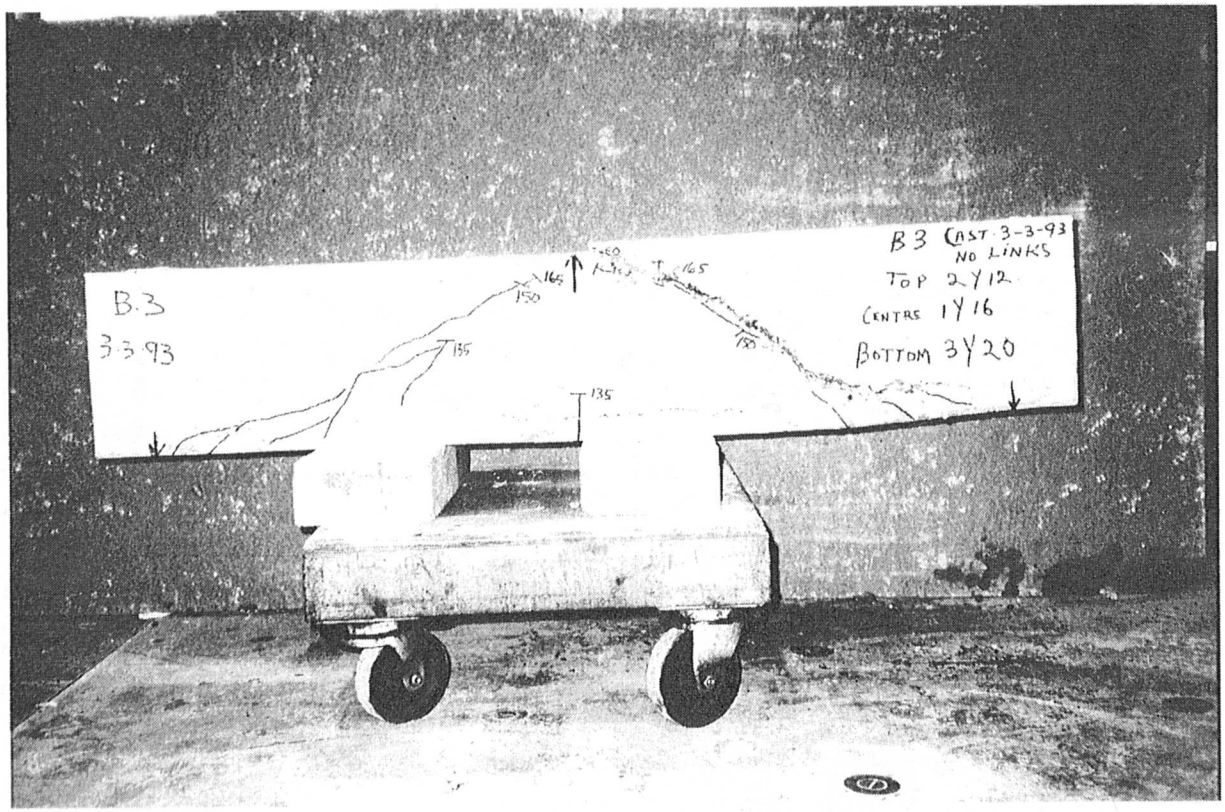

3 **BEAM B3 - 3T20 @ BOTTOM & 1T16 CENTRAL BAR**

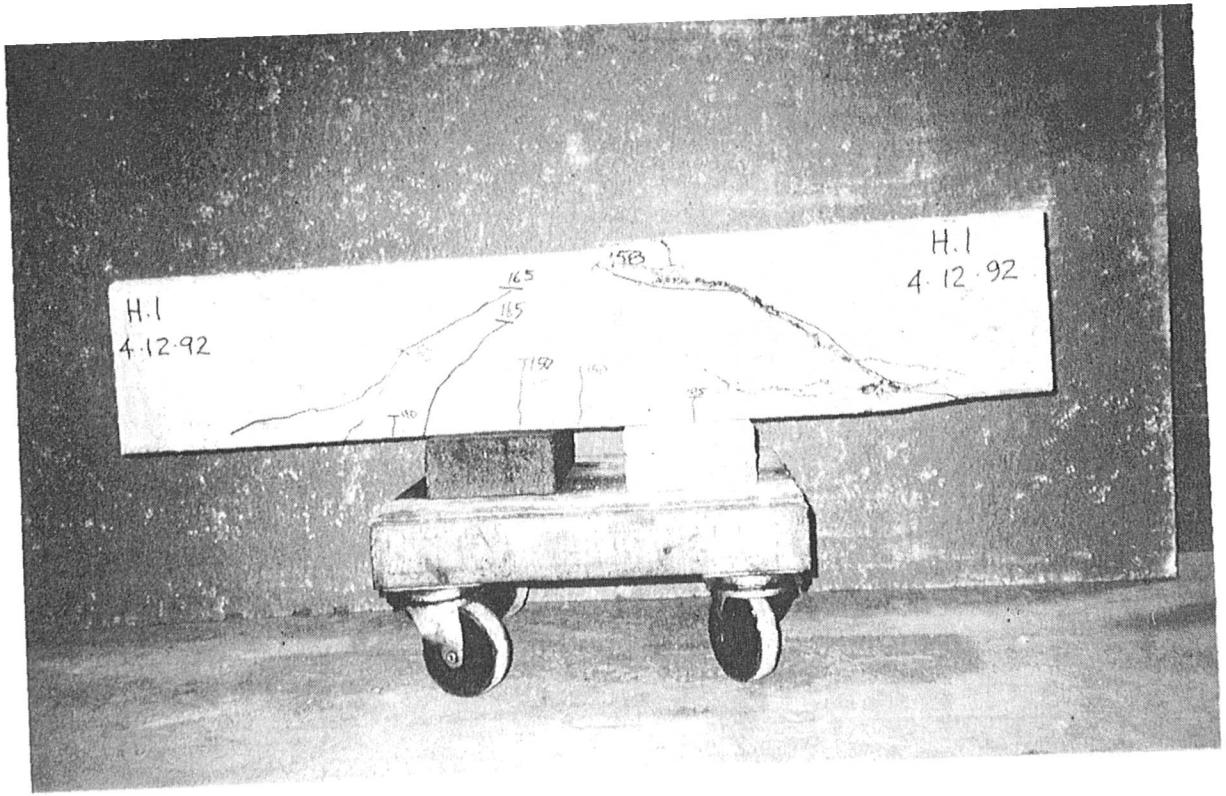

4 **BEAM E4 - 3T25 @ BOTTOM & 1T16 CENTRAL BAR**

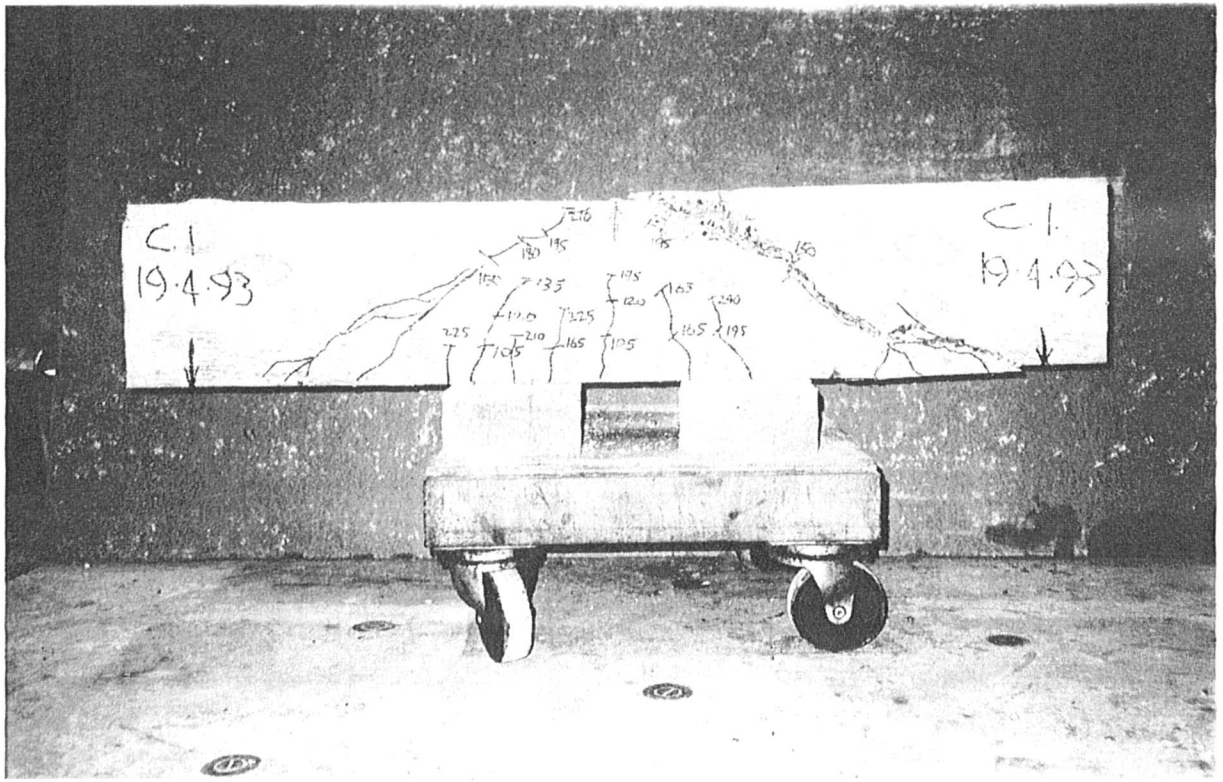

5 BEAM C1 - 3T20 @ BOTTOM, LINKS 6T@200 C/C

& NO CENTRAL BAR

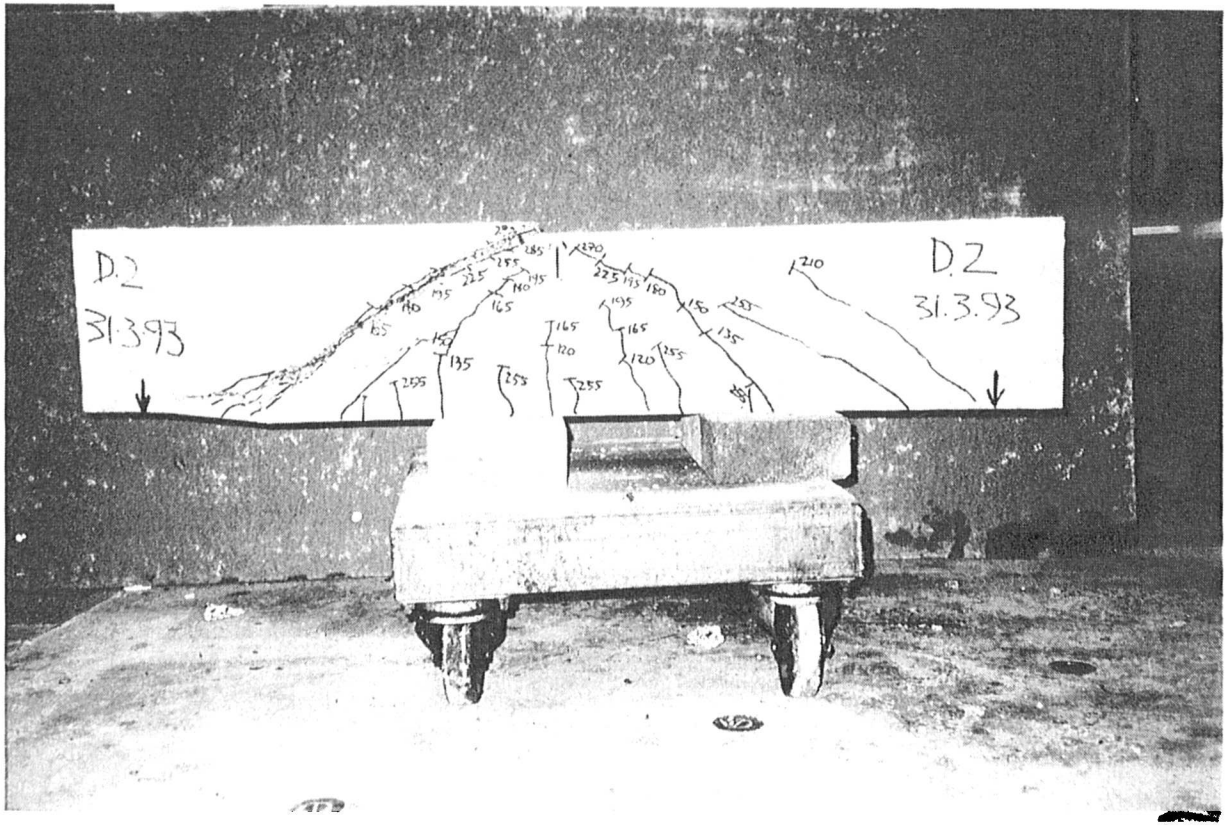

6 BEAM D2 - 3T20 @ BOTTOM, LINKS 6T@200 C/C

& 1T16 CENTRAL BAR

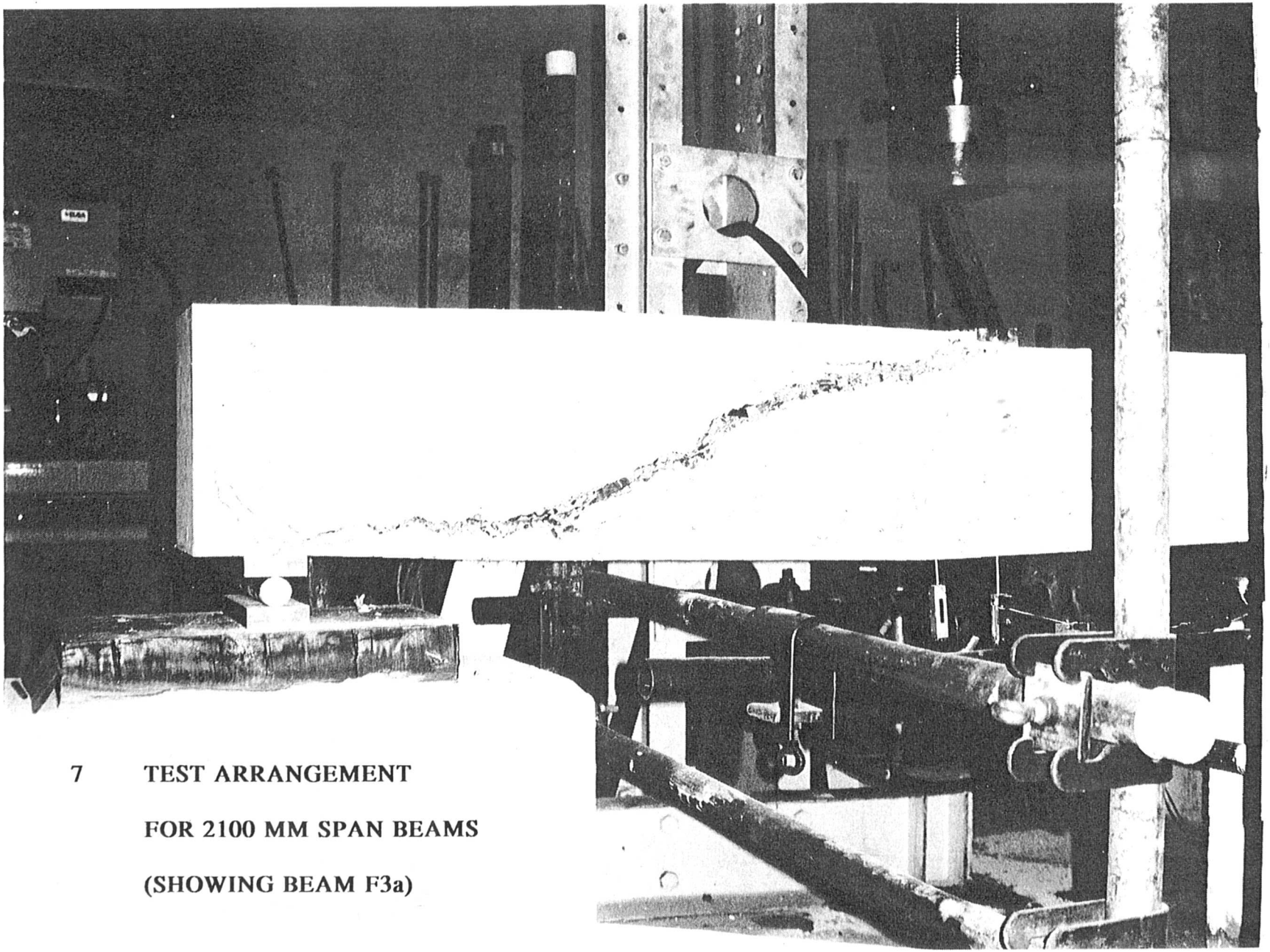

7 TEST ARRANGEMENT

FOR 2100 MM SPAN BEAMS

(SHOWING BEAM F3a)

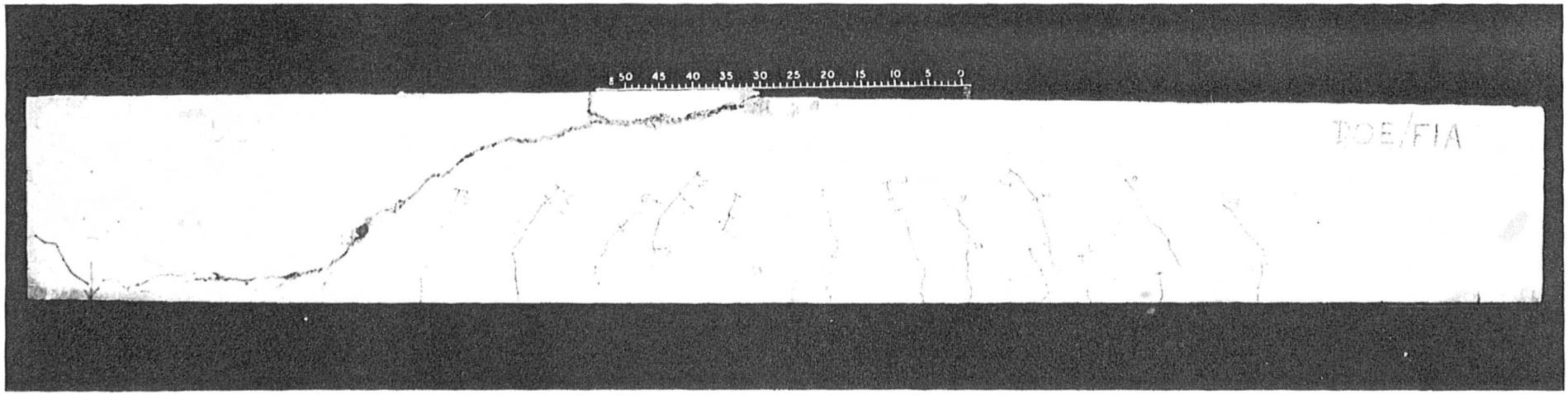

8 BEAM F1 - 3T20 @ BOTTOM & NO CENTRAL BAR

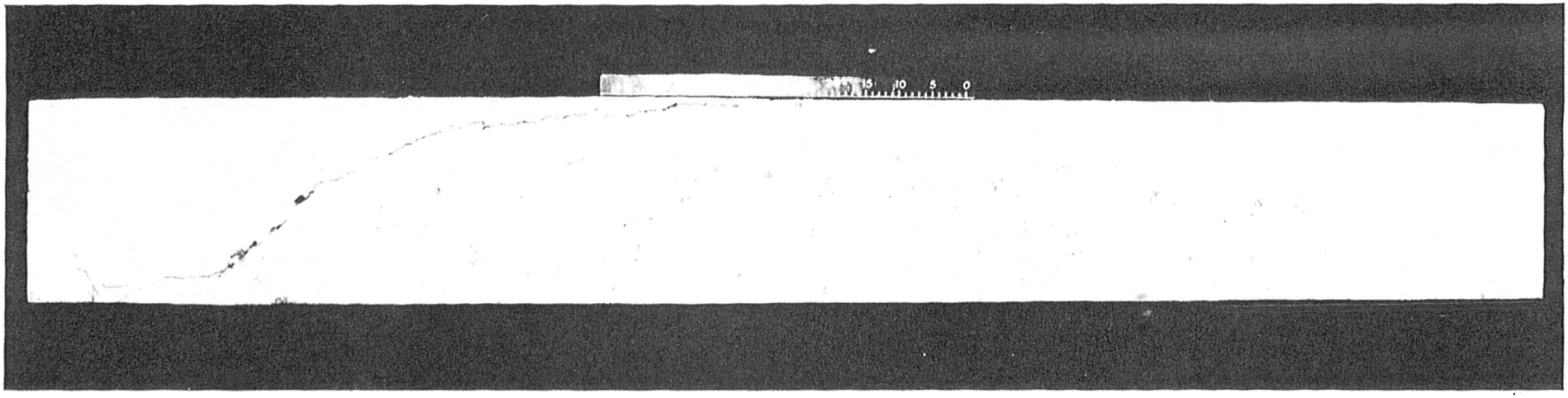

9 BEAM F4 - 3T20 @ BOTTOM & 1T20 CENTRAL BAR

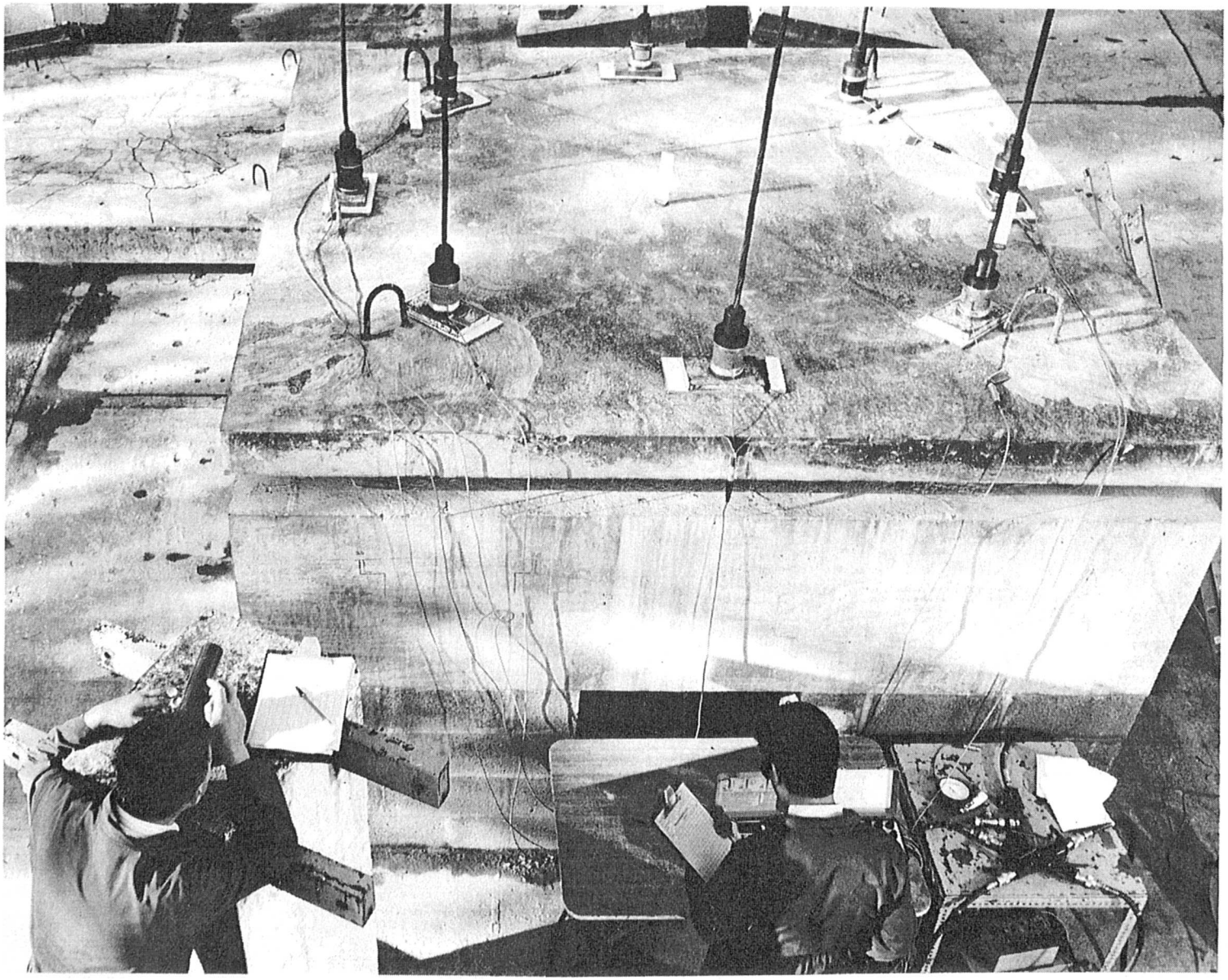

10 TEST ARRANGEMENT FOR SLABS

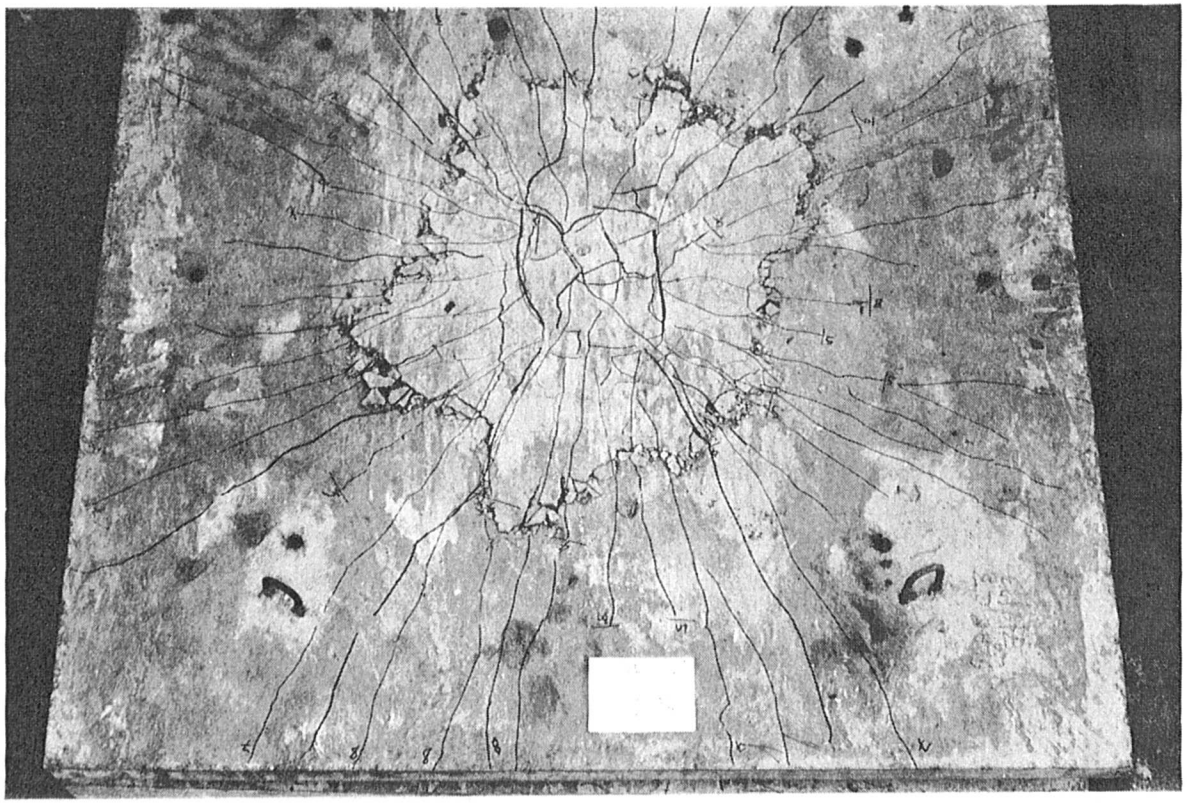

11 150 MM SLAB - T10@80 (T) & NO CENTRAL MESH

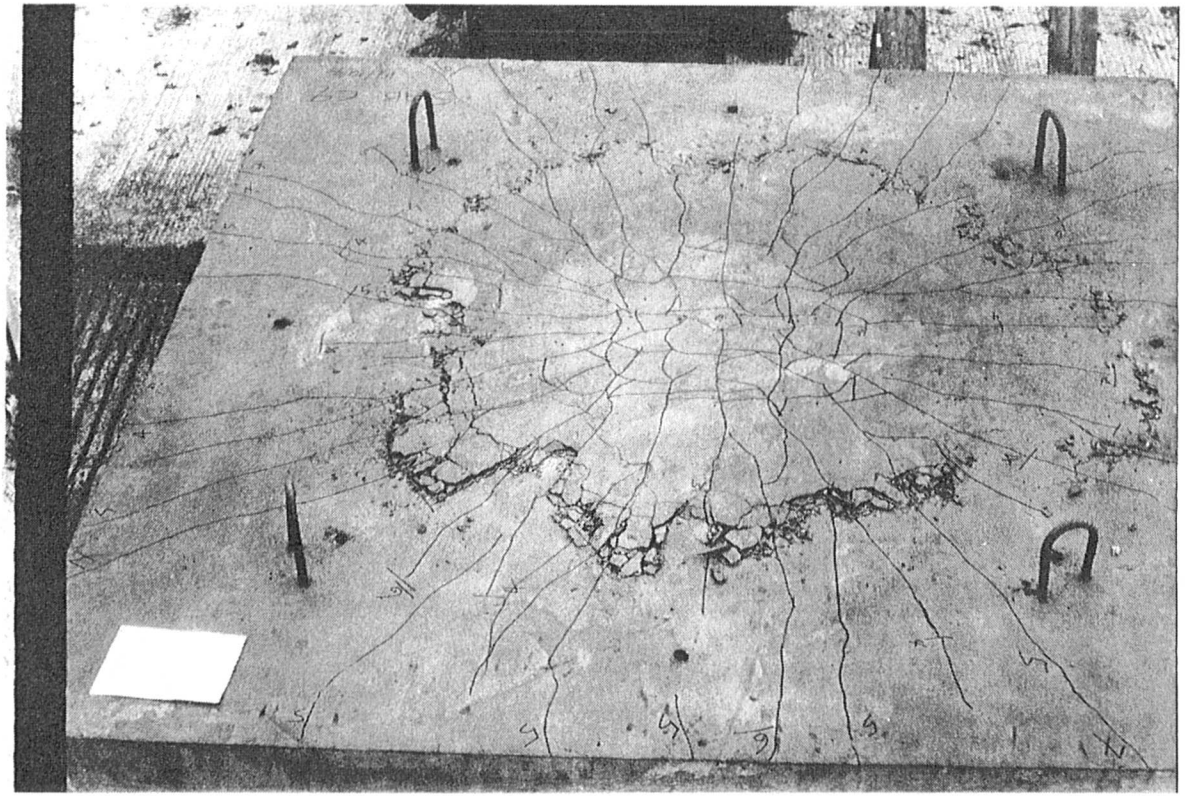

12 150 MM SLAB - T10@80 (T) & T8@160 CENTRAL MESH

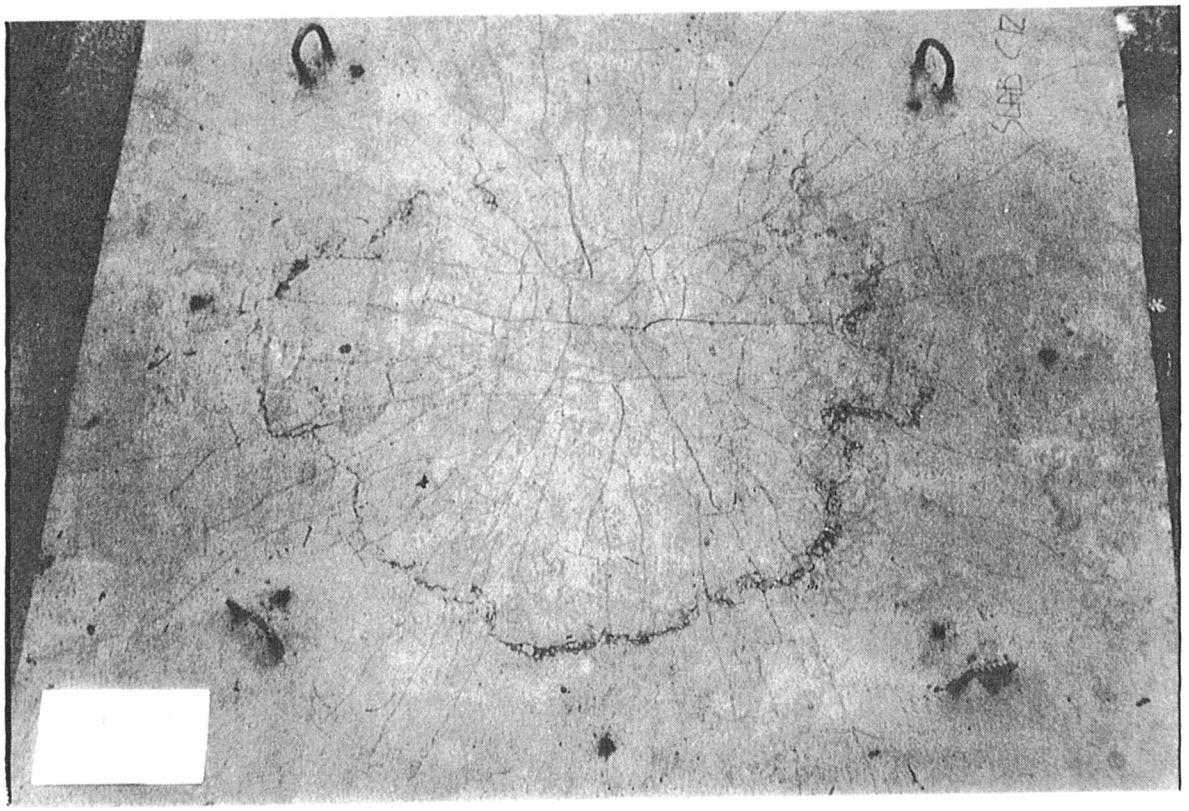

13 200 MM SLAB - T16@160 (T) & NO CENTRAL MESH

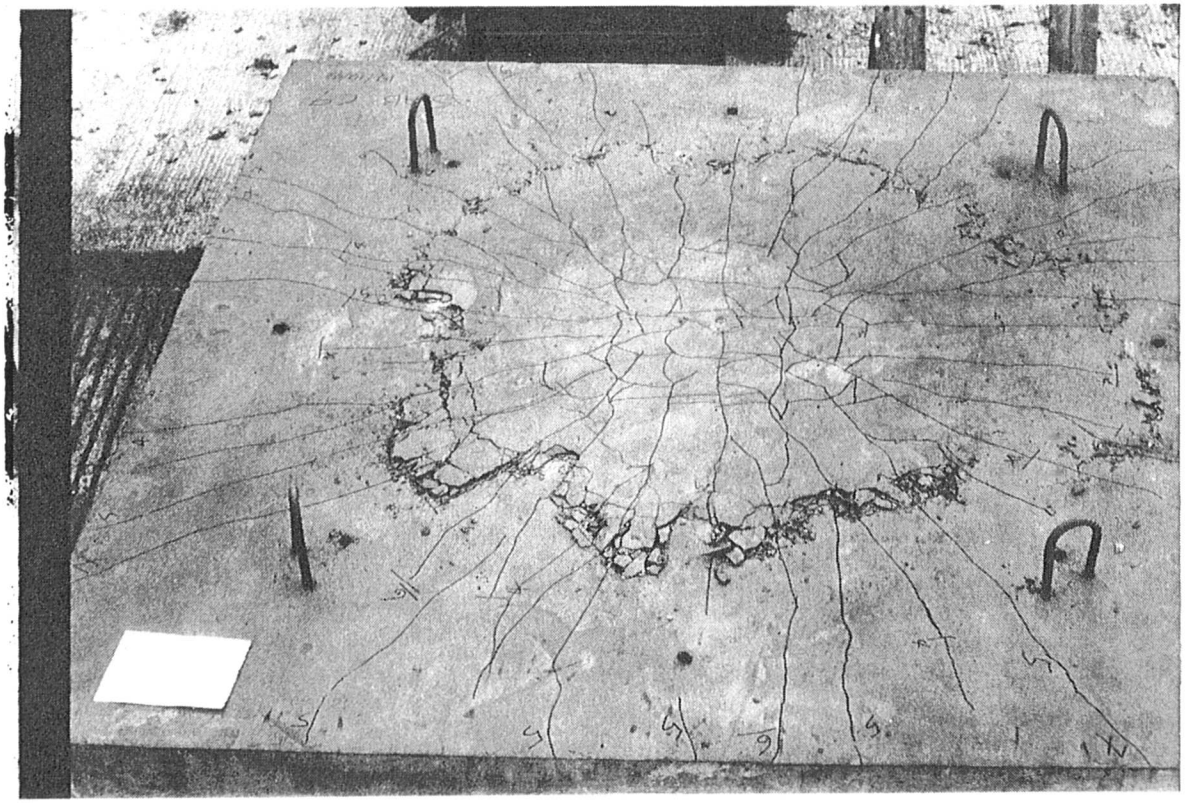

14 200 MM SLAB - T16@160 (T) & T16@160 CENTRAL MESH

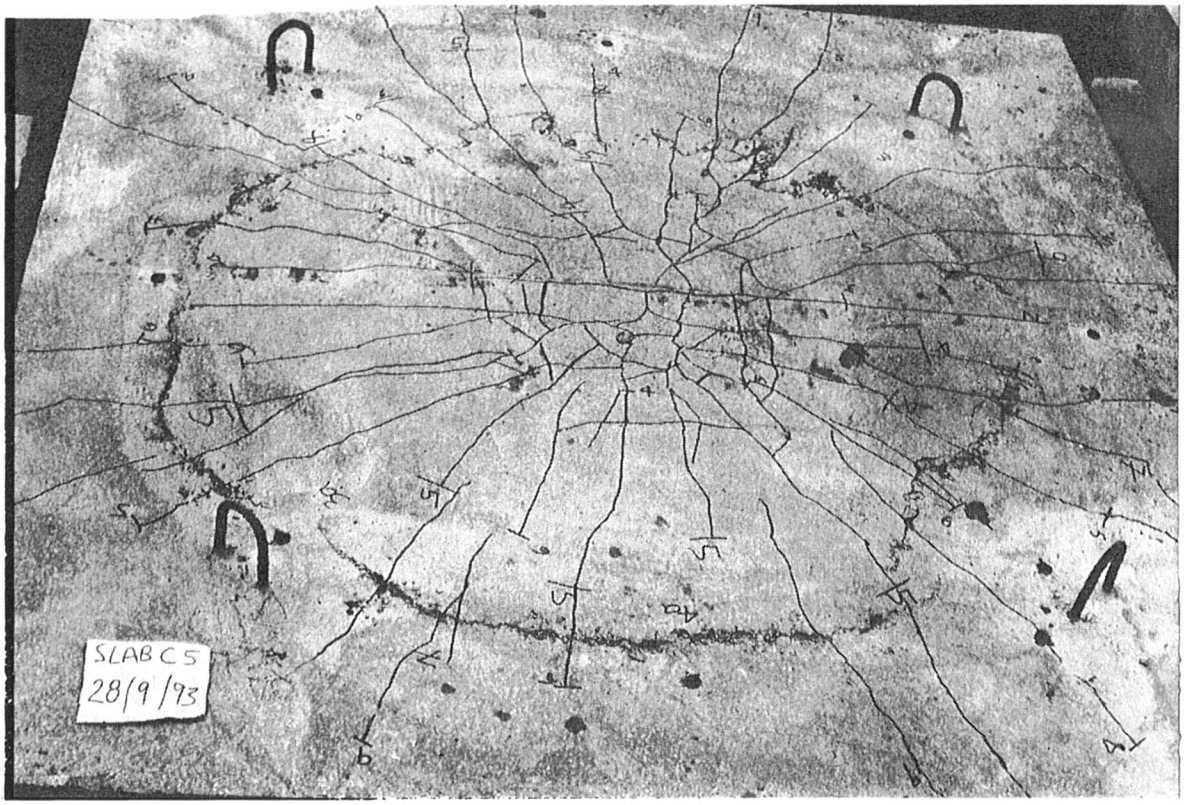

15 250 MM SLAB - T20@175 (T) & T12@175 CENTRAL MESH

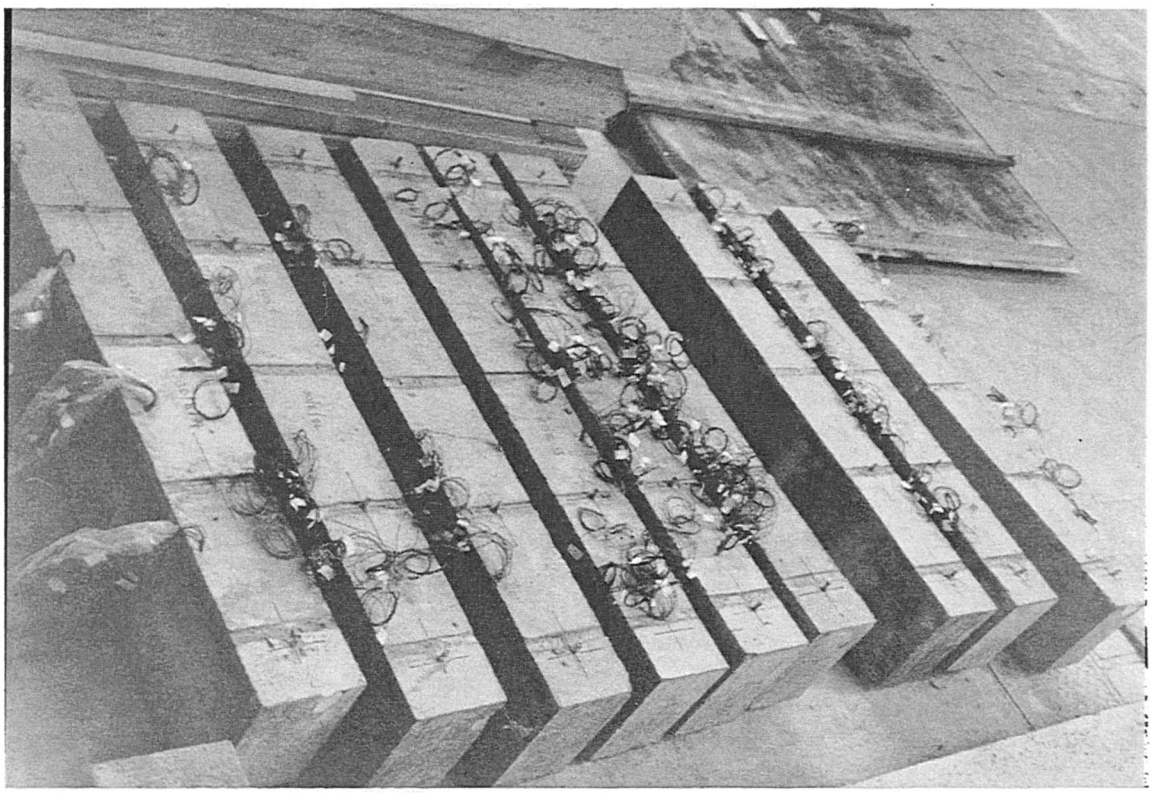

16 BEAM SPECIMENS WITH THERMOCOUPLES

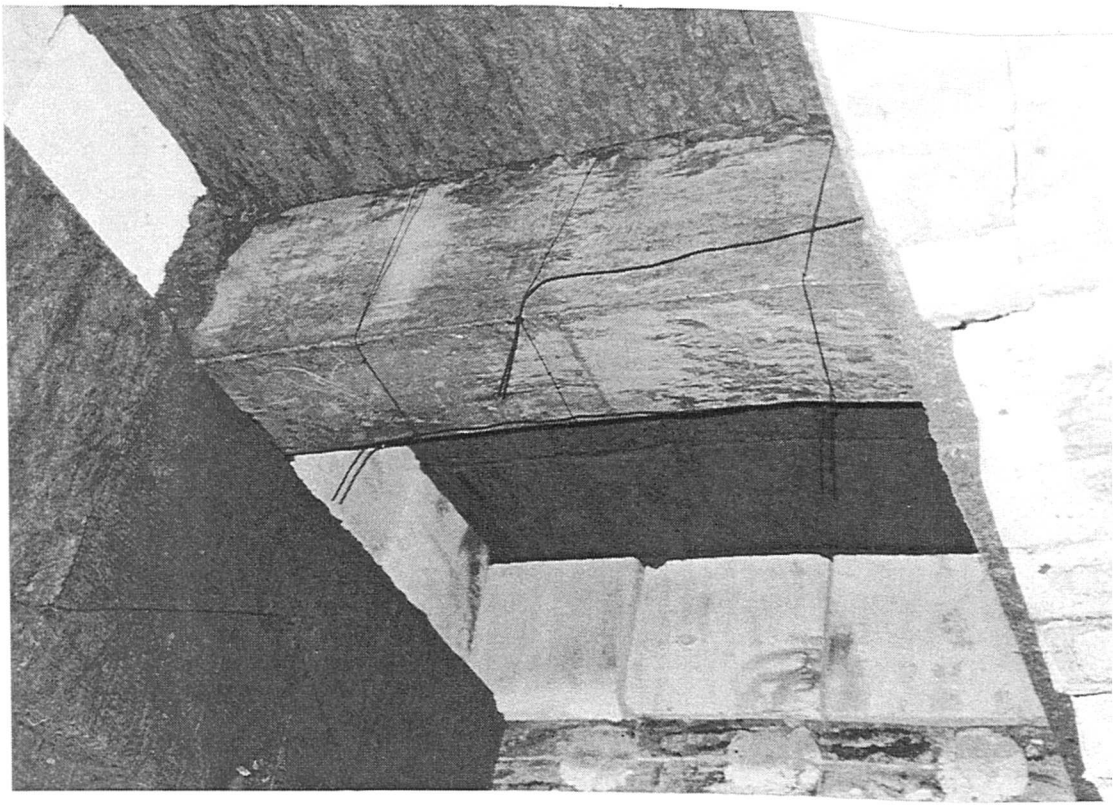

17 INTERIOR OF THE FURNACE SHOWING THE BEAM B101 AND THE THERMOCOUPLES

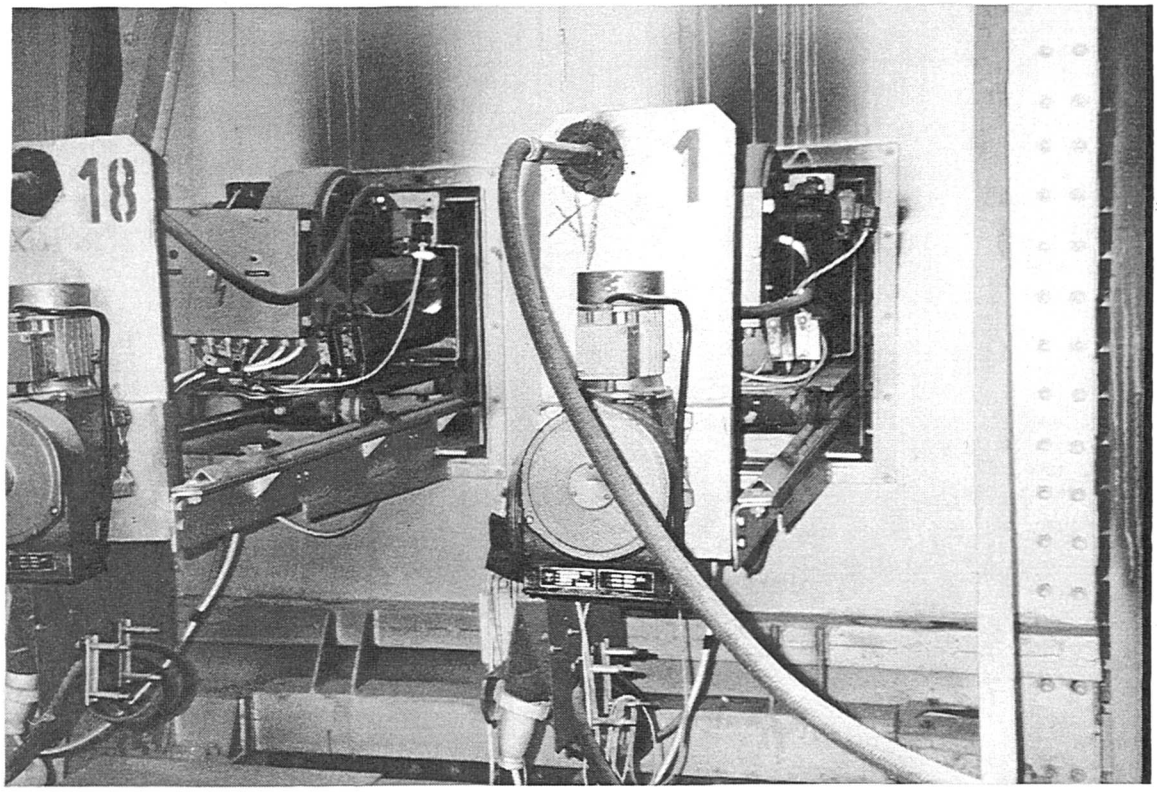

18 EXTERIOR OF THE FURNACE SHOWING BURNERS

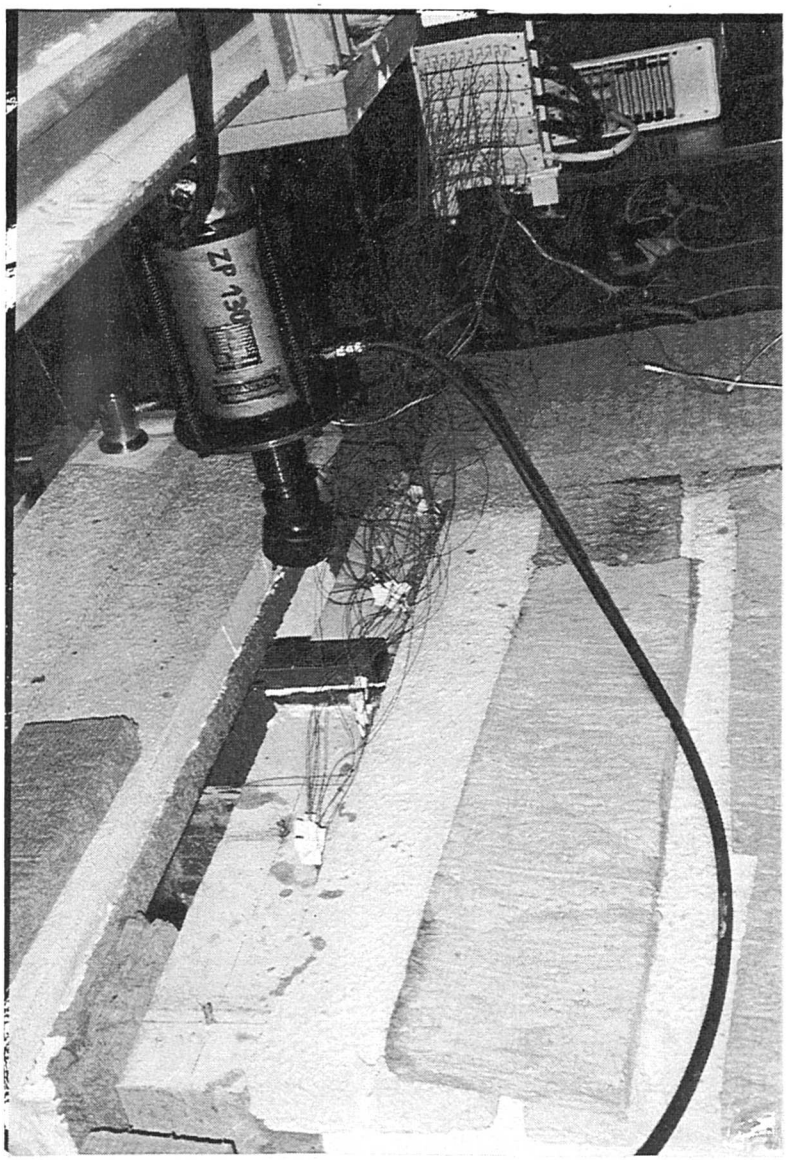

19 ROOF OF THE FURNACE SHOWING SLABS, INSULATION, THE BEAM AND THE LOADING JACK

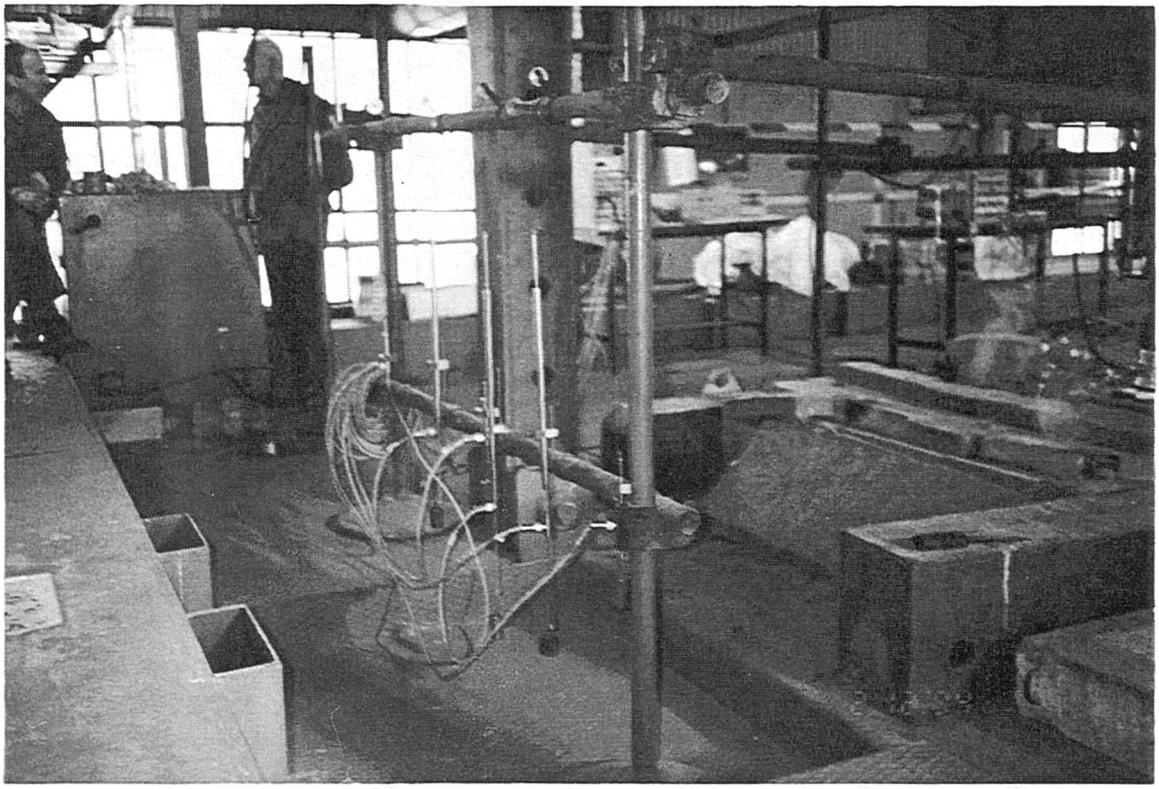

20 INSTRUMENTS FOR MEASUREMENT OF DEFLECTIONS.